



HAL
open science

Combining a real-time closed-loop system with neuromodulation: an integrative approach to prevent pathological repetitive behaviors

Sirenia Lizbeth Mondragón González

► **To cite this version:**

Sirenia Lizbeth Mondragón González. Combining a real-time closed-loop system with neuromodulation: an integrative approach to prevent pathological repetitive behaviors. *Neurons and Cognition* [q-bio.NC]. Sorbonne Université, 2019. English. NNT: 2019SORUS259 . tel-03194990

HAL Id: tel-03194990

<https://theses.hal.science/tel-03194990>

Submitted on 10 Apr 2021

HAL is a multi-disciplinary open access archive for the deposit and dissemination of scientific research documents, whether they are published or not. The documents may come from teaching and research institutions in France or abroad, or from public or private research centers.

L'archive ouverte pluridisciplinaire **HAL**, est destinée au dépôt et à la diffusion de documents scientifiques de niveau recherche, publiés ou non, émanant des établissements d'enseignement et de recherche français ou étrangers, des laboratoires publics ou privés.

Sorbonne Université

Ecole doctorale 391 - Sciences mécaniques, acoustique, électronique et
robotique de Paris (SMAER)
Institut du Cerveau et de la Moelle Epinière / Neurophysiology of Repetitive Behaviors

Combining a real-time closed-loop system with neuromodulation

*An integrative approach to prevent pathological repetitive
behaviors*

Par **Sirenia Lizbeth Mondragón González**

Thèse de doctorat

Dirigée par Eric Burguière et Jean-Luc Zarader

Présentée et soutenue publiquement le 08/04/2019

Devant un jury composé de :

Burguière Eric (CR1)

Directeur de thèse

Zarader Jean-Luc (Professeur Universitaire)

Co-directeur de thèse

Welter Marie-Laure (PU-PH CHU)

Rapportrice

Willuhn Ingo (Professeur associé et leader de groupe)

Rapporteur

Arleo Angelo (DR2)

Président du jury

Fino Elodie (CR1)

Examinatrice



A ma grand-mère

ACKNOWLEDGMENTS

First, I would like to thank the members of my committee, Dr. Marie-Laure Welter and Dr. Ingo Willuhn for kindly accepting to review my thesis manuscript and to Dr. Elodie Fino and to Dr. Angelo Arleo for accepting to evaluate my work.

I would like to extend deep gratitude to my advisor Eric Burguière. Eric, I am glad to be your first PhD student, I truly consider myself lucky to have worked under your supervision. These have been some remarkably interesting and exciting years. I have learned so much thanks to our (sometimes super) long conversations. I am extremely grateful to you for introducing me to the wild world of extracellular electrophysiology. For always being open minded but with a critic eye to my ideas, I know that you trusted me in so many ways for the experiments, for this and more I am incredibly grateful to you.

I owe thanks to my co-advisor Jean-Luc Zarader, I know that you always made our appointments a priority in your busy schedule, we had very stimulating discussions when we were trying to find out how to attack the pattern recognition problem, I remember finishing our discussion with so much motivation and excitement to implement a new approach, and I am grateful for that.

A big thanks to Christiane Schreiweis, not only did I learn a lot about mice with you but also you provided invaluable help for the animal preparations in Chapter 6. Thank you for the not so easy and long surgery sessions.

To Pauline and Nabil, I am glad we did his journey at the same time, we have had some good laughs and I am happy that we shared these last years together. A special thanks to Marine, for all the conversations (and free chouquettes) and for kindly helping me take care of my mice when I could not.

Thanks to everyone in the now NERB team of the ICM for their hospitality when I first joined the lab. To the first members of the BEBG team, to Luc, Margot, Jérôme, Karim, Philippe, and Christian, for making the lab a lovely place to be in.

Thanks to the current graduate students, Lindsay, Oriana, Eliana, and Sami for the encouraging words while writing my manuscript. To the old interns Celine and Maeva that regularly asked for news on my thesis.

All the mice without whom none of this work would have been possible.

To my dear friends Jean-Luc, Cri cri, Oscardo and Sandy, and to my Cinves girlfriends for helping me forget my project when it was necessary.

To Claude and Christian for always worrying about me and the advancement of my project, I really appreciated it.

To my parents, who have always supported me in all my decisions and provided unlimited encouragement. To my "little" brothers, Ricardo who did his PhD at the same time, it has been fun to share our lab adventures. To my little brother Victor who has always helped me to side the bright side of all situations.

To my grand mother Maria, who I know would have been proud, I dedicate this manuscript to you.

And finally, to my brilliant husband. Vince, you probably do not realize how much your never-ending positive attitude toward life and support was my daily battery charger. You inspired me to want to make the best of my PhD years.

TABLE OF CONTENTS

<u>ACKNOWLEDGMENTS</u>	1
<u>TABLE OF CONTENTS</u>	3
<u>SUMMARY</u>	5
<u>PART I: INTRODUCTION</u>	7
<u>CHAPTER 1. PHENOMENOLOGY OF REPETITIVE BEHAVIORS</u>	8
1.1 NORMAL REPETITIVE BEHAVIORS	8
1.2 PATHOLOGICAL REPETITIVE BEHAVIORS.	11
MAIN POINT SUMMARY	18
<u>CHAPTER 2. NEUROPHYSIOLOGY OF COMPULSIVE BEHAVIOR</u>	19
2.1 THE ANATOMICAL-FUNCTIONAL ORGANIZATION OF THE BASAL GANGLIA	19
2.2 THE MICROCIRCUITRY OF THE STRIATUM	30
2.3 NEUROPHYSIOLOGY OF COMPULSIVE BEHAVIOR	38
2.4 ANIMAL MODELS OF COMPULSIVE BEHAVIOR	40
2.5 RODENT SELF-GROOMING PHENOTYPE FOR UNDERSTANDING COMPULSIVE BEHAVIOR	50
MAIN POINT SUMMARY	54
<u>CHAPTER 3. CLOSED-LOOP NEUROMODULATION</u>	55
3.1 OPEN-LOOP BRAIN STIMULATION	55
3.2 CLOSING THE LOOP	76
3.3 CLOSED-LOOP APPROACH RELATED TO RB	87
MAIN POINT SUMMARY	90
<u>PART II: EXPERIMENTAL WORK</u>	91
<u>CHAPTER 4. BENCHMARK GENERATION OF BIO-INSPIRED NEURAL SIGNALS</u>	93
SUMMARY	93
<u>CHAPTER 5. TECHNOLOGICAL DEVELOPMENTS FOR NEUROPHYSIOLOGY</u>	117
SUMMARY	117
5.1 NEUROPHYSIOLOGICAL DEVICE IMPROVEMENTS FOR ANIMAL MODEL EXPERIMENTS: CHRONIC RECORDING IMPLANT AND RECORDING CHAMBER	119

5.2 REAL-TIME FPGA PRE-PROCESSING MODULES	122
5.3 NEURAL STREAMING DEVICE	127
<u>CHAPTER 6. ADAPTIVE OPTOGENETIC STIMULATION TO REDUCE REPETITIVE BEHAVIORS</u>	<u>131</u>
SUMMARY	131
<u>PART III: DISCUSSION AND PERSPECTIVES</u>	<u>157</u>
<u>TABLE OF ABBREVIATIONS</u>	<u>171</u>
<u>TABLE OF ILLUSTRATIONS</u>	<u>173</u>
<u>REFERENCES</u>	<u>175</u>
<u>RESUME EN FRANÇAIS</u>	<u>211</u>

SUMMARY

Summary

For efficient everyday behavior, we rely on habits and routines, i.e. abilities that we have acquired and automatized. As behaviors are repeated in a consistent context, the associative link between the context and the action incrementally increases until, through regular repetition, automaticity of the behavior is established. While the ability to automatize more efficiently might be beneficial, the ridge of healthy repetitive behaviors (RB) is narrow. Indeed, cortico-striatal circuits are affected during various pathological conditions where a dysregulation of the expression of automatized actions, leads to pathological RB. A neuropsychiatric disorder well characterized by pathological RB as a core symptom is obsessive-compulsive disorder (OCD), where repetitions of complex rituals and routines (compulsions) can seriously affect the patient's quality of life. The emergence of pathological RB could result from an overexpression of habitual complex behavioral sequences (compulsions), functions that have been shown to be supported by the cortico-striatal circuits. In this thesis project, we focus on a neurophysiological substrate that is suspected to have a crucial role in the emergence and regulation of RB: the striatal interneuronal network. Indeed, striatal interneurons exert a powerful control over striatal excitability by dynamically controlling the input and output of medium spiny neurons (MSNs). Among those, the inhibitory network of parvalbumin (PV)-immunoreactive interneurons (PVI) form a wide network of feed-forward inhibition onto MSNs and is crucial for the functional regulation of the striatal output networks. A lack of inhibitory PVI control is correlated with increased firing of MSNs in the *SAPAP3-KO* mice, an animal model of compulsive behavior that we used for our studies and that exhibits compulsive self-grooming behavior. Through optogenetic stimulation of PVI in the dorsal medial part of the striatum we were able to effectively prevent compulsive RB and reduce them to normal levels. Moreover, we identified a non-sustained internal electrophysiological pattern in the delta band in the lateral orbitofrontal cortex (lOFC) preceding the emergence of self-grooming. This RB-related preceding activity was used as a biomarker to trigger optogenetic stimulation of the PVI in an online closed-loop approach as a reliable predictive electrophysiological biomarker. On-demand optogenetic stimulation effectively reduced grooming events initializations. In line with our interest in closed loop experimentation, we contributed to the neuroscience toolbox with a series of technical developments that helped us to acquire neural data online and that provide a framework that will be useful for further hard real-time closed loop approaches. Our results helped to understand the biological mechanisms underlying the regulation of RB by proposing that striatal PV-interneurons are essential to regulate the expression of repetitive behaviors. We also provided a new experimental framework for predicting RB that could be used to test other therapeutic targets or hypothesis using a closed-loop approach. Taking together, these results are not only of interest for advancing the understanding of the circuitry behind pathological RB in fundamental research but also of immediate clinical interest for therapeutical purposes regarding RB-related disorders.

PART I: INTRODUCTION

Chapter 1. PHENOMENOLOGY OF REPETITIVE BEHAVIORS

In this this first chapter, I will introduce repetitive behaviors, which can be expressed as a variety of actions, ranging from very simple motor behaviors to extremely complex rituals. I will present their importance in habit formation and how they are necessary for efficient daily life. When repetitive behaviors are over-expressed they become symptoms that characterized a variety of psychiatric disorders. I will also discuss their heterogeneous nature and their phenomenological overlap while focusing on compulsive behavior.

1.1 NORMAL REPETITIVE BEHAVIORS

When introducing repetitive behaviors (RB), intuitively a cluster of broadly associated concepts appear in the same context, such as habits, rituals, routines, mannerisms, and customs. The reason is that repetitive behaviors have multiple connotations and in a general definition they are considered together. Much current work on habit learning in neuroscience has moved apart this broad view (Ann M Graybiel, 2008). From a general perspective, these are sequences of actions in our daily life that we tend to repeat with more less the same frequency, they range from very simple motor behaviors to extremely elaborate rituals, for example washing our hands before cooking or engaging in our morning routines. These actions are so nearly automatic in our life that we execute them without paying too much attention to them and we repeat them regularly. We act according to these behaviors as they take a significant part of our lives. From an intuitive perspective, they can be evaluated as neutral behaviors, desirables or undesirable. It takes time and effort to abolish them. Since these actions take such an essential part in our lives and because of their power over behavior, the motivation for understanding their origins, how to suppress them and create new ones have long fascinated philosophers, psychologist, psychiatrists, ethologists, neuroscientist, and the general population. It comes as no surprise that we can easily find a multitude of podcasts, blogs and even coaching programs suggesting tips and strategies on how to build new habits or how to break them to get positive results and take more control in certain aspects in our lives.

In the literature, we can find different definitions of habits, but most of them agree on two facts, the first is that these are actions that are repeated regularly and the second is that, we rely on these repetitive behaviors, that we have acquired and automatized, to adapt to our environment optimally, these are seen as normal repetitive behaviors. We can break down the characteristics of normal repetitive behaviors in the following points:

- They are characterized by a lack of awareness, unintentionality and the need for a stronger inhibition to prevent its expression.
- Habitual behaviors repeatedly occur throughout days or years, and they can become notably fixed.
- Fully acquired habits are executed automatically allowing attention to be focused elsewhere.
- Habits tend to include an ordered structure of motor actions that are often associated with a context or stimulus.
- Habits can be defined experimentally as being persisted event if the reward value becomes less attractive. They are performed not in relation to a future goal but rather to previous rewarding behavior (Bernard W. Balleine & Dickinson, 1998).

Undoubtedly, RB are an essential part of our lives, not only they are necessary for habit formation but also they seem to be present in normative development. Specific rhythmical, transient stereotyped movements are a normal developmental phenomenon in healthy infants (Rubenstein & Rakic, 2013). These behaviors show great uniformity in form and regularity in a developmental course. RB in normative development include motor behaviors such as swaying, bouncing, waving and flapping in very young children and a variety of repetitive behaviors that reflect ritualization or insistence of sameness (IS) of daily activities in older children (for example, insistence on specific clothing or bedtime rituals). Although these kinds of RB have a peak at 2-3 years, they begin to decline after about age 5 with emerging voluntary motor control (Thelen, 1980). Whereas it is difficult to assign a goal or particular purpose to these behaviors it is hypothesized that these RB are necessary for neuromuscular maturation and as a way to repeat an interesting effect on the environment.

1.1.1 IMPORTANCE OF RB FOR GOAL-DIRECTED TO HABITUAL BEHAVIOR

Regular repetition is a critical factor to habit formation, when behaviors are repeated in a consistent context, the associative relationship between the context and the action increases until, automaticity of the behavior is established, and habits are formed, this means that habits are mostly learned (Ann M Graybiel, 2008). As a consequence of people repeating a behavior in a stable context, their intentions and goals to perform it gradually become less influential and habits become stronger (Carden & Wood, 2018). The studies of habit formation of Dickinson and his collaborators lead to a definition of habits based on reward learning experimentation in rodents. They showed that when actions are performed with some regularity the associations between environmental context and the specific action are strengthened, such that appropriate actions can be more easily accessed in the future, what they called behavioral autonomy (Dickinson, 1985). They showed that in the initial stages of habit learning, behaviors are not automatic, the animal had to work to get a reward, and they are therefore *goal-directed*. Dickinson defined goal-directed behavior as purposeful and nonhabitual actions. After repetition and continued training, animals typically performed the behaviors repeatedly, on cue, even if the reward to be received is reduced or had no longer the same rewarding value, this kind of

operationalized diagnosis of habits is called goal devaluation. Another manipulation for detecting habits is *contingency degradation*, whereby the connection between an action and an outcome is degraded (Robbins & Costa, 2017), an example of goal-directed vs. habitual actions is illustrated in **Figure 1**.

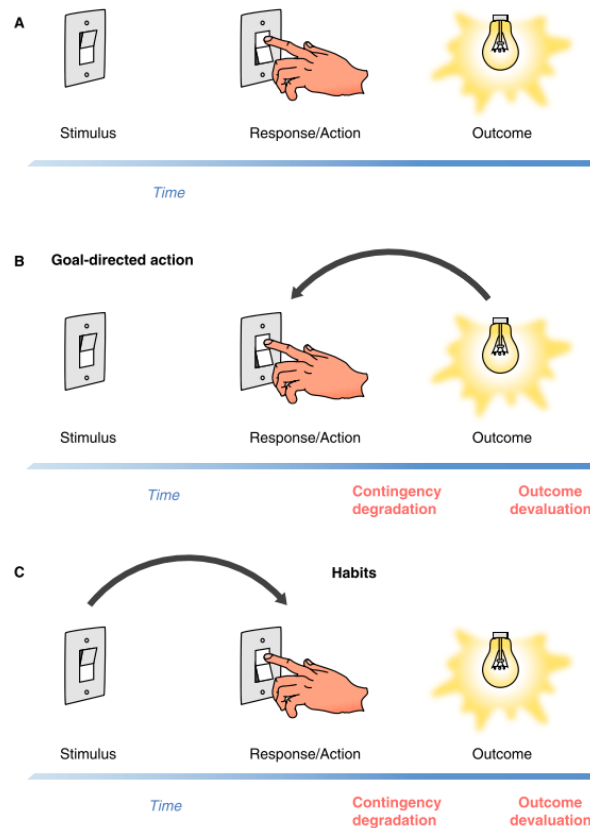


Figure 1 Habits and goal-directed actions. (A) Example of a sequence involving a stimulus (someone sees a light switch), a response or action (flips the light switch) and an outcome (the light comes on). (B) In this example, goal-directed actions are performed in order to obtain a desired outcome, if the outcome becomes less valuable, the action will not be performed (for example, if the room is already well illuminated). In the same way, if the contingency between the action and the outcome is reduced then the action will not be performed; For example, an automatic switch is installed and the light comes on in the absence of the action (contingency degradation). (C) Habits are elicited by previous stimuli and not performed to obtain future outcomes. Therefore, the response (flipping the switch) will be performed upon sight of the switch (stimulus), even if the outcome has been devalued or the relation between action and outcome degraded. Figure from (Robbins & Costa, 2017).

The mechanism of habit formation allows us to automate behaviors that do not require specific planning or organization (Gillan, Robbins, Sahakian, van den Heuvel, & van Wingen, 2016) and is highly dependent on historical information. Because these mechanisms are slow to develop and to modify in comparison to other implicit processes such as classic Pavlovian fear conditioning (Amodio & Ratner, 2011), then again repetition is the primary accelerator of learning and extinction rate.

A collection of neuroscience studies converges on the idea that the neural substrates of both systems, the goal-directed and the habit system may be distinguishable (Dolan & Dayan, 2013). Many of the original discoveries related to the existence of the neural substrates of two relative independent, although interacting, systems for goal-directed

and habitual behaviors which depend on distinct cortical-striatal loops (Anatomical functional organization on Chapter 2). Most evidence points to the notion of the associative cortical-striatal loops and their modulatory inputs to be important for goal-directed behavior, while sensorimotor loops and their modulatory inputs are critical for habit formation (Robbins & Costa, 2017). Indeed, a variety of studies that include brain lesioning, optogenetics, functional and structural imaging points out the importance of the caudate nucleus (anterior caudate nucleus in humans and dorsomedial striatum – DMS- in rodents) and medial orbitofrontal cortex (OFC) for goal-directed control over action and the putamen (posterior lateral putamen in humans and dorsolateral striatum –DLS- in rodents) for the gradual add up of habit formation over time (Bernard W. Balleine & O’Doherty, 2010). The DMS, receiving inputs from associative cortices, is crucial for developing conscious behaviors in response to novel or changing contingencies and environments and is thus pivotal early during learning as well as for the reprogramming of habitual behaviors in case of changing contingencies and environmental conditions. The dorsolateral striatum (DLS) receives input from sensorimotor cortices and becomes increasingly important during the course of learning, when consciously established associations become habits and routines. Moreover, when faced to new contexts or rapid changes in the environment, in isolation, the habit system is not an optimal way to face the situations. There is control over habits given new information by the goal-directed system including the change of eventuality between actions and possible results (for example when we need to adjust the lever to change the temperature in a sink that we have never used before). Indeed, without familiar habit cues, we are forced to make decisions about how to act. Thus, a correct recruitment and dynamic equilibrium of both dorsal striatal regions seems important to develop and execute efficient, adaptive behaviors. Because of the importance of these mechanisms in human behavior, habit research has blossomed over the past few years, in one hand working is being made on how basic cognitive mechanisms (like attention) relate to repetitive behaviors in habit formation and in the other hand on what are the neuro-mechanisms related to habit formation, maintenance and suppression as a way to understand pathologies related to excessive expression of repetitive behaviors.

1.2 PATHOLOGICAL REPETITIVE BEHAVIORS.

When RB are executed excessively often, they become symptoms that characterize a spectrum of neurodevelopmental and neuropsychiatric disorders including obsessive-compulsive disorder (OCD), addiction, eating disorders, schizophrenia, Tourette’s syndrome, autism, and social anxiety disorder. Repetitive behaviors are non-specific symptoms, and they refer to a broad class of actions that are characterized by their increase frequency or repetition, their rigidity or inflexibility and their apparent absence of obvious function (Lewis & Kim, 2009) and historically they have been considered as a marker of psychopathology. The disorders characterized in the compulsive spectrum share similarities in terms of phenomenology, associated features (age of onset, clinical

course, and comorbidity), behavioral treatments and selective pharmacologic take(American-Psychiatric-Association, 2013). There is a different symptomatic phenomenology of RB encountered in stereotypies, tics, compulsions, where RB is a core feature.

1.2.1 HETEROGENEITY IN RB-RELATED DISORDERS

1.2.1.1 STEREOTYPIES

Stereotypies are purposeless, involuntary, patterned, repetitive movements. They are usually rhythmic, continual and tend to change little over time. Examples of stereotypes include head nodding, walking in circles, hand flapping or clapping and facial grimacing, between others. Some may occur with object manipulations, including spinning or twirling items. Unlike tics, stereotypies tend not to change in anatomic location nor complexity over time, and are not preceded by an urge or thought, as is usual with tics or compulsions (Zinner & Mink, 2010). Stereotypies are most commonly associated with Autism spectrum disorder (ASD) and other developmental disabilities, indeed, stereotypies are present in most autistic children.

The category of RB in Autism spectrum disorder (ASD) is broad and heterogeneous, including the inflexible nonfunctional behaviors with high frequency, stereotyped and repetitive motor mannerisms, and desire for sameness in the environment. They are referred to as restricted and repetitive behaviors (RRBs), and according to the DSM-5 they are expressed by at least two of the following: (1) stereotyped or repetitive motor behaviors, use of objects or speech, (2) inflexible adherence to routines or ritualized patterns of verbal or nonverbal behaviors, and (3) high preoccupation with restricted interest. They fall in two clusters: 'lower order' motor actions that are characterized by the repetition of movement (1) and 'high order' behaviors that have a distinct cognitive component (2 and 3)(American-Psychiatric-Association, 2013). RRB in ASD often have a strong sensory component (such as spinning objects), but they do not necessarily include sensory feedback (for example lining up objects). Reports suggest that lower order RRBs are more apparent in younger patients and high order RRBs such as preoccupations, particular interest and obsessions are more often found in older patients. Nevertheless, low order RRBs continue to be seen in high functioning cases (Leekam, Prior, & Uljarevic, 2011; Zandt, Prior, & Kyrios, 2007).

Treatment of stereotypies include pharmacologic and behavioral approaches. Clomipramine (serotonin-norepinephrine reuptake inhibitor –SNRI-), risperidone (dopamine and serotonin antagonist), and fluoxetine (selective serotonin reuptake inhibitor –SSRI-) have been shown to reduce RB in children and adolescents who have autism. These pharmacologic treatments in children are only indicated if stereotypes are causing great discomfort, otherwise behavioral approaches such as habit reversal training (HRT) are preferred(Miller, Singer, Bridges, & Waranch, 2006). Some of these treatments are also used for OCD, which is not surprising since some behaviors shade over into

similar features observed in OCD and can sometimes lead to an additional or alternative OCD diagnosis. It is estimated that around 30-40% of autistic patients are also diagnosed with OCD (Leyfer et al., 2006). Other frequency co-occurring conditions apart from OCD include disorders such as tic disorders, Attention deficit hyperactivity disorder (ADHD), and problems with anxiety and disruptive behavior. Attempts to treat RB in ASD center on the same systems and approaches used in OCD and TS (Lai, Lombardo, & Baron-Cohen, 2013).

1.2.1.2 TICS

Tics are repetitive, non-rhythmic and intermittent muscle contractions resulting in stereotyped movements. When they involve laryngeal-pharyngeal muscles and produce noise, tics are named “vocal”, all other tics are named “motor” tics. Both can be characterized as simple or complex. Simple tics are anatomically isolated, be of brief duration but appear excessive in frequency or/and intensity. Complex tic may mimic a gestural or linguistic purpose, involve several muscle groups and are more sustained in time (Zinner & Mink, 2010). According to the last edition of the Diagnostic and Statistical Manual of Mental Disorders (DSM-5)¹, tic disorders are categorized as neurodevelopmental disorders and include transient tic disorder (with one or more vocal or motor tics that occur for less than 12 months in a row), chronic motor/vocal tics (CMVT) (involves motor or vocal tics, but not both), and Tourette syndrome (TS). RB in tic disorder corresponds to motor tics; stereotyped movements that range from very brief and usually rapid movements, such as eye-blinking, nose-twitching, head-jerking or shoulder-shrugging, to more complex movements, usually performed in the same order, for example, a person might kick out with one leg and then the other. Vocal tics similarly range from simple, such as throat clearing and grunting to more complex, including complete phrases. Moreover, patients might describe a premonitory urge or sensory experience preceding the tic, but no internal experience is necessary to make the diagnosis (Rubenstein & Rakic, 2013). TS patients seem to have impaired habit learning relative to normal controls (Marsh et al., 2004) and some studies showed that TS patients have consistently shown difficulties with fine motor controls, motor inhibition and visual-motor integration (Crawford, Channon, & Robertson, 2005; S. V. Müller et al., 2003; Swain, Scahill, Lombroso, King, & Leckman, 2007).

Regarding treatment, behavioral therapy which includes monitoring of urges and the use of voluntary replacements behaviors has been proven effective in many patients (Piacentini et al., 2010). These include HRT, exposure and response prevention, and comprehensive behavioral intervention (Novotny, Valis, & Klimova, 2018). Medication using antipsychotics (especially dopamine receptor antagonist drugs) tested in TS

¹ The DSM-5 is the 2013 version of the *Diagnostic and Statistical Manual of Mental Disorders*, a taxonomic and diagnostic tool published by the American Psychiatric Association (APA). It is considered as one of the authoritative published works that define and classify mental disorders to homogenize diagnosis, treatments and research.

patients has shown favoring results as well as the use of norepinephrine alpha-2 agonist drugs such as clonidine (Swain et al., 2007). The last treatment option is deep brain stimulation (DBS), reserved for patients who do not respond to behavioral therapy or pharmacotherapy.

Although OCD and tic-related disorders are classified as separate disorders, the overlap between the symptoms of complex motor tics and compulsions associated with OCD is considerable (Franklin, Harrison, & Benavides, 2012). Patients with tic disorders also often present comorbid condition with attention deficit hyperactivity disorder (ADHD). In TS, the first symptoms of OCD appear up to several years after the beginning of tics with maximal severity in late adolescence. And both of these psychiatric comorbidities often persist until adulthood, even during TS remission (Novotny et al., 2018). Apart from repetitive behaviors, tic-related disorders and OCD can also share similar clinical presentations including intrusive sensations and impairment in behavioral inhibition (Lewin, Chang, McCracken, McQueen, & Piacentini, 2010).

1.2.1.3 COMPULSIONS

Compulsions are defined as repetitive behaviors which persist inappropriate to the situation, have no apparent relationship to the targeted goal and often result in undesirable consequences, they can be considered RB or repeated mental acts that are aimed at reducing distress (A Vahabzadeh; CJ McDougle, 2014) according to self-invited rules that must be applied rigidly. Compulsions may persist in repetition without them leading to an actual reward and despite deleterious consequences. The most extensive research work in human compulsivity is conducted in OCD patients. OCD is a common and debilitating neuropsychiatric disorder (A Vahabzadeh; CJ McDougle, 2014). The DSM-5 classifies OCD in the category of obsessive-compulsive and related disorders (that include body dysmorphic disorder, hoarding disorder, and trichotillomania) and no longer in the category of anxiety disorder. The diagnostic criteria of OCD present as core symptoms obsessions and compulsions. Obsessions are mental processes such as thoughts, images or impulses that are undesired, persistent and recurrent causing distress and anxiety. The most commonly encountered obsessions among OCD patients include contamination, a need for symmetry, safety, harm and religious or sexual issues (A Vahabzadeh; CJ McDougle, 2014). These symptom categories all have features of repetitive thoughts and actions, they often appear in a ritualized form and are expressed in relation to internal and external stimuli (E. Burguiere, P. Monteiro, L. Mallet, G. Feng, 2016). Compulsions, as previously described, are typically excessive and often performed within a set of rigid, self-enforced rules. Compulsive behaviors described in patients with OCD include high-order behaviors that reflect inflexibility. Most OCD patients recognize that their concerns are unrealistic and that their behavior is excessive or unreasonable (Edna B. Foa & Kozak, 1995). The severity of compulsions may vary between individuals and so the time spent on their compulsions. As a matter of fact, essential to the diagnosis of OCD is the demonstration that the symptoms result in significant distress and that they may be

excessively time-consuming. Therefore OCD can become a crippling disorder gravely affecting the quality of life of the individuals concerned. Regarding epidemiology, some studies have attempted to estimate the prevalence of OCD in the general population using standardized instruments². The prevalence rates in seven international communities range from 1.9% to 2.5% for lifetime prevalence (Fontenelle, Mendlowicz, & Versiani, 2006; Kessler et al., 2005) and these results were consistent across sites.

Treatment for OCD is usually in a certain degree effective but rarely relieves symptom completely. Cognitive behavioral therapy (CBT), which involved exposure to the triggering stimulus without engaging in compulsive behavior, has been shown to be beneficial in many patients (Franklin, Abramowitz, Kozak, Levitt, & Foa, 2000). Medication including serotonin reuptake inhibitors (SRI's) are considered helpful, particularly when combined with CBT, dopamine receptor D2 antagonist drugs can also be helpful when added to SRI's (Bloch et al., 2006). Medications acting on the glutamate system may also be helpful to treat OCD symptoms (Pittenger, Krystal, & Coric, 2006). Severe cases of OCD have been successfully treated with DBS in the ventral internal capsule/ ventral striatum region (more in Chapter 3).

Compulsive behaviors are the main symptom not only of OCD but also of different groups of neuropsychiatric disorders (**Figure 2**). The DSM5 classifies some of these in the obsessive-compulsive spectrum or in the autism spectrum. Since it is relatively common for OCD patients to be diagnosed with other psychiatric disorders OCD is associated with considerable psychiatric comorbidity (Nestadt et al., 2003). The disorders that are diagnosed more frequently along OCD include tic disorders (Grados et al., 2001), anxiety disorders specially for generalized anxiety disorder, panic disorder and agoraphobia (Nestadt G et al., 2001), Body-Focused Repetitive Behaviors (BDRB) such as trichotillomania, pathologic skin picking and nail-biting, somatoform disorders (such as hypochondriasis and body dysmorphic disorder) and eating disorders (O. Joseph Bienvenu et al., 2000). Important to highlight is that particularly OCD and tic disorders have phenomenological and familial-genetic overlaps. There are several studies (Diniz et al., 2006; Franklin et al., 2012; Grados et al., 2001; Holzer et al., 1994) that reported high rates of tics in OCD patients and they are reported to be more frequent in adults and children with OCD than in the general population. Additionally, one study reported that patients with OCD and CMVT presented more severe OCD than patients with OCD plus TS or patients with OCD alone (Diniz et al., 2006) and that the presence of repeating behaviors well characterizes this comorbidity. At least two studies are suggesting that hoarding and somatic obsessions are more associated with OCD plus Tourette's syndrome than in those with OCD-CMVT. Consequently, clinical decision-making with respect to treatment recommendations can be challenging.

² These studies include the Diagnostic Interview Schedule (DIS; Robins et al., 1981, 1985), the Composite International Diagnostic Instrument (CIDI; Robins et al., 1988a,b), the Schedule for Affective Disorders and Schizophrenia (SADS; Endicott and Spitzer, 1978) and the Clinical Interview Schedule-Revised (CIS-R; Lewis et al., 1992).

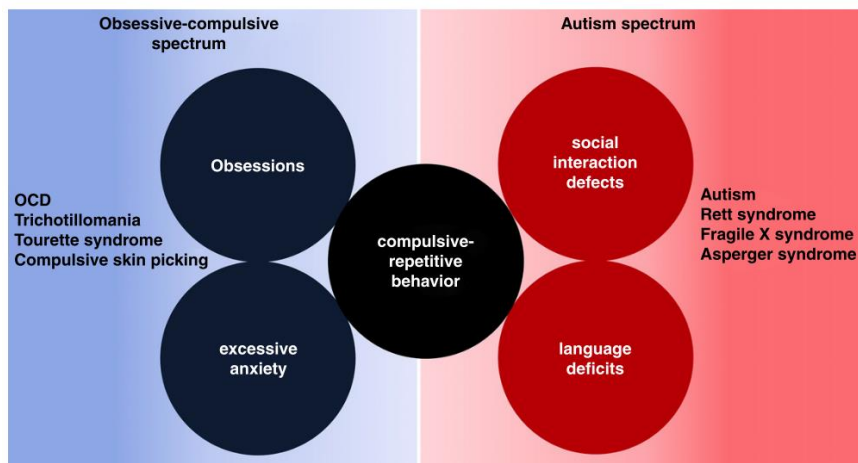


Figure 2. Compulsive repetitive behavior as a core feature shared between obsessive-compulsive (OC) and autism spectrum disorders. Specific features in the OC spectrum disorder include obsession and anxiety whereas social interaction defects and language deficits are specific features of autism spectrum disorders. Figure from (Ting & Feng, 2011)

1.2.2 COMPULSIVE BEHAVIOR AND HABITS

There is no doubt that habits take an important part in human life, their dominance over behavior has been hypothesized to manifest when the stimulus-response link become very strong, or/and by a diminution of goal-directed control over action (a reduction in of the ability to take control over habits) (Gillan et al., 2016). There is a significant interest in investigating the role of habits in human compulsivity, especially in the case of OCD. One hypothesis suggested that habit biases in OCD patients could be explained by a selective deficit in goal-directed control over the action. Another point of view indicates that compulsions result from failure of habitual inhibition in motor and non-motor domains (Jahanshahi, Obeso, Rothwell, & Obeso, 2015). Specifically, there is an interest to reveal if compulsivity could result from deficits in goal-directed control or an excessive build-up of stimulus-response habits (Gillan et al., 2014). A series of human studies showed that OCD patients had a shift in balance away from goal-directed control and towards habits (Gillan et al., 2011). OCD patients showed a deficit in their ability to take control over Stimulus-Response behavior considering the change in the value of outcomes (Gillan et al., 2014; Voon et al., 2015), which means that patients, compared to controls, were more likely to continue to perform an action even though this action no longer served its original purpose. For instance, Gillan and colleagues demonstrated with a goal devaluation procedure (**Figure 3**) that OCD patients had greater avoidance habits than control subjects, and these habits were associated with a subjective urge to respond. In this study the authors suggested that excessive habit formation may be a contributor reflected in compulsivity in OCD (Gillan et al., 2014).

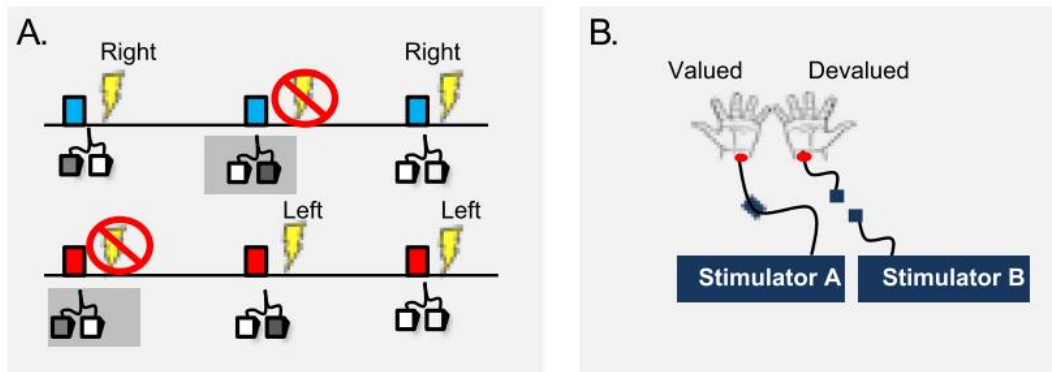


Figure 3. Goal devaluation procedure to test if OCD patients have a bias toward habits. (A) The blue stimulus predicts a right shock and the red one a left shock. If the correct avoidance response is executed on time, subjects avoid shock (left pedal to avoid left shock). In this shock avoidance task, habits were induced through overtraining which were identified using goal devaluation. **(B)** In the devaluation procedure the electrodes on one side are disconnected (devaluated) while the electrodes on the other side are unchanged (valued). Figure from (Gillan et al., 2011)

Habits have become a popular model of compulsivity, in part because how relatively well characterized are the supportive processes at the neurobiological level. Indeed, there is evidence of a neurobiological overlap regarding neural substrates of habit formation and the pathophysiology of OCD (discussed in Chapter 2). Notably, emerging evidence points to the striatum as a critical structure involved to the establishment of ritualized sequences of actions (Barnes, Kubota, Hu, Jin, & Graybiel, 2005; Ann M Graybiel, 2008; Yin et al., 2009). Given the number and diversity of disorders related to repetitive behaviors (RB), the obvious question arises as to whether they share a common etiology. The disorders mentioned before, share high frequency of comorbidity, symptom domains and associated mechanisms, resulting in overlapping diagnostic criteria. Concerning cognitive correlates, deficits in executive function³ are often reported in individuals with persistent RB (Benzina, Mallet, Burguiere, N'Diaye, & Pelissolo, 2000). Although the etiology and pathophysiology of compulsive related disorders are still under investigation, converging evidence from functional neuroimaging studies, analysis of the lesions that result in for example OCD and the observations regarding neurosurgical interventions that can improve compulsive symptoms implicate the prefrontal cortical-striatal circuits in its pathogenesis. These circuits appear to be involved in habit formation and repetitive behaviors and will be explained in the next Chapter.

³ Executive function refers to a broad category of cognitive processes involved in the planning and execution of flexible and goal directed behavior.

MAIN POINT SUMMARY

- For optimal everyday life, we rely on habits, i.e., actions that we have acquired and automatized. In order to obtain a specific outcome, the activity of a goal-directed system drives us to maintain certain behaviors. After repetition of this goal-directed behavior, a shift to the habit mediating system allows us to optimize our behavior for greater efficiency.
- When over-expressed, RB can become symptoms that characterized some neuropsychiatric disorders such as OCD, TS, and ASD.
- RB-related neuropsychiatric disorders have high rates of comorbidity, and are often diagnosed together in the same patient.
- It has been proposed that compulsive behavior may result from dysfunction in the goal-directed system, increasing the dependence on the habitual responding system.

Chapter 2. NEUROPHYSIOLOGY OF COMPULSIVE BEHAVIOR

This chapter aims to review the neurobiological mechanisms that are involved in compulsive behaviors, highlighting the role of the cortical-basal ganglia circuitry and its importance as a putative doorstep to be used in a symptom preventing strategy. Here I summarize the anatomical-functional organization of the basal ganglia, and review the data implicating the cortico-basal ganglia circuits in a variety of compulsive-related disorders including OCD. The center of the attention will be the striatum with a particular interest in its different functional domains and its microcircuitry in the context of compulsive symptoms. This chapter includes a small review of the animal model studies related to compulsive behaviors and the relevance of rodent self-grooming behavior for translational research.

2.1 THE ANATOMICAL-FUNCTIONAL ORGANIZATION OF THE BASAL GANGLIA

To understand the underlying neural correlates of pathologies involving compulsive behavior, it is necessary to know how the cortico-basal-ganglia-thalamocortical loops (CBGTC) are engaged in the normal sensorimotor function. Indeed, to make advances in understanding the clinical aspects of RB, investigators have been studying the basic brain circuits that underlie habit formation and internally guided motor control. Progress has been made particularly studying the multisynaptic neural loops that link the cerebral cortex with several subcortical regions. Research into the underlying mechanisms of RB has focused on microcircuits and the role of different cell types, especially interneurons, suggesting that the same neural cell-types are likely to underlie the emergence of pathological RB in a range of disorders.

The basal ganglia (BG) is a group of forebrain nuclei that is present in all vertebrates, and that interconnects with neural systems that affect behavior such as the cerebral cortex, the thalamus, and the brainstem. At the beginning of the '90s the BG was assigned a role in motor function, and the cortex more a cognitive role. Now we know that the role of the BG is more elaborate than that, it also plays an essential role in many other cognitive functions such as decision-making (B. W. Balleine, Delgado, & Hikosaka, 2007) or learning (Hélie, Ell, & Ashby, 2015). The anatomy of the BG is complex, not to mention that the terminology has changed over the years. Several component nuclei compose the BG at various levels in the brain, and two of them (the globus pallidus (GP) and the substantia nigra (SN)) are divided into anatomically (in terms of connectivity) different elements. The BG include the striatum, the subthalamic nucleus (STN), the globus pallidus (internal segment (GPi), external segment (GPe), and ventral pallidum), and the substantia nigra (pars compacta (SNc) and pars reticulata (SNr)) (**Figure 4**). The ventral BG consists of the

nucleus accumbens, the ventral pallidum and the medial parts of the STN and SN and is primarily involved with limbic or emotional functions, while the dorsal aspect is primarily involved in motor and associative functions (J. M. Tepper, Abercrombie, & Bolam, 2007).

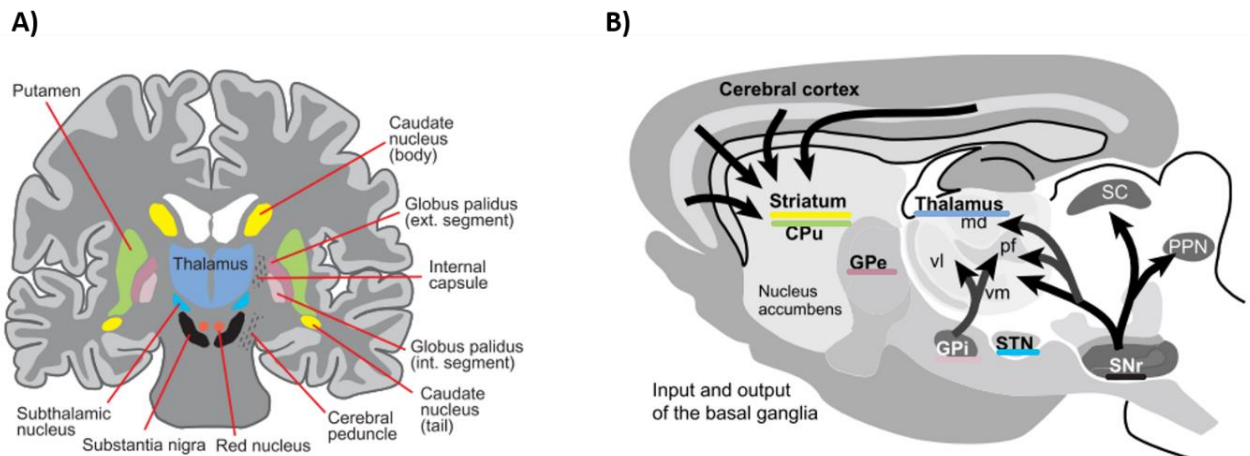


Figure 4. Location of basal ganglia nuclei in the human and rat brain. (A) Diagram of a coronal section of the human brain. Figure from (Squire, Larry; Berg, Darwin; Bloom, Floyd; du Lac, Sascha; Ghosh, Anirvan; Spitzer, 2008). **(B)** Black arrows show the primary input and output connections of the basal ganglia on a sagittal diagram of the rat brain. Figure modified from (Gerfen & Bolam, 2010).

The striatum and the STN are primary receivers of information from outside the basal ganglia. Most of those inputs are excitatory cortical inputs, but thalamic nuclei also provide a broad spectrum of inputs to the striatum. The cortical input uses glutamate as a neurotransmitter and terminates mostly on the heads of the dendritic spines of spiny projection neurons (SPNs). Distinct cortical input can overlap to the same local regions within the striatum (Flaherty & Graybiel, 2013) and inputs from a single cortical region project to multiple striatal zones. The information received is then processed by the BG circuitry through different pathways, generating output to frontal lobe and brain stem areas that are involved in the planning and execution of movements. The basal ganglia output (GPi and SNr) is inhibitory and projects to motor areas in the brain stem and thalamus; thus an increase in the BG outputs leads to a reduction in the activity of its targets. The fact that the BG output is inhibitory to thalamocortical and brainstem targets are relevant to understand its normal motor function. The spinal or brainstem sensory or motor systems do not project directly to the basal ganglia, and there are no direct outputs from BG to spinal motor circuitry. The GPi and the SNr are the primary inhibitory outputs to thalamic nuclei and brain stem.

2.1.1 STRUCTURE

The striatum is in the forebrain and includes the caudate nucleus, the putamen (CPu) and nucleus accumbens. It is named striatum because the axons fibers that pass through it give it a striped appearance. It sends inhibitory projections to the BG output nuclei, the GPi, and the SNr (**Figure 5**). The striatum is one of the regions that is densely innervated by cortical afferents. It is a crucial region for motor programming, habit formation, and social behavior(Hélie et al., 2015). The striatum does not have a highly organized structure like the cortex or the hippocampus but it does present a functional segregation (section 2.1.3). It is compartmentalized on an overall level in the dorsal and ventral striatum and neurochemically into the matrix/ striosome system (A. M. Graybiel & Ragsdale, 1978).

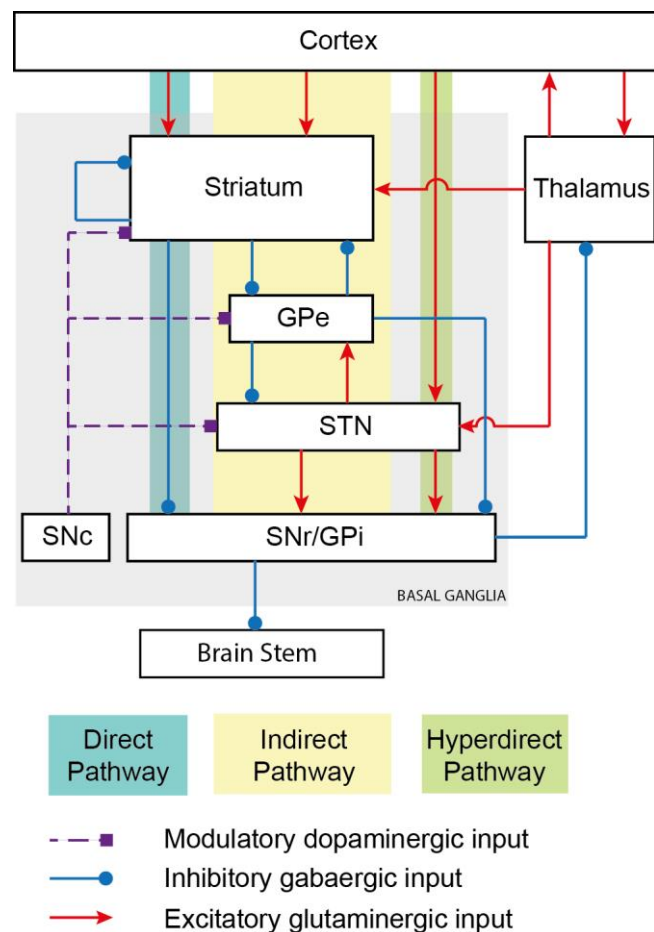


Figure 5. A simplified view of the basal ganglia circuitry showing the direct, indirect and hyperdirect pathways. Glutamatergic inputs are represented in red, gabaergic in blue and dopaminergic in violet. Figure modified from (Fino & Venance, 2010)

The external segment of the pallidum (GPe) is a relatively large nucleus located caudomedial to the striatum(Hitoshi Kita, 2007)(H. Kita & Jaeger, 2017). GPe together with the SNc can be viewed as a central nuclei of the BG because they both receive inputs from BG and send outputs to other BG nuclei. GPe receives excitatory projections from the

STN and inhibitory projections from the striatum (GABA and enkephalin). It projects in the majority to the STN, and there is an inhibitory GABAergic monosynaptic output directly to GPi and SNr and a GABAergic projection back to the striatum (Squire et al., 2008). This organization means that GPe's neurons can provide feedback inhibition to the striatum and STN, but also feed-forward inhibition to neurons in GPi and SNr, suggesting that the GPe may act to restrain the effect of the striatum and STN projections to the GPi and SNr.

The globus pallidus internal segment (GPi) is the primary BG output for limb movements. Indeed, the GPi has large neurons that project outside the BG. Most of these outputs sent via collaterals to the thalamus and the brain stem. The principal inputs to GPi come from inhibitory neurons projecting from the striatum and the STN, indeed GPi cells have dendrites that can span up to 1 mm in diameter allowing them to receive many converging inputs (Squire et al., 2008). GPi and the substantia nigra pars reticulata (SNr) are rather similar since they both receive inputs from the GPe, striatum and subthalamic nucleus, they both project to the cerebral cortex through the thalamus, and are separated by dense fiber bundles of the internal capsule. The GPi has strong interactions with motor cortices and is believed to control somato-motor behaviors. On the other hand the SNr has interactions with the prefrontal cortex and is considered to control associative functions (Nambu, 2007).

The substantia nigra pars reticulata (SNr) is the segment of the SN that is more sparsely cellular (compared to the SNc). Like the GPi, the SNr contains large neurons that project outside the BG (Squire et al., 2008). It receives inhibitory inputs from the striatum, and excitatory inputs from the STN. It provides inhibitory outputs to the thalamus (ventrolateral and ventral anterior thalamus). These thalamic areas in turn project to the premotor and prefrontal cortex (Deniau, Maily, Maurice, & Charpier, 2007).

The substantia nigra pars compacta (SNc) contains large DA-containing cells, DA neurons contain a substance called neuromelanin which gives a dark pigmentation to the SNc therefore it gets its name "substantia nigra" (Squire et al., 2008). SNc receives input from the striatum a sparse input from the prefrontal cortex. In return, the SNc DA neurons project to the CPU in a topographic organization. Nigral DA neurons receive inputs from one striatal circuit and project back to the same or adjacent circuit, modulating activity across circuits (Haber, Fudge, & McFarland, 2000). The action of the DA cells depends on the receptors located on target neurons.

The subthalamic nucleus (STN) has been considered as an important modulator of the BG output. It receives major excitatory glutamatergic inputs from the frontal cortex with significant contribution from motor areas (frontal lobe only) especially from the motor, premotor and supplementary motor cortex and from the frontal eye field. It also receives inhibitory inputs from the GPe. The STN projects to both segments of the globus pallidus (GPi and GPe) and the SNr. Its outputs are excitatory and is essentially composed of projection glutamatergic neurons (Hamani, Saint-Cyr, Fraser, Kaplitt, & Lozano, 2004).

Most details of the neuroanatomical organization of the basal ganglia circuits come from rodent studies. The most notable differences between primates and rodents are the anatomy of the basal ganglia nuclei. The striatum in primates is subdivided into the caudate nucleus and putamen by the internal capsule. This separation results in functional segregation in which we can distinguish that the caudate nucleus is mainly the target of prefrontal cortical inputs and that the putamen is the target of motor and somatosensory inputs. However, the internal capsule is not a strict divider of functional regions, and there is some overlap of prefrontal cortex's inputs to the putamen (Gerfen & Bolam, 2010). In the rodent, we can still find striatum's regional differences that are comparable to those of primate's and that are determined by the distribution of cortical inputs. In primates, the internal segment of the globus pallidus is adjacent to the external segment, in rodents the equivalent nucleus is known as the entopeduncular nucleus is separated from the GPe and embedded in the fiber tract of the internal capsule (**Figure 4-B**). Despite these differences, the major connective organization of the basal ganglia in rodents and primates is highly similar.

The basal ganglia participate in control movement and behavior. Indeed the most substantial portion of basal ganglia inputs and outputs relate to motor areas. In the history of basal ganglia study, it has been shown that basal ganglia lesions cause severe movement anomalies. In addition to its essential role in motor control, the basal ganglia have an essential role in cognitive function. A considerable portion of the cortical areas provides inputs to the basal ganglia, which reciprocally provide outputs to brain systems involved in the generation of behavior (Gerfen & Bolam, 2010). Indeed, frontal cortical areas involved in the planning and execution of movement behavior provide direct projections to the spinal cord that are responsible for the generation of movement, and the cerebral cortex and its connection to the basal ganglia are known to influence or affect behavior. Activity in the basal ganglia does not cause movement directly. Instead, it influences activity in other brain regions like the motor cortex that affects movement. This motor execution has been hypothesized to be via different circuits in the basal ganglia that promote and inhibit movement respectively. Following a top-down description, these neural circuits continue from cortical areas and pass through the basal ganglia through the direct, indirect or hyper direct pathways with a final projection through the thalamus.

2.1.2 BASAL GANGLIA TRIPLE-CIRCUIT MODEL

The direct and indirect basal ganglia pathways have, via glutamatergic and GABAergic neurotransmission, opposing actions on the thalamus and therefore on the frontal cortex. They appear to work oppositely to modulate the thalamic and cortical activation. Activation of the direct pathway projections to the GPi and SNr exerts a powerful inhibition effect over these regions that in return relieves the inhibitory brake on the thalamus. The thalamus then sends glutamatergic projections that activate the frontal cortex. In contrast, the indirect pathway results in the inhibition of the thalamus and the frontal cortex. Activating the indirect pathway results in inhibition of the GPe which produces decreased inhibition on the subthalamic nucleus, which increases its excitation

over the GPi/SNr. When this occurs, the GPi/SNr then increases its inhibitory drive over the thalamus, resulting in a reduced glutamatergic output to the frontal cortex (Rapanelli, Frick, & Pittenger, 2017). The hyperdirect pathway is the pathway from cerebral cortex to STN, which in turn sends outputs to the GPi and SNr. This pathway passes on powerful excitation effects from motor-related cortical areas to the pallidum, bypassing the striatum, and therefore having shorter conduction time than the direct and indirect pathways (Squire et al., 2008). Nambu and colleagues baptized it the hyperdirect pathway precisely because it is the fastest route for information flow from cerebral cortex to the basal ganglia output (**Figure 5**). A simplified center-model of the BG to control voluntary limb movements that include these three pathways would start when a voluntary movement is about to be initiated by cortical mechanisms. The hyperdirect pathway would first inhibit large areas of the thalamus and cerebral cortex that are involved in the selected motor program and other competing programs, this, because it is the fastest route for information flow from the cortex of the BG output. Then disinhibition of specific targets and release of the selected motor program would be possible via an intervention through the direct pathway. Finally, the indirect pathway would allow extensive inhibition of their targets (Nambu, Tokuno, & Takada, 2002). This is a simplified sequential view of information processing where only the selected motor program would be initiated and executed at specific timing whereas other competing programs are canceled.

2.1.3 FUNCTIONAL SEGREGATION OF THE CORTICO-BASAL GANGLIA LOOPS

A general organization plan of the CBGTC is represented in **Figure 6**. The components of this system include the prefrontal cortex, the striatum (composed of the caudate and the putamen) and the thalamus. Cortical and striatal circuits are integrated in various ways. Starting from a broad perspective, CSTC circuits are functionally distinct neural “loops” originating from cortical regions and these regions are as well the site of feedback projections from the thalamus. In these circuits, the striatum does not have direct reciprocal projections to cortical regions, instead, its effects are indirect as they are sent back to the cortex through thalamic projections.

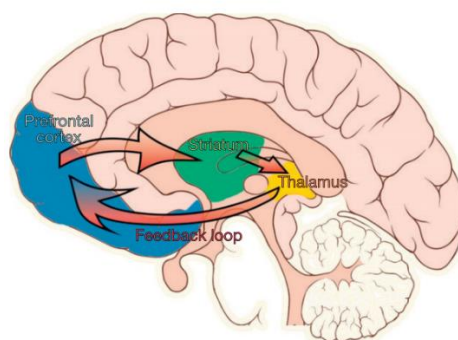


Figure 6. A simplified representation of a CSTC circuit in a sagittal view of the human brain. Figure from (A Vahabzadeh; CJ McDougle, 2014)

The view on the BG has changed over the years from being principally motor-based to include the cognitive and emotional domains. In addition to the BG involvement in the expression of behaviors through movement, the BG is also involved in the process that leads to movement such as the elements that drive actions, including motivation, cognition, and emotions (Haber, 2016). The first models were “box and arrow” models that considered each nucleus of the basal ganglia as a unique and homogeneous structure (a box) that communicates with one or several nuclei by connections characterized either as excitatory or inhibitory (the arrows) (Albin, Young, & Penney, 1989). Nowadays we know this view to be more complicated than that, the basal ganglia not only connect to motor areas of the cortex (motor cortex, supplementary motor cortex, premotor cortex, cingulate motor area, and frontal eye fields) but also to more cognitive associated areas, with converging properties at several levels (Yelnik, 2008). An alternative model of the basal ganglia organization is the five-circuit model proposed by Alexander and DeLong (G E Alexander, M R DeLong, 1986; Mahlon R. DeLong & Thomas Wichmann, 2007) (**Figure 7**). In this model, the cortical projections from the frontal cortex comprise five different circuits: one limbic, two associative, and two motor circuits. It comprises, an oculomotor circuit with origins in the frontal eye field, a motor circuit originating in the frontal supplementary motor area, two associative circuits originating in the dorsolateral prefrontal cortex (DLC) and the lateral orbitofrontal cortex (IOFC), and one limbic circuit originating in the anterior cingulate cortex. Within each of these circuits, there are the indirect and direct pathways, both projecting to the thalamus (Jeffrey L. Cummings, 1993) and sharing the common structures described. In the five circuit model, the cortical projections to the striatum arise only from the frontal cortex, whereas the other cortices (temporal, parietal and occipital) are not integrated into this model.

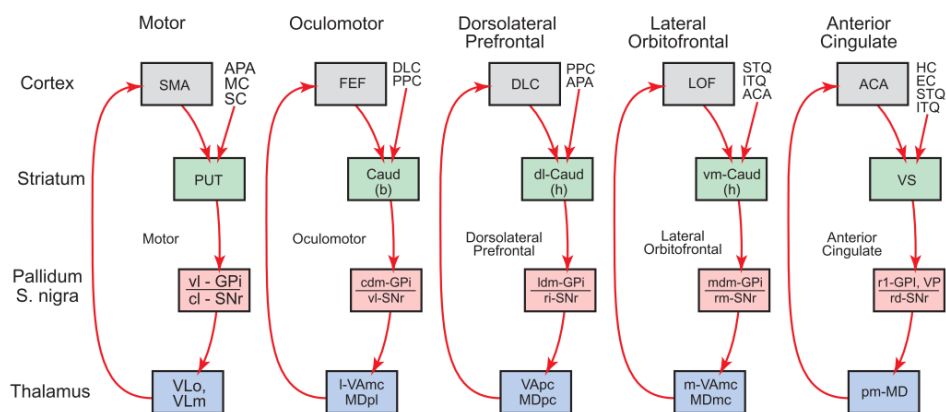


Figure 7. The five circuit model of the BG. It includes parallel circuits connecting the basal ganglia, thalamus and cerebral cortex. ACA, anterior cingulate area; APA, arcuate premotor area; CAUD, caudate; b, body; h, head; DLC, dorsolateral prefrontal cortex; EC, entorhinal cortex; FEF, frontal eye fields; GPI, internal segment of globus pallidus; HC, hippocampal cortex; ITG, inferior temporal gyrus; LOF, lateral orbitofrontal cortex; MC, motor cortex; MDpl, medialis dorsalis pars paralamellaris; MDme, medialis dorsalis pars magnocellularis; MDpc, medialis dorsalis pars parvocellularis; PPC, posterior parietal cortex; PUT, putamen; SC, somatosensory cortex; SMA, supplementary motor area; SNr, substantia nigra pars reticulata; STG, superior temporal gyrus; VAmc, ventralis anterior pars magnocellularis; Vapc, ventralis anterior pars parvocellularis; VLm, ventralis lateralis pars medialis; VLo, ventralis lateralis pars oralis; VP, ventral pallidum; VS, ventral striatum; cl, caudolateral; cdm, caudal dorsomedial; dl, dorsolateral; d1, lateral; 1 dm, lateral dorsomedial; m, medial; mdm, medial dorsomedial; pm, posteromedial; rd, rostrorodorsal; rl, rostromedial; rm, rostromedial; vm, ventromedial; vl, ventrolateral. Figure from (Squire et al., 2008)

Since the entire cerebral cortex projects to the basal ganglia (Yelnik, 2008) there is a more global subdivision of cortical activity including three functional territories (**Figure 8**) (Parent, 1990). Indeed, the five circuit model can be simplified into three circuits when the motor and oculomotor pathways are grouped into one motor pathway, and the DLC and IOFC are grouped into one cognitive/associative circuit, leaving the limbic circuit involving the projections from the ACC (Squire et al., 2008). These subdivisions take into account the fact that terminals from the cortex in the striatum are organized in a topographic manner (**Figure 8**). The sensorimotor territory in the dorsolateral part, the limbic territory in the ventromedial part and the associative territory in the central intermediate part of the striatum. Nevertheless, when terminals from various cortical regions are examined closely, there is a convergence of inputs from different functional regions (Jahanshahi et al., 2015). In a more detailed manner, the sensorimotor territory includes the primary motor, the somesthetic cortices, the premotor cortex, supplementary motor area, and the oculomotor areas. It processes motor and somesthetic information. Following the somatotopic organization, the dorsolateral striatum is therefore linked to motor function. This projections were some of the first to be identified (McFarland & Haber, 2000) and supported by physiological studies demonstrating somatotopic maps and neural responses to specific movements (Kimura, 1986). The associative (or sometimes called cognitive) territory includes the prefrontal dorsolateral and lateral orbitofrontal cortices as well as the parietal, temporal and occipital cortices. It processes cognitive information such as the ability to attend external stimuli or internal motivation, to identify the significance of such stimuli, and to plan meaningful responses to them (Purves et al., 2001). The limbic (or sometimes called emotional) territory comprises the hippocampus, the anterior cingulate and medial orbitofrontal cortices. It processes emotional and motivational information. These three functional regions can be mapped in the striatal regions according to the received cortical inputs.

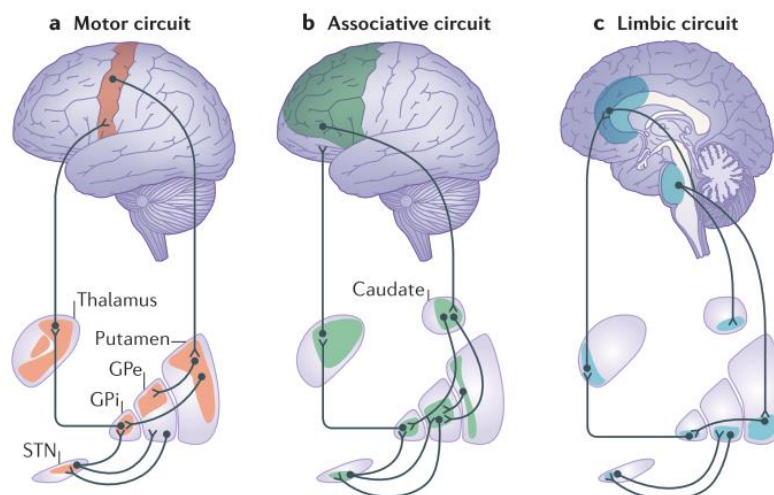


Figure 8. Principal functional subdivisions in the cortico-basal ganglia circuits within the human brain. These include (a) the motor loop, (b) the associative loop and (c) the limbic circuit sensorimotor. Figure from (Jahanshahi et al., 2015) and the original figure from (Jose A. Obeso et al., 2009).

The pattern of cortical inputs helps to define the corresponding striatal regions between humans and rodents (**Figure 9**). The human dorsolateral putamen and dorsolateral caudate (sensorimotor territory) correspond to the lateral portion of the dorsal striatum in rodents. The large parts of the rostral putamen and most of the head, body and tail of the caudate (associative territory) correspond to the medial portion of the dorsal striatum in rodents. The ventral striatum in humans comprises the nucleus accumbens (NAc) and ventral parts of the caudate and putamen (the limbic territory). In rodents the ventral striatum corresponds to the NAc and the striatal portion of the olfactory tubercle. In rodents the NAc is subdivided into core and shell regions with different connectivity and function, while this division is not clear in primates (Chuhma, Mingote, Kalmbach, Yetnikoff, & Rayport, 2017).

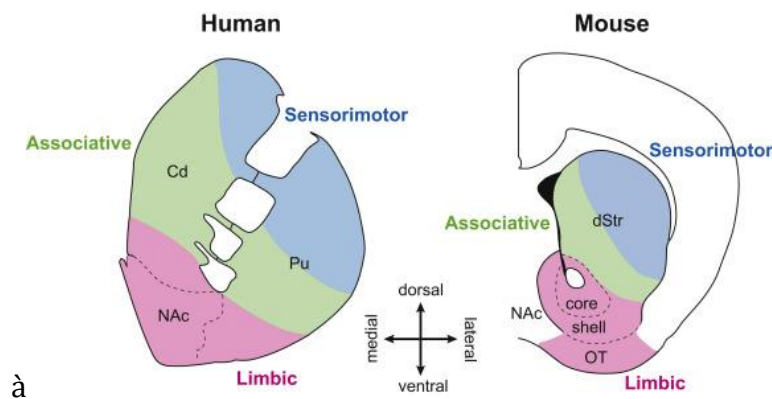


Figure 9. Striatal functional subdivisions between humans and mice. The homologous functional territories in the striatum in humans and rodents can be determined by cortical inputs mediating each function. (Cd: caudate, Pu: putamen, NAc: nucleus accumbens, dStr: dorsal striatum, OT: olfactory tubercle). Figure from (Chuhma et al., 2017).

Interesting to add is that the basal ganglia has unique integrative properties, it seems to have beautifully evolved to optimally receive a great sample of three specific functional aspects of cortical information. These characteristics include its anatomical volume configuration, the number of neurons at different levels and the geometry of its projections (**Figure 10**). First, the volumes of the successive nuclei that each circuit cross decrease in proportions (the subthalamic nucleus is 3000 times smaller than the emitting cortex). Because of volume and cell density, the number of neurons in each nucleus also decreases (subthalamic nucleus neurons are 4000 times fewer than in cortex). Third, the pallidal dendritic arborizations are arranged perpendicularly to striatal afferent axons, maximizing the number of possible connections (Yelnik, 2008).

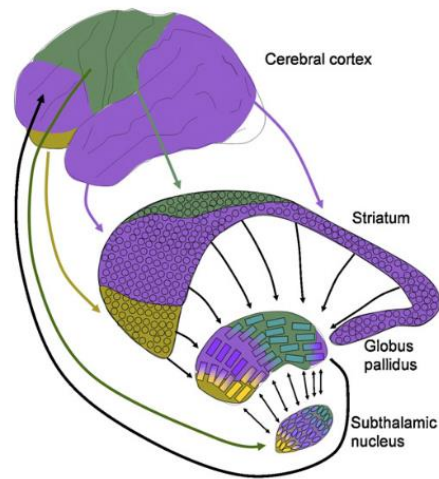


Figure 10. Schematic representation of the integrative properties of the basal ganglia. The basal ganglia receive overlapping information from three functional territories of the cerebral cortex. Volume and cell density decrease in each level. In the globus pallidus, even if neurons are fewer than in the striatum, their flattened and large dendritic arborizations make transmission of striatal information onto pallidal neurons highly converging. In the subthalamic nucleus, information comes not only from the three functional territories but also directly from motor cortices, which makes it a convergence node in the circuit. Figure from (Yelnik, 2008).

Within the associative territory, the existence of a lateral orbitofrontal loop was proposed, involving projections from the orbitofrontal cortex (OFC) to the head of the caudate and ventral striatum, following to the mediodorsal thalamus via the internal pallidus and finally returning to the OFC. From an anatomical perspective, the OFC is a prefrontal brain area with an abundance of reciprocal connections to other brain structures, including the striatum, amygdala and cingulate cortex. The OFC is a focus center for sensory inputs of all five traditionally recognized senses (gustatory, auditory, olfactory, somatosensory and visual). It is composed of several functionally distinct areas that make it highly heterogeneous. So, what exactly is its role? Evidence from lesion studies in animals and humans suggest that the OFC has a crucial role in the emotional and motivational aspects of behavior. Patients with orbitofrontal lesions show behavioral changes related to inappropriate affect, poor decision-making and disinhibition (Namiki et al., 2008). Moreover, functional imaging studies showed that the OFC has a role in monitoring changes in reward value (including anticipation of expected rewards and the probability that rewards will occur) (Gorka, Phan, & Shankman, 2015). Further work dissociate medial and lateral regions of the OFC into different functions, with the lateral OFC (lOFC) being likely to be activated when a response (previously associated with a reward) has to be suppressed, indicating that the lOFC may play an inhibitory role (Elliott, Frith, & Dolan, 1997). In coherence with these findings, orbitofrontal lesions in animals and humans lead to reward-related learning deficits in tasks such as reversal learning⁴ and this could be reflected in inability to detect changes in the motivational value of stimuli and to then modify behavior accordingly (Rudebeck & Murray, 2009) Therefore the OFC is known to

⁴ In a reversal learning task the individual first learns to make a discrimination and then is supposed to learn to reverse its choice. It is useful to study the process of learning to inhibit previously rewarded actions.

be implicated in decision-making, response inhibition, sensory integration, emotional operations, and learning. The utility of investigating the cortical function in the segregated view of the frontal-subcortical circuits has its value as a unifying framework for understanding human behavioral disorders. Indeed, a wide range of behavioral alterations, including OCD can be linked to dysfunction of frontal-subcortical circuits. For example, animal and human imaging studies have shown that behavior controlled by a goal-directed system and a habitual system are mediated via the associative and motor circuits respectively (Bernard W. Balleine & O'Doherty, 2010).

2.2 THE MICROCIRCUITRY OF THE STRIATUM

The striatum is strategically located in the forebrain, it receives inputs from all cortical areas and has an essential role in processing convergent inputs through different pathways. It plays a central role in motor learning, motor control and cognitive process such as decision making in motivated behaviors. The most abundant and studied neuron in the striatum is the medium spiny projection neuron (SPN, but found in the literature also as MSN) because they are the primary and only output neurons of the striatum. Nevertheless, recent studies have shown that striatal interneurons, even though being very few, may play a dominant role for the regulation of the striatal microcircuitry. In this section, we review the basic neurocytology and micro circuitry of the striatum with a focus on parvalbumin-positive interneurons.

2.2.1 MEDIUM SPINY PROJECTION NEURONS

The first and by far most numerous neuron in the striatum is the medium spiny projection neuron (MSN). They make up as much as 80-95% of the total number of striatal neurons, depending on the species (Kemp & Powell, 1971). They are homogeneously distributed in the striatum, and they constitute the output of the striatum via axonal projections to the GP and SN, so they can be categorized as either striatopallidal (indirect pathway) or striatonigral (direct pathway). Cortical input to the striatum targets mainly MSNs through monosynaptic contact, making them the major input target and the major output neuron of the striatum. MSNs have also local axon collaterals within the striatum that form synapses with other spiny neurons (Somogyi, Bolam, & Smith, 1981) (**Figure 11**). In terms of morphology they have large dendritic trees that stretch over 200-500 μm from the cell body of origin (Wilson, 1980), this property makes them perfect receivers from adjacent projections coming from multiple areas of the cortex. They have a cell body of approximately 12-20 μm and from this cell bodies expand 7-10 dendrites that are moderately branched but densely charged with spines.

Besides cortical inputs that make contact primarily with the head of dendritic spines, MSNs receive inputs from a number of afferents from outside the striatum and from within (**Figure 11**), specifically: (1) Inhibitory GABA inputs from small striatal interneurons. This correspond to a subpopulation that is positive for the calcium-binding protein parvalbumin (H. Kita, Kosaka, & Heizmann, 1990). (2) Cholinergic inputs from large aspiny neurons (striatal interneurons). (3) Inhibitory GABA, neuropeptide substance P and enkephalin inputs from adjacent MSNs. (4) A broad input from dopamine (DA) neurons from the SNc and VTA. Five type of G protein DA receptors have been found (D1-D5) and they are classified into two families based on their response to agonist; D1 family (D1 and D5 receptors) increase the effect of cortical input to striatal neurons and D2 family (D2,D3,D4 receptors) have the opposite effect. (5) Glutamatergic excitatory inputs from the thalamus (intralaminar and ventrolateral nuclei). These form asymmetric synaptic contacts and have strong excitatory effects on the MSNs. Regarding cortical

inputs to the striatum, the first quantitative study in rats showed that of all cortical terminals within the striatum about 90% are contacted with dendritic spines, 5% with dendritic shafts and 5% with the soma (Z. C. Xu, Wilson, & Emson, 1989).

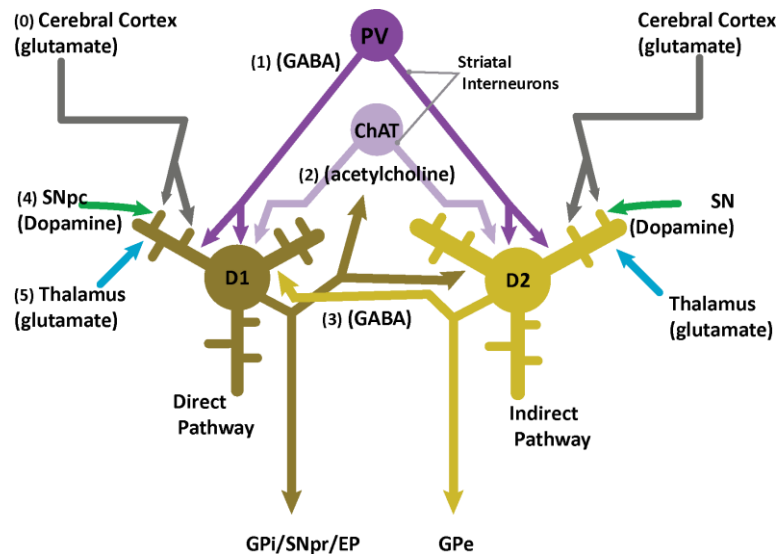


Figure 11. Organization of synaptic afferences on a medium spiny neuron. Figure modified from (Gerfen & Bolam, 2010)

MSNs utilize the inhibitory gamma-Aminobutyric acid (GABA⁵) as a neurotransmitter and have colocalized peptide neurotransmitters. The MSNs are morphologically indistinguishable but chemically heterogeneous, indeed based on their neurotransmitters and type of DA receptors MSNs can be divided into two groups. The first group is a population that contains GABA, substance P and dynorphin and expresses D1 receptors, they project to the SNr and GPi. The second group is a population that contains GABA and the neuropeptide enkephalin and expresses D2 receptors, they are inhibitory and project to the GPe. Nevertheless, approximately 6% of MSNs in the dorsal striatum express both D1 and D2 receptors. These cells produce both GABA and glutamate, allowing presumably to modulate the BG in a bidirectional manner (Perreault, Fan, Alijaniaram, O'Dowd, & George, 2012).

Although there is no evident regional sectioning in the striatum based on cell morphology, in 1978 Ann Graybiel and colleagues showed that when striatum is stained through different immunohistochemical techniques, including staining for acetyl-cholinesterase (AChE), there are clusters in form of patch distribution that protrude more (**Figure 12**). The AChE-poor areas are called striosomes, they send output to the SNc, and the rich areas are called the extrastriosomal matrix and send output to the GP and SNr (A. M. Graybiel &

⁵ GABA is a neurotransmitter used by at least 40% of inhibitory synapses in the mammalian mature brain (Bowery & Smart, 2006) its principal role is reducing neural excitability throughout the nervous system.

Ragsdale, 1978). Within this matrix there are clusters of neurons that receive similar inputs called matrixomes.

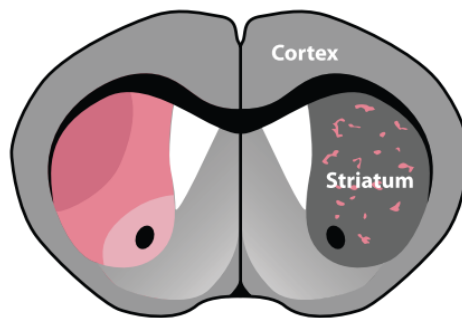


Figure 12. Functional organization of the rodent striatum. Representation of a coronal schematic of the mouse forebrain where striatal patches (pink) are illustrated in the right hemisphere, and the dorsolateral, dorsomedial, and ventral divisions of the striatum are illustrated in the left hemisphere. Figure from (Kreitzer, 2009)

2.2.2 STRIATAL INTERNEURONS

The remaining striatal neurons are interneurons and represent 5% (or less) of the striatal population (Kemp & Powell, 1971). They do not provide axonal projections outside the striatum. Instead they provide axonal projections within, much of which involves synaptic contact with MSNs. In the DMS action initiation or suppression is thought to be triggered by MSNs through coordinated complex activity (Tecuapetla et al., 2016) where MSNs are subjected to strong modulation by ChAT or PV interneurons (**Figure 11**). Despite being few in numbers, striatal interneurons are diverse regarding neurochemical and morphological categories. Two major subtypes are identified: (1) the first one is the large aspiny neurons that use acetylcholine (Ach) as a neurotransmitter. (2) The second one is the medium aspiny GABAergic interneurons of which diverge into different varieties. These inhibitory interneurons are more common in primates than in rodents and play an important role in regulating the medium spiny output neurons (Squire, Larry; Berg, Darwin; Bloom, Floyd; du Lac, Sascha; Ghosh, Anirvan; Spitzer, 2008).

Compared to other brain areas, the striatum contains high levels of Ach, and the principal source of striatal Ach are the large aspiny cholinergic interneurons, which comprises a small portion of striatal cells (about 1-2 %)(Lim, Kang, & McGehee, 2014). Nevertheless, large aspiny cholinergic neurons are large sized cells with cell bodies that go up to (>15 μm) in diameter. They have long aspiny dendrites which split into secondary or tertiary branches, covering an area of over 1mm. Their axon is extremely fine and covers an extensive area (as much as 2mm) (Gerfen & Bolam, 2010). They display a tonic firing rate of 3-10 Hz and their discharge seems not related to movement. One of the two electrophysiological well-characterized striatal interneuron groups are the tonically active neurons (TANs) which are presumably cholinergic interneurons, and the other group is the fast-spiking interneurons (FSIs) presumably PV expressing GABAergic interneurons. These tonically active neurons are not active by electrical stimulation of the GP, they seem to fire with sensory stimuli related to reward (Pisani et al., 2001). TANs are

thought to be large aspiny interneurons that drive MSNs. Apart from MSNs approximately 4% of striatal neurons are GABA-ergic interneurons. These are locally projecting inhibitory cells, and can be classified in three types: (1) approximately 0.7% are parvalbumin-expressing fast-spiking interneurons (PVI/ FSIs) , 0.5% NPY/SOM/NOS expressing low-threshold spiking interneurons and 0.6% are calretinin-expressing low-threshold calcium spike interneurons(Kawaguchi, 1993; James M. Tepper, Tecuapetla, Koós, & Ibáñez-Sandoval, 2010).

2.2.2.1 FOCUS ON PARVALBUMIN-IMMUNOREACTIVE NEURONS

An important subset of striatal neurons are the fast spiking GABAergic inhibitory interneurons that show to be immunolabelled positively to the calcium-binding protein parvalbumin. They are the PV+ interneurons (PVI) and are the most abundant type of GABAergic interneurons. Still, in terms of numbers, estimates of the number of PVI from stereological counting suggest that in the rat striatum only 0.7% are actually PVI (Rymar, Sasseville, Luk, & Sadikot, 2004). These interneurons represent such a small number of cells in the striatum that *in-vivo* recordings with multiple identified GABAergic interneurons are relative rare. In terms of morphology, PVI seem to be a heterogeneous cell population in the striatum. Most PV+ striatal interneurons are classified as medium-sized neurons, although a small subset has been described to be as large as cholinergic interneurons (Bennett & Bolam, 1994) (**Figure 13-C**). (Kawaguchi, 1993) described two distinct sets of PVI, one that has a medium size soma and more compact axonal and dendritic fields, and another set that has larger somatic diameter, axonal and dendritic fields. Some studies reported that PVI have between five and eight aspiny dendrites that can be almost smooth to extremely varicose(Hitoshi Kita, 1993). Their dendritic branching is compact and rather spherical, extending around 200-300 μm in diameter around the soma (**Figure 13-A**). There is however a small fraction of PVI that exhibit more elongated dendritic field(Kawaguchi, 1993; James M. Tepper et al., 2010) (**Figure 13-B**). In contrast, PVI's axon is highly branched and extends beyond the dendritic field. Between the striatal cells, it has one of the densest axonal arborizations. It is roughly spherical/ovoid and spreads about 1.5 to 2 times the diameter of the dendritic field(Kawaguchi, 1993). Although they are distributed along the striatum, PVI are more frequent in the dorsolateral region and display a ventral to dorsal, and caudal to rostral gradient of augmenting density(Luk & Sadikot, 2001). These observations of PVI enriched more in the DLS have been observed in 1-2 month old animals and maintained in adult animals (Fino, Vandecasteele, Perez, Saudou, & Venance, 2018) (**Figure 14**).

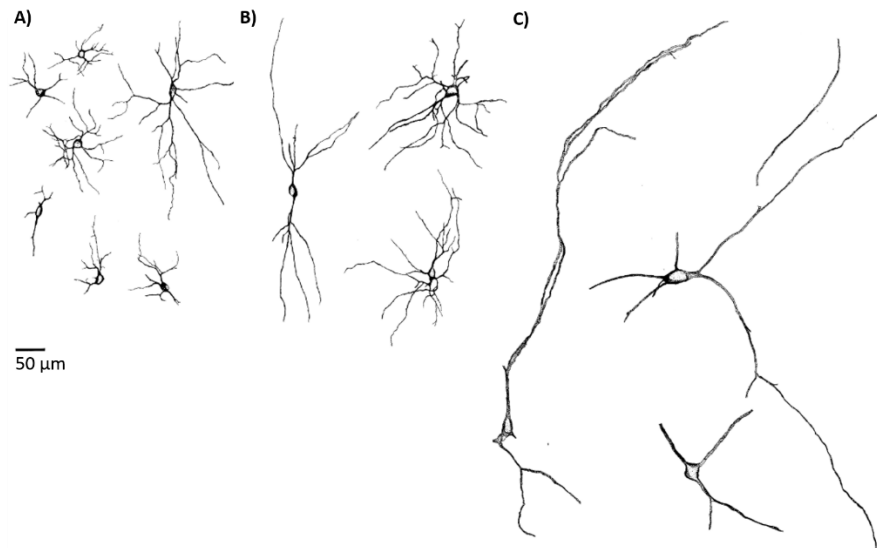


Figure 13. Heterogeneity in PVI morphology. (A)-(B) Drawings reconstructing different striatal parvalbumin-immunoreactive interneurons studied in isolated slices from juvenile rats. Two categories were found according to the dendritic fields: (A) PVI with local dendritic field and (B) PVI with extended dendritic field. Dendrites and axons are separated for each category for easier comparison. Figure taken from (Kawaguchi, 1993). (C) Drawings reconstructing giant PVIs found in the caudate-putamen of primates. Figure taken from (Bennett & Bolam, 1994).

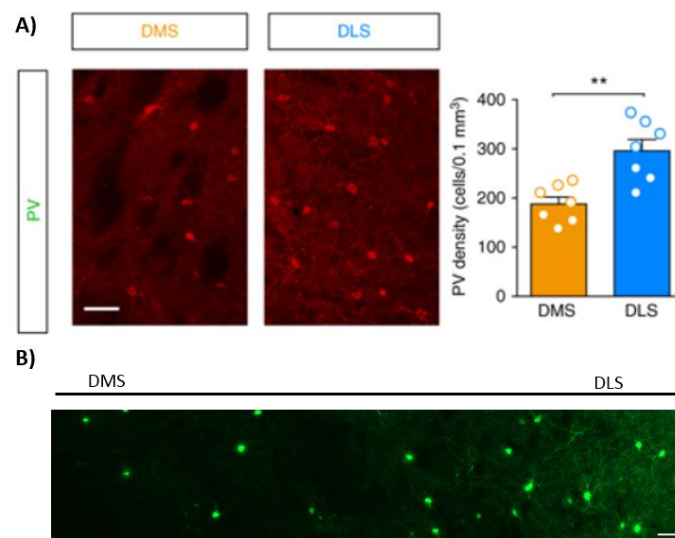


Figure 14. Gradient distribution of striatal PVI. (A) Anatomical distribution of PVI in DMS and DLS from confocal microscopy images ($n=7$ mice). Image taken from (Fino et al., 2018). (B) Gradient density of striatal PVI (unpublished image from Christiane Schreiweis/Oriana Lavielle). Scale bar for both figures is $50\mu\text{m}$.

Kawaguchi and colleagues not only described and categorized them morphologically, they were also the first to identify their electrophysiological characteristics using sliced from juvenile rats (Kawaguchi, 1993). Striatal PVIs display a unique electrophysiological signature that allow us to identify them with confidence based on intracellular or whole cell recordings *in vitro* and *in vivo*. They are called fast-spiking interneurons (FSI) because of their high firing frequency; it has been showed *in vitro*, that in response to strong depolarization currents they can fire at frequencies over 400 Hz. Indeed PVI are highly sensitive to depolarizing input. *In vitro* studies using current injection showed that PVIs

cannot sustain repetitive firing at low frequencies, instead it is necessary a tiny increment in stimulus (10 pA above threshold) to make the PVI firing at its minimal sustainable frequency typically exceeding 20 Hz (**Figure 15-A-B**) meaning that PVI have non-linear spiking response to intracellular depolarization . Action potentials induced by depolarizing current injection are of short duration (<0.5 ms), they show rapid onset and short duration after hyperpolarization (**Figure 15-C**). They are strongly hyperpolarized *in vitro* and do not exhibit spontaneous activity. PVIs have low input resistance, short duration action potentials, abrupt repetitive firing and they show a low input resistance similar to that of MSNs (50-150 M Ω) (James M. Tepper et al., 2010).

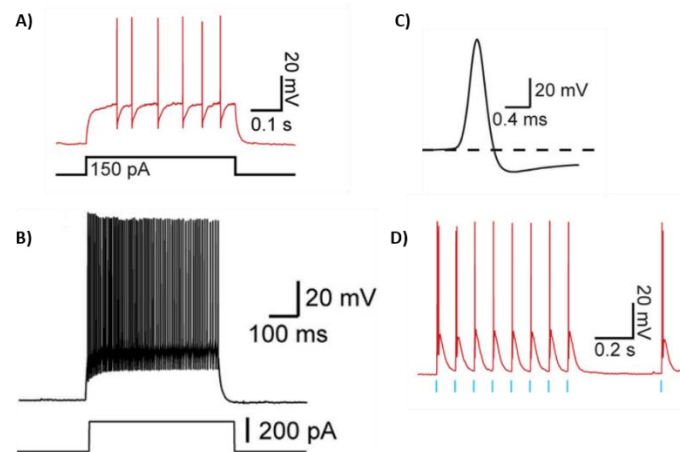


Figure 15. Electrophysiological properties of striatal FSIs recorded in vitro. (A) Typical firing response of a FSI to a suprathreshold step current injection, note that (B) a stronger pulse induce continuous firing at higher frequency with little spike frequency adaptation. (C) Illustrates the brief duration of the FSI action potential. (D) Show the response of a striatal PVI to optogenetic manipulation using a train of light pulses (10 Hz, 2ms width). (Figures A,D were taken from (Szydlowski et al., 2013) and figures B,C were taken from (James M. Tepper et al., 2010)

Putative FSI have been identified in-vivo in unanesthetized behaving rats. Tetrode recordings captured a population of neurons that were tonically active and with average firing rates of 5-30 Hz spikes/s with narrow duration waveforms and that during slow wave sleep displayed high frequency bursts. These putative FSI were more active when the rats were awake and freely moving (Berke, 2008). Indeed, striatal FSI and MSNs can be distinguished from electrophysiological recordings *in-vivo* based on the width or shape of the waveform, interspike interval and average firing rates (Friend, Kemere, & Kravitz, 2015). For example, MSNs typically fire in bursts separated by periods of rest and maintain average firing rates that are inferior to 5 Hz, while FSI generally fire approximately between 10-30 Hz and present a characteristic narrow waveform (Berke, 2008).

FSIs receive inputs from the cerebral cortex, thalamus and globus pallidus and they preferentially make synapses with the soma and dendrites of MSNs. (H. Kita et al., 1990).

PVI have both symmetric and asymmetric synapses⁶ that contact their dendrites and soma. On the one hand, the symmetric synapses arise from dopaminergic and GABAergic extrinsic and intrinsic inputs. On the other hand, most afferents from asymmetric synapses (approximately two-thirds) originate from the cortex with few synaptic inputs from the thalamus (Hitoshi Kita, 1993) having one single cortical neuron making multiple contacts with PVI (Ramanathan, Hanley, Deniau, & Paul, 2002) and having individual PVI receiving synaptic inputs from axon terminals originating from motor and somatosensory cortical regions. The fact that PVI receive multiple connections with single cortical axons suggest that PVI might need less synchronized or/and weaker cortical inputs to be activated than that required to activate MSNs, making them more responsive to coherent cortical inputs. Indeed, Parthasarathy and Graybiel showed in an early study that weak levels of corticostriatal stimulation failed to activate a large number of MSNs but in the contrary was able to induce activation in PVI. Only a stronger and synchronic cortical activity was able to break through inhibition and activate MSNs within the PVI inhibitory field (Parthasarathy & Graybiel, 1997). In terms of connections with other cells, striatal PVI were observed to form dendro-dendritic gap junctions with other PVIs (H. Kita et al., 1990) but not with other cholinergic or low threshold spiking interneurons (James M. Tepper et al., 2010). Striatal PVI are interconnected by electrotonic synapses and although the coupling ratio is usually not strong enough to induce spiking, it is powerful enough to have as consequence evoked spikes in electrotonically coupled FSI via intracellular depolarization and therefore have almost firing synchronicity due to the effects of the coupling (J. M. Tepper & Koós, 2017) (**Figure 16**). This is a very interesting observation as it suggests that groups of FSI may form an inhibitory grouped entity capable of exerting powerful enhanced synchronous control over large number of MSNs with temporal specificity. This phenomenon would influence PVI spike trains forming entities of cells with behavioral relevant functions and could explain why such a small number of cells in the striatum could be enough to exert control over MSNs. This electrotonic coupling between pairs of PVI has also been observed in PVI of the cortex and the hippocampus (Freund & Buzsáki, 1998; Galarreta & Hestrin, 2002).

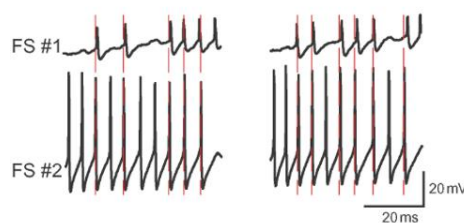


Figure 16. Synchronous spiking induced by electrotonic coupling of two FSIs. Figure from (J. M. Tepper & Koós, 2017)

⁶ Asymmetric synapses are characterized by rounded vesicles in the presynaptic cell, and a prominent postsynaptic density, they are typically excitatory. Symmetric synapses in contrast have flattened or elongated vesicles, and do not contain a prominent postsynaptic density, they are typically inhibitory.

PVI are likely to play an important role in regulating the role of MSNs. Synapses between striatal PVI and MSNs are strong enough to block or delay spiking in postsynaptic MSNs. They are unidirectional from the interneuron to the spiny cell but never in the other direction. Studies in mouse slices showed that the probability of a synaptic connection between an FSI and a MSN within the radius of the PVI axonal field is extremely high, ranging from 48-75% (Gittis et al., 2011; Planert, Szydlowski, Hjorth, Grillner, & Silberberg, 2010). Striatal FSIs make synapses with MSNs on both direct and indirect pathway, and often a single FSI makes synapses with both types (Gittis, Nelson, Thwin, Palop, & Kreitzer, 2010). Using transgenic and viral approaches it is possible to selectively express, for example, channelrhodopsin 2 (ChR2) to FSIs to study them within the striatal microcircuit. (Szydlowski et al., 2013) used transgenic PV-Cre mice and targeted ChR2 to PVIs in the mouse striatum and showed from slice preparations that FSI form a feedforward inhibitory circuit that inhibits MSN while avoiding cholinergic interneurons. They showed that FSI responded to light pulses with strong and immediate polarization causing action potentials in most cases (**Figure 15-D**). It is also possible to recruit striatal FSI from cortical inputs to the striatum as shown by Eric Burguière and colleagues (Burguière, Monteiro, Feng, & Graybiel, 2013b). Indeed, corticostriatal projections recruit striatal PVI to regulate MSN function. This evidence leads us to ask what the behavioral consequences of PVI dysfunction in the striatum could be and what could cause these abnormalities.

A few studies have looked at PVI cell populations in patients that suffer from RB-related disorders. (Kalanithi et al., 2005) investigated postmortem basal ganglia tissue from individuals with TS and compared to normal controls through unbiased stereological techniques. This study demonstrated a consistent PVI imbalance in the BG of the three patients examined but no changes were detected in the density of MSN projections. Statistically significant decreases in PVI density were detected, 51% in the caudate and 37% in the putamen of TS patients. Another study with more postmortem brains of TS patients also showed a 50-60% decrease in PVI in the caudate and in the putamen (Kataoka et al., 2010). They didn't find a statistically relation with decrease PVI numbers and patient's diagnosis or a particular striatal region, suggesting that PVI were equally diminished in the whole striatum. They also didn't find significant differences in the densities of MSNs and or in medium-sized calretinin positive interneurons. Confirmation from animal studies show also the implication of PVI deficits related to abnormal RB. The *dt^{sz}* hamster model (Löscher et al., 1989) shows several features observed in paroxysmal dystonia and in TS such as facial contortions, motor disturbances such as co-contractions of opposing muscle groups and a similar age course. This animal model has also reduction a reduction of 41% in striatal PV (Gernert, Hamann, Bennay, Lo, & Richter, 2000). In a causal recent study, Pittenger's group reduced in normal adult mice approximatively the same proportion of PVI than what was reported in previously postmortem TS studies (M. Xu, Li, & Pittenger, 2016). They used a transgenic-viral cell ablation approach to reduce bilaterally in the striatum the number of PVI. They obtained a very interesting result; the ablation of PVI produced increased RB such as stereotypic

grooming (quantified in two stress protocols) and increased anxiety-like behavior a phenotype that has also been described in animal models of compulsive-like behaviors such as the *SAPAP3-KO* (more about this animal model in the next section). In the contrary, they did not observe spontaneous stereotypies or tic-like movements nor alterations in motor learning or in impulse inhibition. In a later study, it was showed that depletion of conjoint cholinergic interneurons and PVI produced behavioral abnormalities in male mice, such as marked deficit in social interaction and stereotypies in males, in the contrary this phenomenon was not replicated in female mice (Rapanelli, Frick, Xu, et al., 2017).

2.3 NEUROPHYSIOLOGY OF COMPULSIVE BEHAVIOR

In order to create new effective approaches of treatment for RB-related disorders a clear understanding of the underlying physiopathology and neural circuits involved is required. From this perspective, the center of attention of many studies is the disruption of the cortico-striatal-thalamo-cortical (CSTC) circuits. For instance, in 2012 Milad and Rauch (Milad & Rauch, 2012) proposed three parallel segregated circuits that are important for compulsive behaviors. The pathways that link selected areas of the cortex and the basal ganglia have been hypothesized to be implicated in the expression of repetitive behaviors. Indeed, the circuits arising from the OFC, the DLPFC and the ACC are of interest for the study of compulsive behavior. These circuits have different primary functions; the OFC circuit being responsible for context-related processing and response inhibition, the DLPFC circuit involved in working memory⁷ and the ACC being accountable for emotion and reward processing. In the context of compulsivity, the study of the OFC circuit is of special interest because besides being associated in detecting salience and motivational value of stimuli, it has an important role in inhibitory control. Dysfunction of the lateral OFC–centromedial striatum circuit is associated with the loss of the ability to inhibit stimulus–response associations. When this circuit is disinhibited, urges of compulsive behaviors are triggered (Jahanshahi et al., 2015). This theory is supported by evidence in OCD patients using functional magnetic resonance imaging (fMRI) and positron-emission tomography (PET)(Menzies et al., 2008). Particularly, imaging studies showed a hyperactivity of the OFC-caudate circuit that is increased by compulsive symptom provocation (McGuire et al., 1994; Milad & Rauch, 2012; S. L. Rauch et al., 1994; Simon, Kaufmann, Müsch, Kischkel, & Kathmann, 2010). Activity in these regions was elevated at rest and accentuated during exposition to compulsive triggers. Normalization of neural activity has been observed following treatments that include psychopharmacological, behavioral and psychosurgical (Saxena & Rauch, 2000a). An early study PET study (S. L. Rauch et al., 1994), made the explicit distinction between lateral OFC and medial OFC dysfunction; it was suggested that compulsive symptoms

⁷ Working memory is a central concept in neuroscience, it refers to a cognitive system responsible for holding temporally information for further processing. It is important for logic thinking and decision-making.

were positively correlated with glucose metabolic rates in the IOFC and negative correlated with mOFC. This was confirmed with fMRI studies that reported positive correlations between hyperactivity of the IOFC and symptom provocation (Adler et al., 2000; Breiter et al., 1996). Additionally; it was shown that the degree of IOFC hyperactivity prior to therapy could predict the degree of treatment-refractoriness, in this study it was compared to serotonergic reuptake inhibitors (SRIs⁸) treatment; the greater the magnitude of IOFC hyperactivity, the more inefficient the response to treatment (S. Rauch, 2002). Furthermore, fMRI studies have shown that when required to inhibit responding, OCD patients showed under activation of a circuitry that included the OFC (Roth et al., 2007), meaning that there is a negative correlation between symptom severity and inhibition-related activity of the OFC. In terms of morphology, volumetric differences of the putamen and caudate between OCD patients and healthy controls have been reported (Atmaca, Yildirim, Ozdemir, Tezcan, & Kursad Poyraz, 2007; Pujol et al., 2004), but these results have not been accordant. Moreover, meta-analysis (Rotge et al., 2009) haven't found clear volumetric differences in striatal grey matter in OCD patients.

OCD is not the only psychiatric disorder in which abnormalities in corticostriatal circuits are common. Other RB-related disorders such as in TS and ASD present abnormalities in corticostriatal circuits. Additionally to the difference in PVI densities in TS previously mentioned, brain imaging studies in patients suffering from TS have shown aberrant hyper connectivity between the cortical regions and the striatum (Worbe et al., 2015). Abnormal structural organization and volumes in the corticostriatal circuitry have also been seen in TS patients (Greene, Williams, Koller, Schlaggar, & Black, 2017; Müller-Vahl et al., 2014). Patients with ASD have also showed an increase in the growth rate of striatal structures, this change was associated with one particular cluster of RB: insistence on sameness (Langen et al., 2014). Additionally to changes in striatal growth, ratio and shape alterations in the striatum have been shown (Schuetze et al., 2016) in ASD patients. This evidence points to RB-related disorders sharing a dysfunction or imbalance in the corticostriatal circuits, and although the etiology might not be the same for all the disorders the compromised circuits are overlapping. In this sense, patients diagnosed with one RB-related disorder might be also diagnosed with a secondary RB-related disorder, for instance comorbidity between TS, OCD and ADHD is common. Even though human patient studies have offered insights into the dysfunction of the corticostriatal circuits, we cannot decode the precise molecular or cellular mechanisms altered in patients due to ethical and technological limitations. For this purpose, multiple animal models based on clinical and genetic data have been developed to provide a closer investigation into the pathophysiology of these disorders. This is the subject of the next section.

⁸ It has been proposed that SRIs might enhance serotonergic transmission within OFC and consecutively modulating GABAergic tone within the region

2.4 ANIMAL MODELS OF COMPULSIVE BEHAVIOR

As explained in Chapter 1, although a great effort has been put in the characterization of compulsive related disorders through imaging studies in humans, there is a need to understand more precisely the neurobiological basis of this deficit. One way to do so is through animal models of compulsivity where one can for example, causally test the relationship between the activity in a given brain region and the compulsive behavior. The Cambridge Dictionary and the Oxford Dictionary define a model as a “representation of something that can be used to tell what is likely to happen if particular facts are considered as true” and “simplified description of a system to assist calculations and predictions” respectively. As defined, a model is a simplified representation of something, and regarding animal models in psychiatry, a model represents only a part of the disorder being modeled.

Animal models of psychiatric disorders imitate symptoms; they allow us to investigate underlying mechanisms of the disorder, to conduct preclinical treatment evaluations and to test specific theories regarding the causation of the disorder(Szechtman et al., 2017). There is a clear interest in developing animal models to better explain the genetics, the neurochemical and the neuroanatomical causes of this compulsive-related disorders. In the more applied aspect of research, their use is capital in developing new pharmacological and neurosurgical treatments that would improve the likely course of the disorder. To picture the clear interest and importance of the use of animal models of compulsive behaviors let us take the case of OCD, a disorder for which compulsive behaviors are the characteristic symptoms and for which there is a lifetime prevalence of 2.3 of patients not responding to currently available therapies(Kessler et al., 2005). An ideal model of OCD would imitate both types of characteristic symptoms; obsessions and compulsions. Obsessions in patients are subjective clinical features accessed by verbal and sometimes written communication, while compulsive behaviors can be evaluated without dialog. OCD animal models are models of compulsive behavior for which the repetitive actions are observable. Even though the given simplification, the growing area of research using animal models of OCD has provided interesting convergence into brain circuits and neurotransmitters in the behavioral dimension of this disorder(Szechtman et al., 2017).

Invasive techniques in animal models of compulsive behavior are a crucial necessity to accelerate advances in this field and to eventually provide therapeutic relief to patients. In this perspective, three criteria are typically used to assess the potential of a given animal model(Chang et al., 2017): 1) construct validity, 2) face validity and 3) predictive validity. Construct validity is how well the mechanism used to induce the disease phenotype in animals reflects the currently pathology studied. It takes sense in the context of genetics models where a putative gene is manipulated to observe its behavioral and neurobiological consequences. Regarding compulsive behavior research, the most important criterion is face validity which is defined as how well a model replicates the

disorder. In this case, it is usually based on observable equivalent behaviors of compulsive human behavior. The most commonly observed rodent behavior that support face validity is excessive grooming(Chang et al., 2017). Indeed, excessive grooming behavior correspond to the well characterized increase in a behavior that follows a complex stereotyped pattern of actions (more on section 2.4.3). Predictive validity is defined as how well a model can be used to predict currently unknown aspects of the disease. In the case of compulsive behavior this would include reaction to medications, what we can learn from invasive treatments, such as capsulotomy or tests for brain-stimulation protocols(Pinhal et al., 2018). These characteristics that can be evaluated in an particular animal model help to assess the strength of the model and eventually can help to dissect the human population that it models(Chang et al., 2017).

2.4.1 CURRENT ANIMAL MODELS OF COMPULSIVE BEHAVIOR

Decades of research with different functional brain imaging technologies have converged on the cortico-basal ganglia circuits as a key pathway involved in compulsive behaviors particularly observing hyperactivity of the orbitofrontal-subcortical loops caused by an imbalance of activity in these pathways(Saxena & Rauch, 2000b). Such studies provided a useful framework to test hypothesis on the mechanisms of circuitry dysfunction related to compulsive behavior. To test such hypothesis, invasive procedures are sometimes necessary and require various manipulations to investigate deep brain regions in human patients at the cellular and molecular level. Nevertheless, such procedures include ethical issues concerning human experimentation. Translational *in-vivo* research is therefore necessary, especially when trying to dissect the neurobiological basis of psychiatric disorders related to compulsive behaviors where observable behavior is a key factor of interpretation.

In this perspective, animal models of compulsive behavior have been an important focus of research. Several mouse models have been proposed using genetic, pharmacological and optogenetics tools (Table 1). Animal models of repetitive behaviors in humans are categorized into three classes(Lewis & Kim, 2009): (1) animal models that exhibit compulsive-like behavior induced by administration of pharmacological agents or other artificial techniques such as optogenetics or cell ablation, (2) animals exposed to specific environments and/or training or that reveal naturally repetitive or stereotypic behaviors (3) animal models with targeted dysregulation in the central nervous system, these are genetic animal models.

Table 1. Overview of the most common animal models of compulsive behavior. Animal models of compulsive behaviors are classified in three categories depending on the techniques applied to obtain them. The table presents a short description of each animal model, as well as a note on the construct, face and predictive validity of each model.

	Animal model	Short description		Studies
Pharmacological induced and alternative models	8-OH-DPAT	A serotonin 5-HT1A receptor agonist	Perseverative behavior in the T-maze and open arena. Chronic fluoxetine prevents this behavior. No compulsive response in humans in response to 5-HT1A agonist.	C:+ F:++ P:+ (Dek, van den Hout, Engelhard, Giele, & Cath, 2015) (Alkhatib, Dvorkin-Gheva, & Szechtman, 2013)
	Quinpirole	A D2/3 receptor agonist	Perseverative exploration and ritual-like motor behaviors (compulsive checking). High frequency stimulation of the STN and nucleus accumbens reduced the induced checking. SRI treatment delayed the checking behavior.	C:+ F:++ P:+ (Szechtman, Sulis, & Eilam, 1998)
	RU24969	A serotonin 5-HT1B receptor agonist	Similar drugs to treat migraines worsen OCD. Perseverative circling around the perimeter of an open field and prepulse inhibition, chronic fluoxetine rescue both.	C:++ F:+ P:+ (Shanahan et al., 2009)
	Neonatal clomipramine	An SRI in the tricyclic class	Increased anxiety-like behavior on the elevated plus maze, increased marble burying and food hoarding, and deficits in OCD relevant tasks such as reversal learning.	C: F:+++ P: (Ansorge, Zhou, Lira, Hen, & Gingrich, 2004)
	Optogenetics	Optogenetic stimulation of OFC-VMS projection	Repeated hyper stimulation generated a progressive increase in grooming behavior. Increase in VMS light-evoked firing parallel the increase in grooming behavior. SRI treatment rescued induced grooming.	C:++ F:+++ P:++ (Ahmari et al., 2013)
	Transgenic-viral PVI ablation	Induced ablation of a percentage of striatal PVI (as reported in post mortem TS studies)	Increased stereotypic grooming and increased anxiety-like behavior.	C:++ F:++ P: (Rapanelli, Frick, Xu, et al., 2017).
Genetic models	Sapap3 null	Post-synaptic scaffolding protein at excitatory synapses that is highly expressed in the striatum.	Perseverative grooming resulting in open skin wounds, increased anxiety-like behavior, and deficient in OCD relevant tasks such as reversal learning. Sub-chronic SRI alleviates over grooming. Present reductions of PVI. Electrical stimulation of same clinical DBS targets (IC and dorsal part of ventral striatum) robustly decreased grooming. Optogenetic activation of l-OFC input to the striatum decreased grooming in conditioned and spontaneous grooming.	C:++ F:+++ P:+++ (Burguière, Monteiro, Feng, & Graybiel, 2013a; Pinhal et al., 2018; Welch et al., 2007)

<i>Slitrk5 null</i>	<i>SLITRK proteins are widely expressed through the brain and highly enriched in the post-synaptic densities in striatal neurons. Though to direct neurite outgrowth.</i>	<i>Compulsive self-grooming and increased anxiety-like behavior, corrected by chronic SRI.</i> <i>It has reduced striatal volume and elevated neuronal activity in the orbitofrontal cortex.</i>	<i>C: ++</i> <i>F:+++</i> <i>P:++</i>	<i>(Shmelkov et al., 2010)</i> <i>(Abelson et al., 2005)</i> <i>(Katayama et al., 2010)</i>
<i>HoxB8 null</i>	<i>Hoxb8 is involved in development. The only cells that label with Hoxb8 appear to be peripherally derived microglia.</i>	<i>Compulsive self-grooming and allogrooming rescued with bone marrow implant transplant.</i>	<i>C:</i> <i>F:+</i> <i>P:</i>	<i>(Greer & Capecchi, 2002)</i>
<i>Sic1a1 / EAAC1 null</i>	<i>Neuronal excitatory amino acid transporter capable of altering the glutamate diffusion in extra synaptic regions. Strongly expressed in the cortico-striatal regions implicated in OCD.</i>	<i>Increased aggressive and decreased spontaneous open-field locomotor activity. Linkage data points to SLC1A1 in OCD.</i>	<i>C:++</i> <i>F:</i> <i>P:</i>	<i>(Aoyama et al., 2006).</i> <i>(Scimemi, Tian, & Diamond, 2009).</i>
<i>Marble burying</i>	<i>Burying of harmless objects. Requires no behavioral training.</i>	<i>Burying behavior is decreased by SSRIs at low doses. Aripiprazole (an antipsychotic) reduced burying without reducing locomotion. Ovarian and related hormones influence marble-burying behavior.</i>	<i>C:++</i> <i>F:+</i> <i>P:+</i>	<i>(Gyertyán, 1995)</i> <i>(Londei, Valentini, & G. Leone, 1998)</i>
<i>Schedule-induced polydipsia</i>	<i>Food-deprived rats with free water access trained to collect a food reward on schedule, develop a polydipsic behavior considered as a compulsive-like behavior.</i>	<i>Induced polydipsia is reduced by chronic administration of clomipramine, fluoxetine and fluvoxamine. High stimulation of the nucleus accumbens, mediodorsal thalamic nucleus also reduced polydipsic behavior. Schedule-induced polydipsia is modulated by serotonergic agents.</i>	<i>C:+</i> <i>F:+</i> <i>P:++</i>	<i>(Woods et al., 1993)</i> <i>(Kuyck, Brak, Das, Rizopoulos, & Nuttin, 2008)</i>
<i>Spontaneous stereotypy in deer mice</i>	<i>Stereotypic vertical jumping, backward somersaulting and patterned running.</i>	<i>There are high, low and non-stereotypic mice. The high and low are considered animal models of compulsive behavior. SRI, and blocking the striatal D1 and NMDA glutamate receptors decreased stereotypic behaviors. Imbalance in the direct and indirect pathways with a preponderance of the direct one. Elevated frontal cortex activity. Chronic SSRI (fluoxetine) decreased stereotypic behaviors.</i>	<i>C:++</i> <i>F:++</i> <i>P:++</i>	<i>(Korff, J. Stein, & H. Harvey, 2008)</i> <i>(Wolmarans, Stein, & Harvey, 2017)</i>

In the first category, pharmacological models are animals that followed drug-treatments to induce behavioral alterations that are similar to compulsive behavior. These aberrant repetitive behaviors observed include perseveration, indecision compulsive checking and increased anxiety-like behavior (Alonso, López-Solà, Real, Segalàs, & Menchón, 2015). These animals' models based their construct validity on manipulations of the serotonin and dopamine neurotransmitter systems that are thought to be related with OCD. In this category we include another type of artificially induced models. These models include animals models obtained from optogenetics manipulations or transgenic viral cell ablation.

In the second category, behavioral models include naturally occurring repetitive or stereotypic behaviors, such as fur chewing, and innate motor behaviors that occur during periods of stress or conflict, these can be seen as displacement behaviors such as, grooming or cleaning (Alonso et al., 2015). In this category, the most widely used compulsive behavioral types include marble burying, induced polydipsia, and spontaneous stereotypy in the deer mice. In the first two categories, we can find several rodent models that focus on compulsive behaviors and that have been used to investigate the effects of DBS in various targets.

In the third category, current genetic engineered animal models of compulsive behaviors include the *SAPAP3-KO* mice (described in detail in a further section), the *Slitrk5* null mice, the *Hoxb8* null mice and the *Sic1a1/EAAC1* null mice. These animal models are often compared to human OCD. (**Figure 17**)

Slitrk5 null mice

Mice in which the *Slitrk5*⁹ coding region was replaced with the LacZ reporter gene express compulsive self-grooming and increased anxiety-like behavior, and is corrected by chronic fluoxetine treatment (Shmelkov et al., 2010). The findings in this model mouse resemble to those of the *SAPAP3-KO* in terms of over grooming and response to fluoxetine. Moreover, the *Slitrk5* mice has reduced striatal volume and elevated neuronal activity in the orbitofrontal cortex.

The Hoxb8 null mice

The *Hoxb8* null mice also exhibited compulsive grooming and excessive grooming of wildtype cage mates. Its expression is found in adult brain, including regions of the cortico-basal ganglia circuits (Greer & Capecchi, 2002). In the brain the only cells that label with *Hoxb8* appear to be microglia, indeed the expression of *Hoxb8* was shown to come from bone marrow-derived microglia that migrate into the brain in the postnatal period and that gives rise to nearly half of all micro glia (S. K. Chen et al., 2010). Bone marrow transplantation from *Hoxb8* mutants into wildtype mice led to increased grooming and the opposite, bone marrow transplantation from wildtype into *Hoxb8* mutants completely rescued the pathological grooming. Even with these remarkable

⁹ *Slitrk5* (*SLIT and NTRK-like protein-5*) is a neuron-specific transmembrane protein.

experiments, the role of Hoxb8 mutation in microglia in the dysfunction of neural circuitry involved in the grooming behavior was not clear. In a very recent study, Nagarajan and colleagues showed that Hoxb8 mutants also present social behavioral deficits and that aberrant behaviors were rescued with long-term fluoxetine. They showed that Hoxb8 null mice presented synaptic modifications, reflected in increase cortical synapse and spine density within the frontal cortex (cortical synapse expansion) and in the contrary, striatal synaptic contraction (dorso and ventro medial regions) implicating that in those mutant mice there might be a potential increase in the excitatory corticostriatal synapse (Nagarajan, Jones, West, Marc, & Capecchi, 2017).

The Slc1a1 / EAAC1 null mice

The EAAC1 null mice over 1 year old exhibit increased aggressive and self-grooming behavior (Aoyama et al., 2006). The EAAC1 is a neuronal excitatory amino acid transporter that is capable of altering the glutamate diffusion in extra synaptic regions (Scimemi et al., 2009). EAAC1 homozygous loss-of-function mutations are very rare in humans and cause the renal condition dicarboxylic aminoaciduria, but it is still an interesting model because there are genetic links found between OCD patients and Slc1a1, the gene that encodes EAAC1 (Grados, 2010).

2.4.1.1 A COMMON NEURAL CIRCUITRY DEFICIT

We have reviewed different genetic animal models of compulsive behavior and although the causative agents in these models are all very different in the end, behavioral deficits (analog to those of compulsive disorders) such as over grooming and anxiety-like behaviors are very similar.

Additionally, these genetic mouse models show in one way or another, a convergence deficit in the cortico-basal ganglia pathways, including synaptic alteration and orbito-frontal hyperactivity, both which are consistent with diverse functional imaging studies from human OCD. Regarding the specific genes that are disrupted in the different animal models previously described, there is an astonishing overlap of expression across the brain (**Figure 17**). These overlapping brain regions identified in rodents are also identified in human patients suffering from CB such as OCD and TS. These results support the hypothesis observed also in human patients, confirming that the absence of proper regulation of cortical-basal ganglia circuits result in very similar behavioral pathology.

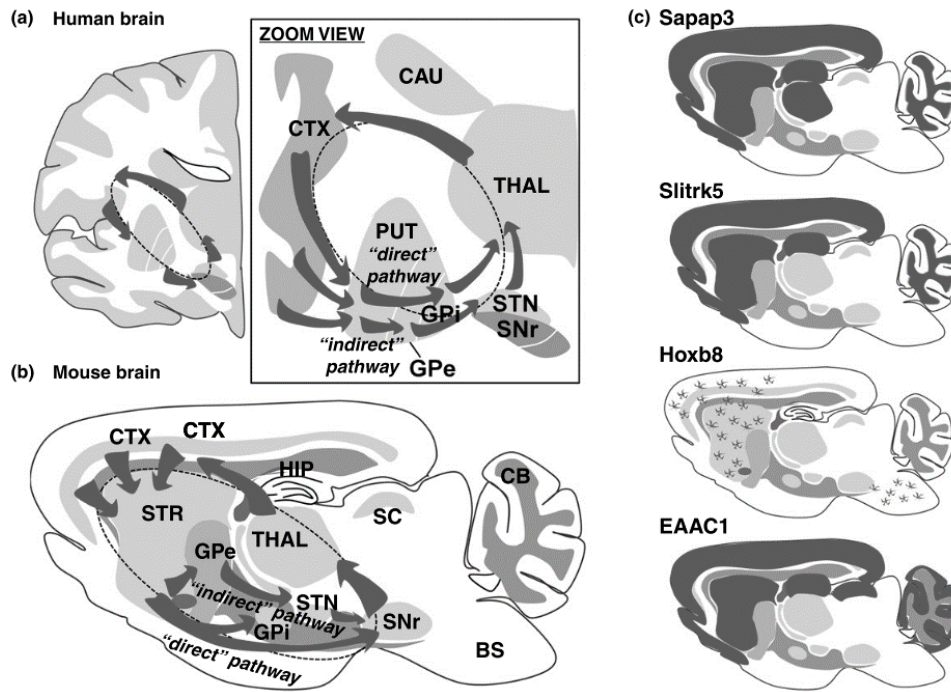


Figure 17. Role of the CSTC circuitry in obsessive-compulsive disorder in humans and compulsive-repetitive behaviors in mice. (a) Human brain coronal section (coronal) illustrating a simplified CSTC loop. Right panel, zoom view of the CSTC loop illustrating 'direct' and 'indirect' projection pathways of the basal ganglia. **(b)** Diagram of a mouse brain sagittal section illustrating the equivalent CSTC loop in the corresponding rodent brain structures. CTX, cortex; STR, striatum; CAU, caudate; PUT, putamen; HIP, hippocampus; THAL, thalamus; STN, sub-thalamic nucleus; SNr, substantia nigra pars reticulata; GPe, globus pallidus externa; GPi, globus pallidus interna; SC, superior colliculus; BS, brain stem; CB cerebellum. **(c)** Genetic animal models of compulsive behavior Figure taken from (Ting & Feng, 2011).

2.4.2 FOCUS ON THE *SAPAP3* KNOCKOUT MURINE MODEL

A relevant animal model of compulsive behavior is the *SAPAP3-KO* knock out murine model. In 2007 Feng's group reported for the first time that the deletion of *SAPAP3-KO* in mice lead to a behavioral phenotype similar to compulsive behavior (Welch et al., 2007). This was a relevant discovery as it is the first genetic mouse model to show compulsive behavior and predictive validity for OCD. The SAPAP family proteins are post synaptic density (PSD) components that interact with two other postsynaptic scaffolding proteins at excitatory synapses, the PSD95 and Shank family proteins. From the genes encoding members of the SAPAP family, the *SAPAP3-KO* has the characteristic of being highly expressed in the striatum (Welch et al., 2007) (**Figure 18-A**).

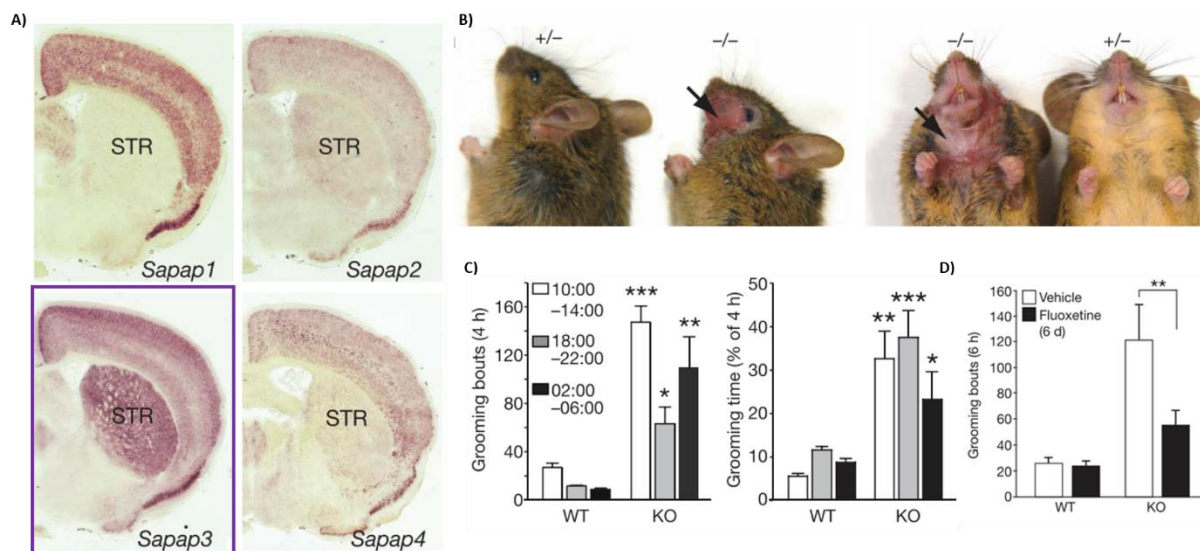


Figure 18. The *SAPAP3-KO* mice. (A) Only *SAPAP3* is highly expressed in the striatum (STR). (B) *SAPAP3-KO* mice develop self-inflicted facial and neck lesions from excessive grooming and scratching and presented anxiety behaviors. (C) *SAPAP3-KO* spent more time grooming and executed more grooming bouts than wildtypes during different schedules of the day. (D) Fluoxetine treatment over 6 consecutive days significantly reduced grooming behavior in *SAPAP3-KO* mice. Figure modified from (Welch et al., 2007).

Mice homozygous for the *SAPAP3* deletion (*SAPAP3-KO*) presented an interesting phenotype of self-inflicted facial and neck lesions by the age of 4-6 months (**Figure 18-B**). These mice develop the lesions independently of their housing situation excluding the possibility of these lesions being provoked by allogrooming or aggressive encounters. These mice have been tested for peripheral cutaneous defects such as inflammation or abnormal afferent sensation, hair nerve and organs that could explain the important lesions observed, but any differences were found when compared to control mice. (Welch et al., 2007) performed a series of extensive behavioral tests to measure the grooming behavior and anxiety phenotype. They found that not only *SAPAP3-KO* mice groom excessively compared to control mice, but their increased activity was present throughout the day and it was increased during the period of 18-22 hr (**Figure 18-C, D**). The lesion itself was not the cause of excessive grooming as mutant mice presenting lesions and mutant mice yet to develop lesions had similar degrees of grooming activity.

Mutant mice have an anxiety-like phenotype confirmed by three different tests. In the open-field experiment, mice spent more time along the walls avoiding the center zone. In the light-dark emergence test the mutant mice took longer to cross from the dark zone into a brightly area (considered a stressful environment) and spent less time in it. In the elevated zero maze test the mutant mice took longer to cross into open areas (considered risk environments) and spent less time exploring such areas. Continuous treatment of fluoxetine, the first-line treatment of OCD, remarkably reduced excessive grooming in *SAPAP3-KO* and reduced anxiety-like behaviors measured in the anxiety tests.

The SAPAP family proteins are postsynaptic proteins of excitatory but not inhibitory synapses and directly bind PSD95 proteins that influence trafficking of glutamate receptors. This is very interesting because most glutamatergic synapses in the striatum are cortico-striatal synapses. In the case of *SAPAP3-KO* mice's recording of brain slices, the field excitatory postsynaptic potentials (fEPSPs¹⁰) were significantly reduced, suggesting that this reduction was due to a postsynaptic impairment in synaptic transmission. Synaptic and behavioral defects were rescued by virus-mediated reintroduction of the *SAPAP3* in the striatum. The spine density of MSNs in the mutant mice's striatum in postnatal (day 21) and adult mice did not show any significant difference compared to control mice, suggesting that at this level there were not morphological changes indicating that the spine formation and maintenance were affected by the lack of *SAPAP3* proteins. The above results strengthened the face validity and predictive validity of the *SAPAP3-KO* animal model more than any other animal model making it a quite appealing model to study compulsive behavior.

It is with no surprise that the findings on *SAPAP3-KO* animal model lead to genetic studies of this protein in patients suffering from compulsive disorders. (Zuchner et al., 2010) performed a human study that supported the role for *SAPAP3* in trichotillomania and OCD, finding through gene re-sequencing analysis seven genetic heterozygous *SAPAP3-KO* variants in 4.2% of diagnosed TTM/OCD patients and only 1.1% in controls, nevertheless it is not stated how these variants may contribute to the pathology risk. Additionally, a large family-based gene association study of *SAPAP3* suggested that multiple variations in the *SAPAP3* gene are associated with grooming disorders (O. J. Bienvenu et al., 2009). Moreover, additional defect in inhibitory transmission in the *SAPAP3-KO* animal model have been identified, including reduced number of PVI in the dorsomedial striatum compared to control animals. Additionally, this decrease in numbers was accompanied by decreased feed-forward inhibition of MSNs by FSI (putative PVI), as shown by paired FSI-MSN recordings, showing abnormally high spontaneous activity of MSNs in the dorsomedial striatum (Burguière et al., 2013b). Together these studies support the hypothesis of deficits within the cortico-striatal circuits, particularly indicate overactive striatal activity and provide evidence of construct validity for the *SAPAP3-KO* animal model. In terms of predictive validity of the *SAPAP3-*

¹⁰ fEPSPs are graded potentials that provide a small local depolarization and can initiate an action potential.

KO model, a recent study investigated the effect of DBS in the internal capsule (IC) and the dorsal part of the ventral striatum (dVS) (Pinhal et al., 2018). DBS in both targets showed to decrease time spent grooming, and stimulation in the IC had stronger immediate effects with grooming returned to excessive levels after stimulation. These changes after stimulation are consistent with the results from DBS in OCD patients (de Koning et al., 2016).

2.5 RODENT SELF-GROOMING PHENOTYPE FOR UNDERSTANDING COMPULSIVE BEHAVIOR

In the first chapter, we defined repetitive behaviors seen as sequential, motor behaviors that once started can continue to completion without constant monitoring and that are often elicited by external or internal triggers. In rodent behavior, one often observed repetitive behavior is self-grooming or auto-grooming. Mature self-grooming or auto-grooming is a complex model of self-directed, repetitive, sequential motor behavior. In rodents, this behavior can take up to 30% of their awake time (Spruijt, van Hooff, & Gispen, 1992). By means of its high predominance and stereotyped patterning characteristics, its study offers us important insights into how complex repetitive behaviors are regulated by the brain under normal conditions and how they are affected under pathological conditions.

Self-grooming is a primary biological function that involves the care of the body surface (Spruijt et al., 1992), it helps to rearrange hairs, to remove dirt, parasites and other strange objects or substances. This self-directed behavior has other possible secondary functions (Kalueff et al., 2016) such as thermoregulation, social communication, de-arousal and in wound healing by the antibacterial properties of saliva. It is seen as an evolutionarily well-conserved innate behavior or rodents that is important for survival. Rodent self-grooming assembles several grooming acts often encapsulated into distinguishable phases and these phases form functional sequences, including highly stereotyped patterns (**Figure 19**) (Kalueff et al., 2016). Mature rodent self-grooming include four distinct phases that usually follow a cephalocaudal or head-to-body rule, although in addition to stereotyped grooming, adults also show flexible, less stereotyped facial grooming movements (Berridge, Aldridge, Houchard, & Zhuang, 2005; Berridge & Whishaw, 1992) that can be seen unpredictable isolated or non-chain grooming phases (that is, flexible mixtures of strokes and licks that are components of a functional sequence). Phase 1 or nose grooming consists of a series of elliptical bilateral paw strokes made near the nose. Phase 2 or facial grooming consists of a series of unilateral strokes from the mystacial vibrissae to below the eyes. Phase 3 or head grooming consists of a series of bilateral strokes backwards and upwards made by both paws simultaneously and usually touching the ears, these are wider movements than those observed in Phase 2. Finally, Phase IV consist of body licking.

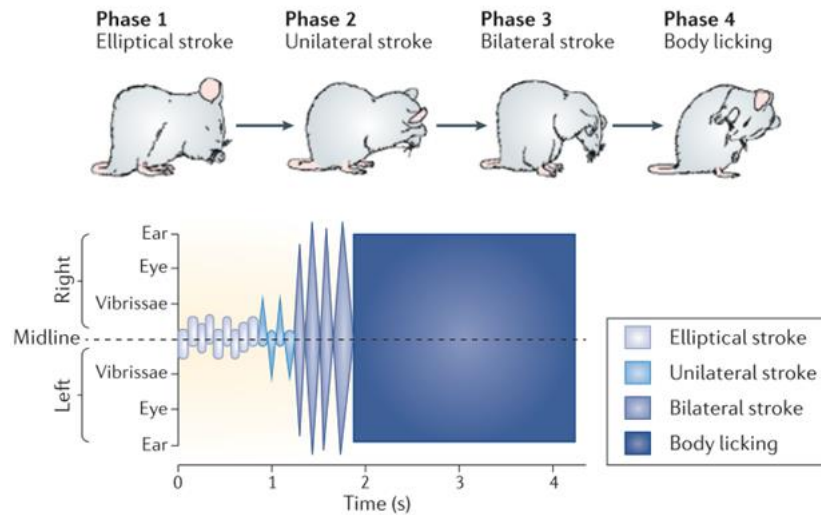


Figure 19. Rodent self-grooming syntactic chain. In mice it represents an important load of time spent exclusively on this activity (Spruijt et al., 1992). The complex sequenced structure of self-grooming can be divided in four distinct phases or classes. These phases form a predictable sequence that goes from phase one to phase four, but single isolated phases are also commonly observed in rodents. Figure taken from (Kalueff et al., 2016)

Grooming behavior can be scored manually or with automatic tools. For acute scoring, where highly precise time onset and termination of grooming events is crucial, or for experiments requiring precise decomposition of the grooming microstructure, the human scoring of videotaped behaviors by trained observers is the most common method. Nevertheless is extremely time consuming. For experimental paradigms that allow a less strict but still accurate scoring assessment of grooming behavior, recent automatic experimental frameworks have proven to be highly effective (Reeves, Fleming, Zhang, & Scimemi, 2016; van den Boom, Pavlidi, Wolf, Mooij, & Willuhn, 2017; Wiltshcko et al., 2015). These approaches uses pre-defined databases selected by users or predefined region of interests in pixels, therefore the performance of these algorithms depend on a certain extend to the appropriate parameters used to train the algorithms or the pre-defined settings entered by the users.

Different grooming metrics could provide insights into different neurobiological mechanisms. Overall there are two approaches to assess rodent self-grooming, in one hand metrics that give information on grooming patterning and classes and in the other hand metrics that indicate the amount of animal grooming (Table 2). Depending on the experiment, different grooming metrics should be analyzed, for example, stressors usually increase the percentage of incomplete or single bouts and disorganize the cephalo-caudal grooming sequences (Kalueff & Tuohimaa, 2005; Kalueff, Wayne Aldridge, Laporte, Murphy, & Tuohimaa, 2007).

Table 2. Common grooming metrics used in neurobiological research.

Grooming metrics	Possible use
Chain and non-chain bouts	Assess the global adherence to the cephalocaudal rule.
Complete caudal grooming (going through the four phases)	
Correct and incorrect cephalocaudal transitions between stages	Assess disturbance in grooming patterning
Interruptions in grooming bouts	
Number of grooming bouts	
Grooming event duration	Assess global grooming activity
Percentage of time spent in grooming (from a period of time assed)	
Percentage of grooming events of different classes	
Syntactic chains per minute	
Probability of chain Initiation	
Grooming events per minute	

From the point of view of complex patterning of motor behaviors, it is interesting to study rodent self-grooming as and indirect phenomena that could be useful to study human brain disorders that include compulsive repetitive behaviors. We have mentioned that despite the interesting findings using animal models of compulsive behavior, especially in the *SAPAP3-KO* mice, there is no single model that could merge the entire conditions observed in compulsive-related disorders. Thus, it is important to focus on robust, easily observable and quantifiable behaviors for which we can probe hypothesis regarding the underlying neural circuitry defects. Although self-grooming is seen as a hygiene self-care behavior, to study grooming behavior and its neurobiology relationship, the context in which it occurs is often more informative than seeing it only as care routine. This assumption means that these behaviors may be expressed in other situations than the presumed body surface care routine. Indeed, when studying the behavioral phenotype of self-grooming it is important to realize that it may result from different mechanisms having very different neurobiological origins. For example, it has been showed that self-grooming in rats is also a response to exposure to novelty and other stressors (Bindra & Spinner, 1958; Smolinsky, Bergner, Laporte, & Kalueff, 2011) suggesting that self-grooming can be considered as a displacement behavior. This characteristic makes it an interesting feature for translational research. In experimental paradigms, triggering grooming is achieved by introducing stressful components such as novelty (Bindra & Spinner, 1958), by sprinkling or dropping water (Burguière et al., 2013b) and by the injection of different drugs (Kalueff & Tuohimaa, 2005; Moody, Merali, & Crawley, 1988).

Human's repetitive motor behaviors such as self-grooming behaviors when executed excessively can become pathological and are considered symptoms in certain neuropsychiatric disorders. The study of rodent self-grooming is useful for translational research as aberrant or excessive rodent grooming can be indirectly related to human repetitive actions that becomes over-expressed. Not that rodent self-grooming could be directly translated to observable symptomatology in humans but rather because of its

complex nature as a fine motor patterned sequence it is indeed an interesting indicator, when excessively executed or dysregulated, of a phenomenon that might be consistent to what is observable in certain human brain disorders.

MAIN POINT SUMMARY

- The basal ganglia system is a collection of nuclei that are interconnected with each other through a complex series of loop circuits, it assures a flow of information that originates in the entire cerebral cortex and projects back to the frontal cortex.
- A principal role of the striatum is to integrate a great number of cortical inputs and process this information to select motor and/or cognitive programs which are then carried out by the diverse pathways of the basal ganglia.
- A prominent model of compulsive behaviors is that there is a deficient in the orbito-frontal-basal ganglia circuits. This hypothesis are supported with various functional imaging studies in patients presenting compulsive behaviors, particularly fMRI studies in OCD patients have shown dysregulation in the corticostriatal connectivity, as a hyperstriatal activation pointing to a deficit in striatum overall inhibition.
- Cortical and striatal interneurons modulate neural circuits to orchestrate a behavioural output appropriate to environmental challenge.
- Striatal PV FSI receive strong afferences form the cortex and are the major elements of a powerful but small feedforward inhibition network that control spike timing in MSNs, thereby are a key element that regulates striatal output.
- The *SAPAP3-KO* mice exhibit compulsive and anxiety behaviors (excessive self-grooming that causes serious facial and neck lesions). This model has proven to response to fluoxetine (the first selected treatment for OCD).
- The observations that *SAPAP3-KO*, a highly expressed postsynaptic scaffolding proteins at excitatory synapses in the striatum, in KO mice indicate that there are defects in striatal neurotransmission in those mice.
- PVi may have an implication in the over-expression of grooming, for instance *SAPAP3-KO* mice have reported to have a decreased number in the centromedial striatum
- Compromised inhibitory striatal interneurons have been implicated in the expression of excessive repetitive behaviors, particularly in TS.

Chapter 3. CLOSED-LOOP NEUROMODULATION

This chapter aims to review how closed-loop experiments are being used on clinical trials as novel treatments and in basic research paradigms to investigate brain function or dysfunction. To first understand the potential of closed-loop neuromodulation it is necessary to understand how open brain stimulation is carried out. We will briefly review the exciting history of brain stimulation and its attached path to technological developments, as well as its role in RB-related disorders. We will see how closed-loop brain stimulation has appeared in the last decades as a promising new research area that aims at modulating, interfering and understanding neural activity with a temporal and spatial specificity by delivering stimuli in response to a specific behavior or a physiological biomarker. Finally, we will discuss the general principles and constrains of combining optogenetics with cellular electrophysiology in a closed-loop approach. We will explain the cycle of operations involved in such experiments, with a focus on signal pre-processing methods that are relevant for this thesis manuscript, as well as the advantages of using machine learning techniques, and we will mention the challenges faced at every step. In this chapter when talking about “Neuromodulation”, we will be referring to the therapeutic or experimental alteration of nerve cell activity through targeted delivery of a stimulus, and we should not confuse it with the meaning that it takes in biology as a natural physiological process in the nervous system.

3.1 OPEN-LOOP BRAIN STIMULATION

3.1.1 A CONDENSED HISTORY OF BRAIN STIMULATION AND ITS PARALLEL PATH WITH TECHNOLOGICAL INNOVATIONS

An interesting way to look at the history of brain stimulation is by exploring different periods in time and relating to each period the significant technological advances that allowed a step forward in developing new neuromodulation techniques. Some of these inventions or developments were not, at the time of the invention, thought to be of use for neuromodulation but thanks to the synergy between the different fields it was possible to achieve a more efficient, better controlled and more specific way to provide neuromodulation. **Figure 20**Error! Reference source not found. summarizes the following timeline.

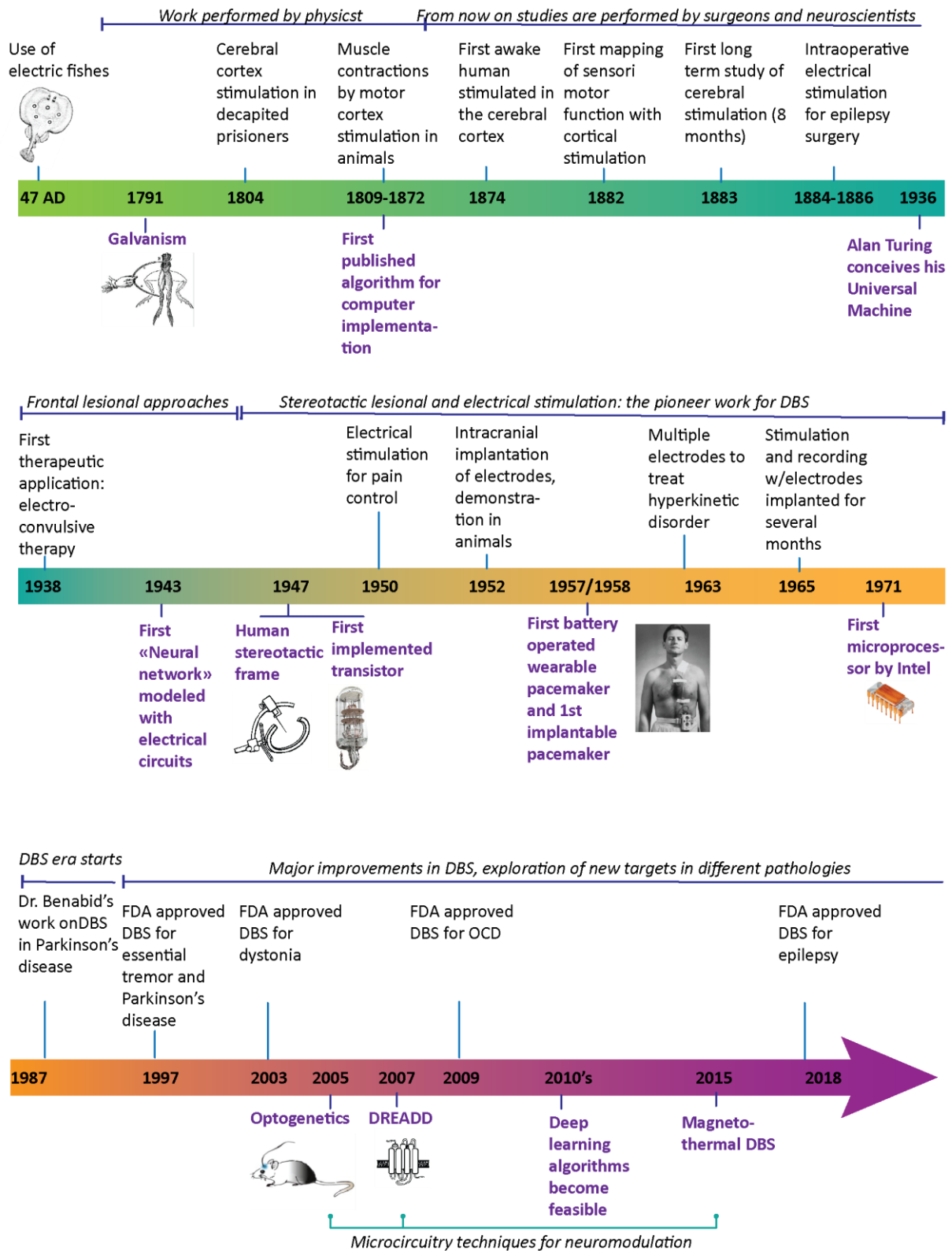


Figure 20. The condensed history of neuromodulation and how it is closely related to the technological developments of each era. The timeline shows the origins and evolution of neuromodulation, and how technological developments parallel the advances in different brain stimulation techniques, from ancient times to the present.

The idea of using electrical stimulation to modulate the nervous system comes from ancient times, the first published record goes back to the time of roman emperor Claudius (about 47 AD). His court physician, Scribonius Largus, recommended in his "*Compositioned medicamentorum*" the use of a live Torpedo fish¹¹ on the human cranial surface to treat chronic headaches. The use of electric fishes was in the following decades explored to try to treat depression, chronic pain and as a post-stroke therapy (Debru, 2006).

In the early eighteenth century, it was the work on animal bioelectricity by Luigi Galvani and his wife Lucia Galeazzi Galavani that immediatly opened the door to the first experimentation on human cortical brain stimulation. Physics professor Giovanni Aldini performed a series of experiments in decapitated prisoners and showed that facial grimaces and contortions by the contractions of muscles of the head and face followed cerebral cortex stimulation (Aldini, 1804). These experiments lead to the hypotheses that brain stimulation could be used to investigate the neurophysiology of the brain and that it could be used as a technique for therapeutic purposes. In 1703 Gottfried Leibniz published his binary system, and although his invention was the first to allow to transform verbal logic statements into mathematical ones, his invention did not have much application, at least not at this point in history, when the mechanical calculators were slowly starting to emerge. It was with the industrial revolution of the 18th century that the need for repetitive operations executed efficiently boosted the creation of calculators and with it the need for a limited language to control its functions. With calculators came the creation of programming languages, by 1842 Ada Lovelace published the first algorithm destined to be executed by a calculator and so the advances of programming language started (Paul A. Freiburger, Hemmendinger, Pottenger, & Swaine, 2018).

Regarding neurophysiologic research, in the ninetieth century most of the published reports concerned experiments that highlighted how cortical direct current stimulation using needle electrodes in live dogs, cats, bulls, and monkeys resulted in motor functions of the body. These experiments were the first piece of evidence of the motor cortex and the main work of Luigi Rolando, Gustav Fritsch, Eduard Hitwing and David Ferrier. In the following years, a series of converging studies helped to confirm the electrical excitability of the cortex and gave the first insights into the cortical hemispheric representation of motor functions. These studies included: (1) the first report of electrical stimulation in the cerebral cortex of awake humans in 1874 by physician Robert Bartholow (Bartholow, 1874), (2) the series of experiments on sensorimotor function with cortical stimulation mapping on a trepanned¹² patient, who had traumatic brain injury, performed by Ezio Sciamanna(Sciamanna, 1882). Finally, (3) the first long-term experiment lasting more than eight months in a patient whose brain tumor destroyed part of the skull bone and

¹¹ *The common torpedo (Torpedo torpedo) is a species of electric ray in the family Torpedinidae. It can reach 60 cm long and can deliver up to 200 volts either in a single shot or in a bursty way with a discharge frequency up to 600 Hz.*

¹² *Trepanation was a surgical practice that consisted in drilling a hole into the human skull in order to expose the dura mater to treat to release blood pressure but also used to try to treat health various health problems.*

allowed easy access to the dura mater surface executed by surgeon Alberto Alberti (Alberti, 1886). In this period, worth mentioning is the pioneering work of neurosurgeon Victor Horsley, he made several studies on motor response through electrical stimulation of the cerebral cortex. He was the first to use intraoperative electrical stimulation of the cortex for the localization of epileptic foci in humans between 1884-1886 (Tan & Black, 2002).

The first therapeutic applications using brain stimulation with electroshock included severe psychosis performed by Ugo Cerletti in 1938. Three years later, Alan Turing introduced his "Universal machine" which is considered to be the origin of stored program computers, and an idea later used and implemented by John von Neumann, this progress served as the precursor for digital computers (Paul A. Freiberger et al., 2018). Only a few years later, in 1943 neurophysiologist and mathematician Warren Sturgis McCulloch and Walter Pitts co-worked to modeled how human neurons might work, they illustrated their theory with electric circuits (McCulloch & Pitts, 1943). Their work would lay the foundations of artificial neural networks and would be a useful input for machine learning tools used nowadays in neuroscience to decode brain signals. In 1947 Henry Wycis and Ernst Spiegel produced the first human stereotactic frame that helped greatly to determine Cartesian coordinates to localize specific targets (Gildenberg, 2002). In the same year, the first transistor was implemented by Nobel Prizes John Bardeen and Walter Brattain (Bardeen & Brattain, 1948). The transistor is perhaps indirectly the most relevant event associated to the history of neuromodulation as it revolutionized the field of electronics and directly opened the way for smaller and cheaper electronics that would be necessary later for implantable neuroprosthetics devices, and particularly microprocessor-driven pacemakers and stimulators, and in general for the construction of future microprocessors.

The '50s were a decade of exciting inventions and productive work of stereotactic lesional and electrical stimulation. In 1950 neurosurgeon Wilder Penfield contributed with fundamental studies (Penfield, W., and Rasmussen, 1950) for brain stimulation of the human cortex that gave a more accurate representation of cortical and somatosensory areas. At this time in history, there was a lot of lesional neurosurgery work being done, in this practice, intra-operative electrical stimulation, used for target exploration was used prior to lesioning. Indeed, electrical stimulation was used only used as part of the protocol to identify the correct position of coagulant electrodes in deep brain regions. Intra-operative electrical stimulation started later to be used for localization of deep nuclei and as a therapeutic method itself for movement disorders (Blomstedt & Hariz, 2010), starting a new exciting era of therapeutic brain stimulation thanks in significant part to the stereotactic method. Another important development in this decade was the neurostimulator, invented in 1957. Earl E. Bakken, an electrical engineer and TV repairman and later founder of Medtronic Inc. produced the first battery-operated wearable pacemaker. One year later in 1958, the first pacemaker implantation would be performed in Sweden with the device entirely hand-made (Aquilina, 2006). We can say that the origins of deep brain stimulation (DBS) are linked to stereotactic lesional

functional neurosurgery for treatment of dyskenetic disorders and tremor in Parkinson but also to the advances in the fabrication of implantable neurostimulators. It was also in this decade that the first experimental brain stimulation protocols started for pain control. Parallel, an exciting era in the field of mathematics was about to give the most fruitful advances in what would be later known as the machine learning domain. Despite the pioneer ideas and innovative algorithms being developed the following years, engineers and mathematicians had to wait for advances in computer processing and memory capacity to catch up with their algorithms in order to be applied in diverse fields, including in neuroscience.

The pioneers of DBS were neuroscientist José M. Delgado, Natalia Petrovna Bekthereva and psychiatrist Carl Wilhem Sem-Jacobs. In 1952, José M. Delgado first described a technique of intracranial implantation of electrodes in humans (Delgado, Hamlin, & Chapman, 1952), he also performed several experiments in animals, in the most famous one, he stopped a bull in mid-charge by electrically stimulating the basal ganglia and thalamic structures (**Figure 21Error! Reference source not found.**). In 1963, Natalia Petrovna Bekthereva achieved excellent results using multiple electrodes for the treatment of hyperkinetic disorder (Bekthereva, Grachev, Orlova, & Iatsuk, 1963), because her work was written in Russian her work was better known latter in history (Sironi, 2011). In 1965, Carl Wilhelm Sem-Jacobsen first used deep electrodes not only for stimulation but also for recording in patients with epilepsy and psychiatric disorders (Sem-Jacobsen, 1965). He implanted multiple electrodes in the thalamus that remained in the patient's brain for several months; he used those electrodes as a way to select the best target for a lesional site in Parkinson's disease. Levadopa, one of the main drugs used to treat Parkinson's symptoms, was introduced in the late 1960s and its success provoked a decline in surgical treatment experimentation of Parkinson's disease, nevertheless ablative procedures continued targeting the thalamic ventral intermediate nucleus and the globus pallidus. It was not until 1987, when pioneer French neurosurgeon Alim Louis Benabid reported its results on thalamic DBS for tremor, that thalamotomy and eventually lesional techniques started to be replaced with DBS (A. L. Benabid, Pollak, Louveau, Henry, & De Rougemont, 1987). A few years later, in 1989, the US Food and Drug Administration approved the DBS for essential tremor and Parkinson's disease. In 1992 stimulation of the globus pallidus was shown to be safer than pallidotomy (Laitinen, Bergenheim, & Hariz, 1992). A couple of years later, Pollak's group stimulated the sub-thalamic nucleus (STN) as a new target for Parkinson's disease, and this target was found to be effective for bradykinesia, tremor, and rigidity (Pollak et al., 1993). These previous studies were only the beginning for DBS in movement disorders, and since then, DBS has been applied in many treatment-refractory psychiatric disorders, in translational models, and in patients. A prove of the interest in this approach is that in the subsequent years DBS was approved for dystonia, OCD and more recently for focal epilepsy in 2018. Although DBS is now used to treat different disorders, the procedure is similar and involves chronic implantation of electrodes stereotactically implanted in a specific brain target and driven by an internal pulse generator to correct abnormal neural activity. A subcutaneous wire travels from the

electrode to the pulse generator that is implanted subcutaneously on the chest wall. After DBS implantation, clinicians use a computer to communicate transcutaneously with the implanted pulse generator and to configure the stimulation parameters. These parameters include the selection of which contacts on the electrode will deliver the stimulation, the amplitude, the frequency and the pulse width (Dougherty, 2018).

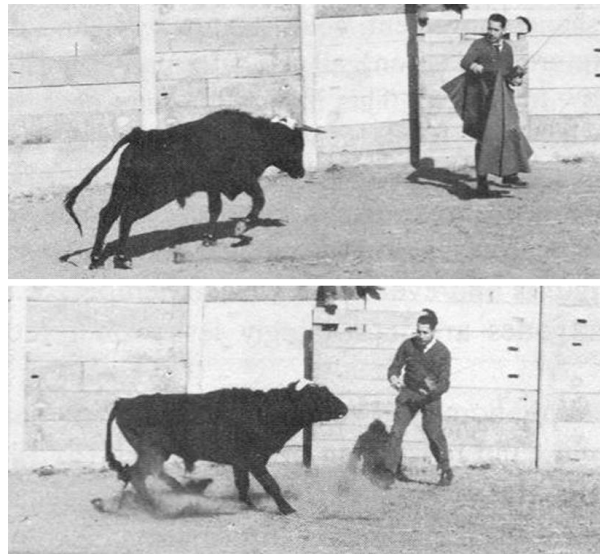


Figure 21. Pictures from the famous experiments in bulls by José Delgado. The pictures show the effect of brain stimulation in stopping the bull in mid-charge. (Pictures were collected from personal correspondences of Dr. Delgado and published in (Marzullo, 2017)).

Lesioning, chemical modulation and electrical stimulation were the vendetta tools in the '90s regarding brain stimulation, and although they have proven to be effective at a brain structure level, they lack selectivity. In the early 2000's more advances in neuromodulation techniques would be invented to overcome selectivity and specificity limits and these techniques would once again change the course of neuroscience. These techniques include optogenetics, chemogenetic tools and the most recent magneto thermal neuromodulation, so far, all these technics are currently used only in animal experimentation. Optogenetics came as a powerful technique that allows selective activation of neurons using light, rather than electrical currents. A viral vector engineered to target specific neural population can be used to carry genes for light sensitive proteins (ion channels, pumps or metabotropic receptor) called opsins which can be triggered by light pulses (More on section 3.2). Their light activation will result in the excitation or inhibition of the targeted neuron depending of the type of opsin used. The birth of optogenetics is often related to the publication of Karl Deisseroth's group in 2005 (Boyden, Zhang, Bamberg, Nagel, & Deisseroth, 2005), he infected rat hippocampal cells with a virus carrying the ChR and demonstrated through electrophysiological recordings cell activation through different light wavelengths. Some might discuss (Vlasits, 2016) that a more precise date was actually in early 2004 when Pan's group submitted his findings on successful transfection of ChR in ganglion cells of mice (Bi et al., 2006) (but were finally accepted later than Deisseroth's publication). In any case, the idea of using light for precise control of neural activity was suggested previously to that, in 1999 by

molecular biologist Francis Harry Compton Crick, in an article suggesting how molecular biologist could help neuroscientist to develop biological tools (Crick, 1999).

Analogous approaches to optogenetics are chemogenetic tools such as designer receptors exclusively activated by designer drugs (DREADD) in which receptors are engineered to respond to synthetic small molecule ligands. This approach was introduced soon after the first optogenetics articles in 2007 (Armbruster, Li, Pausch, Herlitze, & Roth, 2007). A few years later, in 2015 a new technique to provide wireless deep brain stimulation was reported by Ritchie Chen and colleagues (R. Chen, Romero, Christiansen, Mohr, & Anikeeva, 2015), they called it magnetothermal neuromodulation. This technique allows specific neurons to be activated by heat-emitting nanoparticles that respond to external magnetic fields. The neurons are made heat-sensitive by introducing the heat-sensitive calcium ion channel TRPV1 into neurons via delivery of the corresponding encoding gene. Weeks later, magnetic particles are injected in the same region. An external alternating magnetic field redirected to the region of interest causes the magnetic nanoparticles to emit heat enough to activate the TRPV1 neurons and provoke membrane depolarization and excitation. Although very recent and still under investigation, it is certainly a clever approach that will be explored and improved in the following years, probably as much as optogenetics of chemogenetics. It is too soon to know if micro circuitry approaches that require viral delivery or genetic manipulations will one day be commonly used as clinical treatments. One thing is sure, is that, these techniques being used in translational models have enhanced knowledge of the brain microcircuitry in functional or dysfunctional states. In the case of optogenetics, a few companies are currently working on the area of optogenetics for therapeutics purposes. Including Circuit Therapeutics co-founded by Dr. Karl Desseiroth and Dr. Zhou-Hua Pan's startup (acquired by Allergan) which is conducting the Phase 1 clinical trial for vision restoration. The treatment, which aims at treating retinitis pigmentosa received Orphan Drug Designation by the FDA in 2014.

After a fast review of the history of brain stimulation and seeing the big picture with some (and not exhaustive list) of the relevant technological developments it becomes clear that the advances in brain stimulation and particularly deep brain stimulation goes hand by hand with technological inventions. Advances in the comprehension of electricity lead to galvanism experimentation and later, to the first cortical brain stimulation in animals, then electrodes placed temporarily in deep brain areas became more popular. The development of the stereotactic method helped surgeons greatly, they were able to use a three-dimensional coordinate system to locate specific regions in the brain, and they were able to approach precisely deep brain regions with more precise lesional surgery. Parallel, engineers, and mathematicians focused significantly on programmable computers, giving birth to analog, then digital, and finally stored-program computers. These were enormous machines that work first with vacuum tubes. The invention of the bipolar transistor allowed later for integrated circuits and later for microprocessors, and a new era of smaller and more efficient computers appeared. The transistor opened the way for miniaturization of electronics allowing for continuous brain stimulation through the creation of pacemakers and finally through implantable stimulators. The joint effort

between biologist and mathematicians gave, as a result, the basis for artificial neural networks. Years later, advances in computing power made possible the application of machine learning algorithms to help solve multiple challenges in biology and medicine.

Currently, we stand in a decade in which viral delivery, genetic manipulations, and electrophysiology are the triple alliance for newer micro-circuitry neuromodulation techniques. The fast development in recording techniques including microelectrode arrays (MEAs) and probes with hundreds of electrode sites require the processing of a large amount of data and therefore the actual need for efficient algorithms. Nowadays, in the field of DBS, a promising approach is adaptive deep brain stimulation where stimulation is only delivered when neural activity related to abnormal behavior starts. A recent experimental framework of clinical interest is closed-loop optogenetics, a challenging technique that allows to selectively inhibit or activate a population of neurons with temporal specificity only when aberrant physiological or behavioral activity is detected. We further discuss these exciting neural stimulation approaches in section 3.2 of this manuscript.

3.1.2 BRAIN STIMULATION AND PATHOLOGICAL RB

The modulation of brain activity is a reality since the '80s, and it has become the basis of successful therapies to alleviate the symptoms of treatment-resistant disorders such as chronic pain, Parkinson's disease, tremor, and dystonia (Kringelbach, Jenkinson, Owen, & Aziz, 2007). As far as RB-related disorder concern, years of research and clinical trials have given us valuable insights into the pathophysiology of these disorders, yet much more needs to be understand. We can see the progress made by brain stimulation in this area with two magnifying glasses, on the one hand, what macro circuitry stimulation has provided in terms of therapeutic applications and this concerns especially DBS, and on the other hand, what micro circuitry stimulation has brought to light, and this concerns especially studies in animal models. To narrow the review of literature relevant to this manuscript, when talking about human macro stimulation we will not cover other alternative therapeutics technics for OCD such as transcranial magnetic stimulation, and electroconvulsive therapy.

3.1.2.1 MACRO CIRCUITRY STIMULATION

The implantation of electrodes and the delivery of electric current through them allows functional modification of the brain region targeted. This technique has the advantage of modifying brain activity in a non-permanent manner, contrary to surgical removal or lesioning techniques of brain structures. One of the essential parameters for efficient DBS is the stimulation frequency: for instance, in Parkinson's disease, stimulation frequency has effects over tremor when configured between 50-200 Hz (Krack, Hariz, Baunez, Guridi, & Obeso, 2010). Despite its long history of use, understanding how DBS works, what are the best target areas, and how to optimize stimulation protocols are still under investigation. Some mechanisms have been proposed to explain DBS effects, and they come from clinical trials and investigational models. The initial hypothesis regarding DBS mechanisms was that DBS would have an inhibitory effect under high-frequency stimulation on the neurons stimulated, this hypothesis was confirmed by the observation of STN activity in the rat (Benazzouz et al., 2000) and human patients (M. L. Welter et al., 2004). This idea was in agreement with the clinical effect of DBS and their resemblance to that of anatomical lesioning (Ashkan, Rogers, Bergman, & Ughratdar, 2017). The previous hypothesis relied on the assumption that the most relevant or submitted to change activity was the activity local to the electrodes. However, further studies confirmed a more decentralized mechanism involving the excitation of afferent and efferent axons to the site of stimulation. In human (Perlmutter et al., 2002) and rodent studies (Windels et al., 2000), an increase in neurotransmitter release in the downstream structures was observed. Other studies measuring the activity of the structures that receive connections from the STN like the GP were observed to show augmented subthalamic activity contradicting previous inhibitory hypothesis (Hashimoto, Elder, Okun, Patrick, & Vitek, 2003; Jech et al., 2001). In the same optic, Benabid and colleagues postulated that DBS does not reduce neural firing, but instead, HFS induces modulation of

pathological neural activity, causing a network-wide change (Benabid, Benazzouz and Pollak, 2002).

Another theory to explain the DBS's effects, states that DBS disrupt or suppress pathological oscillations. This theory is based on observations of pathological beta-band (13-30 Hz) oscillatory activity in the sensorimotor loops between the cortex, basal ganglia, and cerebellum that is thought to contribute to the motor symptoms of PD. The most relevant proof-of concept study of this theory was demonstrated in eight patients with PD when stimulation was delivered in the STN as a response to this beta-oscillatory activity, symptoms were improved by 50% (Little et al., 2013). This approach is known as on-demand or adaptive brain stimulation, and it will be further discussed in section 3.2. Decades of research point to DBS not acting exclusively as a local excitatory and inhibitory mechanism but through a diversity of effects on local and remote factors. It is likely that the mechanisms of DBS are multifactorial and that may include immediate neuromodulator effects, synaptic plasticity and long-term neuronal reorganization (Ashkan et al., 2017) (**Figure 22**). To help clarify this view translational research is necessary to clarify not only the targets and neural mechanisms that underline the effects of DBS but also the biological fundamentals that are affected in the disorders in which DBS is used or could potentially be used.

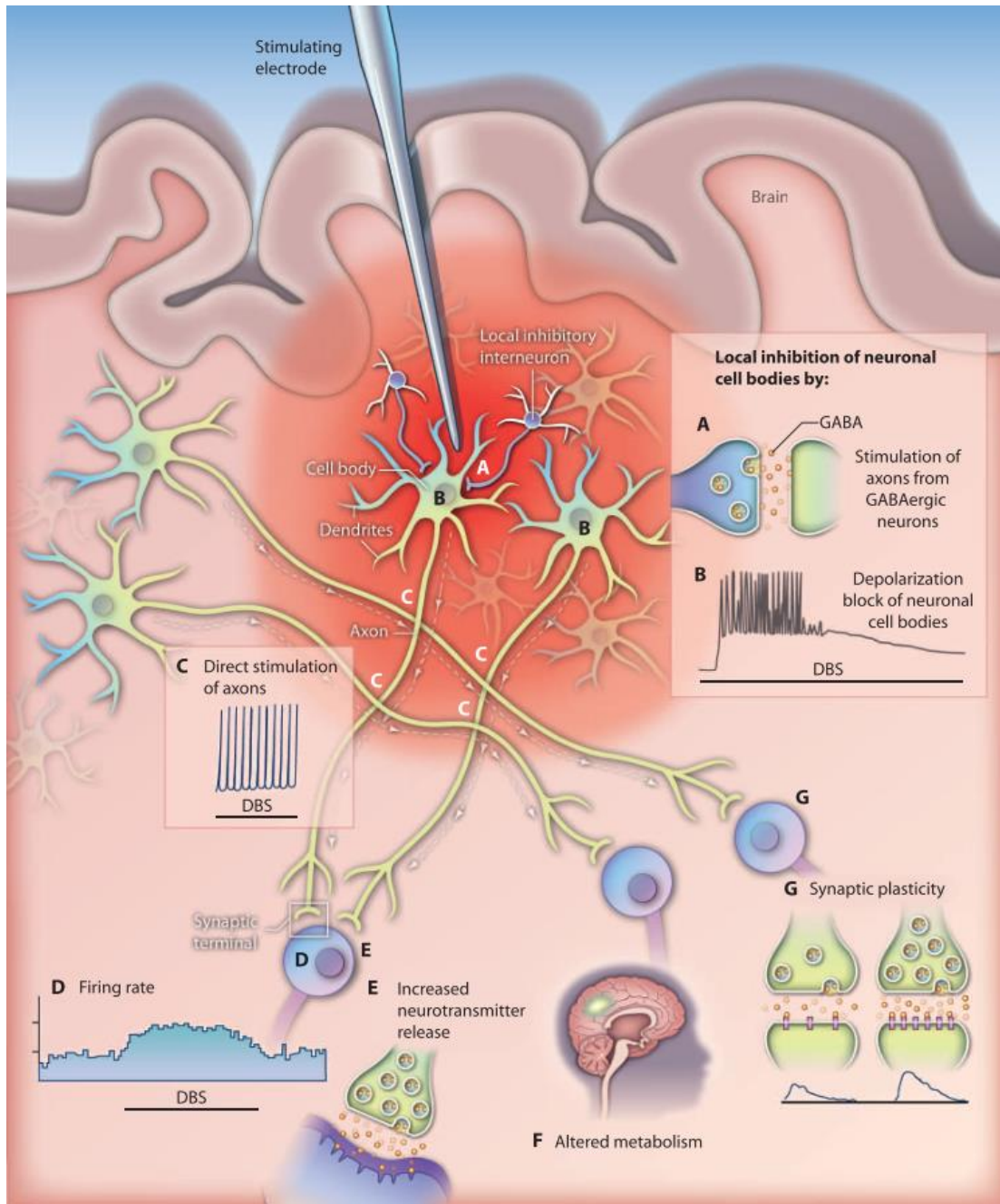


Figure 22. Possible cell effects of high-frequency DBS. Stimulation of brain region targeted by stimulating electrode could cause **(A)** a stimulation of GABAergic terminals, and as a consequence, the release of the inhibitory transmitter GABA and, a **(B)** depolarization block causing decreases neuronal activity. **(C)** The stimulation could also cause an induced artificial, tonic pattern of action potential firing by direct stimulation of local axons, in this way, DBS could influence distant structures from the target. **(D)** If axonal pathways near the electrode are stimulated, this may influence firing rate and pattern in structures receiving these projections. **(E-G)** Altered firing patterns after DBS can be associated with increased neurotransmitter release, alterations in metabolic activity and plastic changes induced as a consequence of long-term potentiation. Figure from (Hamani & Temel, 2012)

[DSB for OCD]

The most explored RB-related disorder with DBS is OCD where it is only indicated for severe, chronic, treatment-refractory cases. Indeed, DBS for OCD is not a default therapy; it is limited in clinical use, reserved for critical cases. Nevertheless it has an FDA approval as a “humanitarian device exemption,” allowing it to advance further from experimentation to clinical use. The first uses of DBS were based on existing literature suggesting that ablation of the anterior limb of the internal capsule was an effective treatment for treatment-refractory OCD. The first DBS use in treatment-refractory OCD included bilateral implantation of electrodes in this zone in four patients and showed clinical benefit in three of them (Nuttin, Cosyns, Demeulemeester, Gybels, & Meyerson, 1999). Over time, the anterior limb of the internal capsule target migrated slowly posteriorly the ventral capsule/ ventral striatum (Vc/Vs). It seemed that, as the target was more posterior, the response rate increased and less energy was required to achieve therapeutic benefit (**Figure 23**). In these cases, effects of the DBS in OCD are thought to manifest through modulation of the white matter tracts rather than the grey matter. It has also been suggested that current spread during DBS of the ventro-caudal anterior limbs of the internal capsule to the shell of the nucleus accumbens (NaC), that is situated directly below is partly responsible for the therapeutic effects and has also become a target (Sturm et al., 2003). Indeed, neuroimaging studies indicate that its therapeutic effect involves an increase in striatal dopamine release(Figee et al., 2014), further amplifying the range of therapeutic mechanism of DBS in OCD. Other studies suggest the ventral anterior limb of the internal capsule (vALIC) as a long-term effective target for OCD DBS, these studies highlight the importance of corticolimbic connections in OCD response to DBS(Schuurman et al., 2018)

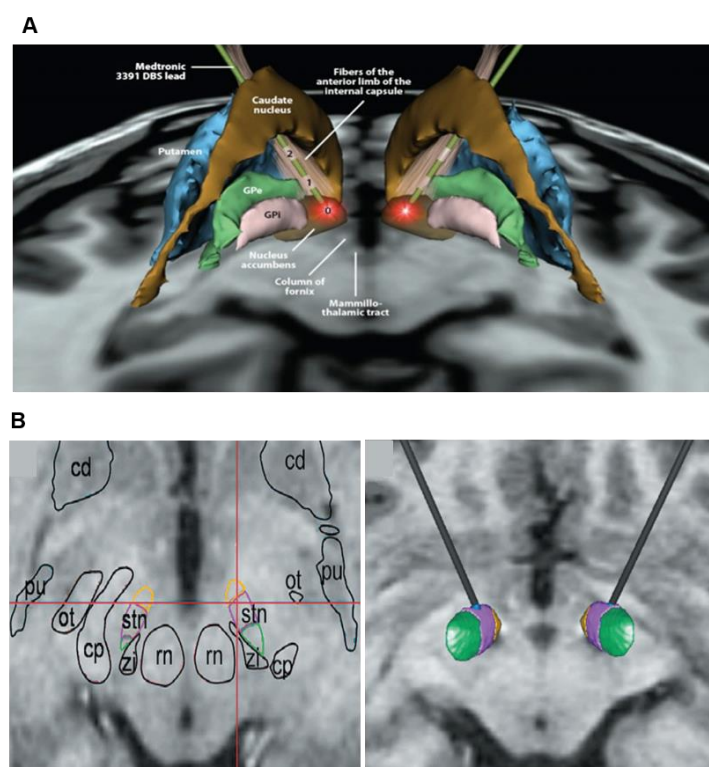


Figure 23. Localization of electrodes for different targets in DBS for OCD. (A) DBS in ventral capsule/ventral striatum, the trajectory follows the anterior limb of the internal capsule. **(B)** DBS in the anteromedial STN near the boundary between associative (violet) and limbic (yellow) territories. Figure modified from (Lapidus, Stern, Berlin, & Goodman, 2014) and (Mallet et al., 2008).

In 2002, Mallet and colleagues were published (Mallet et al., 2002) the result of the first two case reports of DBS in the Subthalamic Nucleus (STN). They implanted subthalamic electrodes to alleviate parkinsonian symptoms in patients who had Parkinson's disease and a history of severe OCD and found remarkable improvements in patients' compulsions. Years later, Mallet and colleagues confirmed with a more extensive study the therapeutic effects of STN DBS in treatment-refractory OCD (Mallet et al., 2008) **(Figure 23-B)** Although these results are encouraging, there is still no FDA approval in place for STN DBS for OCD. Years after the first DBS applications, and with different targets being tested for DBS in OCD (and other disorders), adverse events were noted, including implantation-related hemorrhage and infections. Stimulation effects were also noted, including increased anxiety or depression, mood elevation, impaired cognition and sensorimotor effects (Dougherty, 2018). The long-term effects of DBS and its interactions with neural activity are subjects that are currently under investigation and improvement.

3.1.2.2 MICRO-CIRCUITRY STIMULATION

Advances in micro-circuitry models are of significant interest in macro-circuitry stimulation, as these stimulation methods lack temporal and cellular level specificity. To overcome specificity limitations, optogenetic studies open the possibility to allow temporally and spatially precise manipulation of electrical and biochemical events using fiber-optic light in freely moving animals (Figure 24)

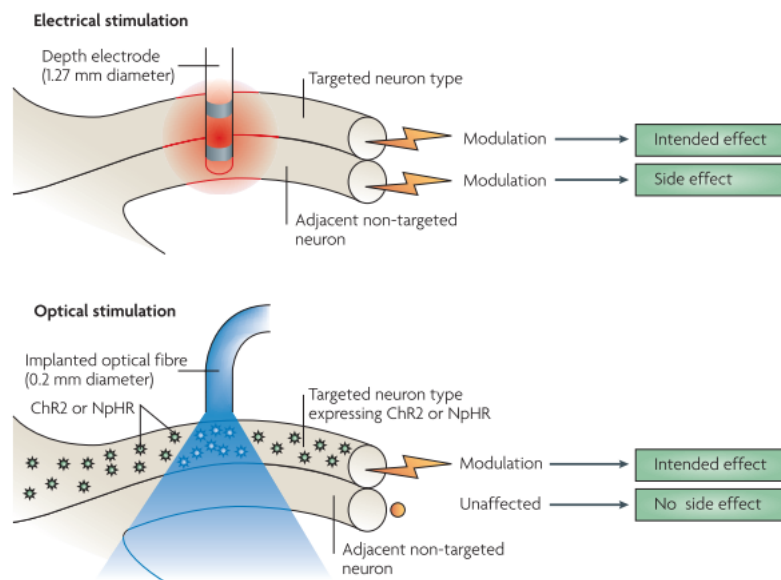


Figure 24. Effects of electrical vs. optogenetic stimulation of neural tissue. Electrical stimulation affects all cells near the electrode while optogenetic stimulation affects only the neurons genetically targeted to express the light-sensitive opsins. Image from (Warden, Cardin, & Deisseroth, 2014) and original from (Zhang et al., 2007).

3.1.2.2.1 OPTOGENETICS

The technology of optogenetics is used to control with light the activity of genetically targeted neurons. First, cells are genetically engineered to express a light-sensitive opsin, which is typically an ion channel pump, or G protein-coupled receptor. Then, after expression of the opsin, targeted cells can be illuminated with light (at the appropriate frequency) to lead to channel opening, pump activation or modulation of intracellular signaling cascades. As a result optogenetic stimulation will elicit cell depolarization or hyperpolarization, and subsequently neural silencing or activation (Guru, Post, Ho, & Warden, 2015). Cell type-specific expression can be achieved with viral vectors using cell-specific promoters, transgenic animals or a combination of both. The effect of stimulation is spatially restricted with light application, allowing for refinement in targeting a specific brain region. Temporal specificity is achieved through a variety of light patterns that allow influencing neural function optimally. This technology requires engineered control tools that can be used to target specific cells, technologies for light delivery, and methods for comparing optical control with measurable readouts such as electrical recording, fMRI

signals or quantitative behavioral analysis (Yizhar, Fenno, Davidson, Mogri, & Deisseroth, 2011).

Different optogenetic actuators can be used for fast, specific inhibition or excitation of neurons. These are proteins that modify the activity of the cell in which they are expressed when that cell is exposed to light (**Figure 25**). The most commonly used actuator are opsins, these are light-sensitive transmembrane proteins that found in a variety of organism, and that can be engineered to optimize functioning. From these opsins, we can differentiate two groups, microbial opsins, and vertebrate opsins. Opsins of both types require retinal¹³ to function. When retinal binds to the opsin, the retinal-opsin becomes light sensitive. If a photon strikes the retinal-opsin complex, its resulting photoisomerization will induce a conformational change leading to neuronal activity change. In mammalian neural tissue retinal is already present to allow the use of optogenetic tools, nevertheless in invertebrate model systems (such as *Drosophila*) a retinal supplement in the diet is necessary in order for optogenetic actuators to function (Guru et al., 2015).

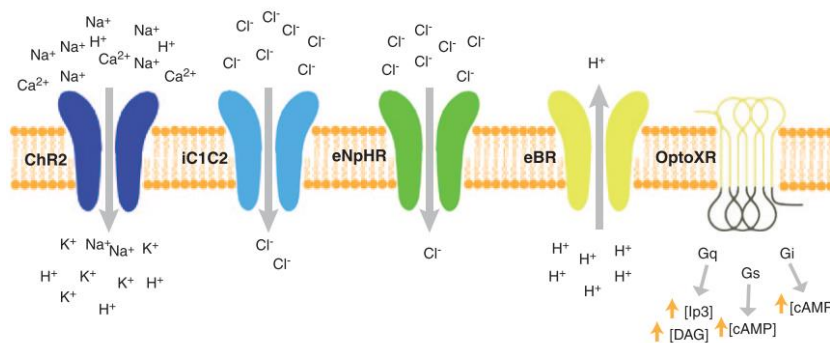


Figure 25. Optogenetic actuator families. A wide variety of opsins are nowadays available. In this figure are illustrated opsins that are used to stimulate neural activity such as the ChR2 (a cation channel), opsins that are used to inhibit neural activity such as iC1C2 (a chloride channel), eNpHR3.0 (a chloride pump), eBR (a proton pump), and to modulate intracellular signaling cascades such as OptoXR (a G-protein-coupled receptor). Image from (Guru et al., 2015)

Microbial opsins are found in eukaryotic and prokaryotic microbial organisms, including algae and bacteria, and are used for a variety of functions including navigation towards sources of energy. They are composed of single membrane-bound protein that acts as a pump or channel. Microbial opsins were first used in optogenetics experiments to control neural function because of their fast kinetics and ease of genetic engineering. Vertebrate opsins are found in animal cells and are primarily used for vision and modulating circadian rhythms (Terakita, 2005). These are G protein-coupled receptors, they initiate a signaling cascade upon activation and by consequence produce slower changes in neural activity than microbial opsins.

¹³ Retinal is one form of vitamin A. It allows certain microorganisms to convert light into metabolic energy. It isomerizes upon absorption of a photon.

In particular, the microbial light-sensitive proteins Channelrhodopsin-2 (ChR2) have been used mainly for *in-vivo* experimentation. They are cation channels that allow Na⁺ ions to enter the cell following exposure to ~ 470 nm blue light. These proteins have fast temporal kinetics, making it possible to drive trains of high-frequency action potentials *in-vivo* (Zhang et al., 2007).

There are multiple ways for efficient delivery and expression of opsin genes. A method that allows tight control over spatial localization of opsin expression is using viral vectors. In this approach, an engineered virus containing an opsin gene driven by a specific promoter is injected into the brain in a region of interest. There are different viral vectors (such as adeno-associated virus (AAV), lentivirus, rabies virus, and canine adenovirus) that can be used to target opsin gene expression in a wide range of experimental subjects from rodents to primates (Zhang et al., 2010). One way to target specific genetically defined cell classes is to use transgenic or knock-in animals that express an opsin in a particular neural population (Zhao et al., 2011). With this technic cell-specificity is conserved but spatial localization is partially lost and will depend of the light delivery site. Another alternative is the use of Cre recombinase-based mouse lines in combination with a viral vector (**Figure 26**). This last method has the advantages of being cell-type specific and being spatial specific.

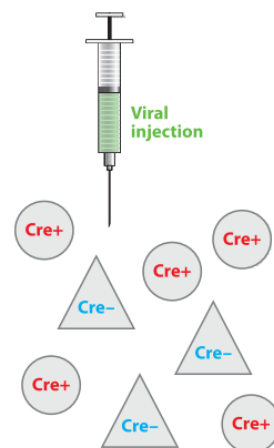


Figure 26. Cre recombinase-based mouse lines in combination with a viral vector. The combination of a transgenic mouse expressing Cre recombinase in specific neuronal subtypes and the injection of a virally encoded opsin allows neural modulation with cell, spatial and temporal specificity. Figure from (Fenko, Yizhar, & Deisseroth, 2011).

Cre recombinase-based mouse lines is a dominant strategy used nowadays to target genetically defined cell types with great spatial specificity achieved with viral vectors carrying the genes encoding specific opsins delivered stereotactically into discrete brain regions. Indeed, different types of neurons are characterized by unique gene expression patterns and can be identified based on neurochemical markers (for example Parvalbumin). This technology allows for deletions, insertions, and inversions at specific DNA sites of cells, all possible thanks to the Cre recombinase which is an enzyme that

recombines a pair of short target sequences, the loxP sites, that flank a gene or other genetic material of interest (Guru et al., 2015). However, this is not the targeting strategy, different targets can be reached using different viral strategies and methodologies for light delivery. **Figure 27** resume the different targeting strategies with optogenetics tools.

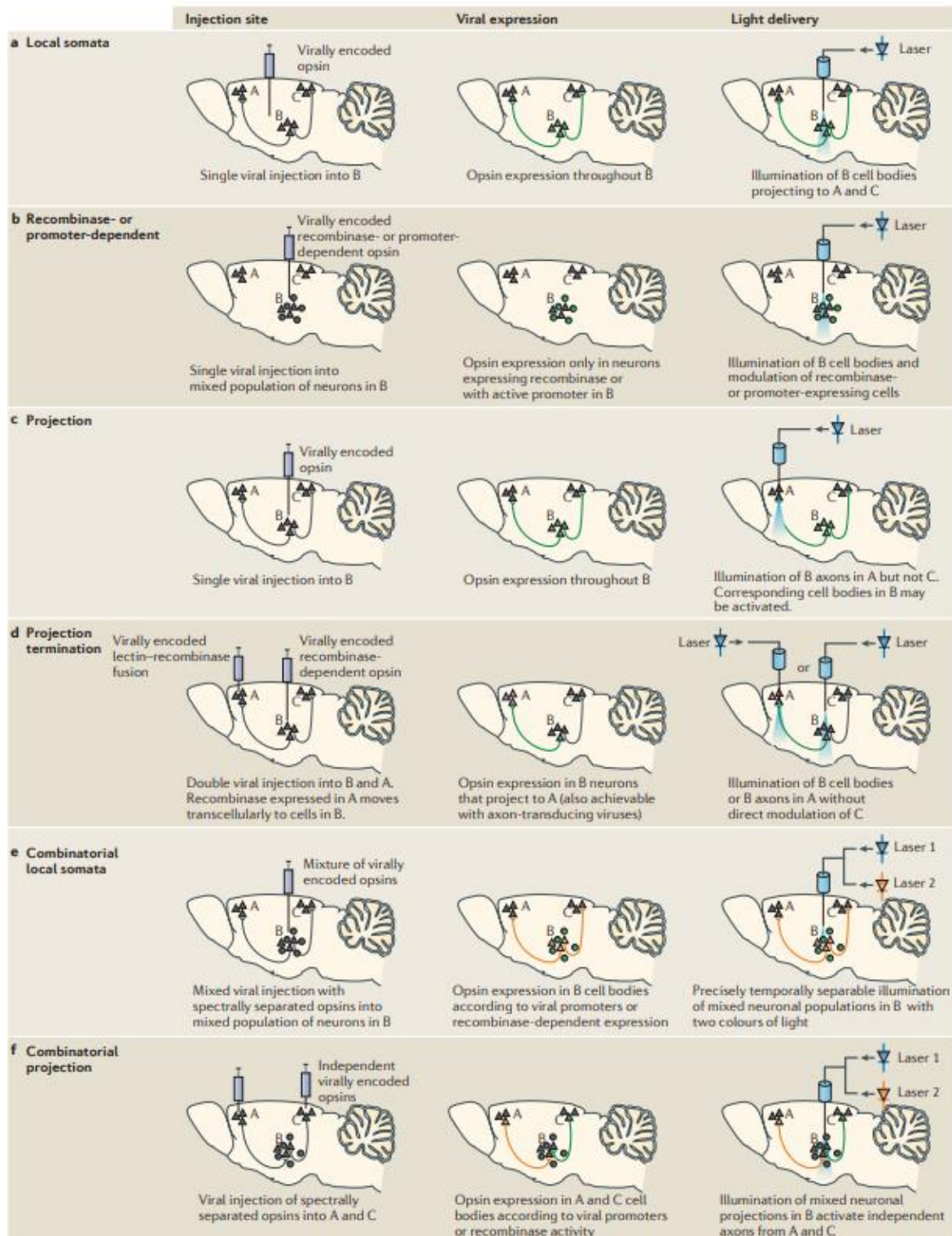


Figure 27. Different targeting strategies with optogenetic tools in vivo. (a) Neuronal cell bodies can be stimulated by injecting a viral vector into the target region and delivering light in the same region. (b) Specific expression of the

transgene in defined cell populations can be achieved by including cell-type-specific promoters within the viral vector or by injecting a recombinase-dependent virus into an animal that is engineered to express a recombinase (such as cre) in particular cell types. (c) Axonal projections can be targeted by injecting the virus at the location of neuronal cell bodies and delivering light to the target region. (d) In projection termination labelling, cells are targeted by virtue of their synaptic connectivity to the target region. In the example shown, transcellular labelling is achieved using a recombinase-dependent system. The synaptic target site is injected with a virus expressing cre that is fused to a transneuronal, and the cell body region is injected with a cre-dependent virus. This results in cells that project to the cre-injected area becoming light sensitive. Similar effects can be obtained using retrograde viruses, although these approaches do not enable control over the postsynaptic cell type. Combinatorial manipulations at either neuronal somata (e) or projections (f) can be achieved with two different optogenetic tools that respond to different wavelengths of light and by delivering multiple wavelengths of light. Figure from (Tye & Deisseroth, 2012)

In any optogenetics configuration chosen, investigators need to include the control condition of “light but not opsin” functional effect to address concerns such as tissue heating effects or long term overexpression of transgenes (Fenno et al., 2011). In order to modulate the activity of opsin expressing neurons light must be delivered to the brain region of interest, for this, there are several factors to be considered, including the intensity of the light needed to activate enough volume of tissue and the pattern of light flashes for the experimental setup. Light sources can be either lasers or Light-Emitting Diodes (LEDs). Lasers allow the application of narrow bandwidth light and the efficient coupling between light source and fiber enables high-powered illumination directly to neural tissue. Despite these advantages, lasers systems are expensive and fragile, and they might require long warm-up delay and the sound produced by the mechanical action of shutters may not be suited for behavioral experiments. LED light sources allow a narrow spectral tuning with various wavelengths. They are less expensive, smaller, and have low power requirements and but its drawback is the relatively weak light source-fiber coupling (Warden et al., 2014).

Optical neuromodulation can be coupled with a quantitative readout, such as electrical recordings or noninvasive forms of output measures, including optical imaging, positron emission tomography (PET), functional magnetic resonance imaging (fMRI) and of course through behavioral assays (Zhang et al., 2007). For the study of circuit-level mechanisms involved in neuropsychiatric disorders, it is particularly interesting to study the effects of modulation on specific cell types *in-vivo* and to quantify its effects in behavior. Indeed, for neuropsychiatric disorders that are linked to specific cell types the ability to mimic putative underactivity, or over activity of candidate neurons can be useful to test the hypothesis of exacerbating or rescuing behavioral phenotypes. In this manner, optogenetics has enabled a new generation of experiments that allow addressing the causal roles of specific neural circuit components in normal and dysfunctional behavior. In particular, there are a few studies using optogenetics in mouse models of compulsive behavior that showed how hyperactivity in the cortico-basal ganglia circuits produced an impaired behavioral performance.

3.1.2.2.2 OPTOGENETICS: THE RESCUE OF EXCESSIVE GROOMING

Eric Burguière developed an optogenetic approach to alleviate repetitive, compulsive behavior in the *SAPAP3-KO* model, a mouse model that expresses excessive grooming.

This study used a delay-conditioning task, in which a tone with a water drop was applied to the mouse's forehead to provoke a grooming response. The behavior of the mutant mice and wild-type littermates strongly varied in the course of conditioning, and the most significant result was observed later in training when wild types inhibited their early grooming to tone and responded immediately after the water-drop release, while *SAPAP3-KO* mutants kept responding to the conditioning tone. This result pointed to mutants having a selective deficit in behavioral response inhibition (**Figure 28-A**). Furthermore, they found that this deficit was associated with a defective down-regulation of striatal projection neural activity, as there was an increased firing of medium spiny neurons (MSN) in the striatum (**Figure 28-B-E**). Interestingly, in cell counts of PV-immunostained sections, they found fewer PV-positive striatal neurons in the mutants than in the wild types, suggesting its relationship to MSN hyperactivity (Burguière et al., 2013b).

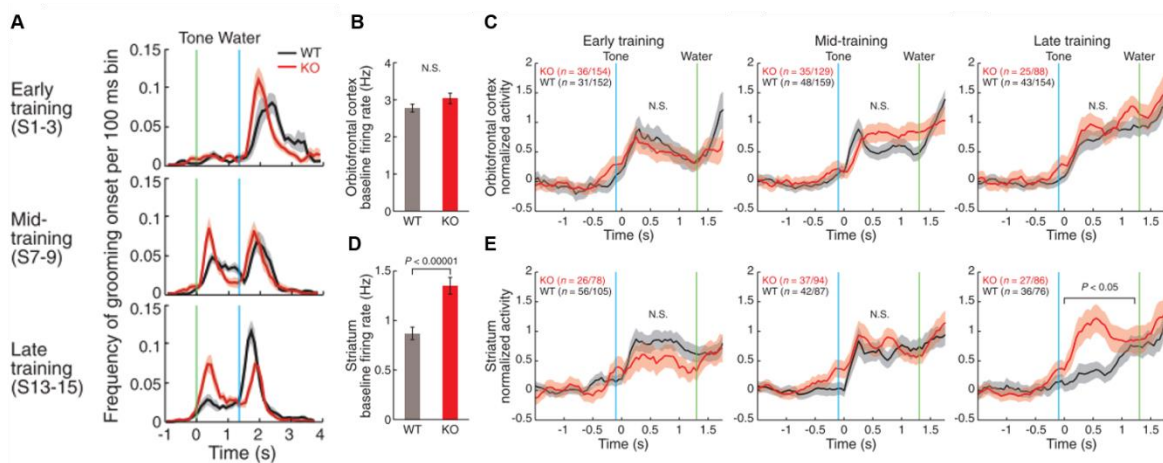


Figure 28. *SAPAP3-KO* mutant mice exhibit a deficit in response inhibition. (A) During a conditioning task, grooming onset distribution in wild types (WT) and knockout mutants (KO) in the different training phases. (B) Average baseline firing rates of IOFC and striatal (D) units. Average activity of IOFC (C) and striatal units (E) classified in the different stages of training.

Furthermore, he optogenetically stimulated either the IOFC projection neurons to the striatum or their terminals, to down-regulate the firing of MSNs of *SAPAP3-KO* mutant mice while recording striatal neurons. This effect can be explained considering one powerful source of MSN inhibition, deriving from striatal FSI, which mediate fast feed-forward inhibition of MSNs in response to cortical activation. The result of this treatment was alleviation of compulsive grooming to a regular basis, leaving other motor behaviors unaffected (**Figure 29-A**). The effects of optogenetics stimulation had an effect not only in conditioned grooming but also in spontaneous compulsive grooming (**Figure 29-B**). The treatment produced increased inhibition of striatal MSNs in the mutants, by increasing excitation of local interneurons, affecting, therefore, the FSI-MSN striatal micro circuitry.

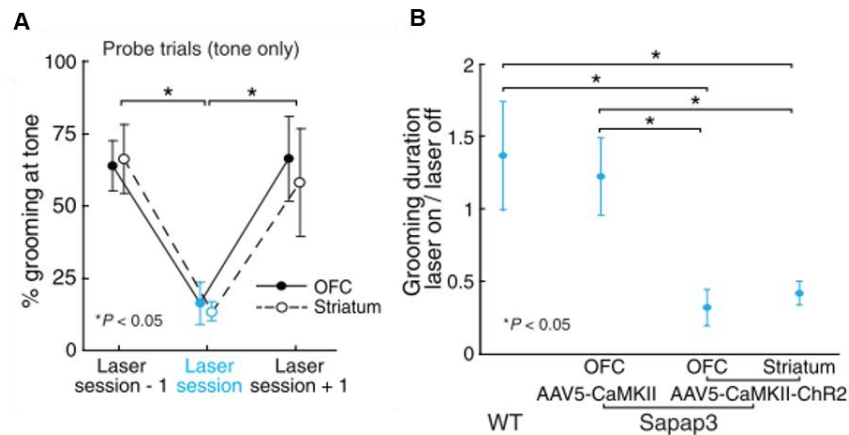


Figure 29. Optogenetic stimulation of IOFC alleviates compulsive grooming. (A) IOFC and striatal stimulation suppressed tone-evoked grooming and (B) spontaneous grooming.

With this study, he showed that involvement of the corticostriatal glutamatergic pathway in behavioral inhibition likely includes not only direct effects on corticostriatal (or other glutamatergic) synapses, but also on local intrastriatal effects on microcircuits that can modulate the efficacy of corticostriatal glutamatergic drive, pointing to FSI to play a crucial role (E. Burguiere, P.Monteiro, L.Mallet, G. Feng, 2016).

3.1.2.2.3 OPTOGENETICS: THE INDUCTION OF EXCESSIVE GROOMING

In a complementary study, another group used chronic optogenetic stimulation as a way to simulate the OFC-ventromedial striatal circuit the hyperactivity seen in OCD (Ahmari et al., 2013). In this study they targeted a different circuit than that of Burguière and colleagues and demonstrated that chronic optogenetic stimulation of the medial OFC, activating the orbitofrontal-striatal pathway, led to the emergence of compulsive behavior accompanied by a sustained increase in MSNs activity. They found causality between this hyperactivity and the onset of compulsive grooming behavior in healthy mice. They showed that by treating the mice with fluoxetine¹⁴ both, grooming behavior and the hyperactivity induced through chronic optogenetic stimulation were remediated.

These two complementary studies indicate that (1) overactive striatal activity as a critical component of the model of compulsive behavior, (2) that there is a lack of inhibitory drive in striatal micro circuitry leading to enhanced MSN spiking in this model and (3) an involvement of the corticostriatal glutamatergic pathway in behavioral inhibition. Confirmation of dysfunction in the corticostriatal circuits using optogenetics has broad implications for understanding disorders that include compulsivity as a core clinical feature. The striatal regions and microcircuit mechanisms identified by (Burguière et al., 2013b) and (Ahmari et al., 2013) have also been implicated in repetitive behaviors seen in addiction, that through drug-induced neuroplasticity become habits (Koob & Volkow,

¹⁴ Fluoxetine is a common treatment for OCD patients, it is a selective-serotonin reuptake inhibitor.

2010). The challenge now for the presented studies is to reveal which dysfunctional functions are embedded within these circuits.

Although micro circuitry stimulation techniques such as optogenetics provide a highly selective mean to control brain circuits, there are still obstacles for its use in clinical settings. These include technical issues (such as the implantation of an optical fiber), ethical and pragmatic concerns, mainly because of the use of viral vectors to express proteins in target cells that create neural sensibility to light. To fully take advantage of microcircuitry stimulation and especially of optogenetics, one approach is to use such a method in a closed-loop manner. Indeed, optogenetics allows millisecond-scale control of neural activity in defined cell types during animal behavior, therefore is well-suited for closed-loop control in behaving animals.

.

3.2 CLOSING THE LOOP

When talking about closed-loop brain stimulation different concepts and approaches emerge, this is because there is a wide diversity of approaches in which closed-loops in neuroscience can be interpreted and implemented either in clinical trials or in animal experimentation (*in-vivo* or *in-vitro*), in an invasive or non-invasive manner and using different techniques. The concept of closed-loop brain stimulation comes from the closed-loop control theory, a theory primarily used in engineering, in this theory, a closed-loop control system is designed to automatically maintain the desired output condition by comparing the actual condition (**Figure 30**). It uses an error signal that is the difference between the measured output and the desired output, to guide changes in the control system. By comparing the generated output with the actual condition, the system decides whether to take measures to correct the output of the next loop. A classic, simple example is temperature control for a house. The thermostat measures the temperature in the house and uses error-sensing feedback to turn on the heater or the AC in order to maintain a target temperature. Inherent of such system is the availability of the target (the desired temperature), system control inputs (the heater and AC on or off) and measured system outputs (measured temperature).

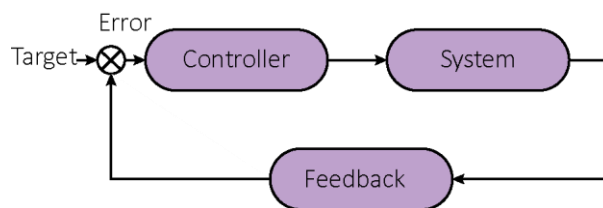


Figure 30. Closed loop control system. In a closed loop control system, the goal is to regulate a system to a desired state using a feedback loop, it involves continuously monitoring without human intervention.

Applied to neurosciences, the closed-loop neuromodulation general principle of operation uses a biophysical type of measure recorded over time and employed to regulate an externally applied stimulus to the biologic system continuously. Closed-loop control could intervene in neural circuits to achieve real-time control over neural dynamics and animal behavior and additionally could be used to generate, refine and confirm circuit-based models (Grosenick, Marshel, & Deisseroth, 2015). Cellular electrophysiology adopted closed-loop protocols and technological approaches since the invention of electronic voltage-clamp feedback amplifiers, and it was crucial for dissecting the ionic bases of the action potentials (Couto, Linaro, Pulizzi, & Giugliano, 2016). Earlier closed-loop protocols relied on custom-made analog electronic circuits and were connected to a conventional electrophysiological amplifier (Robinson & Kawai, 1993; Yarom, 1991). Many closed-loop methods found in the literature are applied to individuals, isolated neurons that through dynamic-clamp¹⁵ are used to recreate

¹⁵ Dynamic clamp is a method that uses computer simulation to introduce artificial membrane or synaptic conductance into biological neurons and to create hybrid circuits of real and model neurons (Grosenick et al., 2015).

synthetic intrinsic and synaptic conductance into living cells, or to study neuronal excitability in *in-vitro* circuits (Couto et al., 2016).

3.2.1 CLOSED-LOOP DEEP BRAIN STIMULATION

The possibility that pathological neural activity can be acquired directly from the target region using DBS electrodes has inspired a different type of paradigm: closed-loop adaptive DBS. This strategy aims at identifying pathological and physiological normal patterns of neural activity that can be used to either help adapt stimulation parameters or to deliver demand-dependent stimulation instead of continuous or random stimulation (W. Neumann, 2019). Closed-loop DBS has, through still a few studies, proved to be more effective than conventional DBS. In humans, closed-loop deep brain stimulation (DBS) paradigms have been implemented for the treatment of advanced Parkinson's disease by applying stimulation whenever recordings of LFP directly via the DBS electrodes exceeded a threshold in beta power (Little et al., 2013), since augmented beta oscillations have been identified as a marker of akinesia and rigidity (Little & Brown, 2012). In this case, adaptive DBS was more effective than open-loop DBS in improving Parkinsonian symptoms, at more than 50% reduction of stimulation time. Previous animal models studies (Rosin et al., 2011) allowed to validate the effectiveness of a closed-loop approach by providing more significant effect on akinesia than standard open-loop DBS (**Figure 31**).

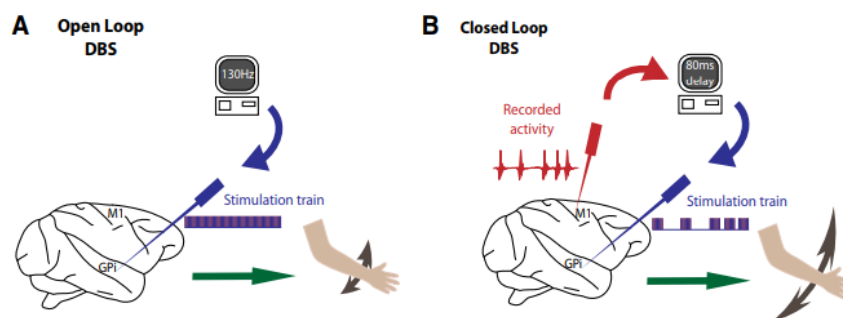


Figure 31. Illustration of an open-loop vs closed-loop DBS paradigm in PD. In this example of application, standard open-loop DBS (**A**) delivers continuous stimulation of a target structure (GPi) through an implanted electrode while closed-loop DBS (**B**) delivers stimulation depending on online activity of a reference structure (primary motor cortex M1). This results in lower stimulation frequency and promotes substantial reduction of Parkinsonian akinesia compared to standard open-loop DBS. Figure from (Santos, Costa, & Tecuapetla, 2011).

This was possible because it has been observed that with movement, high-frequency band activity in the motor cortex increases, and low-frequency band (beta) activity decreases, as it seems to be a suppressive mechanism that gates motor function. This observation has been in part, the basis for closed-loop DBS in PD.

Likewise, essential tremor (ET) is another movement disorder where closed-loop stimulation can be applied. High frequency stimulation of ventral intermediate nucleus (VIM) of the thalamus has shown clinical success in the treatment of ET (Della Flora, Perera, Cameron, & Maddern, 2010; Kumar, Lozano, Sime, & Lang, 2003). ECoG from the

hand sensory motor cortex can provide information on cortical movement intentions and be used to differentiate voluntary and involuntary movements and to drive stimulation (Herron et al., 2017), in this same study using EMG based movement-sensing system they were able to decrease the power usage by 53% at the cost of an additional 8.2% of untreated tremor. Closed-loop DBS in ET is one example of application where inertial external sensors can be used to provide control signals (Elble & McNamers, 2016).

In patients with dystonia, theta/alpha (4-12 Hz) LFP oscillations from the globus pallidus and the subthalamic nucleus are higher compared to PD patients and are associated with involuntary muscle contraction (W. J. Neumann et al., 2017). At present, these oscillations appear to be the most promising candidate for a biomarker, but other signals (EMG, ECoG and inertial sensors) and their interactions are currently being tested for a closed-loop DBS implementation (Piña-Fuentes et al., 2018). In patients with Tourette syndrome (TS) deep brain stimulation is a less established approach compared to PD, ET, and dystonia, but clinical studies are currently increasing in numbers (Martinez-Ramirez et al., 2018; Savica, Stead, Mack, Lee, & Klassen, 2012). LFPs recording from the most common target areas, the centromedian-parafascicular nucleus (CM-Pf) and the GPi (Viswanathan, Jimenez-Shahed, Baizabal Carvallo, & Jankovic, 2012) have reported exaggerated theta activity associated to motor tic severity (Maling, Hashemiyoona, Foote, Okun, & Sanchez, 2012; Priori et al., 2013). It has been shown that theta and beta activities from both target regions, could correctly predict both, motor and vocal tics scores, therefore supporting the implementation of a closed loop DBS approach (Shute et al., 2016). Closed-loop experiments in animals have also provided interesting information on the possible methodologies available. For instance, (Wu et al., 2015) provided an example of conceptualization and validation of an experiment involving closed-loop electrical stimulation. They based their experiment on previous studies of hippocampal theta oscillations related to locomotion as well as on previous results showing how electrical stimulation in the mesencephalic reticular formation (mRt) causes freezing behavior. Regarding input signals for closed-loop DBS, a recent study on the literature of adaptive DBS (Kuo, White-Dzuro, & Ko, 2018) showed that various biological signals coming from kinematic data, EEG, ECoG, LFPs and action potentials have been considered as biomarkers for closed-loop DBS. With the most straightforward approach involving an amplitude response.

When looking for “Adaptive deep brain stimulation” in the life science, search engine PubMed (**Figure 32**) the results points to an exponential tendency in the matter. Standard, current open-loop continuous DBS has already proven to be effective for PD, OCD, hyperkinetic movement disorders and is currently investigated in other pathologies such as epilepsy and drug addiction. The stimulators have been in clinical use for decades now, providing continuous invariant stimulation at a fixed amplitude, frequency and pulse width. The effectiveness of this open-loop therapy relies in great part, in the determination of stimulation parameters by a clinician (Kuo et al., 2018). Why is it then, that closing the loop around DBS seems to be a subject so appealing to clinicians and neuroscientists? We can analyze the answer to this question from two perspectives, the

relevance for therapeutic applications to improve stimulation of already found targets and to ameliorate clinical outcome and the relevance for basic research to investigate on real-time the circuits implicated in the different disorders. From a therapeutic point of view, there are many putative and already proved advantages that make the effort in developing closed-loop DBS worth it. First, chronic stimulation induces adverse effects of stimulation that could potentially be reduced with more precise short duration stimulation. These effects are partially caused by unnecessary or excessive stimulation (Glannon & Ineichen, 2016). Although DBS provide effective treatment, side effects of such therapy can be troublesome. In fact, it is the principal concern among OCD patients, even before the possibility of lack of effect on OCD symptoms (Naesstrom, Blomstedt, Hariz, & Bodlund, 2017).

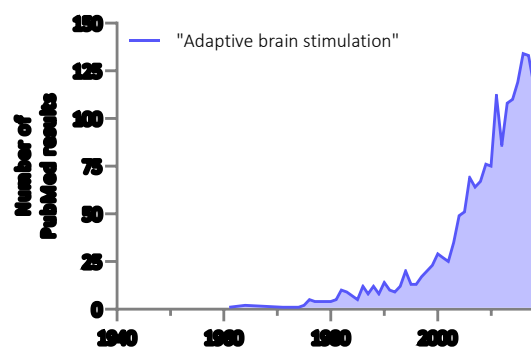


Figure 32. PubMed citations by year that include the terms “Adaptive brain stimulation.”

Second, closed-loop DBS could reduce the amount of labor programming needed. Currently, stimulation parameters are optimized through trial-and-error by a healthcare provider by systematically changing variables such as pulse width, frequency, and amplitude to find a set of parameters that provide the best outcome. Indeed, programmers and clinicians confirmed that the device is a source of an inconvenience since the tuning is far from optimal, it is not only time-intensive but also observer dependent (Glannon & Ineichen, 2016).

Since stimulation parameters are programmed into the stimulator device and set to a constant setting until the next programming session (Gross & Lozano, 1997), the approach does not take into account changes in the neural environment. Therefore it is not sensitive to the changes or fluctuations of the disordered state. Without the necessary feedback, the device cannot adjust to alterations in the brain and is therefore limited in its use. With a closed-loop approach, that takes into account the alterations in the brain that reflect the state of the disorder and therefore decide to provide or not stimulation or decide to change the stimulation setting parameters. Although there is no guarantee of the risk of unintended stimulation, it is most likely that intervention from practitioners beyond the initial programming would still be required. A synergy between engineers, neurologist and neurosurgeons is necessary since the success of the closed-loop brain stimulation approach depends mostly on this. As presented in **section 3.1** the path of DBS is highly dependent on that of the technological advances and algorithm conceptions. We

are currently living in an era in which there is a high enthusiasm in creating automatic and intelligent algorithms to solve problems, in which programming skills are now acquired at younger ages and where miniaturization of electronics becomes more impressive every year. A well-established common ground of communication, understanding and open-minded exchange between the different fields would benefit ones and others and move forward the implementation of closed-loop DBS in the different applications, so in this perspective, a particular effort is worth doing to establish regular contact and shared resources to support one another's work.

3.2.2 CLOSED-LOOP OPTOGENETICS

Classic techniques to study brain function and dysfunction are lesioning, electrical stimulation and chemical neuromodulation. These techniques are effective at the level of brain structure, but they lack a degree of selectivity and specificity. Recently advances techniques are overcoming these limits, including chemo genetic tools, optogenetics and the more recently magneto thermal neuromodulation. Here, we will focus on closed-loop neuromodulation and how optogenetics can be used to provide selective temporal and spatial feedback.

Establishing how a subgroup of neurons controls a specific behavior, or how behaviors can be modified in real-time by complex neuronal network needs sophisticated approaches enabling to drive neuronal circuit's activity with cell-precision and millisecond temporal resolution. In this sense, light sensitive opsins can be used not only to excite or inhibit targeted cell types but also to modulate specific intracellular cascades with temporal specificity.

Optogenetic techniques provide immediate, temporary control of specific cell populations using light-sensitive opsins, making them ideal candidates for on-demand control of aberrant behaviors. Indeed, as optogenetics tools become a standard method of investigating function *in-vivo* of selected neuronal cell types during specific brain states, the ability to introduce light with temporal precision in a responsive manner to state changes is becoming a very interesting approach in neuroscience. Therefore, the term "closed-loop optogenetics" has implicitly the methodology of optogenetics stimulation combined with the closed-loop theory. In closed-loop optogenetics, the control output is a time-varying light stimulus that is automatically modulated or activated based on a particular previous observation, including electrophysiological, behavioral, calcium signaling, behavior marker or other measures of activity generated by the biological system.

In neural systems, experiments involving closed-loop optogenetics allow basic-science investigations of adaptation neural state changes, plasticity and *in-vivo* tuning of stimulation parameters to achieve a specific output (Grosenick et al., 2015). It can also give pre-clinical evidence to inform next-generation neuropsychiatric prosthetics and next-control stimulation systems. They allow the investigation of short or long-term

plasticity associated with the altered activity. Monitoring targeted neural activity in a closed-loop manner, facilitates understanding the amount of activity, and level of synchrony, produced by stimulation, thereby enabling the experimenter to promote or diminish synchronous patterns or activity level depending on the experimental goal, a possibility that cannot be done using electrical stimulation (Grosenick et al., 2015). Despite the now-widespread use of optogenetics in vivo and the significant advances in real-time processing capabilities of computers, there are several barriers to take advantage of the precise spatiotemporal interventions, which are possible with optogenetics.

Because the success of a closed-loop approach depends significantly on the real-time computation, it is essential to make sure that the execution time keeps up with ongoing neural dynamics. In the light to preclinical interest, closed-loop optogenetics has given evidence in some experiments. In seizure detection and prevention, this approach has recently been used to target and optical inhibit thalamo-cortical neurons in the injured epileptic cortex of awake rats based on EEG recordings detecting seizures near onset time, successfully interrupting seizures (Paz et al., 2013). With the same goal in mind, (E. Krook-Magnuson, Szabo, Armstrong, Oijala, & Soltesz, 2014) demonstrated that closed-loop excitation of PVI in the cerebellum reduced temporal lobe seizure duration. Another interesting application of closed-loop optogenetics is in neuromuscular stimulation therapies and neuroprosthetic devices for peripheral limb control (Srinivasan, Maimon, Diaz, Song, & Herr, 2018). A recent example is sacral nerve closed-loop optogenetic stimulation to treat overactive bladder, urinary incontinence, and interstitial cystitis. In this remarkable example, the signals that are exploited online come from a biophysical sensor system based on a strain gauge that allows continues measurements of organ function.

3.2.2.1 THE CYCLE OF OPERATIONS

Closed-loop experimental protocols in neuroscience are challenging to design or implement. A closed-loop experiment requires effective online event detection, fast algorithms to drive procedures and effective stimulus or control strategies to achieve the overall goal. In this section, we inspect the standard operations and challenges necessary to implement a general framework for closed-loop approaches in behavioral experiments.

In general, closed-loop experiments require an acquisition system and a computer (or another processing system) to iteratively monitor the state of the biological system at precise intervals and respond accordingly. This means that closed-loop techniques involve some form of real-time operation within a repetitive cycle while respecting temporal constrains. This cycle runs continuously and for the duration of the experiment. Two main approaches are possible regarding real-time constrains and these depend on the experimental design. The “hard real-time” approach employs strictly constrained time intervals, and the “soft real-time” approach instead works with variable time intervals.

Hard real-time closed-loop approaches require that at each iteration of the cycle all the operations necessary to deliver a stimulus are executed within a specified time constraint. A hard-real-time system can usually guarantee a response within a timeframe. Therefore simulations of the algorithm can precisely predict the number of clocks runs that are necessary to execute the entire algorithm. The goal with this approach is not necessary to achieve high throughput but to guarantee a solid performance in fixed time. Although the previous is true, the processing time of these systems is usually measured in milliseconds or microseconds. A Hard-real-time approach requires either a computer to run a real-time operating system (RTOS) capable of executing real time operations without buffer delays (such as RTLinux, VxWorks and QNX, between others) or a real-time hardware platform (such as Field Programmable Gate Arrays (FPGA)).

Soft real-time closed-loop approaches may use conventional operating systems for which there is no guarantee of strict timing. The implementation of one approach or the other depends on the experiment, protocols that require strict sub-millisecond intervention usually require hard real-time approaches while soft or hard real-time approaches can implement protocols reacting to relative slow changing variables. In paradigms concerning cellular or network electrophysiology hard real-time approaches are more adapted for algorithms that handle single cell resolution, where spiking time detection is relevant to the performance of the closed-loop approach. Soft real-time approaches can be implemented for slow signals such as local field potentials, where changes in signals occur in the millisecond scale. Indeed, dynamical properties of neuronal responses vary on several time scales and the general requirement of reacting to changes on the millisecond timescale depends on the observations that we are interested in.

To fully exploit the potential power of closed-loop experiments, multiple steps including certain technical innovation are needed. In more details, this cycle of operations comprises three significant iterative steps: acquisition, computation, and command (**Figure 33**). In the following sections, we will focus the attention on the methodologies involving extracellular acquisition and recording of neural activity.

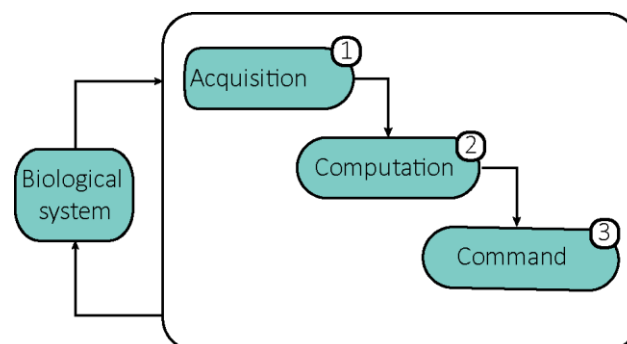


Figure 33. The cycle of operation in a closed loop approach. The continuous loop requires an acquisition phase to acquire physiological data in real-time, a computation stage to process and detect activity of interest that would activate in a last stage a feedback to the biological system.

3.2.2.1.1 ACQUISITION

Signal acquisition is the initial stage of the loop where the acquisition characteristics must be carefully defined according to the experiment as this stage will have an important impact in total processing time, memory capacities and in general in the performance of the closed loop approach. Before this stage, the choice of electrodes, headstages and acquisition interfaces should be made considering the experimental setup and the offline analysis that is meant to be done (**Figure 34**). To acquire signals reflecting the neural activity, it is possible to focus on extracellular action potentials or local field potentials (LFP) depending on the experiment. Electrical acquisition of extracellular action potentials allows after processing of the signals the isolation and identification of the neurons at single-neuron and single-spike resolution of a representative fraction of the neurons in the investigated circuits. If the recordings are done at broadband, it is possible to exploit the superimposed synaptic activity of single neurons in LFPs.

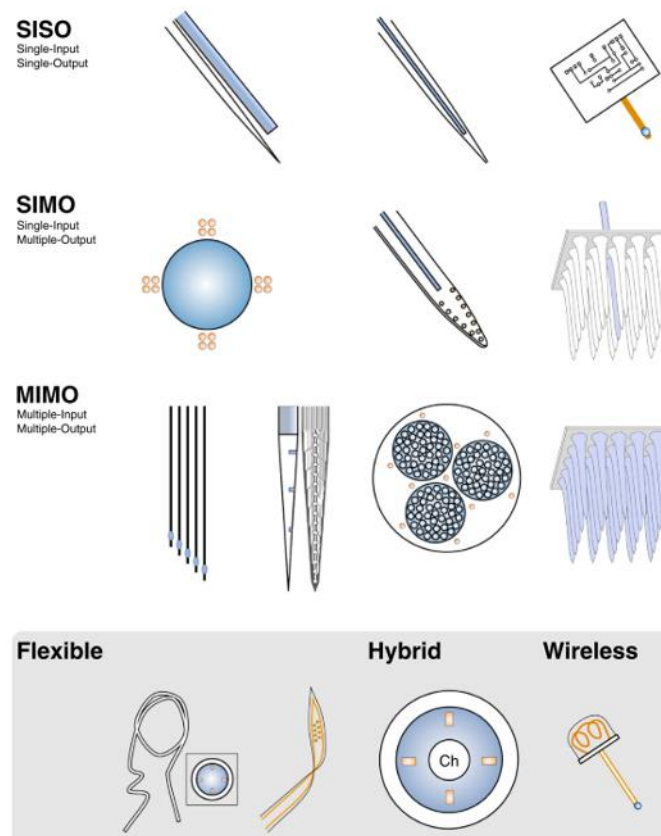


Figure 34. Recording electrodes combined with optical feedback devices for closed-loop neuromodulation. Nowadays, a variety of devices can incorporate guided light source(s) to recording electrodes, the use depend on the control strategies that are meant to be employed. The most recent are the ultrathin flexible electrodes that embed micro LEDs, the hybrid probes that allow simultaneous optical stimulation, neural recording and drug delivery and, the wireless intracranial or external skull-mounted devices.

3.2.2.1.2 COMPUTATION

In closed-loop neuromodulation efficient online algorithms are needed to provide brain stimulation depending on a previously observed neural activity or behavior. Metrics from neural or behavioral activity are used by the controller to estimate the current state of the neural system. This neural state estimate is then used as input to algorithms that compute the necessary control action (e.g., light activation or change in stimulation parameters) to correct or achieve a target activity level or pattern. When this control action is implemented, the reaction of the biological system is again recorded and analyzed, closing the loop (Grosenick et al., 2015). Control algorithms can exploit time representation (continuous or discrete) as well as domain representation (frequency versus time), it depends on the representation of the signal of interest (e.g., LFP biomarkers or a specific action potential pattern). Given that converging evidence points to abnormalities in the synchronized oscillatory activity of neurons to have a role in the pathophysiology of some psychiatric diseases (Uhlhaas & Singer, 2006), one interesting approach is considering oscillations as a direct target of closed-loop optogenetics control.

Regardless the chosen representation of data signals, a limiting factor to implement an efficient closed loop approach is the amount of data and the time that it will take to analyze and extract relevant information from it. Indeed, with the increasing advances in technology, neuroscientists and clinicians are nowadays able to acquire data in greater volume and with finer resolution. The machine learning domain can provide analysis tools to understand brain function or dysfunction (Vu et al., 2018). The term machine learning describes the subfield of computer science that investigates how computers can provide predictions, decisions or perceptions based on data and on continuous experience. Machine learning algorithms have three principal categories: supervised machine learning, unsupervised machine learning and reinforcement learning. In supervised machine learning training data has been previously labelled, usually by human experts. The goal is to learn the relationship between the data content and its labels so that the computer can predict the label of a new data item with accuracy comparable or better than human expertise. As an example, supervised machine learning algorithms have been used to predict freezing behavior in rodents from LFP signals (Karalis et al., 2016). In reinforcement learning, machines are trained to make decision through a dynamic process of trial and errors in order to maximize a desired outcome. In this case the data is not labelled to desired classes but rather, a scoring functions guide the algorithm on how well it performs. In this way, the algorithm continuously updates itself. One way to train a neuroprosthetic device to learn optical motors behaviors is by using reinforcement learning techniques (Iturrate, Chavarriaga, Montesano, Minguez, & Millán, 2015). In unsupervised machine learning the input data is not labelled. The goal is to reveal a certain structure in the data by taking into account similarity between the input data elements. A well-known example in neuroscience is Principal Component Analysis that is used for action potential sorting. A major challenge for this algorithms is dimensionality reduction that is, understanding and providing the most relevant features that best describes the observations of the scientific hypothesis. It is desire that the data provided

has the lowest dimensions without losing relevant information. Regardless of the machine learning algorithm of choice, the preprocessing of data will have a direct impact on the results.

Within the scope of this manuscript, we are interested in the online analysis of local field potentials (LFPs). Indeed, LFPs have several characteristics that allow us to extract rich information from local neuronal populations making them well suited for closed-loop experiments (El Hady, Maling, & McIntyre, 2016). This kind of signals give information of the activity of many neurons in the vicinity, capturing local dynamics that would otherwise be missed by single cell recordings. A control signal for a closed loop approach should be relatively time invariant over the life time of the stimulation device, in this sense, LFPs have the cardinal feature of being more robust and stable in comparison to chronic single cell recordings. The LFPs energy distribution over time can be a useful measure of neural activity. The extraction of this kind of features are of interest not only in the neuroscience domain but also in the speech recognition domain where the interest is also to extract relevant features and patterns from spoken signals. The speech recognition domain has provided useful algorithms for dimension reduction and features extraction. One of these methodologies is the Mel-Frequency Cepstrum (MFC) which is a representation of the short term power spectrum of a signal based on a linear cosine transform of a log power spectrum mapped on the non-linear mel-scale of frequencies. The coefficients resulting from this representation are commonly used as features in speech recognition systems as the scale of frequencies in which they are mapped approximate the human auditory system response (Davis & Mermelstein, 1980). Indeed, the human ear is better at detecting small changes in the low frequency band than in high frequencies.

In pattern recognition of neural signals the MFC could be an interesting approach to discern small variations of a low frequency band while integrating information from higher frequency bands. Since the features extracted depend on a set of filter banks, the space and arrangement can be suited for different requirements. This approach has until now been little exploited in the neurosciences field but recent studies have started to implement it and to profit from it. For example, Al-Galal and colleagues used this approach in a paradigm to recognize emotions based on EEG and ECG signals (Al-Galal, Alshaikhli, & Rahman, 2017). Because it is relatively easy to implement, we can imagine applying it on real-time devices for online analysis in closed loop neuromodulation paradigms.

Independently of the algorithm of choice, execution speed is critical for online neurostimulation applications due to the rapid changes in neural activity and behavior. Nowadays, new techniques for in-vivo imaging allow for the possibility of imaging the same circuit over multiple days with cellular resolution in behaving animals. Although these technologies provide significant advantages, their use in closed-loop applications is still under exploration. The main reasons are that these techniques are not well adapted for sub-millisecond acquisition and analysis as could be in the case of electrophysiology, they require more computationally intensive steps for acquisition and analysis. Indeed,

scanning-image reconstruction time, online image processing that includes online motion correction, cell ROI application, as well as the optical sensors themselves (rise time), together sum to seconds of delay between detecting an event and delivering stimulation. However, in anticipation, computational work has already begun to explore methods that could leave intensive steps offline to work with low-rank dynamics during experimentation. It is likely that in the following decade's closed-loop experiments integrating in-vivo imaging will be more often adopted as they allow for direct observation of a region of interest's neural population and projection dynamics.

3.2.2.1.3 COMMAND

For in-vivo experiments, exciting or inhibiting microbial opsin-expressing projections during behavior are useful for establishing necessity and sufficiency of anatomically defined cells in driving or modifying specific behaviors (Grosenick et al., 2015). A command feedback signal would ideally involve the light stimulation pattern that provides a desired excitatory output while minimizing side effects. This can be achieved by modulating light intensity, duration, and frequency, but calibration is not straightforward, online tuning and further experiments need to be done to achieve the desired activity pattern. In other words, without real-time observation of all the neural activity affected, it is not clear for most observations, including electrical and optogenetic stimulation, whether the intervention chosen to provide stronger, weaker, more or less synchronous activity in the target population than naturally occurs or if this modification is the ideal for the desired output. Indeed, usually for most of the experiments; we have only access to a limited view of the neural dynamics, however one starting strategy is to tune the stimulation to natural activity patterns in order to evoke target activity levels similar to those already observed in the same population of cells, while keeping the evoked activity within the physiological ranges. Another solution could be to use model-based approaches that describe the input-output mechanism of neurons, and that try to find the optimal stimuli to obtain precise spike trains (Ahmadian, Packer, Yuste, & Paninski, 2011).

3.3 CLOSED-LOOP APPROACH RELATED TO RB

The diversity of methods, experiments, and tools involved in adaptive brain stimulation published over the last years proves that many areas of neuroscience research are adopting a closed-loop perspective. Adaptive brain stimulation has been explored especially regarding movements disorders. Converging evidence supports the utility of beta and theta oscillatory activity as biomarkers in the hypokinetic state in Parkinson disease and hyperkinetics disorders (essential tremor, dystonia, and Tourette's syndrome) (W. Neumann, 2019).

Therapeutic effectiveness of brain stimulation for RB-related disorders has already been proven in humans (Mallet et al., 2008; Nuttin et al., 1999; Sturm et al., 2003) as well as in animal models (Burguière et al., 2013b; Pinhal et al., 2018). Although we still need to find and gather all the pieces regarding the underlying neural basis of the therapeutic effects, the principal obstacle moving forward in adaptive brain stimulation comes from finding a trustful biomarker. The lack of a validated biomarker is probably why regarding RB-pathologies, such as OCD, to date, there is no closed-loop strategy already implemented. Indeed, the golden goal is to find a signal predicting the expression of aberrant RB to deliver therapeutic stimulation only when needed.

Few studies have reported specific patterns of LFP and single unit activity in DBS indications for OCD that could eventually be of use as biomarkers of aberrant RB, these studies are summarized in **Table 3**. One of these studies, included two OCD patients implanted with a long term LFP sensing device in the subthalamic nucleus. In this study it was found that the dorsal (motor) area displayed a beta (25-35Hz) oscillatory activity similar to PD patients, while the ventral (cognitive) area displayed different theta (6.5-8Hz) oscillatory activity. This theta oscillatory activity decreased with symptom provocation and was inversely correlated with symptoms severity (Rappel et al., 2018). The authors suggested that theta activity at the ventro medial STN might be used as a biomarker for closed loop feedback control stimulation to treat OCD. They suggested that specific stimulation that increases theta activity might reduce OCD symptoms.

Other studies from intra operative recordings of STN neurons in OCD patients have converged in finding a mean low firing rate compare to PD patients (Piallat et al., 2011; M.-L. Welter et al., 2011). Welter and colleagues not only found that the mean firing rate of the subthalamic neurons was significantly lower in OCD patients compared to PD patients but also found a predominant delta band (1-4Hz) oscillatory activity in the STN associative and limbic parts which was significantly related to OCD symptoms. They reported no significant correlation between firing rate and OCD severity, suggesting that OCD symptoms are not related to a decrease in the STN neuronal firing. Additionally, compared to STN PD neurons, STN OCD neurons had a higher bursting index (longer but less frequent burst), and this was related to OCD severity (M.-L. Welter et al., 2011). Piallat and colleagues also reported a significant proportion of burst neurons found in the non-

motor STN in OCD patients. They suggested that the non-motor STN plays a role in mediating OC behavior and therefore HF DBS-STN would have an effect in altering this abnormal burst pattern (Piallat et al., 2011).

Table 3. Summary of specific relevant LFP activity for a closed-loop approach.

N	Target	Activity	Observations	Study
2	STN (motor)	β (25-35 Hz)	Similar to PD patients (Long term recordings)	(Rappel et al., 2018)
2	STN (associative/limbic)	θ (6.5 – 8 Hz)	\searrow with symptom provocation \searrow with symptom severity \nearrow (Long term recordings)	(Rappel et al., 2018)
12	STN (associative/limbic)	Single unit	\searrow Firing rate compared to PD patients \nearrow Bursting index with more prolonged but less frequent bursts.	(M.-L. Welter et al., 2011)
		δ (1-4 Hz)	\nearrow Oscillatory activity (Intraoperative recordings)	
9	STN (associative/limbic)	Single unit	\searrow Firing rate compared to PD patients \nearrow Burst neurons in the left anterior region of the STN (Intraoperative recordings)	(Piallat et al., 2011)
3	Caudate Nucleus	Single unit	\nearrow Firing rate abnormally high correlated with the presence of obsessions (evaluated by a visual analog scale).	(Guehl et al., 2008)
10	STN (associative/limbic)	Single unit	\nearrow Firing rate when doubt occurred in a verification task (Intraoperative recordings)	(Burbaud et al., 2013)
7	Centro-medial striatum	Single unit	\nearrow Firing rate of MSN in the centro medial striatum	(Burguière et al., 2013b)
	Lateral Orbitofrontal cortex		\nearrow Firing previous to over grooming (SAPAP3-KO animal model)	
24	Lateral Orbitofrontal cortex	δ , θ , β and γ	\searrow Oscillatory activity at rest (SAPAP3-KO animal model)	(Lei, Lai, Sun, Xu, & Feng, 2018)

Pathological checking is thought to be a consequence of great doubt in patients with OCD. Intraoperative recordings of STN activity during a decision making tasks revealed that checking behavior correlated with a higher STN firing rate, and this modification occurred several seconds before the patient had to check (Burbaud et al., 2013). In another study, single unit recordings from the caudate nucleus revealed a high frequency discharge of neurons and variability of inter-spike intervals between patients. This neural activity was related to the presence of obsessions during surgery assessed with a subjective obsession score using a visual analog scale. This study suggested that OCD is associated with overactivity in the caudate nucleus, nevertheless, in this study, there was no direct comparison with human subjects not suffering from OCD (Guehl et al., 2008).

Animal models studies have also contributed with interesting findings in neural activity related to abnormal RB worth being evaluated in the search of a closed-loop useful biomarker. Using the *SAPAP3-KO* animal model, Eric Burguière found abnormal baseline

firing rates of medium spiny neurons (MSN) in the centro medial striatum associated with behavioral response inhibition. Using a delay conditioning task, it was shown that there was an elevation in orbitofrontal cortex firing previous to grooming onset (Burguière et al., 2013b). In a different study in the same animal model, Huimeng Lei and colleagues recorded neural activity in the lateral orbitofrontal cortex and found reduced power in the delta, theta, beta, and gamma oscillations at rest. They suspected that this decreased power in LFP was referred to reduced synchronous activity in the IOFC (Lei et al., 2018). The previous showed interesting findings, considering that different studies in rat showed that therapeutic deep-brain stimulation of the nucleus accumbens, a DBS target for OCD, provoke an elevation of spontaneous LFP power in the same frequency bands (McCracken & Grace, 2007, 2009). Taken together, the above results point to STN oscillatory activity as an interesting source of information regarding the modulation of the cognitive and emotional aspect of OCD. Different bursting properties and low-frequency oscillatory activity in the STN might give correlated information regarding the level of inhibition of OCD symptoms or/and the severity of the symptoms. Striatal and orbitofrontal activity are also attractive candidates for biomarker's exploration. Converging studies in human patients and animal models point to augmented mean firing rate in the striatum and local network dysfunction in low-frequency oscillations in the OFC. The difference in experimental methods might explain the variability in oscillatory activity between some of the studies. Indeed, most of the previous electrophysiological recordings in OCD patients were performed either intra operatively, or in the first post-operative days and only one study included long term recordings with clinical follow-up. It might be difficult to interpret the results since DBS surgery involves considerable stress and anxiety that might alter neuronal activity. Moreover, some of those studies are limited by a small number of OCD patients, but further verification in a large sample of patients might help confirm the results. LFP activity was recorded from the implanted stimulating electrodes limiting the recording area to that of the target regions. Further studies in animal models can help explore other suspected brain regions and give more insights at the micro circuitry level.

Having reviewed the advantages and disadvantages of adaptive brain stimulation, one could ask if closed-loop DBS is the logical future for brain neuromodulation for RB-related psychiatric disorders. There is no doubt that movement disorders have opened the way to reason in an optimistic way of the effectiveness of this approach. In the case of RB-related disorders, a lot still needs to be done, including the finding of a trustful biomarker. The current open questions to address are:

- What are the neural correlates of symptoms that would allow us to implement closed-loop neuromodulation?
- Will a closed-loop neuromodulation approach for RB-related disorders have superior efficacy, compared to open-loop?

MAIN POINT SUMMARY

- An important addition to the current applications of DBS would be the development of robust translational models of RB-related disorders.
- The possibility of recording signals from the DBS electrodes opens up the prospect of developing sophisticated on-demand DBS that is customized to deliver stimulation only when needed.
- Optogenetics is a technique that is well suited for closed-loop control of neural systems since compared to other methods of neural perturbation, it allows increased temporal, regional and cellular specificity.
- Closed-loop optogenetics has the advantage, in the context of pathological behaviors, of adding symptom-related temporal specificity to show the causal significance of inhibition or excitation of a neural population related to a specific behavior.
- Until now, closed-loop optogenetics has proven its valuable input in clinically motivated experiments to quickly stop epileptic activity, in neuroprosthetics devices to restore locomotion, and to modulate learning. It could also play an essential role to lead to effective treatments of psychiatric disorders related to RB.


PART II: EXPERIMENTAL WORK

Chapter 4. BENCHMARK GENERATION OF BIO-INSPIRED NEURAL SIGNALS

SUMMARY

Building a closed-loop interaction with the nervous system require the development of automatic data analysis methods to accurately represent and integrate information to create a targeted interaction with the biological system. In this sense, cutting-edge applications of closed-loop neuromodulation take advantage of real-time or online processing of large amount of neural data. This has become possible thanks to advances in computer processing power, on-board electronics such as micro-processors and field programmable gate arrays (FPGAs). Closed-loop neuromodulation approaches have enabled to understand, modulate and interface with the nervous system in a unique way, as the variables being monitored can influence the biological system in real-time. Nevertheless, the success of this kind of paradigm depends in great part on the implementation of the signal processing algorithms, as well as of the performance of the electronic devices used. Nowadays, the evaluation and optimization of these tools is hampered by a lack of ground-truth databases of neural signals. It is desired for benchmark datasets to include the information necessary to identify the sources that generated in the first place the signals and to include the artefactual features encountered in real-applications, or otherwise a realistic evaluation of the tools will not be possible. This first chapter of the experimental work introduces an original computational approach designed to address the above limitations and is now part of a toolbox developed specifically to help better design and implement real-time closed-loop paradigms. The software presented here generates fully annotated and parametrized benchmark datasets of extracellular neural recordings, which include the integration of three components: neural signals from compartmental models and recorded extracellular action potentials, non-stationary slow oscillations, and a variety of artifacts. This software solution is flexible enough to reproduce a variety of experiments, as a demonstration we presented three examples. We reproduced *in-vivo* extracellular hippocampal multi-unit recordings from a tetrode and polytrode configurations and we showed how the simulator can reproduce ‘virtual’ neural tissue that follows the specific anatomy of a brain structure. We also reproduced experiments from *in-vivo* awake and anesthetized subjects and replicated the previously observed frequency dynamics and action potential content. Lastly, we conducted a series of simulations to study the impact on the frequency domain that artifacts can have in neural recordings. The results presented here are just a glimpse on the many applications that the benchmark dataset generator can have. In the next chapter of experimental results, we will see how it can also be used to calibrate and evaluate hardware solutions for online analysis of neural signals.

SCIENTIFIC REPORTS



OPEN

Bio-inspired benchmark generator for extracellular multi-unit recordings

Sirenia Lizbeth Mondragón-González & Eric Burguière

Received: 22 September 2016

Accepted: 23 January 2017

Published: 24 February 2017

The analysis of multi-unit extracellular recordings of brain activity has led to the development of numerous tools, ranging from signal processing algorithms to electronic devices and applications. Currently, the evaluation and optimisation of these tools are hampered by the lack of ground-truth databases of neural signals. These databases must be parameterisable, easy to generate and bio-inspired, i.e. containing features encountered in real electrophysiological recording sessions. Towards that end, this article introduces an original computational approach to create fully annotated and parameterised benchmark datasets, generated from the summation of three components: neural signals from compartmental models and recorded extracellular spikes, non-stationary slow oscillations, and a variety of different types of artefacts. We present three application examples. (1) We reproduced *in-vivo* extracellular hippocampal multi-unit recordings from either tetrode or polytrode designs. (2) We simulated recordings in two different experimental conditions: anaesthetised and awake subjects. (3) Last, we also conducted a series of simulations to study the impact of different level of artefacts on extracellular recordings and their influence in the frequency domain. Beyond the results presented here, such a benchmark dataset generator has many applications such as calibration, evaluation and development of both hardware and software architectures.

Electrical recording of extracellular action potentials is the “gold standard” technique widely used in electrophysiology¹, where the signals are exploited to correlate neural activity with a behavioural output and/or the electrophysiological consequences of brain lesions or drug infusion, etc. The emergence of novel methods for neural analysis together with high-throughput data acquisition technologies² provide new possibilities for the exploitation of brain activity at the single unit level, for example, giving instantaneous feedback for closed-loop interactions with brain circuits when abnormal neural signals are detected³. This approach has proven effective for several pathological conditions such as Epilepsy, Parkinson’s disease, or Essential Tremor^{4–7}. From a more fundamental perspective, novel algorithms have been recently proposed to process these large amounts of neural data, such as semi-automatic and automatic clustering techniques, to distinguish different neural sources in multi-unit extracellular recordings^{8–12}. In order to validate the performance and accuracy of these different algorithms or devices, reliable datasets, where the majority of the signal content is known, are essential. Ideally, this ground-truth reference should be a completely annotated and parameterised dataset, in which three levels of information should be modifiable and known in detail: the recording environment (e.g. density of active population of neurons or distance from neurons to recording sites), the population dynamics (e.g. firing rate, spike timing of each neuron and spike waveforms) and the noise content (e.g. background noise level contribution and number of artefacts).

There are several applications (Fig. 1) where using a parameterised dataset can be advantageous, ranging from algorithm design to development and evaluation of electronic devices. Moreover, parameterised datasets are needed to evaluate the efficiency of unsupervised classification algorithms. In recent years, several spike sorting algorithms have been proposed^{8–12}, however, it is difficult to assess their sorting efficiency since the datasets used to evaluate their performance were heterogeneous. These studies either used real recording datasets where all the events that constitute the signal were not known, or simulated datasets that did not include all the features encountered in real recording, such as slow oscillations and/or disturbance by artefacts. Therefore, one solution could be to use a fully annotated and parameterised dataset as a ground-truth reference to objectively assess the

Sorbonne Universités, UPMC Univ Paris 06, CNRS, INSERM, Institut du cerveau et de la moelle épinière (ICM), F-75013 Paris, France. Correspondence and requests for materials should be addressed to E.B. (email: eric.burguiere@gmail.com)

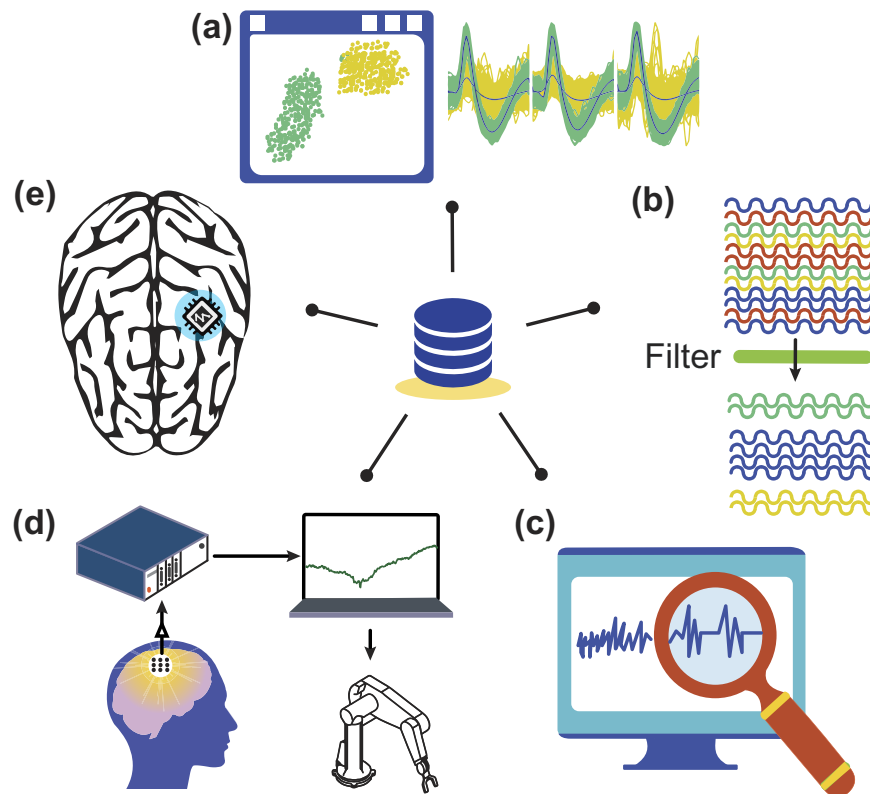


Figure 1. Examples of bio-inspired neural benchmark applications. Such benchmarks are needed in two contexts, on the one hand, in applications that involve fine signal processing usually executed on computers such as (a) neural pattern detection, (b) cluster classification algorithms and (c) signal denoising methods, and on the other hand in applications with direct exploitation of signals, usually executed on electronic devices, such as (d) brain-computer interfaces and (e) on-site decoding neural prosthetics.

performance of these different spike sorting algorithms (Fig. 1a). In the same manner, fully annotated datasets could also be used to challenge event detectors or noise reduction algorithms (Fig. 1b and c).

In addition, these benchmarks could be very useful for brain-computer interfaces and neural prosthetic devices (Fig. 1d and e). The common approach to assess the performance of such electronic devices is to use a large number of neural signal datasets that include a range of various features (e.g. different noise levels, a degree of meaningful information load, signal resolution etc.). For this purpose, parameterised datasets with independently modifiable features would allow the generation of a large variety of neural signal profiles in a controlled manner. This approach could also enable the simulation of experiments for calibration purposes instead of performing labour- and cost-intensive experiments with real subjects.

Several approaches, based either on biological or purely computational models, have been proposed¹³ to generate reliable (in terms of biological constraints), fully annotated, and flexible benchmarks. With *in-vitro* biological approaches^{14,15}, investigators have conducted simultaneous recordings to capture intracellular signals emitted by some neurons located closely to extracellular electrodes. Although this approach relies on real experimental data, the limitation is that only a few neurons could be followed by the intracellular recordings, which represent a small part of the complex signal recorded at the contiguous extracellular recording sites.

Computational approaches use either compartmental or biophysically data-driven models^{13,16–24}. The former are parameterisable but computationally too demanding when required to simulate a large number of neurons. The latter, in contrast, are computationally simpler and faster but not parameterisable given the use of signal templates.

A more recent solution is a hybrid approach, where compartmental and biophysically data-driven models are combined: while the compartmental models serve to generate the neural signal, spike template-based models, on the other hand, simulate the physiological background noise²⁵. Models based on this approach are a good compromise between complexity and bio-realism. Their great potential relies on their ability to generate a simulated signal similar to that arising from a large population of single neurons, leading to a more realistic approach. These hybrid models could be improved by adding other features found in experimental recordings such as corrupting events that could affect signal quality.

In the present study, we propose a computational procedure to generate realistic neural signals based on a hybrid model approach, in which both real and simulated signal features are combined with a relatively low computational requirement. The generated datasets are fully parameterisable and include all the original features found in real recordings such as a variety of different types of artefact and background noise. The validation stage of our procedure explores the similarity between real recordings and our model-generated signals. We show that

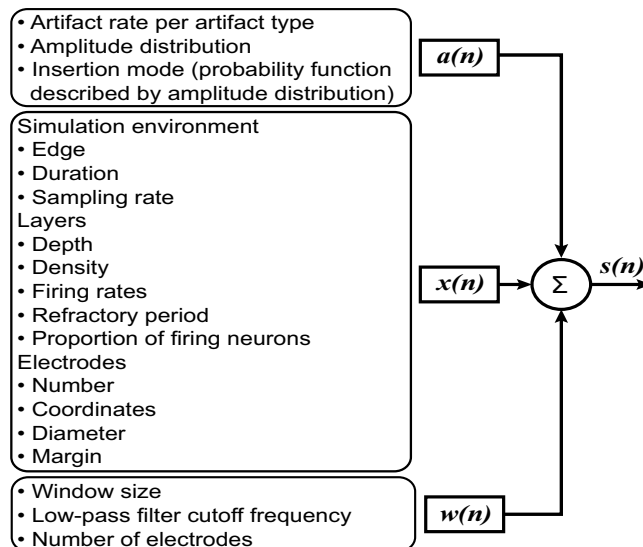


Figure 2. Configuration parameters of the benchmark dataset generator. For each computing module in the benchmark dataset generator, the user has rapid access to allow its modification through a unique file descriptor (.xml file) to easily create different datasets. The parameters are listed inside the text boxes next to each computing module.

our model is easily modifiable and generates synthetic signals similar to those obtained in distinct experimental conditions. We also illustrate the flexibility of our simulator by modelling different types of recording configuration (tetrodes and microelectrode arrays), brain tissue (such as juxtaposed layers) and experimental conditions (awake or anaesthetised animals). To validate our approach, we focus on reproducing hippocampal recording datasets that have been extensively used in previous studies^{14,26}. With our parameterisable bio-realistic procedure, we can also easily simulate different experimental conditions. As an example, we show the incidence of different levels of artefact in anaesthetised or awake animals.

Results

Creation of a three module simulator of extracellular multi-unit signals. Our work proposes a computational procedure to generate datasets that will provide neuroscientists with a ground-truth reference for algorithm and tool evaluation of single and multi-unit signal processing. In our approach, ground-truth from real and simulated signals is obtained by adding spike activity, that is, action potentials from nearby neurons and background noise from distant neurons ($x(n)$), slow oscillations (<300 Hz) from synaptic current inputs ($w(n)$) and artefacts ($a(n)$) that can be expressed as:

$$\begin{aligned} s_1(n) &= x_1(n) + w_1(n) + a_1(n) \\ &\vdots \\ s_e(n) &= x_e(n) + w_e(n) + a_e(n) \end{aligned} \quad (1)$$

In equation (1) $s_1(n)$ refers to bio-inspired simulation of electrode number 1, with n as discrete time variable and suffix e as the total number of simulated electrodes.

Figure 2 summarises the general approach and highlights the modifiable parameters in each individual computing module. The flexibility of this approach is reflected in the creation of different benchmark datasets by simply adjusting the simulation parameters.

Comparison of simulated and real extracellular hippocampal recordings. As a starting point, we created the contribution of the local spike activity to the signal. For this, we modified an existing simulation platform²⁵ designed for a single multi-electrode (i.e. tetrode) to include multiple spatially distinct recording sites. The existing simulator implements a hybrid model that combines detailed compartment models of pyramidal cells and interneurons^{18,27–31} (available via the NEURON³² project) for the closest neurons to the recording sites, coupled with spike templates for the distant neurons, all in a 3D volume of “virtual tissue” (Fig. 3a).

The initial hybrid model²⁵ that generated the spiking activity and background noise also gave the user, via a graphical interface, the option to modify various parameters to generate the datasets. These options allowed the user to select: a single electrode or a tetrode, a uniform (between a minimum and maximum firing rates) or exponential (generalised Pareto) distribution of firing rates, and a proportion of active cells inside a cubic volume. This hybrid model²⁵ was improved in our approach by including any number of recording sites with specific coordinates in a volume of “virtual tissue”. We added the possibility to simulate multiple contiguous tissue volumes (e.g. cortical layers) with individual configurations and the possibility for the user to add customised firing rate distributions by using the Distribution Fitting App in Matlab³³. These modifications gave more flexibility to the original model and enabled us to simulate different experimental scenarios. As an example, we simulated a recording

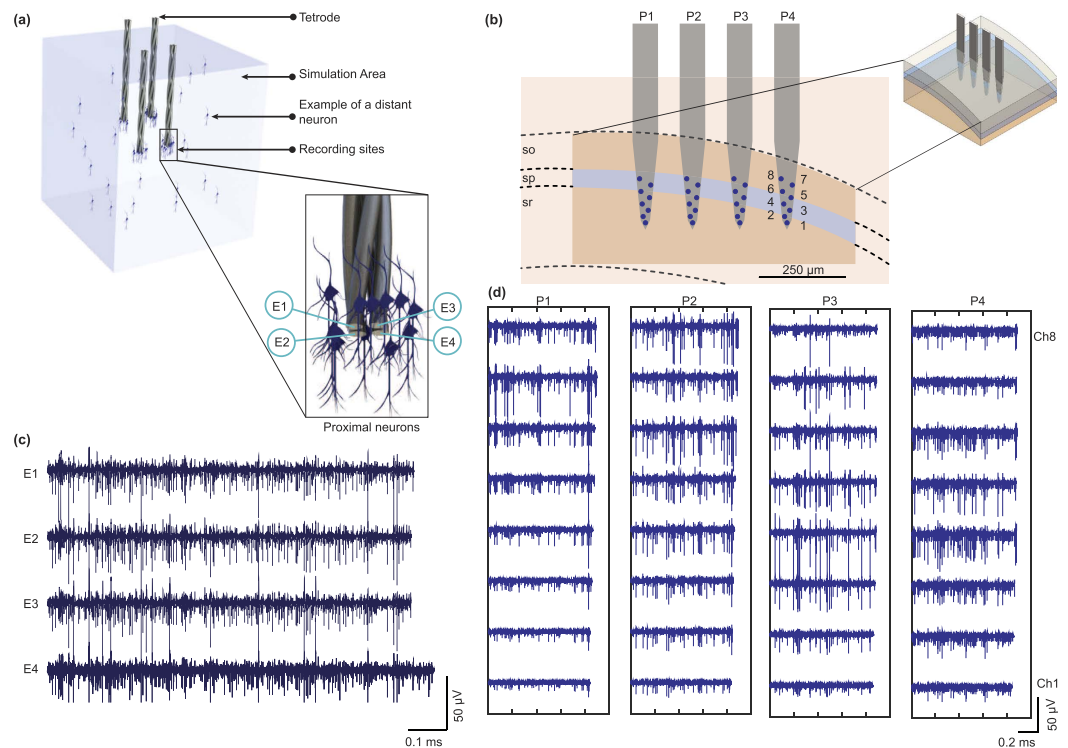


Figure 3. A data-driven model of the neural signal simulator. **(a)** The extracellular action potential simulator was modified from²⁵ to integrate several virtual recording sites (i.e. 4 tetrodes) with different configurations of hippocampal neural populations. The model computes the extracellular action potential waveforms using detailed compartment models of pyramidal cells for nearby neurons and uses action potential templates from real recordings to simulate distant neurons. The result is the contribution of close and distant neurons using the line source approximation (LSA) method⁵⁸ in a 3D virtual volume of tissue. **(b)** Modelling of a portion of virtual rat hippocampus with a 32-channel polytrode array (8 sites \times 4 shanks, dimensions follow Buszaki64 probe from NeuroNexus) superimposed across (following a stereotaxic view) the stratum radiatum (sr), stratum pyramidale (sp) and stratum oriens (so) in the CA1 region of rat hippocampus. Data for dimensions and contours of rat hippocampal regions were measured from Swanson's rat brain atlas to determine the dimensions of our volume, particularly between the atlas levels 30–35. A parasagittal view in the Figure shows atlas level 31⁵⁹ (AP = -3.70 mm relative to Bregma, ML 2–3 mm, DV 2–3 mm). **(c)** Signal samples from one extracellular virtual tetrode. **(d)** Polytrode simulation datasets over one second are shown for each virtual polytrode. The activity across channels reflects the signal location of the virtual recording sites.

Parameters	Stratum oriens	Stratum pyramidale	Stratum radiatum
Firing rate [Hz] ^{60*}	~ 0.6 Hz	~ 0.4 Hz	~ 0.2 Hz
Percentage of active neurons ⁴⁹	10	10	10
Layer thickness [μ m]	120	55	240
Population [neurons/mm ³] ⁴⁷	11 300	272 400	1 900

Table 1. Simulation parameters selected for the multilayer virtual volume experiment. A random distribution of point sources was set for this simulation. The refractory period was 2 ms, the sampling rate was 20 kHz. *The firing rate for each layer followed a probability distribution defined in Supplementary Fig. S3 centred around a certain firing rate.

session with a multi-electrode (polytrode) array in a virtual volume containing different neuronal populations in the hippocampus. We targeted the stratum oriens (SO), the stratum pyramidale (SP) and the stratum radiatum (SR) layers of the dorsal CA1 region of the rat hippocampus with a multi-array of 32 channels (8 channels \times 4 shanks). The design of the spatial distribution of the recording sites were inspired by the Neuronexus “Buzsaki64” probe design (Fig. 3b). The virtual probes were positioned so that the recording sites were present across the three different layers. The characteristics of the neuronal population in each layer (in terms of overall firing rate, proportion of active neurons and neuron density) were determined by following the results reported in previous studies. Details of the configuration parameters for this experimental condition are summarised in Table 1 and in the Methods section. As shown in Fig. 3c the recording sites with the largest action potentials follow the spatial curve of the middle striatum pyramidale layer.

The next feature of our model designed to ensure that simulations were close to real experimental signals was to add the contribution of non-stationary slow oscillations. In the real world an experimenter starts to work with unfiltered raw data before applying further analysis. Those slow oscillations usually refer to the low-frequency part of an extracellular voltage signal recorded inside the brain. We extracted slow oscillations (<300 Hz) from real datasets containing extracellular multichannel recordings made from the CA1 hippocampal region of rats^{14,26,34,35} (and added them linearly to the neural simulations as the non-stationary low-frequency components³⁶). Given that local field potential (LFP) <300 Hz can be contaminated by action potentials, we were aware that the extraction of low frequency components require a preceding exploration³⁷ on the original data to reveal the degree of spike contamination in LFP. In our case, we verified that the contribution of the spectral density of the mean spike waveform was negligible at low frequencies ($\lesssim 300$ Hz).

One element that is often omitted while developing realistic neural simulators is the inclusion of artefacts that contaminate real microelectrode recordings. In any extracellular data analysis, these undesired features should be considered, especially when it comes to unsupervised methods. Many algorithms of detection and artefact suppression have been previously reported, and they all require ground-truth data for evaluation and optimisation purposes. Hence, the inclusion of identified artefacts plays an important role in our neural database creation procedure.

For the artefact component of the benchmark generator, an artefact library was created by extracting artefact events from real data recordings^{26,38,39}. The library contains spike-like sharp artefacts, grooming artefacts and mastication artefacts identified from different *in-vivo* extracellular recording experiments. The library was organised as indicated in Supplementary Fig. S1. The identification was made following multiple validation criteria stages that include: a test for simultaneous cross-channel appearance within an artefact gap of $300\ \mu\text{s}$ in at least 80% of the total number of channels, a visual waveform inspection and a time-coincident comparison with simultaneous video recording (Fig. 4a and b), and a threshold crossing test for the spike-like sharp artefacts (thresholds selected are mentioned in Supplementary Table S1). Each artefact set a_n has between 22 and 32 template waveforms leading to identification and extraction of 40 mechanical shock artefact sets in 28 channels, 20 mastication artefact sequences in 32 channels, and 21 grooming artefact sequences in 28 channels.

The isolated mechanical shock artefacts are characterised by large peak-to-peak amplitudes (between $136.1064\ \mu\text{V} \pm 62.0262$, see details in Supplementary Fig. S2 and Supplementary Table S2) and a peak frequency region around 1000–2000 Hz (Fig. 4c and Supplementary Fig. S2). These results are in line with a study that describes the characteristics of artefacts that are regularly found in *in-vivo* neural recordings⁴⁰.

The mastication artefacts are electrical alterations of the recorded brain signals that appear during chewing events. Solid food provokes strong contractions of the jaw muscles which result in large rhythmic noisy bursts. This rhythmical oral behaviour is specific to mammals⁴¹ and can be identified across channels during electrophysiological recordings (See Supplementary Fig. S3). Characteristic rhythmic noisy bursts of the detected chewing events from rat recordings presented a mean chewing rate of 6.17 bursts/s with a mean duration of 3.3 s and a mean chewing cycle duration of 162.5 ms (see Supplementary Table S3). The identified mean chewing cycle duration results are consistent with previous studies in rat⁴¹.

Grooming artefact sequences across channels were extracted from recordings in mice in a task where they were allowed to groom freely⁴². Identified grooming artefacts appear across channels with large amplitudes and a heterogeneous duration range of ~ 0.4 –28 s. The grooming events identified (phases 1 to 4) constitute a flexible grooming chain. The beginning of each phase of stereotyped movements was annotated within the artefact sequences (Fig. 4c and Supplementary Table S3).

The complete process of database generation is summarised in Fig. 5 and consists of the summing of the following three components: (1) non-stationary low frequencies, (2) annotated and parameterised action potential simulations and (3) the addition of identified artefacts.

Generation of bio-realistic hippocampal benchmark databases in different experimental conditions. To challenge the accuracy and the performance of our model, we aimed to reproduce two types of real hippocampal extracellular multi-unit recording: in awake and in anaesthetised rodents. To mimic the macroscopic population activity of hippocampal neurons used in the real recordings, we set common parameters for both experimental conditions (i.e. those related to the recording environment such as the selected array of electrodes and those related to the simulation environment such as population density) but we differentiated two input parameters for the simulator that best approximated the dynamics of neural populations in our two distinct cases: firing rate and percentage of active neurons (Table 2 summarises the parameters chosen).

Our simulations reproduced neural signals acquired from the hippocampal layer CA1 region^{14,26,34,35}. Different numbers of artefacts were assigned to the neural signals according to each experimental condition since recorded signals in anaesthetised animals tend to be less contaminated by artefacts than in freely behaving animals. For a 10 s simulation, an artefact rate of 1% of the signal was set for the awake condition and 0.1% for the anaesthetised case.

To assess the quality of our benchmark generator, we compared our simulated signals to real recordings. A time-domain examination showed that real and simulated signals had similar profiles in terms of amplitude and action potential distribution, for the two experimental conditions (Fig. 6a). We computed the averaged periodogram of the power spectrum density (PSD) estimate based on simulated and real signals of anaesthetised and awake rodents. The results confirmed that the distribution of power versus frequency components of the recorded signal in anaesthetised or awake animals were accurately reproduced by our model since no difference could be detected between real and simulated signals (Fig. 6b).

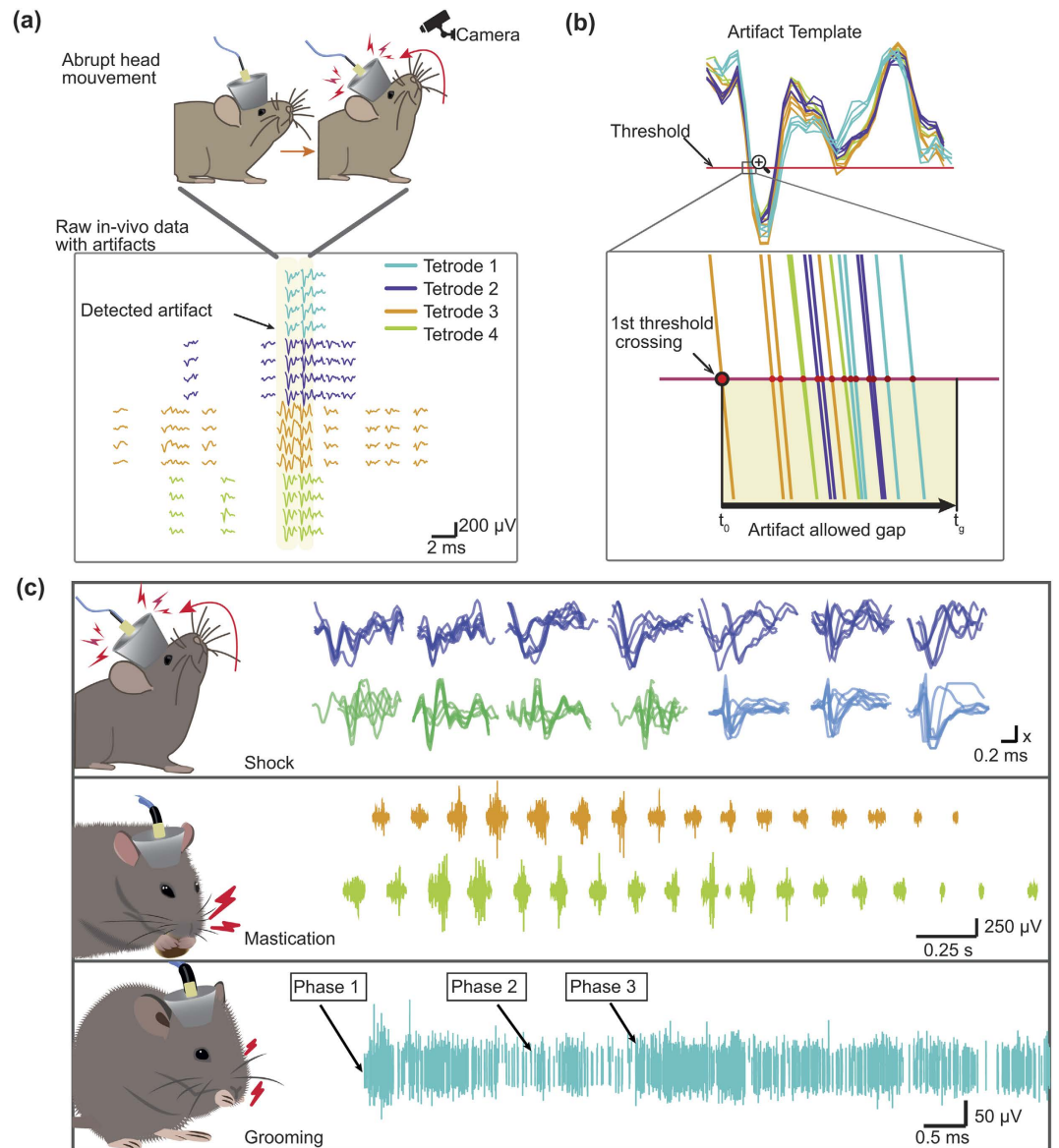


Figure 4. Artefact Library extracted from *in-vivo* real recordings. Artefact extraction is based on multiple validation criteria. (a) The artefact events were identified during unusual physical events captured by video monitoring (e.g. mechanical shock to the headstage, abrupt movement of the animal, grooming events, etc). (b) The artefacts were identified by their time-coincidence across channels ($>80\%$ of the total number of spatially distinct channels) within a width gap parameter ($300\ \mu\text{s}$) starting from the first threshold crossing. (c) The library includes spike-like noise artefacts produced mainly by electronic interference or abrupt head movement, chewing artefacts and grooming artefacts. For the head collision artefacts each set shown in the figure is a superposition of waveforms corresponding to the first channel for each of the 7 tetrodes. The x value of the vertical axis of the scale bar is $20\ \mu\text{V}$, $30\ \mu\text{V}$ and $40\ \mu\text{V}$ for the blue, green and purple waveforms respectively. Mastication artefacts follow well identified rhythmic patterns (shown in Supplementary Fig. S2). Grooming artefacts appear across channels as high level movement artefacts with variable duration (See Supplementary Table 4).

Interestingly, we could illustrate the utility of our parameterisable benchmark generator by looking at the effect at different contamination levels on electrophysiological signals. We explored the effects of application of different perturbation levels of artefacts using our annotated datasets for the two scenarios, in anaesthetised and awake subjects.

Our model predicted that the amount of artefact contamination would differentially affect the extracellular signals from anaesthetised or awake conditions. The evidence shows that, for the same level of signal contamination; the power-spectrum distribution was altered more in the anaesthetised than in the awake condition (Fig. 7). Action potentials contain a wide range of frequencies^{36,43} and the inherent higher frequencies overlap with the high frequency content of sharp artefacts which causes a growth in terms of power content in those frequency bands (as shown in Fig. 7). This phenomenon is more obvious for narrow extracellular spikes and it is easier to

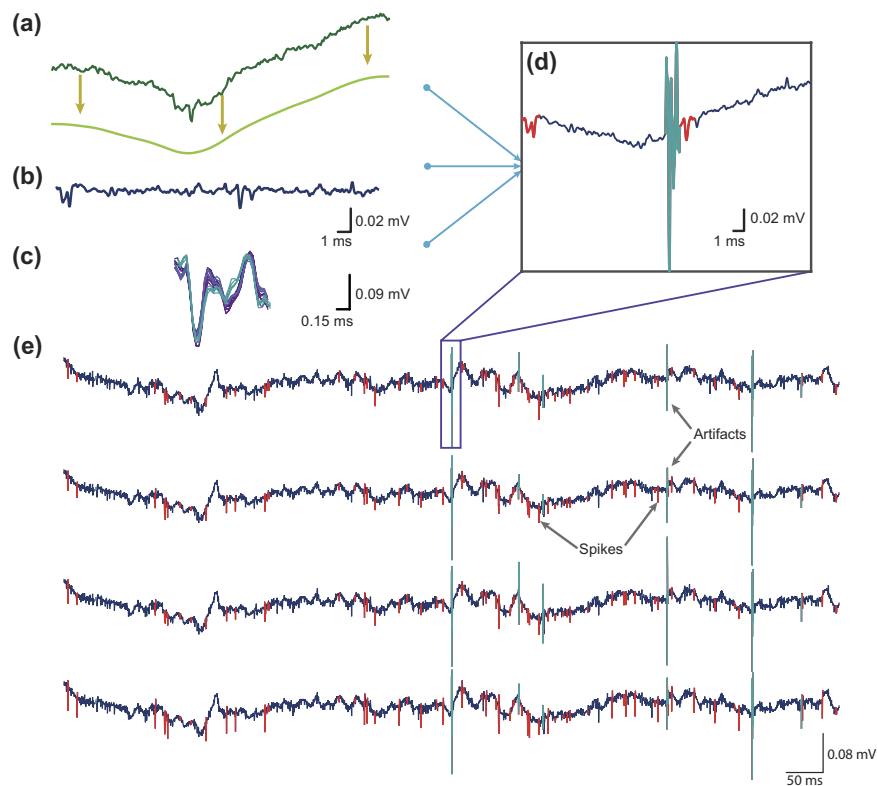


Figure 5. Generation of a ground-truth database of extracellular simulated realistic recordings. (a) Low frequencies extracted from real recordings using a Low Pass Butterworth Filter; (b) Neural data simulated from compartmental models and spike templates. (c) Annotated artefacts. (d) The addition of these three elements forms a completely parameterised benchmark. The action potentials are displayed in red and the artefacts in light blue.

Parameters	Awake	Anaesthetised
Firing rate [Hz] ^{51,61,62}	0.5–12	0.5–5
Percentage of active neurons ⁴⁹	10	4
Population [neurons/mm ³] ^{46,47}	300 000	300 000
% of artefact contamination	1	0.1

Table 2. Simulation parameters selected for both awake and anaesthetised experiments. A random distribution of point sources was set for both simulations. The refractory period was 2 ms, sampling rate was 20 kHz and the simulation duration was 10 s.

observe in contaminated recordings of anaesthetised animals, where the neural activity is lower than for the awake subject experiments.

The results confirmed that spikes and artefacts can be confused, both in amplitude and in frequency content. Thus, multiple testing that relies on other parameters should be taken into account to differentiate them, such as the extracellular spike width, wave shape and time appearance across channels.

Discussion

We are currently witnessing an exponential increase of neural data collection paradigms with massive simultaneous recordings brought forward by the progress of microfabrication techniques and integrated sensors. The collection and use of such large amounts of neural information has stimulated the development of a number of hardware and software tools. Examples are signal acquisition devices, signal processing algorithms, or software for the calibration of brain-computer interfaces. To date, despite the necessity of benchmark datasets to test these kind of applications, there are surprisingly few ground-truth datasets available, and most of these are not parameterisable. Thus, there is an urgent need of such benchmarks to assess the validity of recently developed toolboxes and algorithms aiming to analyse neural data. Evidence of this need are initiatives such as the Spike Sorting Evaluation Project⁴⁴, which aims to gather different benchmark datasets used to compare and evaluate software.

To address this issue, we developed a bio-inspired computational approach to create annotated and parameterised databases of neural signals. The innovative aspect was to combine neural signals simulated by a hybrid model with other components encountered in real recording such as artefact events and low frequency oscillations. To

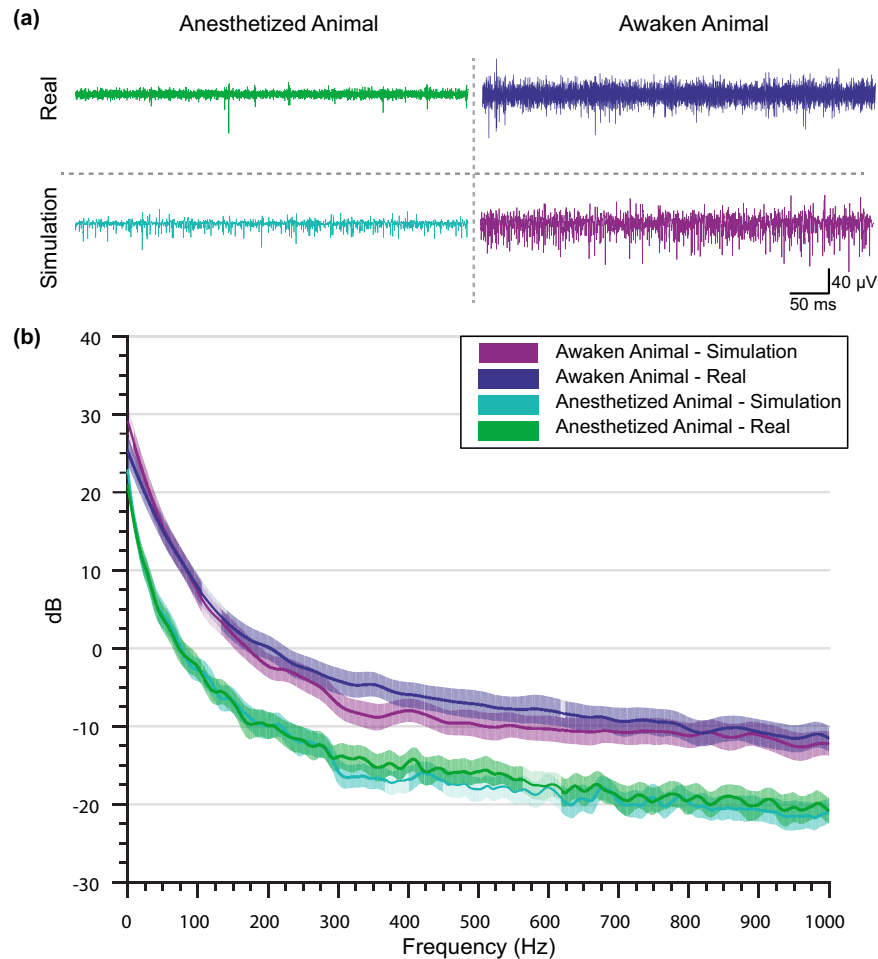


Figure 6. Inspection of simulated and real extracellular traces. (a) Qualitative comparison between real (600 Hz high-pass filtered) and simulated signals. (b) Averaged periodogram PSD estimate vs frequency for the real and simulated versions of the anaesthetised and awake versions of experiments. Low frequencies were extracted from different windows in the same recording session and linearly added to the simulated neural signals.

illustrate the flexibility of our methodology, we simulated two distinct experimental conditions; extracellular signals extracted from anaesthetised or awake rodents. We challenged our generated benchmark dataset by comparing the simulated signal with real experimental recordings.

Our results showed that the synthetic signals generated bore a close resemblance in terms of frequency properties and spike proportions to the recorded ones, and this held for our two different conditions. We showed that the addition to the simulated signal of common features encountered in real recordings (such as low frequency oscillations and artefacts) could have a significant impact on the spectral signature. Indeed, we found that the artefacts extracted tend to have a wide spectrum with dominant content at high frequencies that overlaps the neural spikes. These artefacts affect the frequency components in neural signals in different ways according to the percentage of the contamination of the signal and to the nature of the experimental setup (Figs 6 and 7).

Spectral analysis of our artefact library showed that most of the power of the signal from these events fell within the frequency range of 1000–3000 kHz. These values are similar to those shown for the power spectral density of action potential events³⁶. Taken together, these results showed that the addition of artefact events into simulated signals, an innovation of our benchmark generator, is an essential component to consider as they can drastically corrupt the frequency domain signature of spiking activity.

Additionally, we showed an application example where we simulated a polytrode array across different virtual layers of tissue. Here the aim was to demonstrate how different experimental setups could be configured independently using the same simulator and how the different generated simulations accurately captured the overall neural activity.

One application where our benchmark generator could be of great interest is for testing devices and analysis modules used in closed-loop experiments, in which a stimulus is delivered immediately after a feature of interest is detected. In this configuration, a series of devices and software analysis modules interact to form the closed-loop chain. Between the key elements of the chain, online sorting algorithms and on-chip real-time modules (e.g. Field Programmable Gate Arrays (FPGAs) and Complex Programmable logic devices (CPLDs)) are key

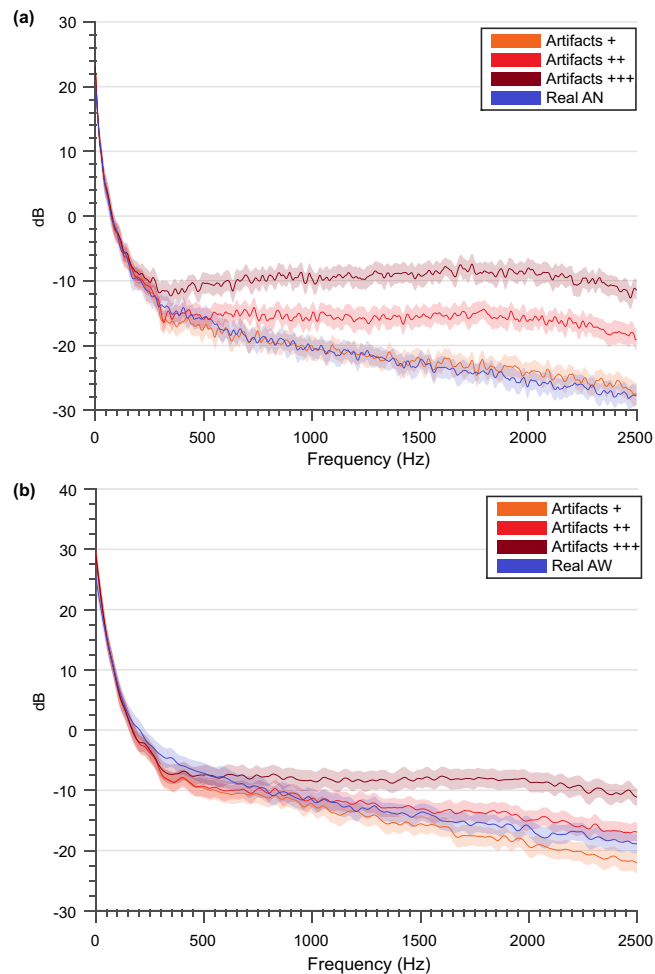


Figure 7. Averaged periodogram for simulations contaminated in different proportions. (a) Averaged periodogram PSD estimate vs frequency for the real and simulated versions of the anaesthetised paradigm. (b) Averaged periodogram PSD estimate vs frequency for the real and simulated versions of the awake paradigm. The signals (with a duration of 10 s) were contaminated with different artefact rates, starting at a contamination percentage of approximately 1% (+), subsequently 10% (++), and 57% (+++) of the signal.

elements for online analysis. To correctly evaluate and compare the performance of these systems, the use of reliable benchmark datasets, such as the ones presented here, are essential. Ideally, this should be done by generating the datasets via the simulator and streaming them directly to the acquisition systems.

The datasets generated could be useful to evaluate the performance of various tools such as denoising and pattern recognition modules or spike sorting algorithms, implemented either in hardware or software.

In the future, this fully annotated benchmark should be optimised to fit more experimental scenarios. Some parameters and features could be added or replaced depending on the experimental conditions and the cellular and physiological properties of the neural substrate chosen for simulation. For example, in our model, irregular interspike intervals reflect a random process bounded between a predefined firing-rate distribution. However, in real recordings, it is common to find some neurons that fire action potentials in a bursty mode⁴⁵. This feature could be added to the model by replacing the instantaneous firing rate with a generated probability distribution train of burst events.

One of the most challenging features to reproduce in synthetic signals is the background noise, given that there are many factors that shape it. Such disturbances can proceed from the subject itself (e.g. physiological background noise produced by the subject's activity, additive and variable sources of current from other cells that are captured by the electrodes), the recording site (e.g. dimension, neural density, whether it be a preparation or not), the electronic instrumentation and the electrodes that couple to the tissue (e.g. thermal noise, shot noise, dielectric noise), external sources (e.g. electromagnetic and electrostatic coupling between the circuitry and external devices), and from the digital conversion itself (e.g. aliasing). Although there are metrics to measure their average contribution, it is still a major challenge to replicate every source of noise. We present here a library of common artefacts found during recordings that can be used to complete the benchmark datasets.

Methods

In this section, we describe in detail the three main components of our benchmark generator.

Hybrid model for neural signal simulation. For our experiments, we fixed the parameters that define the recording environment for both setups: the simulation model was a 1.5 mm^3 cube with known randomly placed neurons with 16 recording sites and an electrode diameter of $13 \mu\text{m}$. We considered a population density of $300,000 \text{ neurons/mm}^3$ ^{46,47} for hippocampal neuronal density and a ratio of 80% pyramidal cells and 20% interneurons⁴⁸.

We set firing rate ranges based on previous studies^{49,50} for the anaesthetised and the awake cases, respectively. Firing rates of interneurons were set by multiplying pyramidal cell average firing rates by a factor of five^{51,52}, both for close and distant interneurons. The irregular interspike interval was defined by a uniform distribution bounded between a minimum and a maximum firing rate, respecting a refractory period. For both cases, anaesthetised or awake subjects, the refractory period was set at 2 ms, the sampling rate was 20 kHz and the total duration of each simulation was 10 s. The spatial distribution of the recording sites for the simulations presented here are illustrated in Supplementary Fig. S4.

Concerning our experiments, the level of artefact contamination of the signal was distinguished for the two experimental conditions, with 0.1% and 1% of the simulated signal contaminated in the anaesthetised and the awake animals, respectively. The number of artefacts for each channel recorded was defined by equation (2):

$$N_a = a_{rate} * \Delta_a \quad (2)$$

where a_{rate} is the average number of artefacts/s and Δ_a is the recording duration in seconds.

For each artefact event, a sample is added to the beginning and the end of the artefact waveform by curve fitting linear interpolation in order to smoothly add this waveform to the neural signal, this is done as follows:

$$V(t_0) = V(ts_n) + \frac{t_0 - ts_n}{t_1 - ts_n} * (V(t_1) - V(ts_n)) \quad (3)$$

where t_0 is the sample added to the beginning of the template, t_1 is the sample where the template starts, ts_n is the sample immediately preceding t_0 and $Vs(ts_n)$ corresponds to the value of that sample in μV . The set of artefacts was integrated over time following a uniform random distribution that uses the Mersenne Twister algorithm⁵³ to generate pseudo random numbers for a Uniform Distribution.

Non-stationary slow oscillations. We used a 10th order low-pass Butterworth filter applied in both the forward and reverse directions to maintain zero-phase distortion. In our design, the dataset used to extract the non-stationary slow oscillation component could be modified by the experimenter according to the nature of the signal intended to be simulated as well as the filter cut-off frequency. For our experiments, we used the real recording datasets previously reported^{14,26}, low-pass filtered with a cut-off frequency of 300 Hz. Spike contamination in this frequency band was verified according to³⁷ to have minimal effects on the extracted LFP. The resulting non-stationary extracted components were linearly added into the simulated signals.

Artefact library. To extract the artefacts and create the library, we analysed neural data recorded from several different experiments. To detect artefacts, the signal had to cross the pre-defined amplitude threshold on at least 80% of the channels simultaneously (within an artefact window of $300 \mu\text{s}$).

The head collision artefacts were recorded from mice during a behavioural task⁴². The original data consisted of seven single tetrode files recorded with a Cheetah160 Acquisition System with a total of 28 valid channels and a total recording duration of 3635.6 s. Each tetrode file is the result of a previous preprocessing analysis of the raw data, band pass filtered between 600–6000 Hz and a preset voltage threshold described in Supplementary Table S1. Individual waveforms were extracted and saved with their corresponding timestamps (Supplementary Table S1 shows the total number of detected waveforms for each tetrode file). Each waveform is $1142 \mu\text{s}$ in length with a pre-threshold period of $285 \mu\text{s}$. The data was sampled at 28 kHz and stored at 32 points per waveform with their corresponding timestamp values and 16 bit A/D resolution.

The waveforms with shapes uncharacteristic of action potentials were marked as type 3 artefacts⁴⁰ if they satisfied complementary verification methods (See Fig. 4). We created a library of 40 different sets of artefacts, where each set has between 14 and 18 artefacts recorded by the electrodes in ref. 42. In the simulation code we defined an average rate coefficient, that is, the number of artefacts/second of 1 and 10 for the anaesthetised and for the awake version of our simulations. The artefacts included present a distribution of amplitudes showed in Supplementary Fig. S2a.

To extract the grooming artefacts, the different grooming events were first identified from video recordings⁴². The different grooming phases were assigned according to a previous study⁵⁴. Identified grooming sequences were paired to the simultaneous extracellular recordings for verification of the appearance of simultaneous artefacts across channels. The different grooming phases described in ref. 54 in the syntactic behavioural chain were annotated together with the artefacts (See Supplementary Table S4) in the library.

The chewing artefacts were extracted from electrophysiological recordings in rat. In this case, the animal was moving freely in a square arena chasing solid food rewards. We explored the recordings using NeuroScope software⁵⁵ to visually identify abnormal augmented activity that stood out significantly from the background noise. We explored the data in the time-frequency domain and calculated the chewing cycle duration (1/mean chewing rate) and duration of the chewing sequence. We compared time-frequency analyses with the high-pass filtered data (300 Hz cut-off frequency) (See Supplementary Fig. S2).

Real databases. The reference neural databases for real signals were recorded from separate groups of awake and anaesthetised animals^{14,26,34,35,38}.

Case 1: Anaesthetised subjects. Real data consists of extracellular recordings in the hippocampus of anaesthetised rat^{14,34,35} with experimental procedures fully described previously^{27,35} and have been used by various laboratories as a benchmark for spike sorting algorithms. Animals (Sprague-Dawley rats) were anaesthetised with urethane (1.5 g/kg; Sigma). Extracellular electrodes were lowered into the CA1 layer of the hippocampus by monitoring for the presence of single unit activity.

Case 2: Awake subjects. The datasets include multichannel extracellular recordings from layer CA1 of the right dorsal hippocampus of Long-Evans rats during an open field task. In the task, the animal was placed on an elevated square platform and was looking actively for water rewards. Full details of the surgical and experimental procedures in awake recording were previously reported^{26,45} and are only briefly described here.

Multi-layer simulation. The overall firing rate distributions of the SO, SP and SR layers were described in a previous study⁴⁵ and reproduced here (see Supplementary Fig. S5), using the Matlab Distribution fitting tool³³ with a logistic distribution and the following mean and scale parameters:

$$\begin{aligned}\mu_{so} &= -0.470 & \sigma_{so} &= 0.278 \\ \mu_{sp} &= -0.288 & \sigma_{sp} &= 0.257 \\ \mu_{sr} &= -0.420 & \sigma_{sr} &= 0.27\end{aligned}$$

Statistical analysis. We computed the Bartlett's power spectrum density estimation (PSD) method⁵⁰ of simulated and real signals to reduce the variance introduced by the periodogram while maintaining the frequency resolution⁵⁶. The original benchmark datasets of 10 s duration were split into 10 non-overlapping 1 s length data segments. For each data segment we computed the periodogram using the discrete Fourier transform (see equation (4)), where $s_{1,1}$ is the data segment 1 from recorded signal from electrode 1).

$$\begin{cases} S_{1,1}(f) = \frac{\Delta t}{N} \left| \sum_{n=0}^{N-1} s_{1,1}(n) e^{-i2\pi n \Delta t f} \right|^2 \\ \frac{-1}{2\Delta t} < f < \frac{1}{2\Delta t} \end{cases} \quad (4)$$

We then averaged the result of the periodograms for the 10 non-overlapping data segments:

$$P_1(f) = \frac{1}{10} \sum_{l=1}^{10} S_{1,l}(f) \quad (5)$$

We finally computed the standard error of the mean by computing the segment standard deviation divided by the square root of the sample size. We performed the local fitting on the averaged result to smooth the data and used the weighted linear least squares and 2n degree polynomial method⁵⁷ with a span of 1% of the data.

Further information. Neural recording data from *in-vivo* rodents was used to assess the quality of our simulator. These datasets were available from previous studies which have been approved by the Institutional Animal Care and Use Committee of Rutgers University^{34,35}. From these studies, we used the datasets "hc1"¹⁴ and "hc2"²⁶ that have been made available to the community.

Software access. Matlab code for generation and use of datasets described here, as well as the artefact library are available at <http://bebgtteam.net/resources>. As previously described, the design is fully modifiable to simulate any specific experimental scenario that the experimenter wants to reproduce (e.g., amount of signal contaminated with artefacts, number of electrodes, distance between electrodes, etc.). To facilitate changes of the model, an XLM file and a Matlab configuration file are available where all the parameters can be rapidly modified.

References

- Scanziani, M. & Häusser, M. Electrophysiology in the age of light. *Nature* **461**, 930–939 (2009).
- Buzsáki, G. *et al.* Tools for Probing Local Circuits : High-Density Silicon Probes Combined with Optogenetics. *Neuron* doi: 10.1016/j.neuron.2015.01.028 (2015).
- Krook-Magnuson, E., Gelinás, J. N., Soltesz, I. & Buzsáki, G. Neuroelectronics and Biooptics. *JAMA Neurol.* **72**, 823 (2015).
- Krook-magnuson, E., Gelinás, J. N., Soltesz, I. & Buzsáki, G. Neuroelectronics and Biooptics: Closed-Loop Technologies in Neurological Disorders. *JAMA Neurol.* 1–7, doi: 10.1001/jamaneurol.2015.0608 (2015).
- Sun, F. T. & Morrell, M. J. *Closed-loop Neurostimulation : The Clinical Experience.* 553–563, doi: 10.1007/s13311-014-0280-3 (2014).
- Rosin, B. *et al.* Closed-loop deep brain stimulation is superior in ameliorating parkinsonism. *Neuron* **72**, 370–384 (2011).
- Brocard, F. D. *et al.* Closed-loop brain-machine-body interfaces for noninvasive rehabilitation of movement disorders. *Ann. Biomed. Eng.* **42**, 1573–1593 (2014).
- Hagen, E. *et al.* Spiking activity for evaluation of spike-sorting algorithms. **6**, 1–23 (2015).
- Friedman, A., Keselman, M. D., Gibb, L. G. & Graybiel, A. M. A multistage mathematical approach to automated clustering of high-dimensional noisy data. *Proc. Natl. Acad. Sci.* **2015**, 201503940 (2015).
- Franke, F., Quiñero, R., Hierlemann, A. & Obermayer, K. Bayes optimal template matching for spike sorting – combining fisher discriminant analysis with optimal filtering. *J. Comput. Neurosci.* **38**, 439–459 (2015).

11. Matthews, B. A. & Clements, M. A. Spike Sorting by Joint Probabilistic Modeling of Neural Spike Trains and Waveforms. **2014** (2014).
12. Quiroga, R. Q., Nadasdy, Z. & Ben-Shaul, Y. Unsupervised spike detection and sorting with wavelets and superparamagnetic clustering. *Neural Comput.* **16**, 1661–87 (2004).
13. Thorbergsson, P. T., Garwicz, M., Schouenborg, J. & Johansson, A. J. Computationally efficient simulation of extracellular recordings with multielectrode arrays. *J. Neurosci. Methods* **211**, 133–144 (2012).
14. Henze, D. A., Harris, K. D., Borhegyi, Z., Csicsvari, J., Mamiya, A., Hirase, H., Sirota, A. & Buzsáki, G. Simultaneous intracellular and extracellular recordings from hippocampus region CA1 of anesthetized rats. doi: <http://dx.doi.org/10.6080/K02Z13FP> (2009).
15. Wehr, M., Pezaris, J. S. & Sahani, M. Simultaneous paired intracellular and tetrode recordings for evaluating the performance of spike sorting algorithms. *Neurocomputing* **26–27**, 1061–1068 (1999).
16. Lewicki, M. S. Bayesian Modeling and Classification of Neural Signals. *Neural Comput.* **6**, 1005–1030 (1994).
17. Pouzat, C., Mazor, O. & Laurent, G. Using noise signature to optimize spike-sorting and to assess neuronal classification quality. *J. Neurosci. Methods* **122**, 43–57 (2002).
18. Gold, C., Henze, D. A. & Koch, C. Using extracellular action potential recordings to constrain compartmental models. *J. Comput. Neurosci.* **23**, 39–58 (2007).
19. Martinez, J., Pedreira, C., Ison, M. J. & Quian Quiroga, R. Realistic simulation of extracellular recordings. *J. Neurosci. Methods* **184**, 285–293 (2009).
20. Thorbergsson, P. T. *et al.* Spike library based simulator for extracellular single unit neuronal signals. *Conf. Proc. IEEE Eng. Med. Biol. Soc.* **2009**, 6998–7001 (2009).
21. Einevoll, G. T., Franke, F., Hagen, E., Pouzat, C. & Harris, K. D. Towards reliable spike-train recordings from thousands of neurons with multielectrodes. *Current Opinion in Neurobiology* **22**, 11–17 (2012).
22. Lindén, H. *et al.* LFPy: a tool for biophysical simulation of extracellular potentials generated by detailed model neurons. *Front. Neuroinform.* **7**, 41 (2013).
23. Lindén, H. *et al.* Modeling the spatial reach of the LFP. *Neuron* **72**, 859–872 (2011).
24. Parasuram, H. *et al.* Computational modeling of single neuron extracellular electric potentials and network local field potentials using LFPsim. *Front. Comput. Neurosci.*, doi: [0.3389/fncom.2016.00065](https://doi.org/10.3389/fncom.2016.00065) (2016).
25. Camuñas-Mesa, L. a. & Quiroga, R. Q. A detailed and fast model of extracellular recordings. *Neural Comput.* **25**, 1191–212 (2013).
26. Mizuseki, Kenji, Anton, Sirota & Pastalkova Eva, B. G. Multi-unit recordings from the rat hippocampus made during open field foraging. doi: <http://dx.doi.org/10.6080/K0Z60KZ9> (2009).
27. Gold, C., Henze, D. a, Koch, C. & Buzsáki, G. On the origin of the extracellular action potential waveform: A modeling study. *J. Neurophysiol.* **95**, 3113–3128 (2006).
28. Rudolph, M., Pelletier, J. G., Paré, D. & Destexhe, A. Characterization of synaptic conductances and integrative properties during electrically induced EEG-activated states in neocortical neurons *in vivo*. *J. Neurophysiol.* **94**, 2805–21 (2005).
29. Destexhe, A., Contreras, D., Steriade, M., Sejnowski, T. J. & Huguenard, J. R. *In vivo*, *in vitro*, and computational analysis of dendritic calcium currents in thalamic reticular neurons. *J. Neurosci.* **16**, 169–85 (1996).
30. Contreras, D., Destexhe, a. & Steriade, M. Intracellular and computational characterization of the intracortical inhibitory control of synchronized thalamic inputs *in vivo*. *J. Neurophysiol.* **78**, 335–350 (1997).
31. Huguenard, J. R. & Prince, D. A. A novel T-type current underlies prolonged Ca (2+) -dependent burst firing in GABAergic neurons of rat thalamic reticular nucleus. *J. Neurosci.* **12**, 3804–3817 (1992).
32. Hines, M. L. & Carnevale, N. T. The NEURON simulation environment. *Neural Comput.* **9**, 1179–1209 (1997).
33. The MathWorks, I. Matlab and Distribution Fitting App Release 2016a.
34. Harris, K. D., Henze, D. A., Csicsvari, J., Hirase, H. & Buzsáki, G. Accuracy of tetrode spike separation as determined by simultaneous intracellular and extracellular measurements. *J. Neurophysiol.* **84**, 401–414 (2000).
35. Henze, D. A. *et al.* Intracellular features predicted by extracellular recordings in the hippocampus *in vivo*. *J. Neurophysiol.* **84**, 390–400 (2000).
36. Fee, M. S., Mitra, P. P. & Kleinfeld, D. Variability of extracellular spike waveforms of cortical neurons. *J. Neurophysiol.* **76**, 3823–33 (1996).
37. Waldert, S., Lemon, R. N. & Kraskov, A. Influence of spiking activity on cortical local field potentials. *J. Physiol* **591**, 5291–303 (2013).
38. Mizuseki, Kenji, Anton, Sirota & Pastalkova Eva, B. G. Theta oscillations provide temporal windows for local circuit computation in the entorhinal hippocampal loop. *Neuron* **18**, 1199–1216 (2009).
39. Burguière, E., Monteiro, P., Feng, G. & Graybiel, A. M. Optogenetic Stimulation of Lateral. *Science (80-)*. **340**, 1243–1246 (2013).
40. Islam, M. K., Rastegarnia, A., Nguyen, A. T. & Yang, Z. Artifact characterization and removal for *in vivo* neural recording. *J. Neurosci. Methods* **226**, 110–123 (2014).
41. Gerstner, G. E. & Gerstein, J. B. Chewing Rate Allometry Among Mammals. *J. Mammal.* **89**, 1020–1030 (2008).
42. Burguière, E., Monteiro, P., Feng, G. & Graybiel, A. M. Optogenetic stimulation of lateral orbitofronto-striatal pathway suppresses compulsive behaviors. *Science* **340**, 1243–6 (2013).
43. Pettersen, K. H. & Einevoll, G. T. Amplitude variability and extracellular low-pass filtering of neuronal spikes. *Biophys. J.* **94**, 784–802 (2008).
44. Franke, F. *et al.* Spikesorting Evaluation. (2012).
45. Mizuseki, K., Diba, K., Pastalkova, E., Buzsáki, G. & Buzsaki, G. Hippocampal CA1 pyramidal cells form functionally distinct sublayers. *Nat. Neurosci.* **14**, 1174–1181 (2011).
46. Boss, B. D., Turlajski, K., Stanfield, B. B. & Cowan, W. M. On the numbers of neurons in fields CA1 and CA3 of the hippocampus of Sprague-Dawley and Wistar rats. *Brain Res.* **406**, 280–7 (1987).
47. Aika, Y., Ren, J. Q., Kosaka, K. & Kosaka, T. Quantitative analysis of GABA-like-immunoreactive and parvalbumin-containing neurons in the CA1 region of the rat hippocampus using a stereological method, the disector. *Exp. Brain Res.* **99**, 267–76 (1994).
48. Markram, H. *et al.* Interneurons of the neocortical inhibitory system. *Nat Rev Neurosci* **5**, 793–807 (2004).
49. Shoham, S., O'Connor, D. H. & Segev, R. How silent is the brain: Is there a 'dark matter' problem in neuroscience? *J. Comp. Physiol. A Neuroethol. Sensory, Neural, Behav. Physiol.* **192**, 777–784 (2006).
50. Bartlett, M. S. Smoothing Periodograms from Time-Series with Continuous Spectra. *Nature* **161**, 686–687 (1948).
51. Marshall, L. *et al.* Hippocampal pyramidal cell-interneuron spike transmission is frequency dependent and responsible for place modulation of interneuron discharge. *J. Neurosci.* **22**, RC197 (2002).
52. Ison, M. J. *et al.* Selectivity of pyramidal cells and interneurons in the human medial temporal lobe. *J. Neurophysiol.* **106**, 1713–21 (2011).
53. Matsumoto, M. & Nishimura, T. Mersenne twister: a 623-dimensionally equidistributed uniform pseudo-random number generator. *ACM Trans. Model. Comput. Simul.* **8**, 3–30 (1998).
54. Kalueff, A. V. *et al.* Neurobiology of rodent self-grooming and its value for translational neuroscience. *Nat. Rev. Neurosci.* **17**, 45–59 (2015).
55. Hazan, L., Zugaro, M. & Buzsáki, G. Klusters, NeuroScope, NDManager: A free software suite for neurophysiological data processing and visualization. *J. Neurosci. Methods* **155**, 207–216 (2006).
56. Kale, R. U., Ingale, P. M., Murade, R. T. & Sayyad, S. S. Comparison of Quality Power Spectrum Estimation (Bartlett, Welch, Blackman & Tukey) Methods. *Int. Journal Sci. Mod. Eng. I*, 28–31 (2013).

57. Cleveland, W. S. Robust Locally Weighted Regression and Smoothing Scatterplots. *J. Am. Stat. Assoc.* **74**, 829–836 (1979).
58. Holt, G. R. & Koch, C. Electrical interactions via the extracellular potential near cell bodies. *J. Comput. Neurosci.* **6**, 169–184 (1999).
59. Swanson, L. W. *Brain Maps: Structure of the Rat Brain.* (2004).
60. Mizuseki, K., Diba, K., Pastalkova, E. & Buzsáki, G. Hippocampal CA1 pyramidal cells form functionally distinct sublayers. *Nat Neurosci* **14**, 1174–1181 (2011).
61. Mercer, L. F., Remley, N. R. & Gilman, D. P. Effects of urethane on hippocampal unit activity in the rat. *Brain Res. Bull.* **3**, 567–70 (1978).
62. Buzsáki, G. & Mizuseki, K. The log-dynamic brain: how skewed distributions affect network operations. *Nat. Rev. Neurosci.* **15**, 264–78 (2014).

Acknowledgements

We thank Luis Alejandro Camuñas-Mesa and Rodrigo Quian Quiroga for sharing their simulator for detailed neuron models on the dedicated website <http://www2.le.ac.uk/centres/csn/software/neurocube>. We would like to thank Mizuseki K., Sirota A., Pastalkova E. György Buzsáki, Darrel A. Henze, Hajime Hirase, Zsolt Borhegyi, Jozsef Csicsvari, Akira Mamimya and Kenneth D. Harris for sharing their hc-1 and hc-2 datasets through the Collaborative Research in Computational Neuroscience (CRCNS) data sharing platform. We would like to extend our thanks to Brian Lau for scientific advice and to Christiane Schreiwies whose comments greatly improved this manuscript. The research leading to these results received funding from the programmes “Investissements d’avenir” ANR-10-IAIHU-06, from the CONACYT graduate programme fellowship and from the CARNOT institute.

Author Contributions

S.L.M.G. and E.B. designed the experiments, S.L.M.G. performed the experiments, S.L.M.G. and E.B. wrote the manuscript.

Additional Information

Supplementary information accompanies this paper at <http://www.nature.com/srep>

Competing financial interests: The authors declare no competing financial interests.

How to cite this article: Mondragón-González, S. L. and Burguière, E. Bio-inspired benchmark generator for extracellular multi-unit recordings. *Sci. Rep.* **7**, 43253; doi: 10.1038/srep43253 (2017).

Publisher's note: Springer Nature remains neutral with regard to jurisdictional claims in published maps and institutional affiliations.



This work is licensed under a Creative Commons Attribution 4.0 International License. The images or other third party material in this article are included in the article's Creative Commons license, unless indicated otherwise in the credit line; if the material is not included under the Creative Commons license, users will need to obtain permission from the license holder to reproduce the material. To view a copy of this license, visit <http://creativecommons.org/licenses/by/4.0/>

© The Author(s) 2017

Supplementary Material

Bio-inspired benchmarks generator for extracellular multi-unit recordings

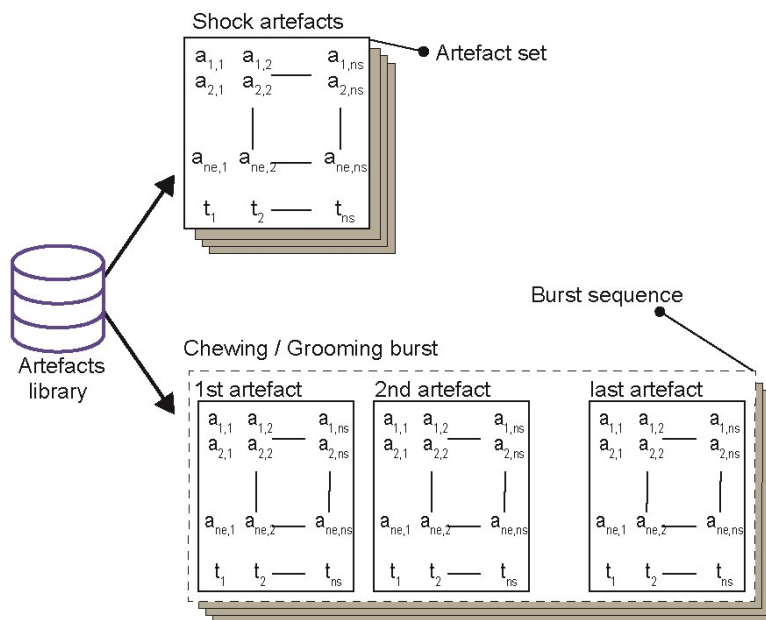
Sirenia Lizbeth Mondragon-Gonzalez¹, E. Burguière^{1*}

¹ Sorbonne Universités, UPMC Univ Paris 06, CNRS, INSERM, Institut du cerveau et de la moelle épinière (ICM), F-75013 Paris, France

*Eric Burguière

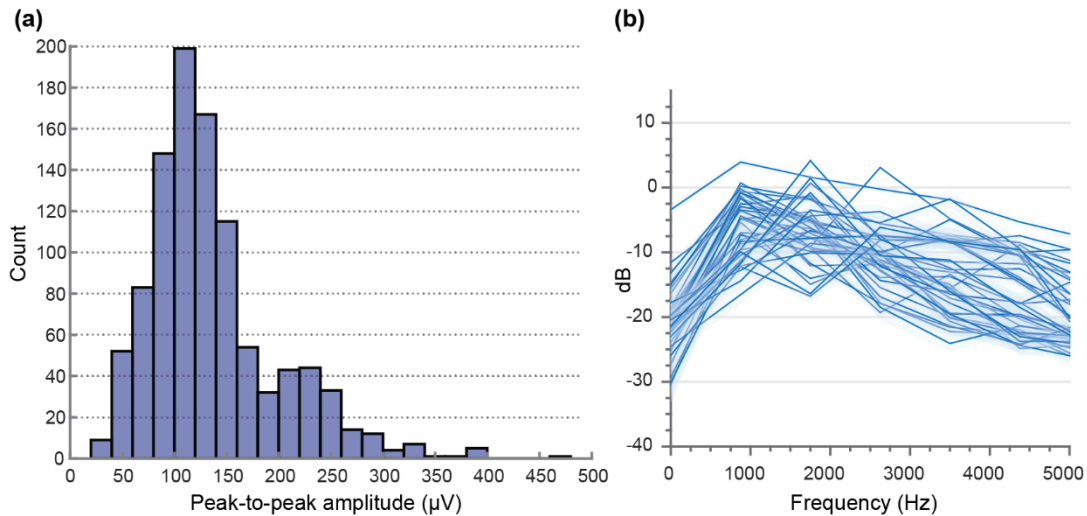
eric.burguiere@gmail.com

1 Supplementary figures

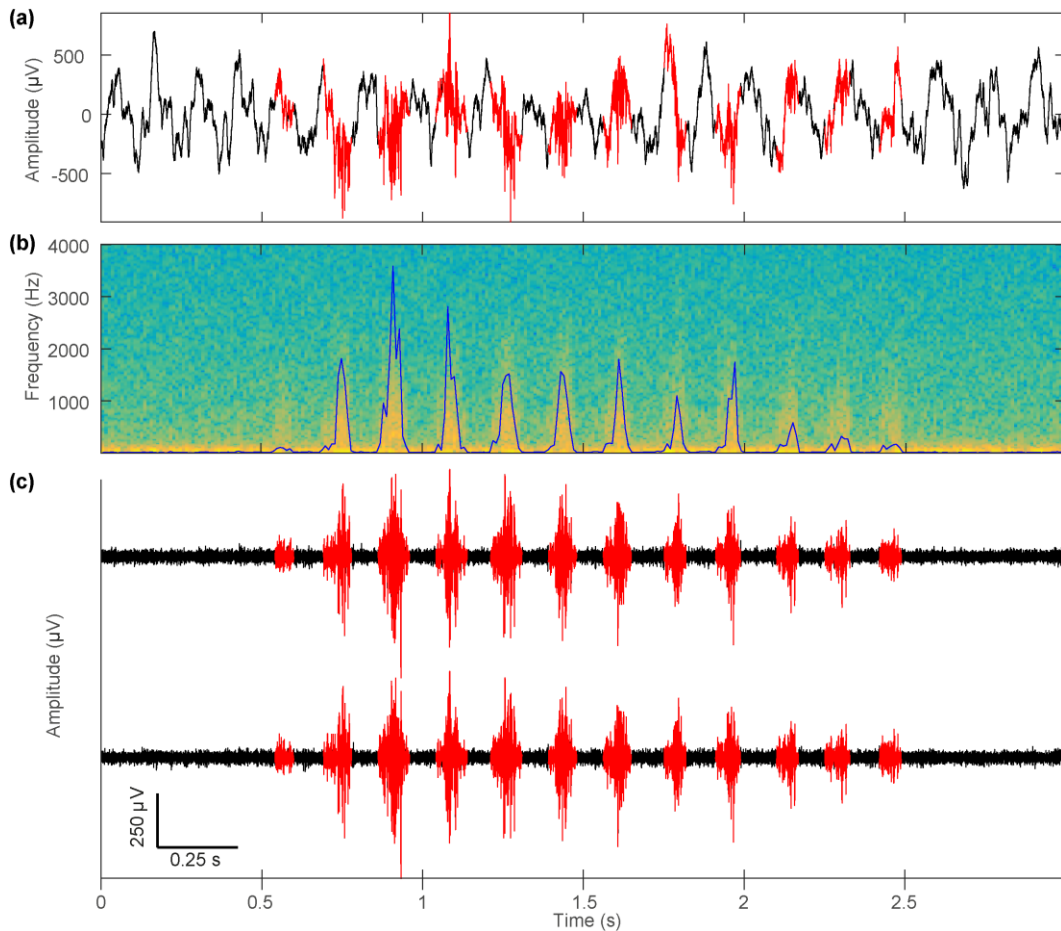


Supplementary Figure S1. Artefact library content. The artefact library contain spike-like artefacts or “head shock artefacts” that arise from headstage implant impacts to the electronics or from abrupt head movements, mastication artefacts and grooming artefacts. We stored the artefacts in artefact sets and artefact sequences that correspond to one single detected event. Every event has a different causal origin and this information is annotated for each set. A single artefact set contains an artefact event across channels. For the “head

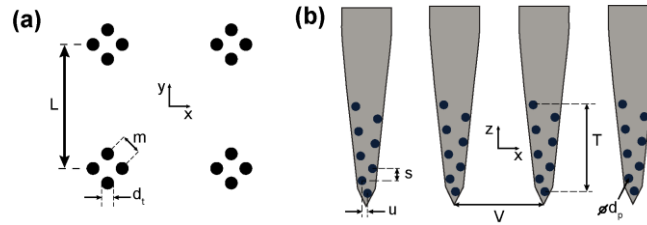
impact artefacts” this is usually a sharp waveform and for the chewing and grooming artefact an artefact set contains one artefactual burst from a sequence. In the figure, $a_{x,y}$ is the value of the x^{th} sample on the y^{th} channel of the artefact, t_x is the timestamp of the x^{th} sample. A single set contains minimum 22 artefacts and maximum 32 artefacts.



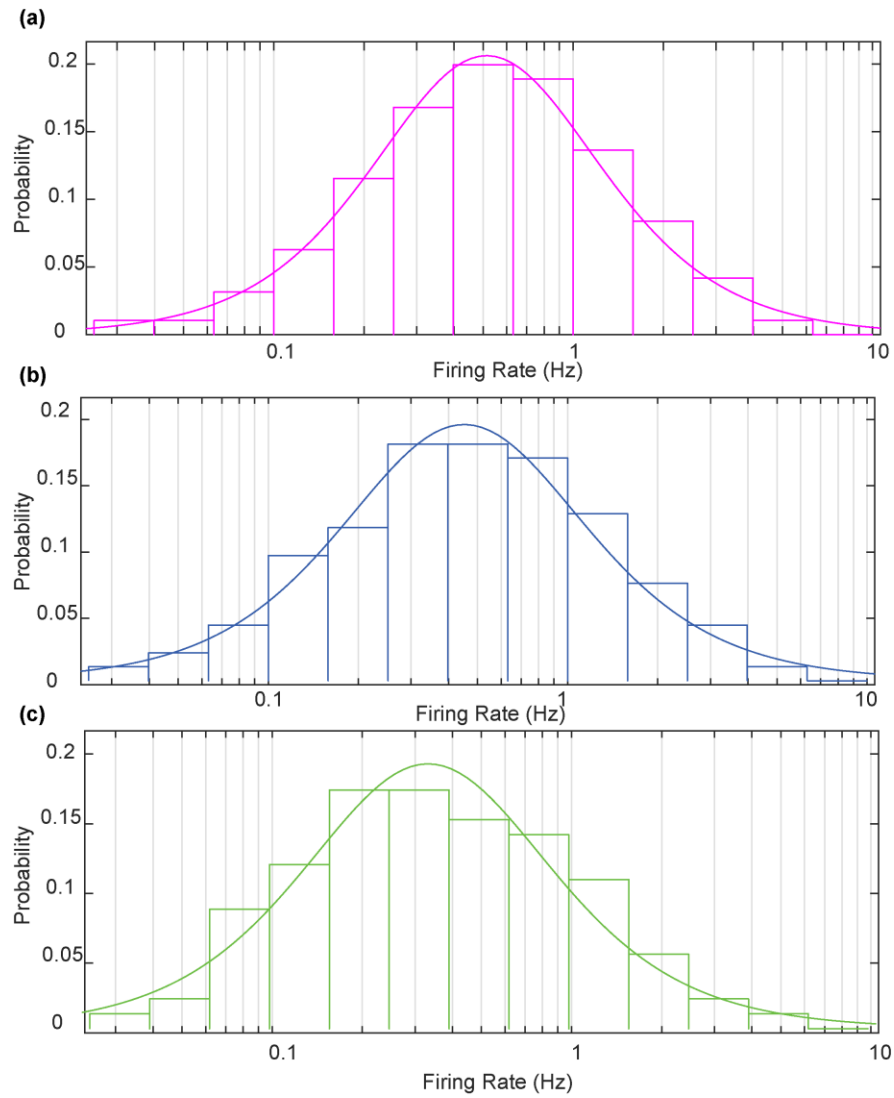
Supplementary Figure S2. Time-frequency analysis to identify signal artefacts of rodent chewing events. Characteristic rhythmic patterns of high-frequency and high-amplitude appear during mastication episodes. Trace (a) was recorded from one electrode during mastication, the chewing artefacts appear in red. In (b), the time-frequency analysis of (a) reveal the periodic bursts of chewing which are easily identified after high-pass filtering (in this case 300 Hz cut-off frequency) in (c). Bursts of chewing artefacts usually appear across channels as shown from the recordings in adjacent electrodes in panel (c).



Supplementary Figure S3. Time-frequency analysis to identify signal artefacts of rodent chewing events. Characteristic rhythmic patterns of high-frequency and high-amplitude appear during mastication episodes. Trace (a) was recorded from one electrode during mastication, the chewing artefacts appear in red. In (b), the time-frequency analysis of a reveal the periodic bursts of chewing which are easily identified after high-pass filtering (in this case 300 Hz cut-off frequency) in (c). Bursts of chewing artefacts usually appear across channels as shown from the recordings in adjacent electrodes in figure (c).



Supplementary Figure S4. Spatial distribution of virtual recording sites for the tetrode and polytrode configurations. All the parameters shown in the figure are easily modifiable within the coordinates configuration file. **(a)** The tetrode configuration array was defined by a distance between tetrode arrays “L”, and a inter separation distance “m”. For our application example values $L=150\mu\text{m}$, $m=30\mu\text{m}$ and $dt=20\mu\text{m}$ **(b)** The polytrodes’ coordinates were defined by distance $V=200\mu\text{m}$, $s=20\mu\text{m}$, $T=120\mu\text{m}$ and $dp=15\mu\text{m}$.



Supplementary Figure S5. Distribution of overall firing rates for each virtual layer. The distributions attributed to the different layers ((a) stratum oriens , (b) stratum pyramidalis, (c) stratum radiatum) follow the overall firing rates reported in a previous study¹.

2 Supplementary tables

Supplementary Table 1. Waveforms summary. It indicates the total number of waveforms for each tetrode. The total number of detected waveforms for all tetrodes is 1112953.

Tetrode number	Number of waveforms	Spike Threshold for channel 1 to channel 4 (μV)
1	68622	40, 40, 40, 40
2	363826	40, 40, 40, 50
3	125357	40, 40, 40, 40
4	44415	60, 60, 60, 60
5	127755	60, 60, 60, 60
6	326093	50, 50, 50, 50
7	56885	50, 50, 50, 44

Supplementary Table 2. Histogram bin counts. Peak-to-peak amplitude for the 1024 artefacts of the database. The bin edge is a uniform width of 20 μV .

Bin Edges (peak-to-peak amplitude in μV)	Number of waveforms	% of total number of artefacts
20-40	9	0.879
40-60	52	5.078
60-80	83	8.105
80-100	148	14.4530
100-120	199	19.434
120-140	167	16.309
140-160	115	11.23
160-180	54	5.273
180-200	32	3.125
200-220	43	4.199
220-240	44	4.297
240-260	33	3.223
260-280	14	1.367
280-300	12	1.172
300-320	4	0.391
320-340	7	0.684
340-360	1	0.098
360-380	1	0.098
380-400	5	0.488
460-480	1	0.098

Supplementary Table 3. Characteristics of chewing cycles detected. Duration, mean chewing rate across channels and chewing cycle duration (1/mean chewing rate) were calculated for each artefactual chewing sequence.

Sequence Number ID	Duration [s]	Mean chewing rate (CR) [bursts/s]	Chewing cycle duration [ms]
1	3.946	6.821	146.6061
2	3.8697	5.168	193.4985
3	3.3603	6.249	160.0256
4	3.9509	6.074	164.6362
5	1.5936	6.275	159.3625
6	2.9935	6.347	157.5548
7	2.746	6.554	152.5786
8	2.7998	6.071	164.7175
9	2.9121	6.524	153.2802
10	3.1005	6.128	163.1854
11	2.684	5.588	178.9549
12	2.426	6.183	161.7338
13	3.504	6.278	159.2864
14	4.169	5.756	173.7318
15	3.995	6.007	166.4724
16	3.388	6.198	161.3424
17	3.27	6.422	155.7147
18	3.6112	6.092	164.1497
19	4.474	6.348	157.5299
20	3.271	6.420	155.7632

Supplementary Table 4. Grooming artefacts.

Sequence Number ID	Duration [s]	Phases identified in the syntactic chain
1	7.9	1, 3
2	2	3
3	1.3	2, 3
4	0.4	1
5	2.2	1, 3
6	0.912	3
7	0.73	3
8	3.187	3
9	20.12	1, 2, 3
10	16.53	1, 3
11	10.96	1, 3
12	1.49	1, 3
13	0.612	1, 3
14	2.432	3
15	1.95	1, 3
16	17.91	1, 2, 3
17	7.68	1, 3
18	1.08	3
19	0.5	3
20	2.757	3
21	1.72	3
22	28.01	1, 3
23	3.536	3

Software

In order to create different simulations there are two files that can be rapidly modified:

- Coordinates.xml: to define recording sites' Cartesian coordinates and diameters.
- Configuration.m: to define the simulation parameters, dimension of the layers of virtual tissue and the population characteristics.

Main.m in the "Creation" folder will add the LFP and Artefacts from the library.

Chapter 5. TECHNOLOGICAL DEVELOPMENTS FOR NEUROPHYSIOLOGY

SUMMARY

In this chapter of the experimental work section, I describe some technical developments that are part of a hardware toolbox for closed-loop neuroscience paradigms. The technological developments were made to ease experimentation involving online neural signal acquisition and processing. In particular, the technical advances presented in part 5.1 were fundamental for the experimental part described in Chapter 6 and were meant to be used in rodent experimentation. The results presented in section 5.2 and 5.3 could be not only useful for animal experimentation but also be of use for the preliminary investigational stage of adaptive-DBS. The first technical developments presented allowed me to record electrophysiological signals from different brain regions as well as to simultaneously provide optogenetics stimulation while recording the behavior in freely-moving mice. These included the optimization of an implantable chronic high channel device that is not only light in weight but also allows stable long-term recordings. The implanted animals used for experimentation were recorded in an experimental chamber that was designed and built to isolate the animal from electrical devices and external stimuli, and that helped to reduce background noise levels.

Closed-loop experimental procedures in neurosciences demand effective online event detection, fast responding devices to execute algorithms and to drive stimulus on the biological system and effective continuous monitoring of the physiological signals. Depending on the features of interest, the procedures might require hard real-time processing or allow for soft real-time processing. For instance, in the case of signal analysis in the time-scale of action potentials, it is likely that the cycle of operations implemented demand strict constrained time intervals that are only possible to achieve with real-time hardware system that can guarantee a response within a timeframe, the main goal being to guarantee a solid performance in fixed time. I will also present the first developments made as part of a real-time processing chain intended for future closed-loop experiments. This include the design of an architecture for action potential pre-processing chain and denoising for Field Programmable Gate Arrays (FPGA) applications. Furthermore, I will describe the electronic solution designed to stream, previously recorded or simulated physiological signals, directly to acquisition systems. This application becomes particularly useful for the evaluation of the different modules involved in the cycle of operations of a real-time closed-loop solution for neuroscience experiments.

5.1 NEUROPHYSIOLOGICAL DEVICE IMPROVEMENTS FOR ANIMAL MODEL EXPERIMENTS: CHRONIC RECORDING IMPLANT AND RECORDING CHAMBER

The results explained in this section 5.1 are meant to be used for rodent experimentation.

The first step in the neural electrophysiology processing pipeline is the transmission of neural signals from implanted electrodes to a headstage, where each electrode interface with a single input channel on the headstage. Chronic electrophysiology allows the ability to record neural signals from multiple depths at once under simultaneous optogenetic manipulation. In this sense, extracellular acquisition during several weeks need stable recordings from large population of neurons. In the case of animal models of psychiatric disorders behavioral observation of awake mice with simultaneous recordings from a large ensemble of neurons is of crucial importance in the study of the neural circuits implicated in the disorder. As shown in **Chapter 6**, I recorded extracellular signals during several weeks from a freely moving murine animal model exhibiting compulsive self-grooming behavior, meaning intense head locomotion. Despite the widespread use of chronic electrophysiology and drive mechanisms available, it is a challenge to count on a light, stable, flexible and yet low-cost drive for behaving mice.

5.1.1 RESULTS

I've developed a drive implant that is based on a previous model (Voigts, Siegle, Pritchett, & Moore, 2013), several improvements were made to make it light in weight yet robust for long-term experimentation, easier to manipulate and that could allow for simultaneous electrophysiologic and optogenetic manipulations. Out of the several modifications done, the most important ones are the following: A change in the model core of the drive holding the electrodes adds the possibility to lower the electrodes via micro screws inserted in the nuts hold by the drive (**Figure 35-A,B**). A plastic spring is attached to the screws and it allows for the electrodes to move up and down (**Figure 35-C**). At the bottom of the drive mini holders give more stability when placing the drive at the animal's head and attaching it with dental cement during surgery. A 3D-printed enclosure cap can be easily removed or secured by unscrewing bilateral lateral screws (**Figure 35-D**). One of the advantages of this drive is that it allows the recycling of materials, for instance the enclosure cap can be disinfected and reused with different animals. In addition, the placement of different recording and stimulation sites can be adjusted easily by changing a single Computer Assisted Design (CAD) file, providing flexibility with respect to the brain regions targeted (**Figure 35-E**). Hence, our home-made drive supplies a simple, effective, flexible and lightweight solution that allows combining the recording of neural activity with optogenetics intervention. It has been

successfully used for chronic experimentation during several months allowing the mice to move without limitations thanks to its light weight and size (**Figure 35-E**).

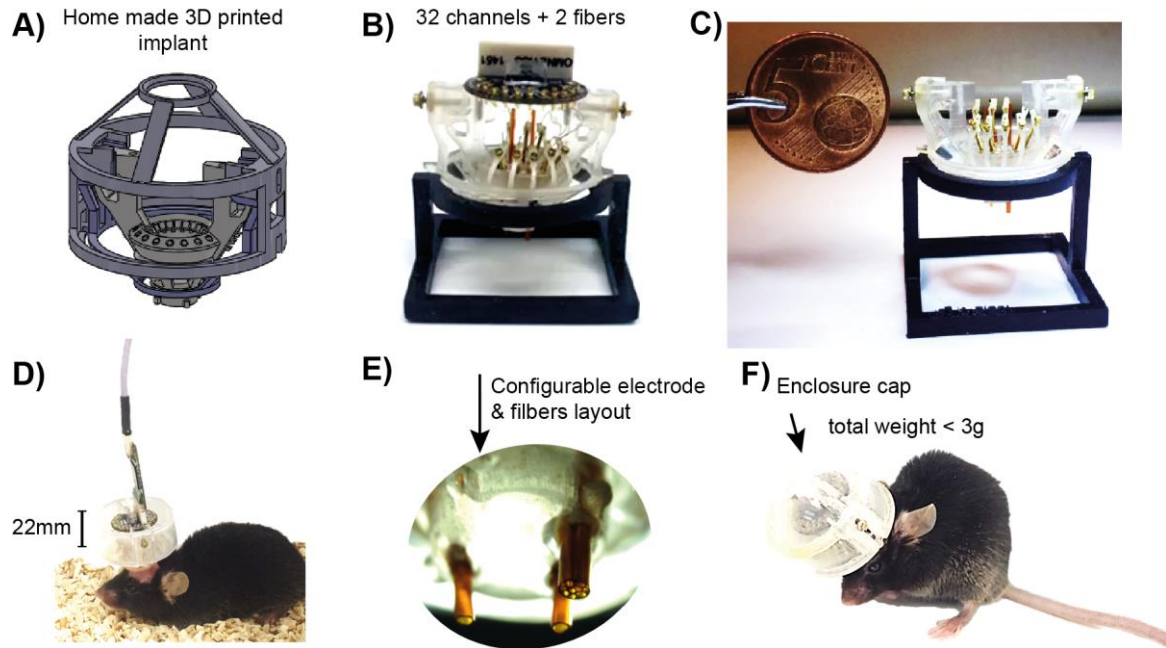


Figure 35. Home-made drive implant. (A) The 3D-printed structure is composed of three units: the drive body, a shielding cap and a protection cone. (B) The drive can hold 32 channels and 2 optic fibers, although with some modifications it can be scaled up to 64 channels. (C) The drive mechanism uses micro screws attached to a plastic spring to individually move each tetrode. (D, F) Mice can naturally move since the total weight is less than 3 g with 22 mm height. (E) The drive bottom is easily configurable to reach a variety of brain targets, in the picture we see a configuration for 2 fibers and one bottom tube guiding 8 tetrodes. (F) The cap enclosure is straight forward to remove and close, and safely protects the electrodes from dirt.

Complementary to the recording drive, I designed and built a recording chamber for electrophysiology and optogenetics experimentation in mice. In opposition to commercial experimental chambers, our home-made cage has all the electronic devices mounted outside the recording chamber, having the advantage of isolating the animal from the experimental devices and therefore reducing noise levels during electrophysiology recordings (**Figure 36**). The recording chamber is composed of two units, one embedded into the other, this allows us to directly remove the unit where the animal was placed to be easily disinfected and prepared for the next utilization without compromising the entire setup.

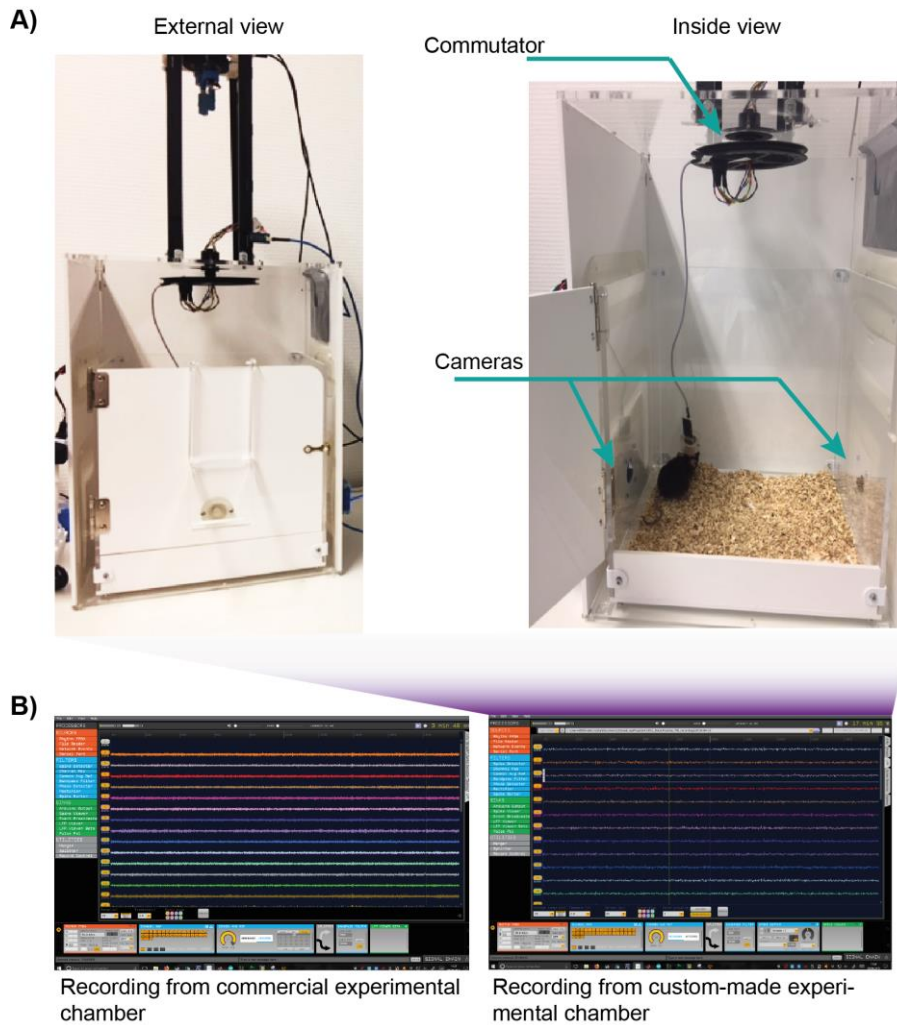


Figure 36. Custom-made experimental chamber. (A) The chamber has an inner unit to isolate the animal from electronic devices, this has the effect of (B) globally reducing the noise level.

5.1.2 METHODS

In our drive implant design, the guide tubes are attached to a plastic core that is manufactured from clear resin using stereolithography (Forms Lab 2, proprietary material). The drive body supports all of the other components and since it is transparent it facilitates the assembly and evaluation during manufacturing. The customization of the localization of the bottom tubes can be easily made by modifying the CAD file.

The position of electrodes in guiding tubes is similar to that reported in (Voigts et al., 2013) with the difference that our guiding screws are held by nuts attached to the drive body and the spring mechanisms instead of having single open springs holding the screws by contact, the springs are closed so that a single screw is inserted in hole of a single spring, allowing for better grip. The springs are made from 0.25 mm PET sheets and cut by laser. The shielding template that is used for the enclosure cap is also cut by laser from 0.1 mm clear acetate sheets. The home-made implant includes a holder for two optical fibers that is attached in top of the electronic circuit, the optical fibers fall to guiding tubes attached to the bottom of the implant to guide their location.

5.1.3 CONTRIBUTION

Here, we have described the design of a drive implant that has allowed us to record from eight individually adjustable tetrodes simultaneously, and at the same time allowed us to perform optogenetics manipulations in closed-loop experiments. By improving a previous drive design, our home-made implant is significantly easier to manipulate and to build. The enclosure cap has allowed to keep the inside of the implant intact over months. The implant is robust and yet light in weight, and its use has been tested to its limits by our animal model that presents excessive scratching and self-grooming.

We have also added to our neuroscience toolbox a simple custom-made experimental chamber that has allows for electrophysiology experimentation as well as for optogenetic light stimulation, and video recording. Our recording chamber has greatly help us to reduce noise levels in neural recordings and to have an improved setup to work with.

5.2 REAL-TIME FPGA PRE-PROCESSING MODULES

There is an increased interest in exploiting closed-loop experiments in which a stimulus is delivered immediately after a feature of interest is detected (Buzsaki et al., 2015; Grosenick et al., 2015). According to the very short latency of neurophysiological events such action potentials, an ideal closed-loop system would require rapid, and precise timing analysis response ($1 < \text{ms}$). These performances cannot be reached using a conventional general-purpose OS-based approach which cannot ensure analysis within specified time limits. Indeed, signal-processing algorithms introduce an inherent delay and the operating system in which they relay introduces latencies and undesired jitters, and together with the delay of data streaming the total mean latency is >10 ms. On-chip implementation of algorithms and precisely on field-programmable gate arrays (FPGAs) have some major suitable advantages for closed-loop designs: high determinism, high reliability, high performance and true parallelism. Executing tasks such as signal filtering, artifact denoising and spike identification using FPGA represent a fast shortcut to feedback generation with lower delays $<1\text{ms}$ (**Figure 37**). To that aim we implemented the basis for a real-time analysis platform that include basic analysis modules FPGAs for closed-loop experiments. The system functionality of our hardware design was verified using completely parameterized realistic simulations of extracellular recordings, by computationally testing its performance and measuring the total processing time.

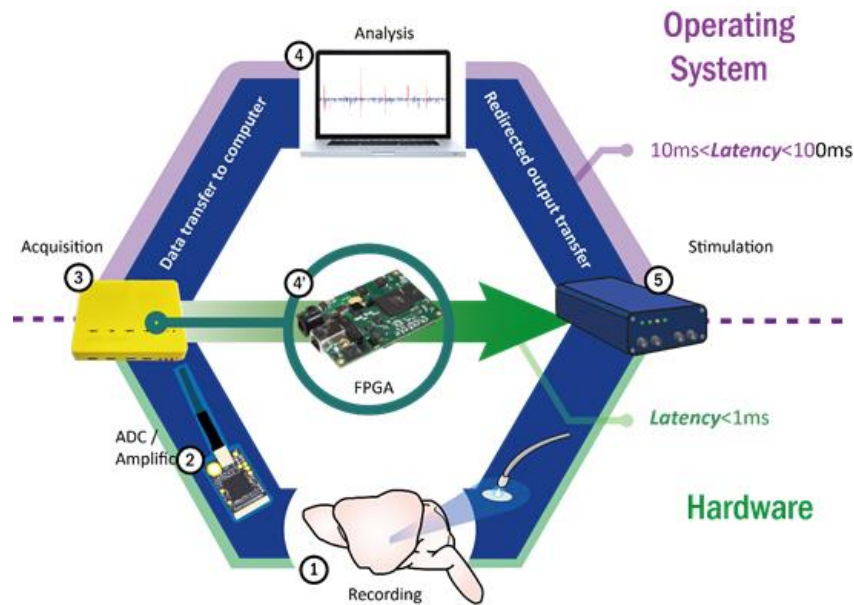


Figure 37. Real-time closed-loop neuromodulation approach. In a classic *in vivo* closed-loop experiment design there are some common operations that are repeated in a cycle. **(1)** Electrophysiological recordings are amplified, and digitalized **(2)**, an acquisition system is in charge of the conditioning and transmission of the signals to a computer **(3)**, the data analysis is executed by PC, where the operating system with signal-processing algorithms introduce an inherent delay and undesired jitter **(4)**, to finally deliver stimulation when required **(5)**. By using performing data analysis under FPGA, we can assure strict timing performance and true parallelism, characteristics that are desired for some closed-loop experiments **(4')**, especially for those that work with single-unit features.

5.2.1 RESULTS

We designed building blocks on Verilog language to form an event-based scheme for on-demand feedback delivery. The designed blocks include 1) IIR band-pass Butterworth 2nd and 3rd order filters, 2) action potential detector module based on threshold crossing and, 3) and artifact denoising module and 4) a transmitter module (**Figure 38**). When used together the artifact detector can be used to confirm the extracted action potentials. The modules were implemented on a FPGA (Spartan 6, XILINX, California, U.S) that is already compatible with existing acquisition systems from Intan (Intan Technologies, California, U.S.) or Open Ephys (Open Ephys, Lisbon, Portugal). The system functionality of our hardware design was verified using our completely parametrized realistic simulations of extracellular recordings (Mondragón-González & Burguière, 2017) (**Figure 38**).

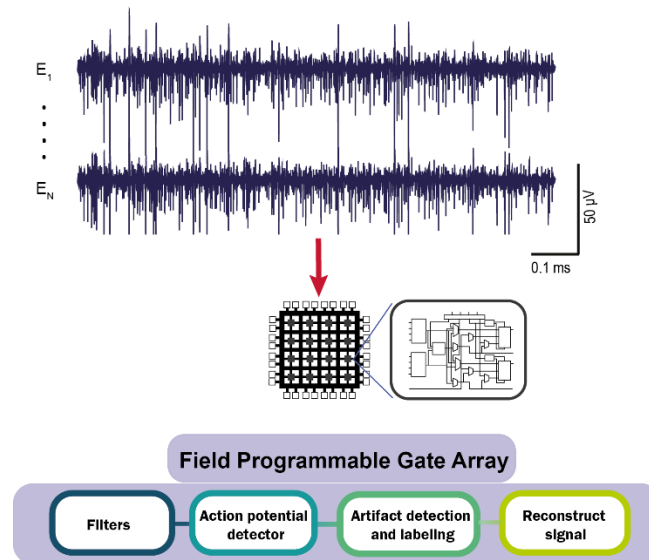


Figure 38. FPGA based analysis modules. The processing analysis modules implemented for a Field Programmable Gate Array (FPGA) includes the essential modules for online action potential analysis.

The tests datasets generated allowed us to test the action potential detector together with the artifact removal module. For this we created two datasets, one including neural signals with low percentage of artifacts (3 artifacts/s) and another with high percentage of artifacts (30 artifacts/s). Computational tests were focused on performance and total processing time measures. We computed a precision index for different detection thresholds (multiplier values for the mean deviation noise measure) and set the band-pass filter to 300-3000. Our results show that adding an artifact detection module can be highly beneficial, to increase the precision of the action potential detector (**Figure 39-a**) while keeping a hard sub-millisecond time response as short as 0.26ms when including an artifact removal module or 0.06ms without this module (**Figure 39-b**).

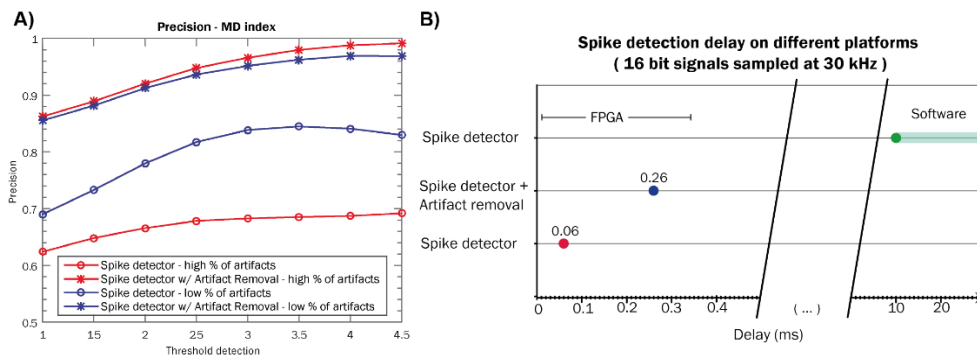


Figure 39 Precision and time response of the FPGA analysis modules. (A) When used, the artifact removal module increases the precision results while keeping (B) an invariant sub-millisecond response time.

5.3.2 METHODS

Building blocks were designed on Verilog hardware description language, we used the Xilinx ISE suite development environment (XILINX, California, U.S) to perform synthesis and implementation in FPGA. Such modules implement a specific function and each one

has different inputs to modify the configuration parameters and one or several outputs to flexibly interconnect them for future and different modules, such as decision making and feedback generation modules. The designed blocks include a band-pass Butterworth 2nd and 3rd order filters, a spike detector module and an artifact denoising module. The filter modules rely on an IIR design where the filter's coefficients are set by input signals. Since the calculation of each analysis module is done by a dedicated circuit, we designed the hardware circuits with simple architectures to gain in processing time, this allow us also to use few logical components. To detect an action potential (AP), the algorithm starts a count back when the signals value crosses a predefined threshold. If the signal value crosses another threshold before the count back reach zero (i.e. within a predefined time window starting at the first threshold detection) then the AP detection output is set to AP detected. Finally, the artifact detector considers the AP detected across channels. If the APs are detected on more than a predefined percentage of electrodes within a predefined time window, then the algorithm classifies the AP an artifact. Indeed, it is likely that an artifact (such a movement, shock or electrical artifact) appears across the majority of channels. In order to test the precision of the AP detection we generated realistic simulated neural data using a data-driven simulator (Mondragón-González & Burguière, 2017) in which extracted artifacts templates and non-stationary components from real recordings of in vivo experiments were linearly added to the reference signal to create a ground-truth annotated benchmark.

5.3.3 CONTRIBUTIONS

In-vivo electrophysiological recordings are characterized by precise time-dependent activity patterns of multiple neurons. Thus, the design of a short latency closed-loop stimulation design is extremely appealing given that it would allow the monitoring and interaction on the spike time-scale that otherwise would be impossible. By using reconfigurable digital hardware to execute signal-processing we can open the door to a complete set of new *in-vivo* closed-loop experiments. With this small contribution to the neuroscience toolbox we achieved the design of an FPGA-based signal processor to detect AP events without confounding artifacts while keeping short-latency processing time (<1 ms) and high precision. By using reconfigurable digital hardware to execute signal-processing we can imagine a whole possibility of *in-vivo* closed loop experiments such as fast detection and modulation of pathological related neural activity that is in the spike time-domain, with this in mind, our modules have been designed to allow further interconnections with more advances processing modules.

5.3 NEURAL STREAMING DEVICE

Closed-loop protocols with strict sub-millisecond intervention usually require hard real-time approaches. These approaches are usually implemented on hardware to allow for on-board electronics and real-time analysis. To correctly evaluate, optimize and compare performance of these systems, the use of reliable benchmark datasets is essential. To test the closed-loop setup at different levels of the loop the previously known signals should be sent and acquired as if they were recorded from a biological system. Nowadays there are limited commercial solutions that allows us to stream data in this manner, and the few available in the market only allow for simple signals such as sinusoid and triangular signals that are useful for simple tests, for instance to verify if a preamplifier is working or not. To this end, we have created an electronic solution 'the Neural streaming device' that allows to replay and stream previously recorded or simulated neural data into the acquisition system.

5.3.1 RESULTS

The Neural streaming device was designed to act as a connected headstage to stream real or bio-inspired neural data coming from different channels directly into the digital acquisition and analysis system (**Figure 40**). The neural signals are saved as uncompressed raw data into a micro SD-card, when the micro SD-card is plugged into the board, the system will be recognized it and wait for an input form the user to start streaming the data.

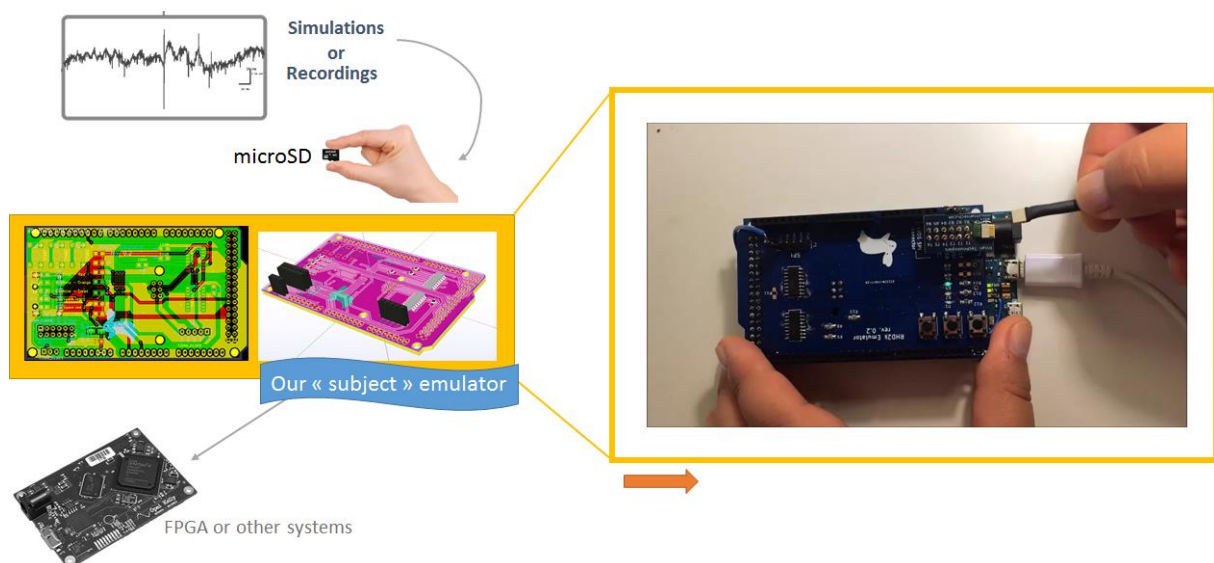


Figure 40. Overview of the neural streamer board. To simulate an online recording, the first step is to save a recorded or generated signal into a microSD card. We designed an extension shield for the Arduino due board that includes a microSD card reader. The neural streamer is connected to the recording system through, for example, a LVDS SPI cable. On the picture on the right, we are plugging this cable on a powered board.

Our system can be used to allow digital data streaming in three modalities: using an arbitrary signal such as a sine wave, a square wave, or a triangular signal, using simulated electrophysiological signals from multiple channels or using pre-recording real electrophysiological signals. Indeed, the board provides a simple way to test preamplifiers, implemented analysis algorithms and electronic devices by generating reference signals that would normally come from implanted electrodes, and therefore is a useful addition to the neuroscience hardware toolbox.

5.3.2 METHODS

The Neural streaming device is an Arduino Due based board, which has the advantage of being low-cost and of having a microprocessor (SAM3X CPU) that operates at maximum speed of 84MHz, a clock frequency sufficient enough to process and stream up to 32 channels at a sampling rate of 20 kHz. Additionally, the microprocessor has a direct memory interface useful to transfer the data from the micro SD card to the SRAM memory without the need of the processing unit. This allows us to preserve the CPU power for the conditioning of the signals to the format required by the acquisition system (in our case Intan RHD2000). The data signals are sent to the acquisition system through the Low Voltage Differential Signaling (LVDS) standard. Since the Arduino board does not natively include a micro SD card reader nor a necessary LVDS interface, we designed a custom shield (**Figure 40**) that included these features, plus additional status LEDs. The custom shield is an extension board that can be plugged directly on top of the Arduino Due board. The Neural streaming device firmware was programmed to execute a state-machine described in **Figure 41**. When the system is powered up, it first initializes the communication interfaces (loading the micro SD card driver and communication driver), and switches on the status LEDs. Once the initialization stage is over, it switches off the status LEDs and waits for a micro SD card to be inserted. Once a micro SD card is inserted, the file is opened and the file header containing the details of the data (e.g. sampling rate, number of channels and duration) is read. The first part of the data is loaded into the buffer memory. During this operation, a flashing orange LED indicates that the system is busy until it is ready to start the streaming (indicated with a green blinking LED). The streaming starts when pushing the start button. The memory containing the preloaded data is divided into two buffers, allowing the system to continuously load the data from the file in a first buffer while streaming the previous data from the other buffer. The streaming of the data stops when all the data is sent or when the stop button has been pushed.

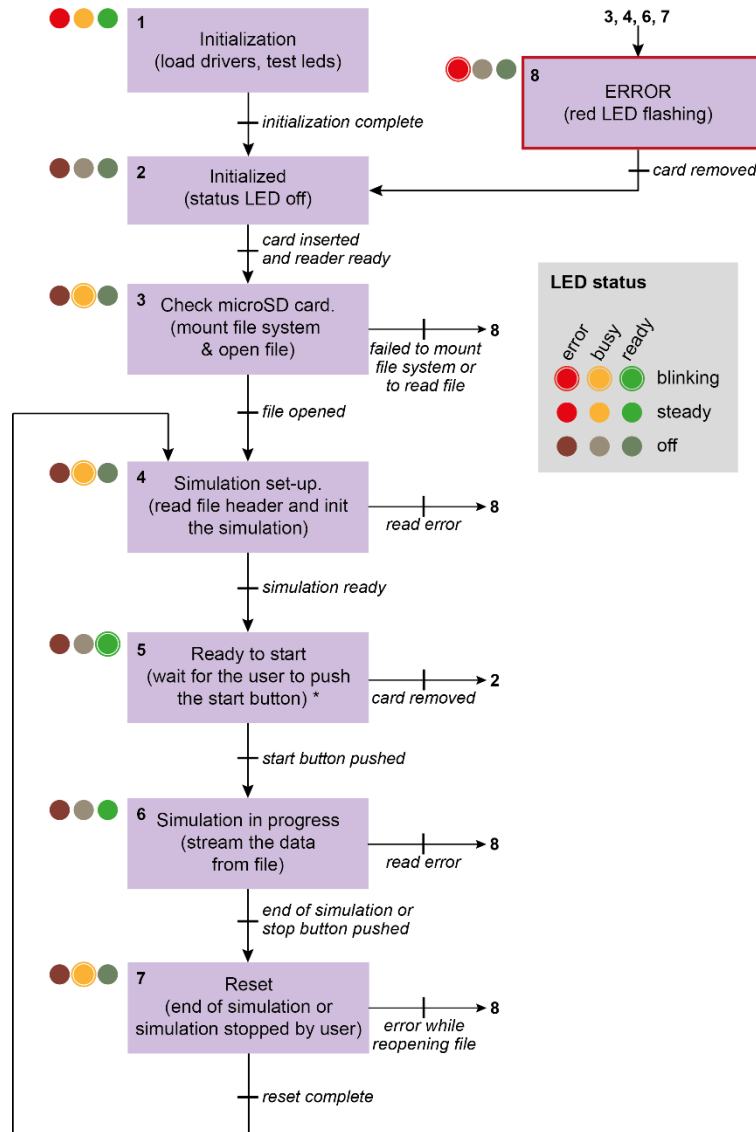


Figure 41. Flow-chart of the “Neural Streamer” software state machine. The figures shows the different steps implemented in a state-machine in order to continuously read and send the pre-saved data until the end of the recording.

5.3.3 CONTRIBUTIONS

When developing algorithms implemented either on hardware or software a data streamer can be useful to test various aspects of our setup. For example, streaming arbitrary signals (e.g. sinusoids) with previously known frequency content allow us to test different common modules such as filters where we can measure its attenuation and evaluate its proper implementation. Streaming neural data to the acquisition system can allow us to test analysis modules that process neural information (i.e. online spike sorting algorithms). In this case we can challenge the designs by feeding the algorithms with different signals with different level of artifacts. Finally, by streaming pre-recorded sessions we could replicate previous experiments and tune our algorithms to get the best configuration for a further experiment with a living subject. In summary, this simple development allows to test, debug and produce robust and reliable hardware-based signal processing algorithms without unnecessary animal experimentation.

Chapter 6. ADAPTIVE OPTOGENETIC STIMULATION TO REDUCE REPETITIVE BEHAVIORS

SUMMARY

In conditions where pathological repetitive behaviors (RB) are expressed, there is an imbalance of striatal activity possibly as a consequence of interneuronal network deficiency (Burguière et al., 2013b). This sixth chapter presents the results of a study conducted on the *SAPAP3-KO* mice, an animal model of compulsive behavior which exhibits excessive self-grooming behavior (Welch et al., 2007). Through optogenetic manipulations, we were able to manipulate precisely the striatal parvalbumin positive immunoreactive interneurons (PVI) network suspected to have a crucial role in the emergence and regulation of RB. This study provided the first evidence that by continuously lifting the PVI network of inhibition in the dorsomedial territory of the striatum it is possible to reduce compulsive self-grooming to normality in all the *SAPAP3-KO* mice. Our results showed that the dimension that seemed to have been modified were the number of initializations of grooming events, and this had a diminishing impact on the total time spent grooming while the quality of grooming events remained unchanged. Our results show that the striatal micro circuitry, and specifically the PVI, are important in inhibiting the onset of compulsive behaviors.

In the past it has been proposed that the activation and inhibition of neurons in a network happens in a rhythmically manner (Buzsáki, Anastassiou, & Koch, 2012) and this is responsible for various brain operations. In the context of compulsive behavior, the study of circuits arising from the orbitofrontal cortex (OFC) are of special interest because of the important role in inhibitory control, indeed, when lateral OFC-centromedial striatum circuit is disinhibited, urges of compulsive behaviors are triggered (Jahanshahi et al., 2015). We investigated the dynamics of local field potentials in the IOFC around grooming events in freely-moving *SAPAP3-KO* mice and found a non-sustained internally generated 1-4 Hz oscillations that temporally predicted grooming initialization. Using this information, we then developed a supervised machine learning approach to provide optogenetic stimulation in a context-specific manner using only LFP signals from the IOFC. Closed-loop optogenetic stimulation resulted to be more effective in alleviating compulsive grooming compared to continuous stimulation while significantly reducing the total stimulation time.

Prediction and prevention of compulsive behaviors by closed-loop optogenetic recruitment of striatal interneurons

S.L. Mondragon-Gonzalez, C. Schreiweis, J.L. Zarader, E. Burguière

ABSTRACT

Dysregulation in the cortico-striatal circuits has been shown to be related to pathologic repetitive behaviors. The cellular mechanisms of dysfunction at the microcircuit level remain still under investigation. Striatal positive parvalbumin (PV) interneurons receive strong afferences from the cortex and are the major elements of a powerful feedforward inhibition network that control spike timing in medium spiny neurons, thereby are a key element that regulates striatal output. To prove the role of PV interneurons in reducing aberrant repetitive behaviors we used the Sapap3 mutant mice, which exhibit excessive self-grooming and increased anxiety. Using optogenetics activation of PV interneurons in the dorsomedial striatum, we were able to reduce compulsive behavior to normality. We found that the development of non-sustained internally generated 1-4 Hz oscillations in the orbitofrontal cortex temporally predicted grooming initialization. Using a combination of extracellular signal acquisition, optogenetics manipulation and online data processing, we were able to predict grooming onset and provide on-demand stimulation of striatal PV interneurons. We found that both, closed-loop optogenetics and continuous open-loop stimulation robustly decreased excessive grooming. Acute on-demand stimulation had the advantage of requiring significantly less total stimulation delivery. These results highlight how the modulation of PVi's can positively influence the rescuing of pathologic repetitive behaviors and point to their involvement in the dysfunction mechanism that is associated to the cortico-striatal circuits. Moreover, we have provided an experimental framework that allows prediction of grooming behavior in Sapap3 mutant mice that may help to causally explore the underlying neuropathophysiology of repetitive behaviors.

INTRODUCTION

For optimal everyday life, we rely on habits, i.e., behaviors that we have acquired and automatized. As behaviors are repeated, the associative link between action and context increments until automaticity is established and habits are formed. Habits are characterized by a lack of awareness, unintentionality and the need of stronger inhibition to prevent its expression in the learnt context (Graybiel 2008; Hilario and Costa 2008; Yin and Knowlton 2006). In pathological conditions, behaviours may become habitual to a degree that they are compulsively executed despite deleterious consequences. Such compulsive behaviours are executed under a subjective urge and have been proposed to represent a core feature of neuropsychiatric disorders with pathological repetitive behaviours (RB) such as Obsessive Compulsive Disorders (OCD) or Gilles-de-la-Tourette Syndrome (TS) (Diniz et al. 2006; Franklin, Harrison, and Benavides 2012; Lewin et al. 2010). Although symptoms are heterogeneous across these pathologies, they share the common characteristics of restricted, repetitive patterns of behavior, which are executed despite their negative consequences.

The key player hypothesized to form and regulate the expression of habits and pathological repetitive behaviors (RB) are cortico-basal ganglia circuits (CBGs). CBGs are topographically organized into parallel cortico-striatal loops (Alexander, DeLong, and Strick 1986; Hintiryan et al. 2016; Hunnicutt et al. 2016; McGeorge and Faull 1989; Oh et al. 2014), which dynamically interact and are recruited to different extents during learning and habit formation (Graybiel 2008; Thorn et al. 2010; White and McDonald 2002; Yin et al. 2009; Yin and Knowlton 2006). Crucial for the adaptation and reprogramming of established routines is the dorsomedial striatum (DMS), which receives inputs from associative cortices. In line with this, a loss of adaptive control has been suggested to underlie maladaptive execution of habitual and pathological repetitive behaviours (Corbit, Nie, and Janak 2012; Fineberg et al. 2011; Milad and Rauch 2012; Murray et al. 2014; Swain et al. 2007). Indeed, fronto-striatal circuits, notably between the orbito-frontal cortex (OFC) and the DMS, have been shown to be recruited when goal-directed reprogramming of habitual behaviors are required (Gremel and Costa 2013). In line with this, a dysfunction of these adaptive circuits has been described in OCD patients as well as animal models of pathologically repetitive behaviors, thus adding evidence to the hypothesis of a lack of executive control over habitual behaviors in diseases with pathologically repetitive behaviors (Burguière et al. 2013; Chamberlain et al. 2008; Joel, Doljansky, and Schiller 2005).

The OFC is the most frequently reported region to present volumetric, functional and connectivity alterations in OCD patients. In the Sapap3-KO mouse model of compulsive-like behaviours, selective stimulation of the lateral part of the OFC (lOFC) corrected over-expression of conditioned pathological grooming behaviours and local field potentials recordings (LFP) in the lOFC showed alterations in certain frequency bands (Burguière et al. 2013). Of particular interest for steering the functioning of dorsal striatal activity, is the striatal microcircuitry. Under normal conditions, cortical and striatal interneurons modulate neural circuits to orchestrate an adapted behavioral output. In this striatal microcircuitry, fast-spiking interneurons, characterized neurochemically through the expression of the calcium-binding protein parvalbumin (PVIs) receive strong afferences from the cortex and are pivotal for striatal functioning through driving activity of striatal output neurons, the medium spiny neurons (MSNs), which with ~95% represent the vast majority of striatal neurons. PVIs form the major elements of a powerful feedforward inhibition network that control spike timing in MSNs, given their earlier and low-threshold activation relative to MSNs (A. H. Gittis et al. 2010; Koos 2004; Mallet 2005; Planert et al. 2010; Silberberg and Bolam 2015).

Recent studies have raised the interest in the possible implication of the striatal PVIs and their relationship to RB-related pathologies. Transient inhibition or a reduction in the numbers of PVI

in rodent models goes in line with the observations of abnormal elevated high firing rates of striatal MSNs as well as aberrantly repetitive behaviours (Burguière et al. 2013; Gernert et al. 2000; a. H. Gittis et al. 2011; Peñagarikano et al. 2011). Causal ablation studies (Rapanelli et al. 2017; Xu, Li, and Pittenger 2016) of striatal PVI in healthy mice resulted in the expression of increased repetitive behaviours such as stereotypic grooming and increased anxiety-like behaviour, a phenotype that has also been described in the SAPAP3 knockout (KO) animal model of compulsive-like behaviors. Postmortem studies in TS patients have reported a decrease in striatal PVI density and thus corroborate the hypothesis of PVI as a neurobiological substrate of the regulation of RB. These shreds of evidence establish the sufficiency of the striatal dysfunction of PVI in the expression of persistent, repetitive behaviours, although such observations cannot elucidate the causal role of this deficit.

In the present study, we have investigated the behavioral consequences of continuous optogenetic stimulation of striatal PVI in the SAPAP3 KO mice model, a mouse model that present excessive pathological self-grooming. We have found that continuous PVI stimulation in the dorsomedial striatum reduces the number of grooming initializations and therefore, the total time spent engaging in such repetitive behavior, but it does not change the nature and proportion of different types of grooming events. We investigated IOFC LFP signal properties in the SAPAP3 KO proving causality for functional changes and repetitive compulsive behavior. Our analysis revealed prominent 1-4 Hz oscillations with a peak frequency at 2 Hz which strongly correlated with grooming initialization, and that arose around 1s before onset. These frequency fluctuations were not seen when the mice were passively resting. Following this observation, we created a supervised learning pipeline that used IOFC LFP features around the previously observed frequency bands and that allowed us to predict self-grooming behavior successfully. To further exploit the effects of optogenetics stimulation of striatal PVI in reducing compulsive behaviors we implemented a closed-loop approach where optogenetic stimulation was delivered with temporal specificity according to online grooming predictions. Our results showed that acute optogenetic stimulation of striatal PVI strongly reduced the number of grooming initializations and reduced the total time spent in such behavior in a similar proportion to continuous stimulation. A key result in this paradigm comes from the demonstration of the efficacy of the approach compared to continuous open-loop stimulation, as we were able to decrease the total stimulation duration significantly.

RESULTS

I. Chronic optogenetic stimulation of striatal positive parvalbumin interneurons alleviates compulsive behavior

We first asked whether, the defect in striatal inhibition of MSNs previously showed to be linked to the expression of pathological repetitive behaviors in *Sapap3* mutants could correspond to a deficit in parvalbumin (PV)-containing interneurons, the major units necessary for mediating fast feed-forward inhibition of MSNs in response to cortical activation. In this case, we investigated whether we could restore the striatal inhibition by optogenetically stimulating the striatal PV interneurons directly. To test this hypothesis, Cre-dependent hChR2(134R)-mCherry ssAAV5 vectors were stereotactically injected into the dorsomedial striatum of *Sapap3*^{-/-} :: PV^{Cre/wt} transgenic mice, yielding hChR2 expression in fast-spiking PV interneurons (Figure 1A) and selective striatal PV-expressing cells were confirmed (Figure 1B).

To assess the impact of PV positive interneurons (PVi) activation on spontaneous compulsive-like behavior, we stimulated the PVi containing hChR2 within the striatum while we video recorded unconditioned and freely-moving SAPAP3-KO mice during their natural behavior, which is characterized by spontaneous excessive grooming. The experimental paradigm included a habituation stage of 10-15 min before the stimulation protocol, and we alternated between 3-min blocks of chronic stimulation and blocks without stimulation (Figure 1C) with three independent sessions of repetition. We delivered pulses of blue light (20 Hz, 5-ms light pulses, 10 mW) through two bilateral optical fibers in the dorsomedial striatum (Supplementary Figure 1). When the SAPAP3-KO mice were under optical stimulation, the PV interneuronal activation significantly decreased the number of grooming events by 55.8% and similarly, the total percentage of time spent in grooming was reduced by 46.25% compared to baseline (n=7) (Figure 1D and E). Opposite to the enhancement effect on the alleviation of compulsive behavior, control *Sapap3* knockout mice injected with a control virus that went through the same procedure (n=2) did not show a reduction effect of grooming bouts nor in total percentage of time spent in grooming (Supplementary Figure 2).

To evaluate how the stimulation of PVi impacted the excessive grooming behavior, we investigated its etiology during both, the stimulation blocks with light stimulation on and off. We examined in-depth patterning associated assessment of grooming behavior by scoring two types of behaviors, sequential patterns of self-grooming that follow a cephalocaudal direction (Kalueff et al. 2007) and single phase grooming events. The question asked was whether the optogenetic stimulation effect on grooming was reflected as an impact in sequential super-stereotypy in the syntactic chains or incomplete or isolated non-chain grooming bouts. We found that grooming sequences and isolated non-chain grooming bouts were consistent in the time duration of individual events, indistinctly of the stimulation protocol. Additionally, the percentage of the distinct type of grooming events was not affected by the stimulation (Figure 1F). These results confirm that the stimulation of PVi had an effect particularly in altering the grooming events initiation and by consequence in the total percentage of time spent rather than in modifying the order, proportion and average duration of individual grooming events. We also assessed whether optogenetic stimulation changes other locomotion activity in *Sapap3* mutants, for this we scored scratching activity in *Sapap3* mutants. The analysis revealed that although it seems to be a tendency in the reduction of scratching events and the percentage of time spent scratching, this difference was not statistically significant. (Supplementary Figure 3. Effect of chronic stimulation of dorsomedial striatal PV interneurons on scratching behavior in *Sapap3* mutant mice. Supplementary Figure 3).

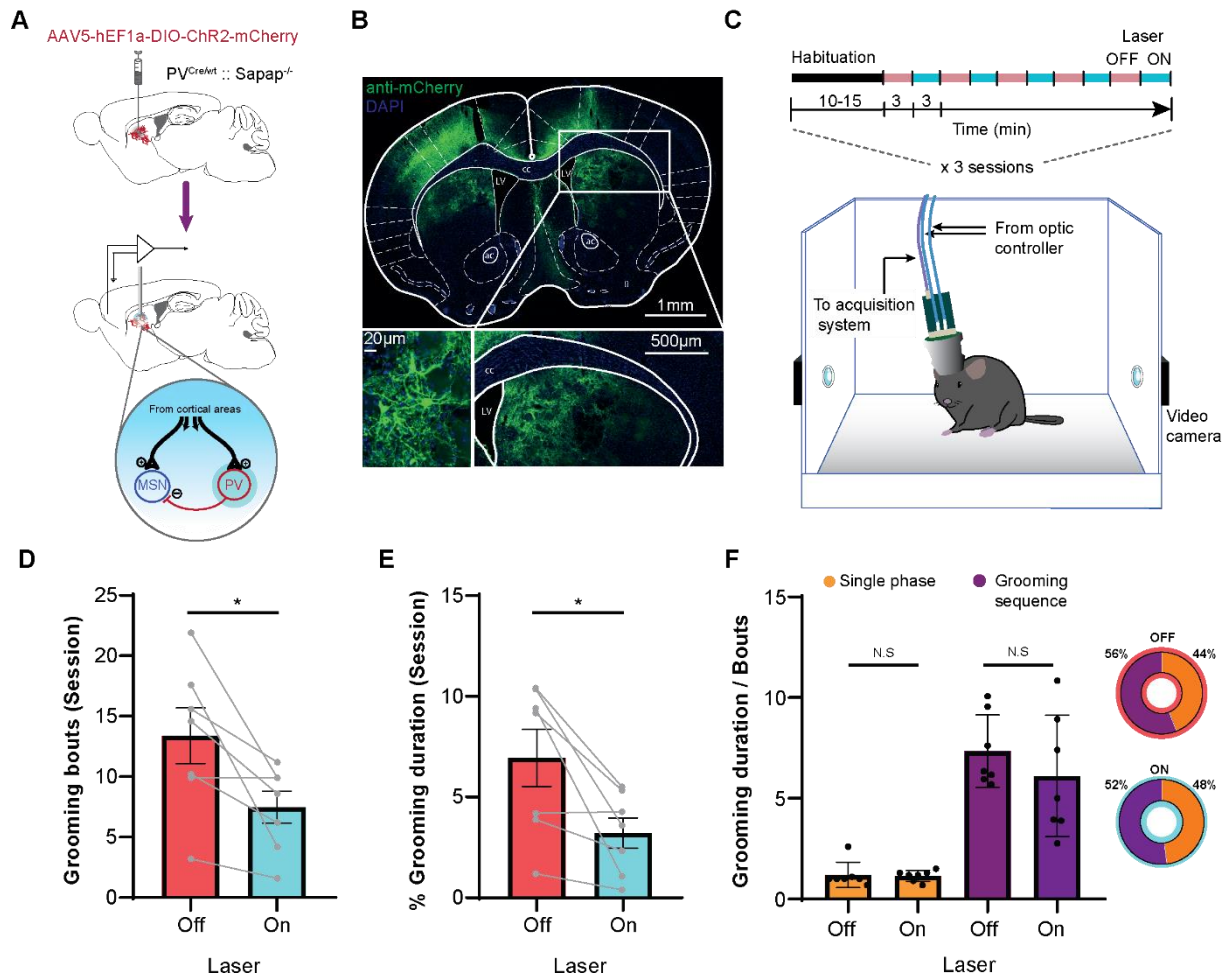


Figure 1. Chronic stimulation of dorsomedial striatal PV interneurons reduces compulsive-like behavior in SAPAP3-KO mice. (A) Schematic illustration of the experimental preparation and simplified model of microcircuitry of striatal PV interneurons. PV interneurons are opto-excited using bilateral fibers implanted in the DMS. (B) Post-hoc histological confirmation of selective striatal PV-expressing cells (anti-PV immunostaining, green). (C) Experimental setup and optogenetic stimulation paradigm. Blue bars denote the duration of bilateral optical stimulation (20 Hz, 5-ms light pulses, 10 mW). (D) Chronic optogenetic activation of DMS PV interneurons in SAPAP3-KO mice reduces by a factor of ~56 % grooming bout initialization and by consequence the grooming duration by ~46% (E). The differentiation of grooming events into grooming sequences (that follow a caudal sense) and single phases does not show a statistical difference during optogenetics stimulation concerning frequency nor the average duration (F) $n=7$ mice. Error bars in D-F represent mean \pm SEM (* $P<0.05$, Wilcoxon matched pairs test).

Previous studies explore the consequences of PVi dysfunction in the striatum, in patients suffering from repetitive-behavior related disorders (Kalanithi et al. 2005; Kataoka et al. 2010) and in animal studies (Burguière et al. 2013; Xu, Li, and Pittenger 2016) where striatal PVi induced deficits are related to abnormal RB, notably reflected in an increase in stereotypic grooming. In the SAPAP3-KO, the abnormal excessive grooming behavior results from a deficit in behavioral inhibition. To our knowledge, this is the first study that causally tests with optogenetics activation the behavioral rescue effect on a genetic model of compulsive behavior that has previously shown to have a disrupt of striatal FSIs. Our finding demonstrates that selective stimulation of PVi activity can help alleviate compulsive behaviors in an animal model expressing insistent spontaneous repetitive behaviors by reducing the number of grooming initializations and therefore by reducing the total time spent engaging in such behavior, and this, without altering the type or average duration of individual grooming events.

II. Low-frequency signature in the IOFC predicts compulsive grooming onset

The cortico-striatal circuits arising from the Orbitofrontal cortex (OFC) are of significant interest in the study of compulsive behavior. Indeed, the OFC circuit is responsible for context-related processing and response inhibition, and dysfunction of the lateral OFC-ventral striatum circuit is associated with a loss of ability to inhibit stimulus-response associations. When this circuit is disinhibited, urges of compulsive behavior are triggered. This observation has been supported by neuroimaging studies in human patients, highlighting the elevated activity accentuated during exposition to compulsive triggers. Studies on animal models of repetitive behaviors have also given us insights pointing particularly to the OFC as a central brain region relevant for pathologic repetitive behavior (Burguière et al. 2013; Lei et al. 2018). Notably, local field potentials (LFP) alterations in different frequency bands and an increased bursting activity have been reported during resting state between *Sapap3* mutants and control animals while baseline activity of IOFC putative pyramidal neurons was similar.

In the present study, we investigated functional grooming-related LFP activity by performing *in-vivo* multichannel recording in the IOFC of freely-moving SAPAP3- KO mice expressing excessive pathological self-grooming while simultaneously video recording its behavior (Supplementary Figure 1A). The initialization of grooming events was scored from the video frames, and the onset annotated when the first evident movement of front limbs to engage in a grooming event occurred (Supplementary Figure 4). Local field potential activity was synchronized with video recordings, and time-windows of 8s around the onset of grooming events were extracted. The analysis of OFC LFPs recordings revealed a pronounced 1-4 Hz oscillation with a peak frequency at 2 Hz which raised previously to grooming initialization. To evaluate if these oscillations could predict grooming behavior, we first computed the grooming-triggered spectrograms centered on the onset of grooming episodes (Figure 2A). We observed that these oscillations directly correlated to grooming episodes (Figure 2A-B) and that these oscillations were more prominent within 1 second before grooming onset (Supplementary Figure 5). Moreover, these oscillations were not present when animals were passively resting during the recording sessions (Figure 2B). These results strongly suggested that internally generated 2 Hz oscillations are a useful predictor candidate of grooming onset rather than a consequence of grooming behavior. As chronic optogenetic stimulation of PVi had an effect on diminishing the grooming initializations, we asked whether on-demand optogenetic intervention could alleviate compulsive grooming by acting upon a prediction signal of the event to come. To this end, we developed a pre-processing stage for feature extraction combined with a supervised classification algorithm to predict a categorical variable, pre-grooming event or other states (Figure 2D). To train the algorithm we created databases of time-windows from pre-grooming events and from other different behaviors extracted from five individual recording sessions (see Materials and methods). This approach allowed us to successfully predict grooming onset by exploiting the rate of change in the 1-4 Hz spectrum band. (Figure 2C). Our results provided a practical framework to predict grooming onset in the *SAPAP3* KO by using OFC recordings uniquely. We did not try to determine the origin of the 1-4 Hz LFP signature but instead use it as a biomarker to implement a temporally restricted therapeutic strategy to deliver acute light stimulation instead of continuous stimulation.

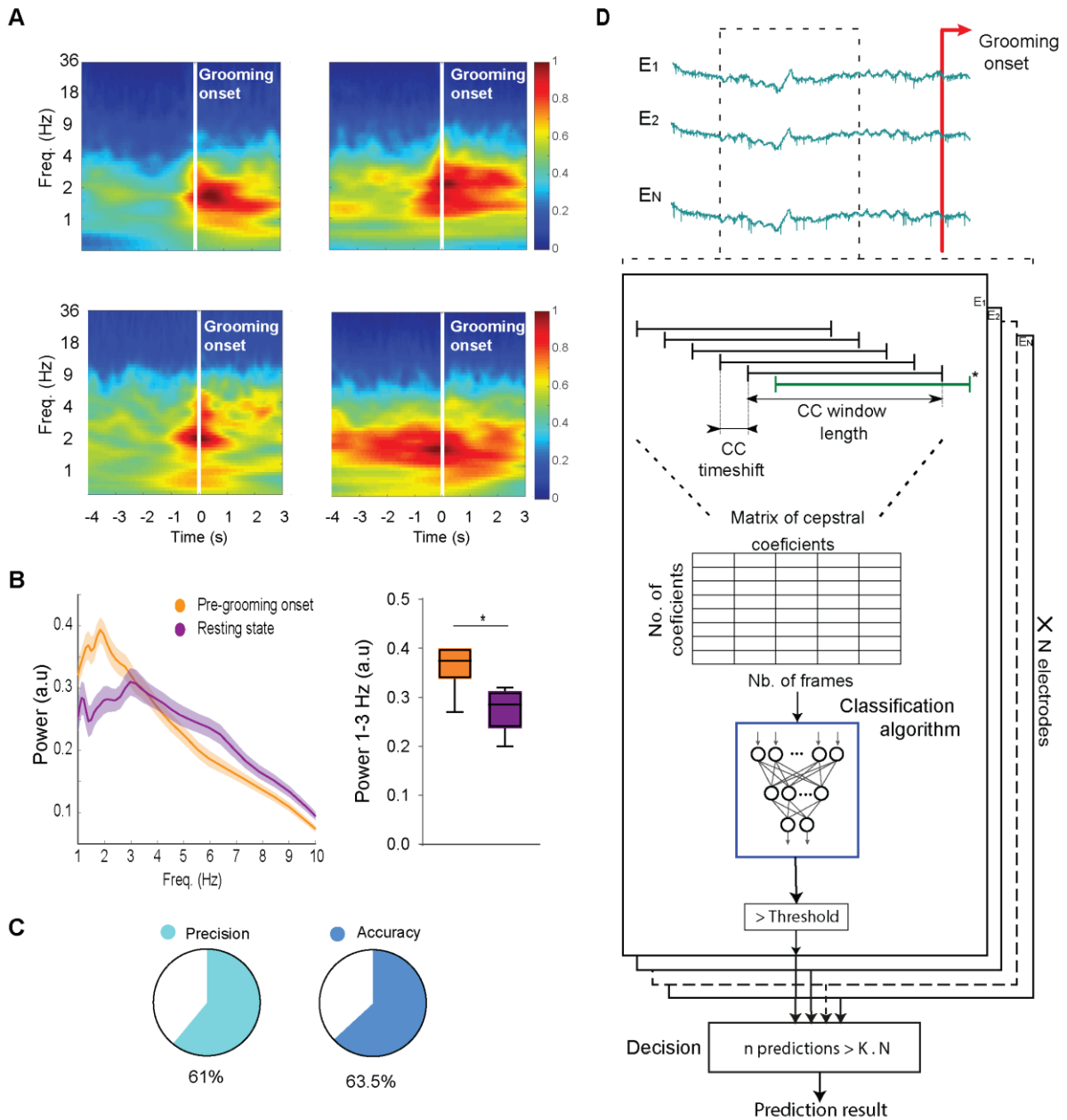


Figure 2. Low-frequency LFP signature predicts grooming onset. (A) Representative spectrograms of OFC activity in SAPAP3 KO mice before and during grooming behavior show an emergence of low oscillations prior to grooming onset. Vertical white lines in the spectrogram indicate grooming start. Each spectrogram represent the averaged LFP normalized activity of 45 grooming events for a single mouse extracted over five different recording sessions ($n=4$, warmer colors represent higher energy). (B) Averaged power spectra of OFC LFPs recorded during pre-grooming and resting state periods (Left) and averaged OFC 1-3 Hz power during pre-grooming and resting state periods ($n=6$, 15 grooming events and 15 resting states for each mouse) ($*P<0.05$, Wilcoxon matched pairs signed rank test) (Right). (C) Average accuracy and precision of the classifier at predicting initialization of grooming bouts. (D) The prediction algorithm exploit power cepstrum coefficients extracted from different electrodes to train a supervised classification algorithm, individual electrodes are treated separately, and if an agreement of results is found across electrodes, then the algorithm decides the outcome response accordingly.

III. ON-demand activation of PVI reduces compulsive grooming

Because continuous excitation of PV interneurons was found to alleviate compulsive grooming behavior by reducing the number of grooming event initiations, we next sought to determine whether stimulating PV cells before grooming onset in a time selective manner could have a significant effect in correcting pathological repetitive behavior. To test this hypothesis, we developed a closed-loop approach where grooming events were predicted as the OFC signals were acquired, triggering short periods of light stimulation. In this approach, the input source is local field potential signals (LFP) from the OFC in the Sapap3 KO x PV Cre, and the decision output is translated in light stimulation delivered bilaterally in the DMS. In this experimental paradigm, the mice were implanted with tetrodes in the IOFC and with optic fibers in the DMS. During the experiments, mice were video recorded while they could move freely (Figure 3).

The experimental paradigm included a habituation stage of 15 min. We then alternated and repeated four times three different experimental blocks of 3-minute period. During the 'off' blocks no stimulation was delivered. During the 'closed-loop' blocks grooming events were predicted online, triggering the delivery of pulses of light for 4 seconds (20 Hz, 5-ms light pulses, 10 mW). Following closed-loop blocks, we randomly triggered light stimulation in a 'yoked' block. The number of light triggers corresponded to the predictions made by the algorithm during the last earlier closed-loop block. Three independent sessions were repeated for each mouse. Closed-loop optogenetic stimulation effectively alleviated compulsive grooming in all Sapap3 KO mice tested. On average, grooming initialization was reduced by 59%, and the percentage of time spent in grooming was reduced by 65%. Additionally, yoked blocks that followed closed-loop stimulation, also resulted in overall decreased grooming activity. The behavioral response to randomized optogenetic stimulation was not homogeneous across mice and the averaged grooming initializations and time spent in grooming was higher than during closed loop blocks but not statistically significant ($n=5$, $P>0.05$, Wilcoxon matched pairs signed rank test) (Figure 3B-C). Moreover, as it was the case during open-loop continuous stimulation, the averaged grooming duration of individual events and the distribution of grooming categories across trials stay unaltered (Figure 3E). We quantified the number of light stimulation initializations triggered by the predictive algorithm during the on-demand optogenetic interventions and calculated the percentage time during which the mice received optogenetic stimulation. The results showed remarkably low duration of time spent delivering stimulation, saving in average 87% of time (Figure 3D). Taking together, our results show that the grooming phenotype observed in the SAPAP3 KO mice can be rescued by correct timed, spatially restricted and cell specific optogenetic on-demand intervention.

There is an intense interest in developing closed-loop systems for the treatment of repetitive behavior associated disorders such as OCD. In the line of clinical interest, we compared the efficacy of the open-loop and closed-loop experiments. The number of grooming initializations was reduced in similar proportions in both, closed-loop and continuous stimulation paradigms (59% vs 55%). Closed-loop stimulation of PVi was more effective in reducing the percentage of total time spent in grooming (65% vs 46.25%). Taken together, our results show that continuous PVi optogenetic stimulation, in an animal model that expresses pathological repetitive behaviors, result in behavioral restoration. Moreover, we discovered a predictive LFP signature in the IOFC that correlates with grooming onset and that was proven to be a useful biomarker candidate for online prediction of pathological repetitive behavior control. In addition, we showed that optogenetics techniques combined with online processing of LFP signals can provide superior restoration on grooming behavior compared to continuous stimulation, while keeping minimum stimulation delivery.

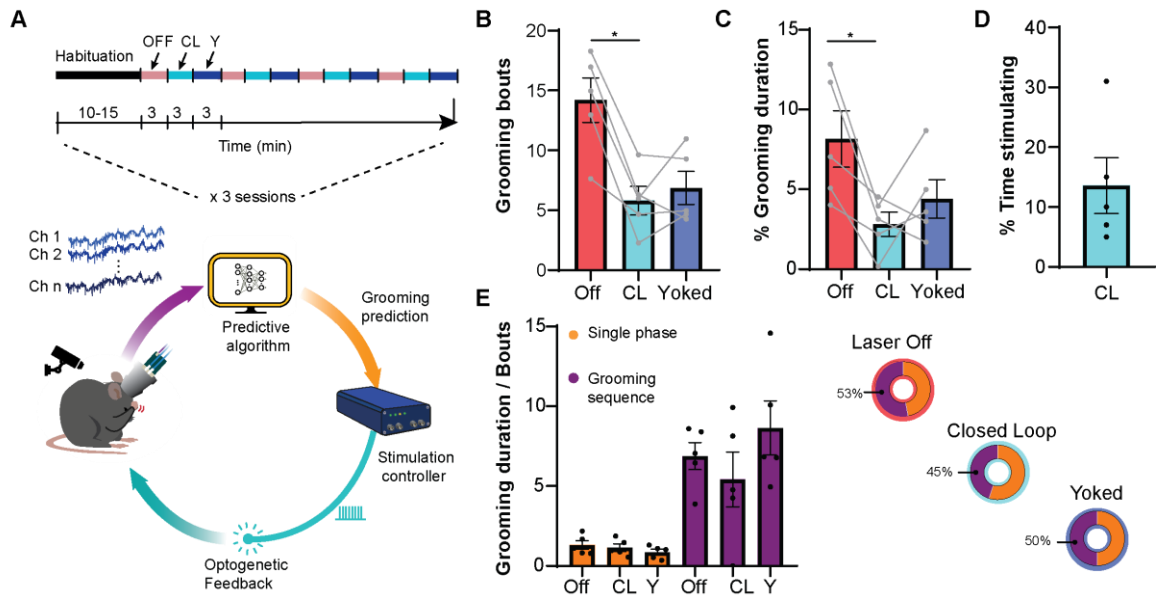


Figure 3. Closed-loop optogenetic intervention alleviates compulsive grooming. (A) Schematic illustration of the closed-loop experimental paradigm implemented for on-demand optogenetic intervention. *SAPAP3 KO* is implanted for both electrical acquisitions of neural activity and light stimulation. The violet arrow indicates IOFC local field potentials acquired and digitalized at the mouse head-level. Based on online cepstral features extracted from LFP signals and a classifier algorithm, a command signal (orange arrow) is sent to activate a stimulation controller to deliver light pulses of blue light during 4s. At the same time, animal behavior is video recorded during the experiment. (B) Averaged grooming bout initializations during the three different blocks of the experimental paradigm as well as percentage of time spent grooming (C). (D) Averaged percentage of time the mice spent receiving optogenetic stimulation ($13.6 \pm 9.3\%$, $n=5$). (E) Distinct self-grooming behaviors do not show a statistical difference during on demand, randomized optogenetic stimulation nor in periods without stimulation. $n=7$ mice. Error bars in D-F represent mean \pm SEM (* $P < 0.05$, Wilcoxon matched pairs test).

DISCUSSION

The results of our study conducted on the *SAPAP3-KO* mice, which exhibit excessive self-grooming, showed that through optogenetic manipulations we were able to manipulate precisely the striatal interneuronal network to reduce compulsive self-grooming to normality. Indeed, continuous optogenetic stimulation of PVI in the dorsal medial striatum had a rapid effect in normalizing grooming behavior in all the *SAPAP3-KO* mice by reducing the number of initializations of grooming events. We then designed a closed-loop stimulation protocol by using a neurophysiological predictor characterized by an increase of delta rhythm in the lateral orbitofrontal cortex shortly preceding grooming onset. By using this predictor, we showed that closed-loop optogenetic stimulation effectively alleviated compulsive grooming in all *SAPAP3-KO* mice. Taken together, our results helped to understand the biological mechanisms underlying repetitive behaviours by proposing that, in the context of compulsive grooming, striatal PV-interneurons are actively recruited at the onset of grooming events to regulate their expression.

In normal conditions, a powerful inhibitory network in the striatum keeps a balance of excitation and inhibition, and therefore is critical for regulating striatal output. In conditions where pathological repetitive behaviors are expressed, there is an imbalance of striatal activity being hyper-active, possibly as a consequence of interneuronal network deficiency. Our results show that the striatal micro circuitry, and specifically the PVI, are important in inhibiting onset of compulsive behavior, these results are in line with a previous hypothesis from a past study (Burguière et al., 2013b), in which the PVI were proposed to be role players in the regulation of RB. Indeed, previous studies have highlighted the role of the dorsal striatum in contributing directly to action selection and initiation through the integration of the different corticostriatal loops (B. W. Balleine et al., 2007). The observation that PVI stimulation was reflected more in a reduction of grooming initiations also echoes a previous study that showed the influence of PVI in choice execution (Gage, Stoetzner, Wiltschko, & Berke, 2010) and how distributed FSI pulse would help to suppress prepotent but currently inappropriate actions. Other recent studies have also looked at the specific roles of dorsal striatal FSI and MSNs during the execution of acquired behavioral sequences, and shown that FSIs interact with MSNs to shape action boundary activation (Burgess, Graybiel, Burgess, & Graybiel, 2018). In this same line, striatal PVI have shown to be capable of suppressing output via competing inhibitory microcircuits (Lee et al., 2017).

We also showed that PVI stimulation didn't change the characteristics of grooming behavior. We separately analyzed scratching behavior from grooming behavior since these instances may reflect two distinct repetitive behaviors (Berridge & Whishaw, 1992). These categories should be analyzed separately since scratching in rodents is a rather simple rhythmic movement made by the hind limbs that can be distinguished from the more complicated patterned grooming sequences (Brash et al., 2005). It might be possible that these distinct behaviors may be regulated by circuits arising from different cortical areas, for instance, it has been shown that striatal inputs coming from the anterior cingulate cortex (ACC) are a specific critical circuit element for regulating scratching behavior (Lu et al., 2018), it would make sense then to categorize it as a different type of RB, one that would fit better into the complex motor tic category.

In the context of compulsive behavior, the study of circuits arising from the OFC are of special interest because of its probable important role in inhibitory control. This theory is supported by evidence in OCD patients where imaging studies showed a hyperactivity of the OFC-caudate circuit that is increased by compulsive symptom provocation (McGuire et al., 1994; Milad & Rauch, 2012; S. L. Rauch et al., 1994; Simon et al., 2010). We thus analyzed functional grooming-related LFP activity by performing *in-vivo* multichannel recording in the IOFC of freely-

moving Sapap3 KO mice. A key finding of our study comes from the demonstration of the development of a non-sustained internally generated 1-4 Hz oscillations in the orbitofrontal cortex that temporally predicted grooming initialization. The rise in this oscillations directly correlate to grooming episodes while being more prominent within the one second preceding grooming onset, and were not observed during resting behavior, suggesting that this acute internally generated oscillation could be useful predictor biomarker for self-grooming onset. To our knowledge, our data provide the first demonstration of a low-frequency biomarker that is correlated to the prediction of self-grooming behavior. Regarding specific IOFC activity, a recent study provided interesting information regarding IOFC dysfunction in the SAPAP3 mice. The authors investigated local field potential oscillations in the IOFC of awake mice during rest. They found that compared to wildtype mice, the IOFC of SAPAP3-KO mice exhibited network dysfunction, demonstrated by a decreased power of local field potentials that included the delta band (1.5-4 Hz) (Lei et al., 2018). It has been shown that an increase of delta power promote the recruitment of cortical pyramidal neurons assemblies (Karalis et al., 2016). As a consequence, a decrease of delta rhythm might result in a dysfunctional cortical drive to recruit striatal PVi network downstream. Therefore, that power decrease in IOFC could result in less PVi recruited leading to a hyper activation of MSNs. Future experiments exploring the synchronization of the delta band with individual neurons may help to challenge this hypothesis.

Although in our study we did not investigated the exact origin of the low-frequency signature we observed in the IOFC, our observations showed that this signature was present across mutant animals. Motivated by this finding, we developed a supervised machine learning approach to provide optogenetic stimulation in a context-specific manner. The classification algorithm was designed to consider the different representation of the underlying neural activity of the different electrodes, indeed although multiple electrodes are implanted into the same brain region the size and shape of the sampling field might lightly vary depending on the impedance of the electrode. We believe that cepstral coefficients are an unconventional but efficient alternative to classic feature extraction methods to feed into a number of supervised learning algorithms, and that this approach could be used in other applications than the one presented in this study. Indeed, if the frequency band of interest is known, the frequency scale of triangular filters can be arranged to focus in such frequency band while taking into consideration the contribution of other frequency bands but reducing its influence since those coefficients provide information about the rate of change in the different spectrum bands. By successfully predicting grooming onset, exploiting the rate change in the delta band, we were able to investigate the effects of acute optogenetic stimulation in a closed-loop manner. Our results show that closed-loop optogenetic stimulation effectively alleviated compulsive grooming in all SAPAP3-KO mice that went through closed-loop experimentation while significantly reducing the stimulation time by 87%. Compared to continuous open-loop stimulation, closed-loop stimulation was more effective in reducing the total time spent in grooming while the reduction in number of events was similar for both approaches. Although having a strong positive efficient effect during closed-loop modulation, it is still not a trivial task to evaluate if closed-loop brain stimulation is a better strategy than open loop. From a translational perspective, we should first investigate the long-term effects of closed-loop stimulation, in particular to investigate if we could induce chronic reduction of compulsive grooming by presumably modifying synaptic events occurring at their initiation time.

Here we have provided the first in-vivo closed-loop experiment to alleviate pathological RB in the SAPAP3 mice. This study gives important evidence of the role of striatal PVi in regulating RB and particularly in their necessity during the temporal window previous to initialization of RB. A crucial point to mention is that the closed-loop approach presented was a predictive one, since it reacted before RB onset and not to the detection of an on-going RB, therefore the predictive

on-demand feedback allowed us to define the temporal specificity characterizing the causal role of PVi in RB. Additionally, the predictive approach implemented may be useful in further experiments as a platform to explore in a closed-loop manner other brain targets for therapeutic purposes. The presented results give a more confident view for future adaptive DBS in patients suffering from RB-related disorders since our online analysis method could be easily implemented in on-board electronics. These findings although they raised some intriguing questions, advance our understanding of the neuropathophysiology and circuitry mechanisms that underlie compulsive behaviors, and may help generate and redefine new hypotheses for further investigation.

MATERIAL AND METHODS

Animals

All experimental procedures followed national and European guidelines, and have been approved by the institutional review boards (French Ministry of Higher Education, Research and Innovation; Protocol APAFIS#1418-2015120217347261 French Ministry; Brain and Spine Institute Animal Care and Use Committee protocol no. 00659.01). Animals were group-housed prior to surgery and individually housed after implantation surgery for the rest of the experimental protocol in order to protect the animal and its implant. All animals were maintained in a 12-hour light/dark cycle (lights on/off at 8:00am/8:00 pm, respectively), and had *ad libitum* food and water access.

In order to specifically modulate PV interneurons in Sapap3^{-/-} mutant mice and Sapap3^{+/+} controls, we crossed the Sapap3-KO colony (provided by Dr. G. Feng, MIT, Cambridge, USA) with Pvalb^{Cre} mice (Jackson Laboratory Stock Number 008069; provided by Dr. A. Bacci, Brain and Spine Institute, Paris, France) in heterozygous breedings in the animal facility of the Brain and Spine Institute. Both intercrossed lines were of C57BL6/J background. Following studies of previously reported grooming phenotype in adult Sapap3^{-/-} animals (Welch et al. 2007), we used 9 adult male Sapap3^{-/-} :: PV^{Cre/wt} and 2 age-matched Sapap3^{+/+} :: PV^{Cre/wt} mice (mean age = 9 ± 1.55 months; mean weight 33.47g ± 6.25).

All animals of our colony were systematically genotyped for the presence or absence of the Sapap as well as Cre-recombinase protein during weaning period and the genotypes of all experimental animals verified at the end of the experiments. For the Cre-recombinase, primers oMR1084 and oMR1085 were used according to genotyping recommendations of the Jackson Laboratory for the Pvalb^{Cre} mice. The presence of both a mutant band (~100bp) and a wildtype band (~500bp) indicated the heterozygosity of our experimental animals.

Viral Vectors

Viral vectors were purchased from the Viral Vector Facility, Neuroscience Center Zurich, University of Zurich and ETH Zurich, Switzerland, aliquoted and stored at -80°C until stereotaxic injection surgeries. Addgene plasmids #20297 and #50459 were used for the generation of adeno-associated viruses of serotype 5, one expressing either an excitatory opsin and a fluorophore reporter (ssAAV-5/2-hEF1 α -dlox-hChR2(134R)_mCherry(rev)-dlox-WPRE-hGHp(A); physical titer: >9.1x10¹² vector genomes/ml) or expressing only the fluorophore reporter (ssAAV-5/2-hSyn1-dlox-mCherry(rev)-dlox-WPRE-hGHp(A); physical titer: >1.3x10¹³ vector genomes/ml). Titers were determined via fluorometric quantification in the providing viral core facility.

Electrode and fiber-optic implants

Implants were home-made designed and constructed around a clear plastic core. The design was made in SolidWorks (Dassault Systems, MA, U.S.A) and printed via stereolithography using a Form2 (Formlabs, Somerville, MA, U.S.A) with clear resin. The plastic drive body core held 8 independently mobile tetrodes and two fixed flat optic fiber stubs (Plexon Inc., Texas, USA) of 200/230 μ m (core/core + cladding) inserted in a zirconia ferrule (Supplementary Figure 1.B). Tetrodes were made from 17.78 μ m (0.0007 inch) Formvar-coated nichrome wire (A-M Systems, WA, U.S.A), twisted and heated to form tetrodes. Tetrodes were fixed to laser-cut plastic springs

(polyethylene terephthalate, 0.25 cm from Weber Metaux, Paris, France) and individually driven via miniature screws (Micro-modele, Strasbourg, France). Electrodes were attached to an electrode interface board (Open Ephys Production Site, Lisbon, Portugal) with gold pins (Neuralynx, MT, U.S.A). Individual electrodes were gold plated to an impedance of 200-350 k Ω . Ground connections were made using 50.8 μ m (0.002 inch) Formvar-coated tungsten wires (A-M Systems, WA, U.S.A). The whole implant (drive body, cap, and cone) weighed less than 3g. (Supplementary Figure 1A, B)

Stereotaxic surgeries

Each mouse was deeply anesthetized (induction at 2.5% % isoflurane; maintenance during surgery at 0.9% isoflurane) and mounted into a digitally equipped stereotaxic frame via ear bars adapted for mouse stereotaxic surgeries. Scalp hair was removed using depilation cream diluted with sterile 0.9% saline and the skin disinfected three times with 70% ethanol and betadine solution prior to skin incision. Four small burr holes were drilled around the perimeter of the exposed skull surface to accept steel anchor screws. Two additional small burr holes were drilled behind the estimated headstage implant volume to insert two separate ground wires; Craniotomies and duratomies (0.8mm diameter) were made bilaterally above the dorsomedial striatum (AP = +1.0 mm, ML = +1.5 mm) and unilaterally above the left lateral orbitofrontal cortex (AP = +2.8 mm, ML = +1.5 mm). Brain surface was maintained humid with sterile 0.9% saline throughout viral injections until headstage device implantation. AAV constructs were injected bilaterally at a constant rate of 50nl/min (0.4 μ l/site) into the dorsomedial striatum (DV -2.4, measured from brain surface) using a motorized micropump? a precision syringe (Hamilton Gastight Series #1701, 10 μ l) and according needles (Hamilton, 33Ga, bevelled end). Precisely, prior to virus injection, the needle was lowered to -DV = 2.5mm and retracted to DV = -2.4 immediately, where the needle was allowed to adapt for 2 minutes. After injections, the needle was let in place for 10 minutes before being retracted for 300 μ m (DV=-2.1) and let rest in place for another minute. Afterwards, the needle was removed from the brain.

After viral injections, a drop of surgical lubricant was applied to the cranial openings and then the headstage was carefully lowered so that the bottom polyamide tubes containing either tetrodes or smaller tubing to hold the optic fibers touched the brain surface. The headstage was then fixed to the skull and screws with dental acrylic. Ground wires were formed into tiny loops, which were inserted below the skull to make surface contact with the brain. Ground wires were then fixed to the headstage construct and connected to the electrode interface board. Optic fibers, fabricated to be inserted 2mm into the brain measured from the surface, were inserted into the according place of the electrode interface board, carefully lowered to the maximal depth, and glued into position. Tetrodes were advanced individually directly after surgery as well as carefully put into position of the targeted recording sites position in the orbitofrontal cortex (DV = 1.5-2 mm)during the following 3-5 post-operative days, with an attempt to maximize the number of recorded units per site prior to the first training session. Animals were closely monitored post-surgery taking into account changes in weight, body score, nesting and overall activity as indicators of surgery recovery. During the experimental, the electrodes were minimally moved to maintain recording quality.

Histological verification of recording sites and viral infections

After experimental procedures, electrolytic mark lesions were made to confirm the localization of tetrode recording sites as well as viral infection *post-mortem*. Animals were anesthetized as described above and constant current was delivered to each electrode with an output discharge of 25 μ A during 10s using a current stimulator (Digitimer Ltd, Hertfordshire, England). After 72 hours mice were anesthetized with an intraperitoneal injection of pentobarbital (200mg/kg) and transcardially perfused with 30ml of 4°C cold 0.9% sodium chloride solution, followed by 60ml of 4°C cold 4% PFA in 1xPBS. Brains were postfixed in the same paraformaldehyde solution over night at 4°C, briefly rinsed three times in 1xPBS and progressively dehydrated for cryosectioning by 24 hours incubations first in 15% and subsequently in 30% sucrose solution, prepared in 1xPBS. Next, brains were embedded in O.C.T. compound and sectioned into six series of 30 μ m sections (Microm HM N°560, Thermo Scientific) into 1xPBS containing 0.1% sodium azide. Prefrontal sections were stained with 1% cresyl violet solution and analyzed for the location of the mark lesions under a brightfield microscope.

Immunofluorescence staining was performed on one series containing striatal sections in 4°C cold solutions on an orbital shaker. Sections were washed three times for ten minutes in 1xPBS, followed by three washes of each ten minutes in 1x PBS containing 0.1% Tween 20 and 0.2% Triton-X. Sections were next blocked for two hours in 5% normal donkey serum in 1 x PBS containing 0.1% Tween 20 and 0.2% Triton-X. Subsequently, sections were incubated in the same blocking buffer containing anti-red fluorescent protein antibody (polyclonal anti-RFP, Rockland, #600-401-379, Lot #35634; dilution: 1:1000) on an orbital shaker at 4°C overnight. Sections were then washed three times for ten minutes in 1 x PBS with 0.1% Tween 20 and 0.2% Triton-X and incubated for two hours in blocking buffer containing a secondary antibody (polyclonal anti-rabbit Alexa488, produced in donkey, xxxxxxxx; dilution 1:400). Afterwards, sections were washed twice for ten minutes in 1 x PBS with 0.1% Tween 20 and 0.2% Triton-X, followed by one washing for ten minutes in 1 x PBS. Sections were next incubated for 2 minutes and 30 seconds in DAPI solution (10 μ g/ml), washed three times for ten minutes in 1 x PBS, mounted in 0.1M phosphate buffer onto Superfrost Plus slides and coverslipped using fluorescence-protecting medium (Fluoromount™, Sigma Aldrich). All striatal sections were imaged using a slide scanner (Axio Scan.Z1, ZEISS) and striatal viral transduction was analyzed and mapped using ZEN software (ZEISS) and a mouse brain atlas(Paxinos and Franklin 2001).

Electrophysiology

Behavioral activity, video recorded using 2 opposite cameras, was recorded along with the neural activity and synchronized through short simultaneous activation of an LED (visible in the video recordings) and of a digital input to the acquisition system (Intan Technologies, CA, U.S.A) at the start of each session. All the devices were properly referenced to ground. Broadband signals were digitalized at 20 kHz and recorded using either Intan GUI (Intan Technologies, CA, U.S.A) or Matlab software (R2016b and R2017b, RHD2000 MATLAB Toolbox).

Optogenetic stimulation

In order to allow for proper viral transduction, all optogenetics experiments were performed at least two weeks after stereotaxic viral injections. All optogenetic manipulations were conducted bilaterally targeting the dorsomedial striatum. The implanted striatal fiber stubs were connected to optical patch cables (200 μ m core and 0.5 m length with a numerical aperture of 0.66) via mating ferrules in a zirconia sleeve. Optical patch cables were connected to Blue light LED source

modules (465 nm) mounted on magnetic LED commutators. The light stimulation patterns were pre-programmed using Radiant Software (Plexon Inc.) and triggered either by TTL signals controlled either by Matlab (R2017b) custom software or using Radiant Software.

Before experimentation, the output power was calibrated with a light power meter (Thorlabs PM100D with S120C sensor). After calibration, light power from optical fiber stubs was measured to be ~ 10 mW. To calculate the theoretical depth of the light irradiance, we used a model based on direct measurement in mammalian brain tissue (Yizhar et al. 2011). Light power was strong up to ~ 0.55 mm depth (2.03 mW/mm²), and light irradiance fell off to 0.8 mW/mm² at a depth of 0.8 mm (Supplementary Figure 1-C). Unless otherwise stated, all devices for optogenetic modulations were purchased from Plexon Inc. (Texas, U.S.A.).

On-demand optogenetic stimulation

A sequence of three stages, each lasting 3 minutes, was repeated four times during one session. During the first stage, no stimulation was performed. During the second stage, an online prediction algorithm triggered a stimulation whenever it predicted the beginning of a grooming event. During the last stage, the same number of stimulations as in the second stage were delivered in a randomly pre-assigned order. Each TTL-triggered optical stimulation lasted 4 s (10 mW, 5-ms pulses at 20 Hz).

Continuous optogenetic stimulation

Each chronic optogenetic stimulation session lasted 30 minutes and consisted of five consecutive repetitions of two stages, a stage of three minutes without stimulation followed by a stage of three minutes with continuous stimulation delivery (10 mW, 5-ms pulses at 20 Hz).

Behavioral experiments

The home-made experimental setup consisted of two units, one nested into the other. The outer apparatus unit was made out of white acrylic and contained passive commutators for electrophysiology and optogenetics, LEDs, which were set to the minimal brightness required for video recording and data synchronization, as well as two cameras, which were connected to a digital video recording system and which allowed for video acquisition from two different perspectives at the height of the mouse (704x576 resolution and 25 frames per second). The inner apparatus unit consisted of a transparent acrylic container with absorbent floor, in which the mouse was allowed to freely move around during experimental sessions. The second unit was placed inside the first unit, the goal being to isolate the mice from any device and from visual external distractions.

Starting between four to ten days after surgery, the animals were habituated for three days to the apparatus prior to experimental onset. Mice were frequently handled, connected to and disconnected from the experimental apparatus. Sessions were performed between 6pm and 8pm, i.e. close to the onset of the animals' active time in order to maximize awake behaviors. At the beginning of each session, mice were gently handled and connected to the electrophysiology acquisition system and/or to the fiber patch cables. Any noises and vibrations were avoided during experimentation. All mice were left connected for 10 to 15 minutes in the behavioral box before the start of the experiment in order to allow them to accommodate to the experimental apparatus. No water or food were provided during the experimental sessions. After each experiment, the behavioral apparatus was cleaned using a deodorant and disinfectant cleaning spray containing 55% ethanol.

Behavioral assessment was done offline manually, using a freely available video scoring software (Kinovea, 0.8.15, www.kinovea.org). Two behaviors were scored, rodent self-grooming and scratching with hind limbs. We quantified grooming duration, number of grooming initialization events, and percentage of time the mice spent grooming as well as scratching duration and number of events. To more precisely capture self-grooming duration than in previous studies (Aldridge and Berridge 1998; Burguière et al. 2013), here, grooming onset was defined as the time point when the front paws of a mouse started to engage in grooming and not when the paws reached the nose (Supplementary Figure 2). End of grooming was defined as the time point when the mouse stopped to groom at least one second or when the grooming behavior was interrupted by another behavior (e.g. scratching). Scratching with the hind limb was also scored in this same manner.

Rodent self-grooming behavior is a complex behavior that usually follow a cephalo-caudal direction and involves distinct phases. We differentiated between two grooming events: (1) complete, typical cephalo-caudal grooming sequences consisting of phases 1 through 4 as previously described (Kalueff et al. 2007) and (2) fragmented grooming activities containing only a single phase. Additionally, we annotated other behaviors such as walking, rearing, sniffing, resting, stretching, heading up, freezing and heading down. These behaviors were used in a database for our supervised learning algorithm.

Local field potential analysis

All data analysis was performed using custom Matlab scripts. Continuous electrophysiological data from Intan RHD2000 system was aligned to behavioral recordings using TTL synchronization signals. Time-windows around manually tagged time points of grooming onset were extracted from the LFP signals. We decreased the broad band data sample rate by a factor of 40 and then low-pass filtered the data using a 10th-order Butterworth filter with a cut off frequency of 10 Hz (Matlab function "filtfilt"). We performed the continuous wavelet transform around grooming events (4s before the grooming onset and 3s after the initialization of the action). We used the Morse wavelet with a symmetry parameter (γ) equal to 3 and a time-bandwidth product equal to 60. For each mouse, we obtained the LFP power spectrum preceding the grooming events by computing the normalized wavelet power spectrum, whereby we averaged all pre-grooming instants over time and events (time-windows of 500ms prior to grooming onset).

Supervised learning algorithm

To obtain the predictive value of OFC low frequency LFP components related to the animal's behavioral state ("about to groom" and "other behavior"), we used a machine learning approach and designed a pre-processing stage that is based on small changes in frequency content over time. For each mouse, we created a database of pre-grooming events and another database that included other timeframes corresponding to other behaviors. The databases were created from five different recording sessions (40 min each) with a minimum of 100 events per database.

For each recorded channel, we calculated Cepstral coefficients (CC) by extracting 1s frames from the LFP signals to have enough samples for a reliable spectral estimate. Two consecutive frames were time shifted by 200 ms to form a matrix of 5 cepstral coefficients frames. The amplitudes of the resulting spectrum were centered and normalized. For each frame, we added the power value defined as:

$$P = \frac{1}{2T} \sum_0^T V(t)^2$$

Hereby, 'T' was equivalent to the number of samples in an input frame (e.g. T=20 000 for a sampling rate of 20 kHz and frame length of 1s). These CC frames and associated power values constituted a single input vector for the classifier representing the features extracted. To each input vector we associated a pair of values representing the expected output of the neural network (pre-grooming = (1, -1) and other behavior = (-1, 1)).

The databases were randomly split into a training data set containing 70% of the events, which was used to train the artificial neural network and into a test data set containing the remaining 30% of events that was used to test the performance of the prediction algorithm. Our artificial neural network had an output (ranging from -1 to 1) for each class (pre-grooming or other behavior). To improve the performance of the algorithm, the classifier used a decision threshold adjustment to decide if the output values of the neural network corresponded to a pre-grooming event or not. The threshold was determined according to a benchmarking dataset. Whenever output values were both either above or below the decision threshold, the classifier didn't choose a class. The decision was computed for each electrode separately; only if more than 80% of these detections pointed to a pre-grooming event then it was counted as such. To obtain the most accurate network configuration, we trained the neural network by changing the preprocessing configuration of the datasets. This included modifying the frequency range for filter bank analysis of the CC, the learning rate and the number of epochs.

Statistical analysis

All data analysis was performed using Graphpad Prism 8.0.1. (GraphPad Software Inc.). P-values were obtained using nonparametric statistical tests. For post-hoc comparisons, we used the Wilcoxon matched pairs test and considered significant difference with $P < 0.05$. Data were expressed as mean \pm SEM values.

ACKNOWLEDGEMENTS

This study was supported by grants from the ANR Jeune Chercheurs Project R16148DD and the Carnot Foundation (to EB), from L'Oréal-UNESCO Postdoctoral Fellowship (to CS) and from the Science and Technology Council of Mexico (CONACYT) and Foundation de France fellowship (to SLMG).

REFERENCES

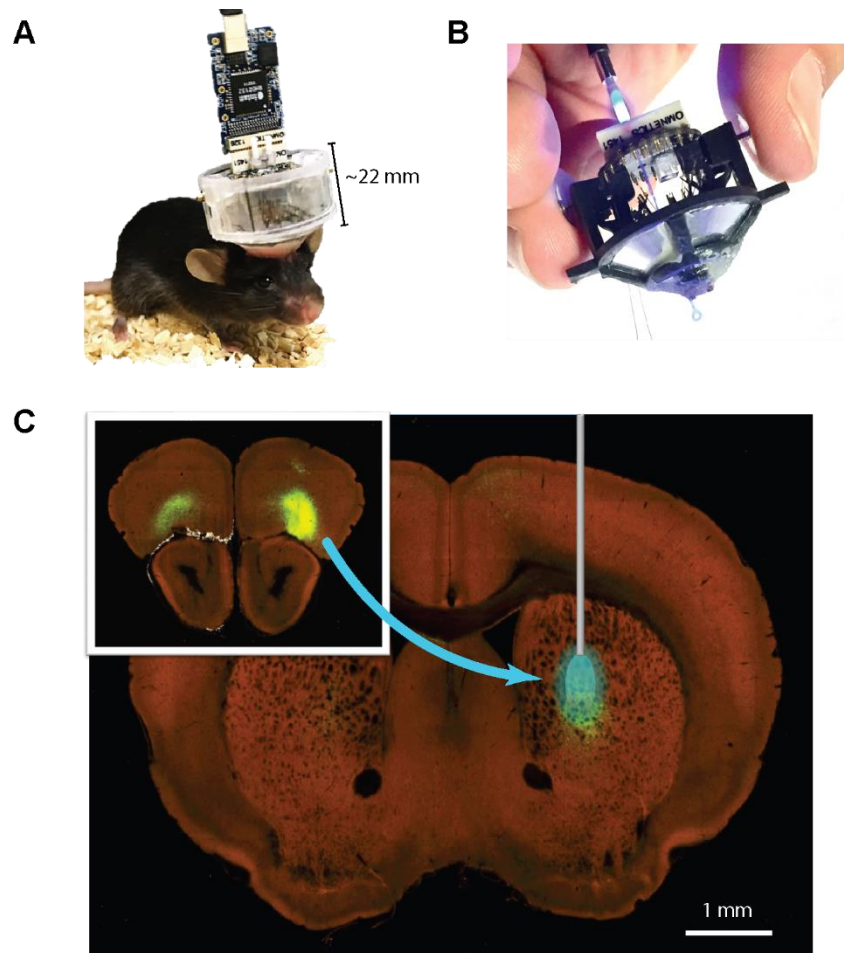
- Aldridge, J W, and K C Berridge. 1998. "Coding of Serial Order by Neostriatal Neurons: A 'Natural Action' Approach to Movement Sequence." *The Journal of neuroscience : the official journal of the Society for Neuroscience* 18(7): 2777–87. <http://www.ncbi.nlm.nih.gov/pubmed/9502834>.
- Alexander, G E, M R DeLong, and P L Strick. 1986. "Parallel Organization of Functionally Segregated Circuits Linking Basal Ganglia and Cortex." *Annual Review of Neuroscience* 9: 357–81.
- Burguière, Eric, Patrícia Monteiro, Guoping Feng, and Ann M. Graybiel. 2013. "Optogenetic Stimulation of Lateral Orbitofronto-Striatal Pathway Suppresses Compulsive Behaviors." *Science (New York, N.Y.)* 340(6137): 1243–46. <http://www.pubmedcentral.nih.gov/articlerender.fcgi?artid=3876800&tool=pmcentrez&rendertype=abstract>.
- Chamberlain, Samuel R. et al. 2008. "Orbitofrontal Dysfunction in Patients with Obsessive-Compulsive Disorder and Their Unaffected Relatives." *Science*.
- Corbit, Laura H., Hong Nie, and Patricia H. Janak. 2012. "Habitual Alcohol Seeking: Time Course and the Contribution of Subregions of the Dorsal Striatum." *Biological Psychiatry*.
- Diniz, Juliana B. et al. 2006. "Chronic Tics and Tourette Syndrome in Patients with Obsessive-Compulsive Disorder." *Journal of Psychiatric Research* 40(6): 487–93.
- Fineberg, Naomi A. et al. 2011. "Disruption in the Balance Between Goal-Directed Behavior and Habit Learning in Obsessive-Compulsive Disorder." *American Journal of Psychiatry* 168(7): 718–26.
- Franklin, Martin E, Julie P Harrison, and Kristin L Benavides. 2012. "Obsessive-Compulsive and Tic-Related Disorders." *Child and adolescent psychiatric clinics of North America* 21(3): 555–71. <http://www.ncbi.nlm.nih.gov/pubmed/22800994><http://www.pubmedcentral.nih.gov/articlerender.fcgi?artid=PMC3401067>.
- Gernert, Manuela et al. 2000. "Deficit of Striatal Parvalbumin-Reactive GABAergic Interneurons Idiopathic Paroxysmal Dystonia." *Journal of Neuroscience* 20(18): 7052–58.
- Gittis, a. H. et al. 2011. "Selective Inhibition of Striatal Fast-Spiking Interneurons Causes Dyskinesias." *Journal of Neuroscience*.
- Gittis, A. H. et al. 2010. "Distinct Roles of GABAergic Interneurons in the Regulation of Striatal Output Pathways." *Journal of Neuroscience*.
- Graybiel, Ann M. 2008. "Habits , Rituals , and the Evaluative Brain."
- Gremel, Christina M., and Rui M. Costa. 2013. "Orbitofrontal and Striatal Circuits Dynamically Encode the Shift between Goal-Directed and Habitual Actions." *Nature Communications*.
- Hilario, M R, and R M Costa. 2008. "High on Habits." *Frontiers in neuroscience*.
- Hintiryan, Hourii et al. 2016. "The Mouse Cortico-Striatal Projectome." *Nature Neuroscience*.
- Hunnicutt, Barbara J. et al. 2016. "A Comprehensive Excitatory Input Map of the Striatum Reveals Novel Functional Organization." *eLife*.
- Joel, Daphna, Julia Doljansky, and Daniela Schiller. 2005. "'Compulsive' Lever Pressing in Rats

- Is Enhanced Following Lesions to the Orbital Cortex, but Not to the Basolateral Nucleus of the Amygdala or to the Dorsal Medial Prefrontal Cortex." *European Journal of Neuroscience*.
- Kalanithi, Paul S A et al. 2005. "Altered Parvalbumin-Positive Neuron Distribution in Basal Ganglia of Individuals with Tourette Syndrome." *Proceedings of the National Academy of Sciences*.
- Kalueff, Allan V. et al. 2007. "Analyzing Grooming Microstructure in Neurobehavioral Experiments." *Nature Protocols* 2(10): 2538–44.
- Kataoka, Yuko et al. 2010. "Decreased Number of Parvalbumin and Cholinergic Interneurons in the Striatum of Individuals with Tourette Syndrome." *Journal of Comparative Neurology* 518(3): 277–91.
- Koos, T. 2004. "Comparison of IPSCs Evoked by Spiny and Fast-Spiking Neurons in the Neostriatum." *Journal of Neuroscience*.
- Lei, Huimeng et al. 2018. "Lateral Orbitofrontal Dysfunction in the Sapap3 Knockout Mouse Model of Obsessive-Compulsive Disorder." : 1–12. <https://jpn.ca/wp-content/uploads/2018/11/44-1-180032.pdf>.
- Lewin, Adam B. et al. 2010. "Comparison of Clinical Features among Youth with Tic Disorders, Obsessive-Compulsive Disorder (OCD), and Both Conditions." *Psychiatry Research*.
- Mallet, N. 2005. "Feedforward Inhibition of Projection Neurons by Fast-Spiking GABA Interneurons in the Rat Striatum In Vivo." *Journal of Neuroscience* 25(15): 3857–69. <http://www.jneurosci.org/cgi/doi/10.1523/JNEUROSCI.5027-04.2005>.
- McGeorge, A. J., and R. L.M. Faull. 1989. "The Organization of the Projection from the Cerebral Cortex to the Striatum in the Rat." *Neuroscience*.
- Milad, Mohammed R., and Scott L. Rauch. 2012. "Obsessive-Compulsive Disorder: Beyond Segregated Cortico-Striatal Pathways." *Trends in Cognitive Sciences* 16(1): 43–51.
- Murray, Jennifer E. et al. 2014. "Increased Impulsivity Retards the Transition to Dorsolateral Striatal Dopamine Control of Cocaine Seeking." *Biological Psychiatry*.
- Oh, Seung Wook et al. 2014. "A Mesoscale Connectome of the Mouse Brain." *Nature*. http://connectivity.brain-map.org/?searchMode=source&sourceDomain=714&primaryStructureOnly=true&tracers=10&isi=false&transgenicLines=177839331&initImage=TWO_PHOTON&experimentCoordinates=2800,3550,6850&experiment=159887627.
- Paxinos, George, and Keith B J Franklin. 2001. Academic Press *Mouse Brain in Stereotaxic Coordinates*.
- Peñagarikano, Olga et al. 2011. "Absence of CNTNAP2 Leads to Epilepsy, Neuronal Migration Abnormalities, and Core Autism-Related Deficits." *Cell*.
- Planert, H. et al. 2010. "Dynamics of Synaptic Transmission between Fast-Spiking Interneurons and Striatal Projection Neurons of the Direct and Indirect Pathways." *Journal of Neuroscience*.
- Rapanelli, Maximiliano et al. 2017. "Targeted Interneuron Depletion in the Dorsal Striatum Produces Autism-like Behavioral Abnormalities in Male but Not Female Mice." *Biological Psychiatry* 82(3): 194–203. <http://dx.doi.org/10.1016/j.biopsych.2017.01.020>.
- Silberberg, Gilad, and J. Paul Bolam. 2015. "Local and Afferent Synaptic Pathways in the

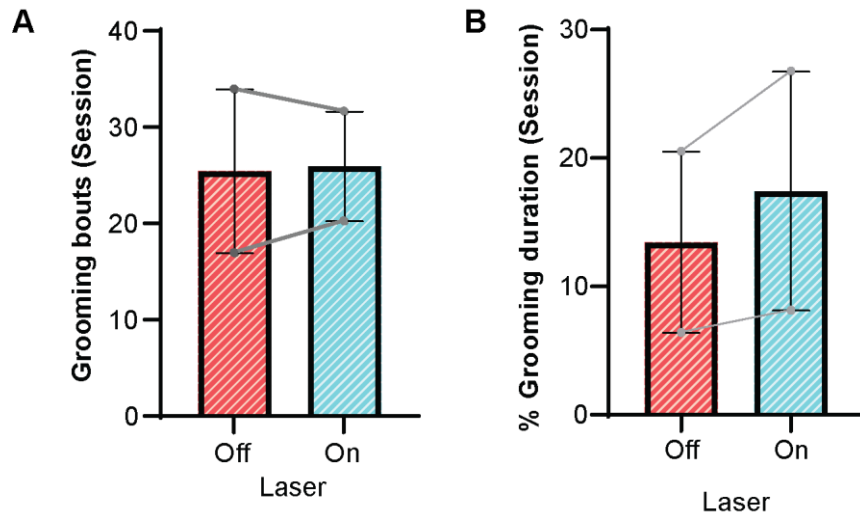
Striatal Microcircuitry.” *Current Opinion in Neurobiology*.

- Swain, James E. et al. 2007. “Tourette Syndrome and Tic Disorders: A Decade of Progress.” *Journal of the American Academy of Child and Adolescent Psychiatry* 46(8): 947–68. <http://dx.doi.org/10.1097/chi.0b013e318068fbcc>.
- Thorn, Catherine A., Hisham Atallah, Mark Howe, and Ann M. Graybiel. 2010. “Differential Dynamics of Activity Changes in Dorsolateral and Dorsomedial Striatal Loops during Learning.” *Neuron*.
- Welch, Jeffrey M et al. 2007. “Cortico-Striatal Synaptic Defects and OCD-like Behaviours in Sapap3-Mutant Mice.” *Nature* 448(7156): 894–900. http://www.ncbi.nlm.nih.gov/sites/entrez?Db=pubmed&DbFrom=pubmed&Cmd=Link&LinkName=pubmed_pubmed&LinkReadableName=RelatedArticles&IdsFromResult=17713528&ordinalpos=3&itool=EntrezSystem2.PEntrez.Pubmed.Pubmed_ResultsPanel.Pubmed_RVDocSum.
- White, Norman M., and Robert J. McDonald. 2002. “Multiple Parallel Memory Systems in the Brain of the Rat.” *Neurobiology of Learning and Memory*.
- Xu, M., L. Li, and C. Pittenger. 2016. “Ablation of Fast-Spiking Interneurons in the Dorsal Striatum, Recapitulating Abnormalities Seen Post-Mortem in Tourette Syndrome, Produces Anxiety and Elevated Grooming.” *Neuroscience*.
- Yin, Henry H. et al. 2009. “Dynamic Reorganization of Striatal Circuits during the Acquisition and Consolidation of a Skill.” *Nature Neuroscience*.
- Yin, Henry H., and Barbara J. Knowlton. 2006. “The Role of the Basal Ganglia in Habit Formation.” *Nature Reviews Neuroscience* 7(6): 464–76.
- Yizhar, Ofer et al. 2011. “Optogenetics in Neural Systems.” *Neuron* 71(1): 9–34. <http://dx.doi.org/10.1016/j.neuron.2011.06.004>.

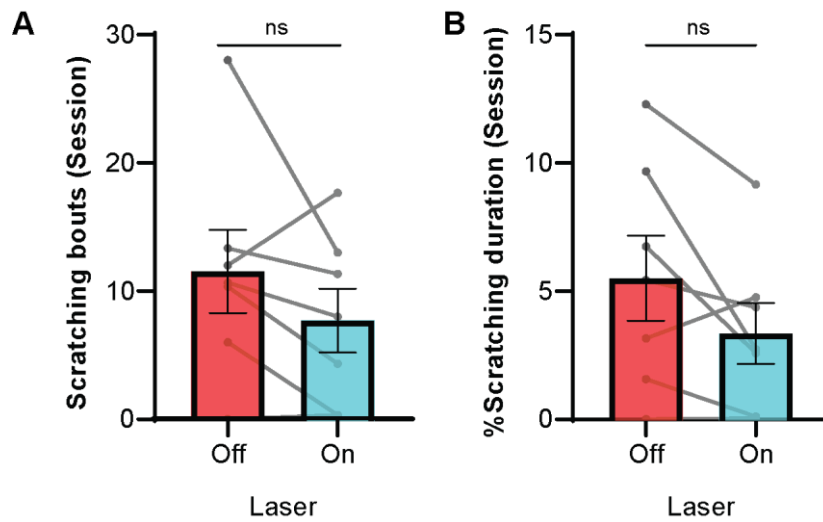
SUPPLEMENTARY MATERIAL



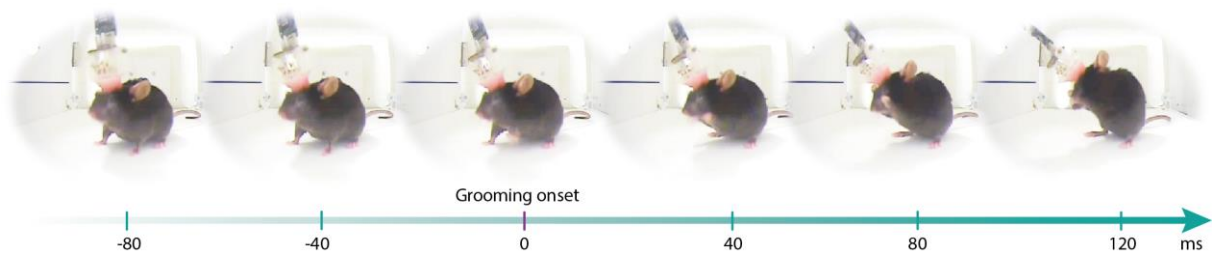
Supplementary Figure 1. Combined optic-fiber and electrophysiology implant for simultaneous neural and optical chronic manipulations in freely moving mice. (A) Picture of a mouse implanted with our custom-build chronic device, the implant weighted < 3g and allowed normal locomotion. (B) Closed-view of the chronic device, bilateral optic fibers were fixed to reach 2-2.2 mm depth in the dorsomedial striatum. (C) The images show the schematic location of the fiber stub and its theoretic depth range of irradiance. Images were modified from the Allen Mouse Brain Connectivity Atlas (Experiment 159887627) to show the axonal projections from the location of our recording sites in the OFC to the location of the fiber stub in the striatum. Axonal projections are labeled by viral tracers and visualized using serial two-photon tomography.



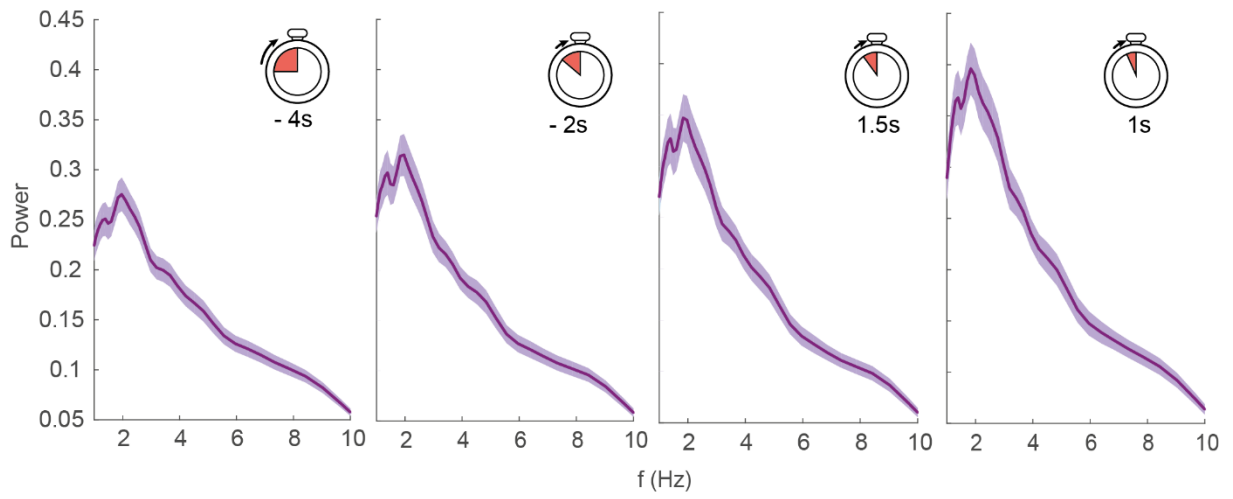
Supplementary Figure 2. Effect of chronic optogenetic activation of DMS PV interneurons in SAPAP3 mice injected with a control virus. The effects do not seem to not reduce number of grooming bouts (A) nor the total percentage of time spent in grooming (B).



Supplementary Figure 3. Effect of chronic stimulation of dorsomedial striatal PV interneurons on scratching behavior in Sapap3 mutant mice. Difference between scratching bouts and percentage of time spent in scratching during stimulation on and off shows no statistical difference. $n=7$ mice. Error bars represent mean \pm SEM ($P>0.05$, Wilcoxon matched pairs test).



Supplementary Figure 4. Continuous images frames from a grooming event. The grooming onset was assigned to the first frame that showed action from anterior limbs to engage in a grooming event.



Supplementary Figure 5. Averaged spectrogram of different time-windows prior to grooming events.

PART III: DISCUSSION AND PERSPECTIVES

Discussion and perspectives

In this final part of the manuscript, we go through the principal results previously described in **chapters 4, 5, and 6**, discussing their contributions, examining what question they tried to address and what other questions our results raised, without forgetting the translational perspective (or the significance for clinical research) that motivated in the first place this project. This dissertation presents the principal results of a thesis project whose central motivation was to investigate a path to a) better understand the pathophysiology and b) optimize treatments for pathological repetitive behaviors. Keeping that direction in mind, we used for our studies a rodent model that expresses pathological self-grooming behavior. The guiding thread was sustained by converging studies pointing to the orbitofrontal-striatal pathway to be abnormally active in OCD patients as well as in animal models of compulsive behavior as reviewed in the introduction section. We focused our attention on a striatal cellular subtype, the parvalbumin-immunoreactive fast-spiking interneurons (PVI), which play an essential role in regulating the expression of striatal-dependent behaviors, and that are likely implicated in the expression of pathological repetitive behaviors. To achieve such goals, some technological developments were necessary to be done in order to move forward in this direction, and these are the results presented in **chapters 4 and 5**.

I. Technological developments for closed-loop experiments

The aim of the first two parts of the experimental work (**chapter 4 and 5**) of this dissertation was to provide a new set of tools for implementing experiments involving closed-loop feedback. In order to take neuromodulation research to the next level, neuroscience needs affordable and extensible platforms for executing hard real-time analysis and stimulation. In this context, the developments presented in **chapter 4** are part of a software toolkit that was developed as a part of this thesis project, while the developments presented in **chapter 5** correspond more to the hardware part of the toolkit. These technical developments were produced in order to fulfill the needs for flexible devices suitable in experimental frameworks for closed-loop neuromodulation. Some of them were directly implemented in the results presented in **chapter 6** of this manuscript, and others are meant to be used for further applications in closed-loop experimentation.

1.1. Software developments

In closed-loop neuroscience, the online analysis of multi-unit extracellular recordings of brain activity has led to the development of numerous tools, ranging from real-time executed signal processing algorithms to electronic devices and applications. Currently, the evaluation and optimization of these tools are hampered by the lack of ground-truth databases of neural signals. Indeed, to assess any toolbox or algorithm aiming to analyze online neural data, the ideal way to proceed is by using benchmarks datasets that could be configurable to match the “real life” situation in which the algorithms would be performing. For instance, for an implanted device aiming at analyzing continuous neural

signals, its validity must be verified with benchmark datasets that would include artifacts encountered in normal conditions.

Moreover, we are witnessing an exponential increase of neural data collection with massive simultaneous recordings and examples of new signal acquisition devices and signals processing algorithms. Despite these technological improvements, there are surprisingly few testing grounded-truth datasets available (D. Henze et al., 2009; D. A. Henze et al., 2000). To address this issue, we developed a bio-inspired computational approach to create annotated and configurable databases of neural signals (Mondragón-González & Burguière, 2017). The neural tissue simulator presented in **chapter 4** aims at combining neural signals simulated by a hybrid model with other components encountered in real recording such as different artefactual events. We proved the utility of our simulator by recreating two experimental conditions: extracellular signals extracted from anesthetized or awake rodents and we compared their resemblance to recorded ones in terms of frequency properties and spike proportions. We were also able to prove how artifacts affect the frequency components in neural recordings with a particular impact in the frequency range of 1000-3000 kHz, the same band where action potentials events fell into. To show the flexibility of our approach, we simulated two experimental setups: simulations from “virtual” arranged tetrodes and polytrodes. We also recreated the spatial neural distribution of the CA1 layer of the rat hippocampus to show how diverse types of neurons can be spatially set to follow an anatomic distribution. Our benchmark generator can be used for testing devices, and analysis modules used in closed-loop experiments, in which a stimulus is delivered immediately after a feature of interest is detected. In this configuration, a series of devices and software analysis modules interact to form the closed-loop chain; we can thereby evaluate the performance of the analysis modules using our bio-inspired simulator (Mondragón-González & Burguière, 2017).

1.2. Hardware developments

1.2.1. Real-time signal processing hardware to optimize the design of closed-loop experiments.

As introduced in this manuscript, optogenetics closed-loop feedback is currently used in animal research for interrupting certain types of undesired neural activity, such as seizures (Esther Krook-Magnuson, Armstrong, Oijala, & Soltesz, 2013; Paz et al., 2013) and we have demonstrated in **chapter 6** that it can be used to help alleviate pathological repetitive behaviors. In this kind of applications, algorithms are implemented in either a soft-time or a real-time manner to detect large amplitude oscillations in the LFP signals, which triggers optogenetics stimulation. While such approaches can be implemented without major limitation in software, single-unit based closed-loop experiments would be most likely incompatible with soft-time solutions due to single-unit fast changing dynamics. For instance, the detection of a specific spiking pattern would need a more immediate and well-controlled reaction time in the processing and analysis compared to

LFP patterns that by nature involve slow fluctuations in time. This was the primary motivation in implementing simple real-time analysis modules for the preprocessing of neural action potentials. The goal, in this case, was to establish the foundation that would allow for single-cell processing in hard real-time and eventually the adding of more complex analysis modules such as clustering or pattern recognition in real-time. In any case, the essential pre-processing stage requires common steps such as real-time acquisition, band-pass filtering, and action potential detection. The design of this hardware circuits was implemented in Field Programmable Gate Arrays (FPGAs) using the Verilog Hardware Description Language, which compared to computers or general-purpose (micro) processors have the advantage of high-speed parallel processing with strict clock dependent execution. We showed the feasibility in implementing such modules on hardware by reporting how little registers and logic usage was necessary, both characteristics appreciated for an application intended to process several channels and react immediately to them. Although our experimental design shown in **chapter 6** did not include this kind of processing, the results that we obtained opened the way to different proposed experiments involving single-unit online analysis that would be interesting to investigate (and that will be discussed in the next section of the discussion). The proof of concept of hardware real-time spike analysis has been previously demonstrated with a system that can be configured to detect specific patterns of firing based on the spatiotemporal characteristics of the signals (J. Müller, Bakkum, & Hierlemann, 2012). We could imagine taking a similar approach to the next level by implementing real-time machine learning algorithms for automatic spiking pattern recognition. There are obvious potential interests in using an FPGA (or similar real-time hardware like Complex Programmable Logic Devices (CPLDs)) to perform signal-processing in the clinical context of brain stimulation. The first is that it gives information on the number of hardware resources needed for an implantable device and the second point is that it allows objective quantification of the power necessary to perform continuous online processing of neural signals plus stimulation delivery.

A crucial step towards this goal is to assess the validity and performance of the hardware architecture; indeed, a degree of trustfulness of this kind of approach needs to be evaluated, and this especially true for closed-loop clinical research. When recording electrical activity from the extracellular medium there is no exact way to know the ground truth of your signals, unless having identified the surrounding cells through patch clamp (D. A. Henze et al., 2000) or with other technics such as two-photon imaging (Kaszás et al., 2014), but these techniques are limited to the number of cells identified. In our case, the performance of our hardware designs, presented in **chapter 5**, was assessed with a set of reliable benchmark datasets of extracellular recordings created specifically for this purpose with a software tool that we presented in **chapter 4** (Mondragón-González & Burguière, 2017). Therefore, to correctly evaluate and compare the performance of on-chip real-time modules (such as FPGAs presented before), the use of reliable benchmark datasets, such as the ones presented here, are essential. Ideally, this should be done by generating the datasets via the simulator and streaming them directly to the acquisition

systems. To that end, I designed an electronic board, 'the Neural streamer' that allows to replay and stream previously recorded or simulated neural data coming from different channels directly into the acquisition and analysis system. The real or simulated recordings are saved into a micro-SD memory card as raw data, and then the Neural streamer is in charge of streaming the data at a pre-defined frequency. This tool allows performing multiple useful tests for real-time closed-loop experiments without the need for an animal implanted. This addition to the toolbox kit can be used for instance to precisely measure the closed-loop time-delay at different levels (acquisition, processing, and feedback).

1.2.2. Neurophysiological device improvements for animal model experiments

Nowadays many commercially available implantable solutions combine electrode recording with light delivery. Nevertheless, the cost of these solutions is not negligible when designing experiments, and most of them are not flexible enough as they offer a single configuration of electrode arrays.

A simple addition to the neuroscientist's toolbox I developed and that is tremendously handy was the optimization of a custom-made light implant for electrophysiology and optogenetics experiments in rodents. As presented in the first section of the experimental work, I optimized a light implant (< 3g, 32 channels) that allows movable tetrode recording and light stimulation. When having all the materials available, the implants can be built within two days and can be easily modified to reach different brain targets. This design was used in the experimental part of **chapter 6**. In our experience, these home-made implants successfully allowed us to record from eight adjustable tetrodes simultaneously for several months in awake, behaving mice while optogenetically manipulating neural activity. As explained in **chapter 6**, we implanted the custom-drives in an animal model of compulsive behavior, the *SAPAP3-KO* mice. The characteristic phenotype of this animal model includes excessive grooming (Welch et al., 2007) and small size compared to wildtypes (our observations) meaning that they execute excessive head locomotion from grooming and weight less than wildtypes. By using such an animal model, we were self-imposed with strict restrictions regarding the robustness and weight of the implant. The implants had to be light enough, so they did not interfere with the phenotype by allowing the animals to easily self-groom. Our home-made implants weight less than 3g (representing on average 9% of body weight for mutant animals for an implant including two optic fibers, and 32 recording channels) and were stable over time. Additionally, the same design could be used for DBS in rodents and was designed to target different brain regions by easily modifying the bottom of the implant.

The second part of hardware development required for our closed-loop experiments was a home-made modular chamber. This development was motivated by the fact that commercial, experimental chambers are expensive and sold as one block-chambers,

meaning that if sensor devices or actuators are needed in the experiments, they are directly mounted on the cage where the animal is left. This has a negative effect on the electrophysiological recording as electrical devices mounted on the cages are considered potential sources of noise. A Faraday cage can help reduce external electrical noise, but this is not a perfect solution and to improve experiments, all electrical sources should be isolated from the animals when possible. A strategy that has worked for us for reducing noise, besides properly grounding equipment and avoiding grounding loops, is to isolate the mouse from as much peripheral equipment as possible. By doing this, the only things inside the experimental chamber are the mouse, the headstage and the fiber patches. I have, therefore, designed and built a low-cost experimental chamber consisting of two units, one nested into the other. The outer unit holds all the electronic components (passive commutators of electrophysiology and optogenetics, LEDs for visual cues and cameras) and the inner apparatus unit was isolated from contact with the first unit. The home-made experimental chamber also had the advantage of limiting visual and device-related distractions for the mouse. The approach is another small contribution to the neuroscience toolbox since it is straightforward to build, easy to modify and low-cost.

The experiments presented in **chapter 6** offer a glimpse of what is possible to do with a part of the toolkit that I developed. The tools developed for implementing closed-loop experiments are well within our research, and it would be advantageous to apply them for a future hard real-time closed-loop application.

1.3. Perspective and potential benefit of closed-loop design for clinical application

An often mentioned advantage of adaptive brain stimulation is that it could reduce stimulation current without the loss of therapeutic effect, by providing a more biologically tuned response, potentially extending the stimulator's battery life, thus reducing the number of surgeries needed for replacement. Most commercially available DBS systems are not rechargeable, and battery depletion requires replacement. Between the top three concerns among patients and clinicians regarding DBS are the complications of surgery and anesthesia. Additionally, there is another concern from the clinical part on patients falling to keep appointments for device monitoring which can result in incomplete or failed neuromodulation (Naesstrom et al., 2017). Having to return to a clinic every few months for parameter adjustment or battery replacement can be a burden to patients since there is a substantial psychological and financial cost associated with returning to the clinic. We could imagine that a closed-loop DBS approach could potentially address this important issue reducing the frequency of costly and time-consuming clinical consultations. The advantage in reduction of the battery's life with closed-loop DBS remains truly advantageous only if the additional cost of signal analysis plus stimulation remains lower. This benefit-cost analysis cannot correctly be evaluated unless performing the estimation in the intended electronic system to use. An alternative solution can be to assess the total power consumption from simulations, but this is only possible with real-

time based systems such as FPGAs or CPDLs, for which the exact delay and number of operations and resources pre-allocated can be known.

Another critical factor to consider for the development of novel closed-loop DBS strategies are the actual concerns among patients and clinicians, and this includes the novelty of the treatment, translated in inappropriate responses to alterations in the brain circuitry. Indeed, new closed-loop DBS paradigms are not immune to malfunction, and in RB-related disorder are still at the beginning of the learning curve concerning closed-loop DBS. The rationale to adopt in this case is that for the first trials, the medical team should be able to change modalities between closed and open loop. As is usually the case for novel therapeutic applications, some limitations have been revealed with the first studies, and some others will be discovered on the go. These limitations are likely to be similar for the different applications in which adaptive DBS is explored. For example, algorithms that require the tuning of a considerable number of parameters lead to a complex relationship between inputs and their effects. This could be translated in a very specific and not trivial manner to interpret the setting's influence in the efficiency of the approach. The only way to know of device malfunction or suboptimal function is through observations or reports of patient's symptoms. In the case of DBS for movement disorders this is easier to notice since adverse effects are immediately detectable but for psychiatric disorders such as OCD, the cognitive or affective symptoms from circuit dysregulation may take weeks to appear (Ineichen, Glannon, Temel, Baumann, & Surucu, 2014). A closed-loop approach that informs on the internal brain state could be useful to address this problem. Moreover, we can cite in a more philosophical level, the idea that a device can control a person's behavior without his conscious awareness raise debates on autonomy, control and identity (Naesstrom et al., 2017), although this can also be questioned on open-loop DBS.

In resume, closed-loop DBS seems a very promising approach worth investing in. Although most of the closed-loop DBS evidence comes from movement disorder studies, there is no reason to think that similar approaches could not benefit RB-related psychiatric disorders. There are still a few examples of clinical applications to know all the variables involved in conducting such a paradigm in psychiatric disorders, including the advantages and long-term inconveniences. Nevertheless, animal research oriented in this direction should first provide the necessary evidence of the cellular mechanism for the network effects of DBS to provide an optimistic framework to rely on, and that would help to design future clinical trials and the next-generation devices for adaptive deep brain stimulation.

II. Insights into the neurophysiology of repetitive behaviors by using closed-loop optogenetics.

Experiments involving closed-loop stimulation are of major interest for basic-science to investigate the underlying neurophysiology of a core symptom of RB-related disorders, as well as to give pre-clinical evidence to inform next-generation therapeutic approaches for DBS. In our case, a closed-loop approach was implemented to investigate the regulation of the expression of RB in the cortico-striatal circuits, particularly in the dorsal striatum, for this we focused our attention on the striatal interneuronal network, a neurophysiological substrate suspected to have a crucial role in the regulation of RB.

2.1. The role of the striatal interneurons in the regulation of repetitive behaviors

In normal conditions, a powerful inhibitory network in the striatum keeps a balance of excitation and inhibition, and therefore is critical for regulating striatal output. In conditions where pathological repetitive behaviors are expressed, there is an imbalance of striatal activity possibly as a consequence of interneuronal network deficiency. The hypothetical model is that in part, as a result of this deficit there will be a hyper activation of the entire cortical basal ganglia loops. In **chapter 6** of this manuscript we presented the results of a study conducted on the *SAPAP3-KO* mice, which exhibit excessive self-grooming and increased anxiety. Through optogenetic manipulations, we were able to manipulate precisely this striatal interneuronal network suspected to have a crucial role in the emergence and regulation of RB. This study provided the first evidence that by continuously lifting the PVi network of inhibition in the dorsomedial territory of the striatum it is possible to reduce compulsive self-grooming to normality. Indeed, continuous optogenetic stimulation of PVI in the dorsal medial striatum had a rapid effect in normalizing grooming behavior in all the *SAPAP3-KO* mice that went through our protocol. This reduction in grooming could have been obtained in different ways, for instance, by having many bouts of short duration or fewer but longer bouts. In order to causally understand the effects in behavior following stimulation, we looked closer into its characteristics during on and off stimulation. Our results showed that the dimension that seemed to have changed were the number of initializations of grooming events, and this had a diminishing impact on the total time spent grooming. Other dimensions such as the average duration of a single event, or the proportion of different grooming types were unaltered. In this study we did not look specifically at the effects of stimulation on excessively rigid serial patterns because the average duration of individual grooming sequences stayed unchanged between the stimulation mode on and off, suggesting that it had no effect in changing the rigid serial patterns of grooming behavior or in completion of the chain pattern. Our results show that the striatal micro circuitry, and specifically the PVi, are important in inhibiting onset of compulsive behavior, these results are in line with a previous hypothesis from a past study (Burguière et al., 2013b), in which the PVi were highlighted to be role players in the regulation of RB. Indeed, previous studies have highlighted the role of the dorsal striatum in contributing directly to action selection and initiation through the integration of the different corticostriatal loops (B. W. Balleine et al., 2007). The observation that PVi stimulation was reflected more in a reduction of

grooming initiations also echoes a previous study that showed the influence of PVI in choice execution (Gage, Stoetzner, Wiltschko, & Berke, 2010) and how distributed FSI pulse would help to suppress prepotent but currently inappropriate actions. Other recent studies have also looked at the specific roles of dorsal striatal FSI and MSNs during the execution of acquired behavioral sequences, and shown that FSIs interact with MSNs to shape action boundary activation (Burgess, Graybiel, Burgess, & Graybiel, 2018). In this same line, striatal PVI have shown to be capable of suppressing output via competing inhibitory microcircuits (Lee et al., 2017). Since the PVI stimulation didn't change the characteristics of grooming behavior this also may suggest that different striatal pathways may regulate the patterning and sequencing of grooming activity.

In analyzing the effect of Striatal PVI continuous stimulation, we confirmed that the *SAPAP3-KO* groom more than the wild-type mice, this is reflected in the duration of grooming and number of events. The *SAPAP3-KO* mice groom approximately 12% of the assed time compared to 5% in the wild-type mice (Protocol Stimulation OFF). This percentage seems inconsistent with a previous study, which characterized the *SAPAP3-KO* mice phenotype (Welch et al., 2007) and found they groom more than 30% of the time (during similar schedules than ours). However, other studies have reported inferior percentages of grooming rates (Ade et al., 2016; P. Xu et al., 2013). This disparity could be explained in part, because of the differences in the experimental conditions when assessing grooming. Potential reasons could include difference in physical motor effort between tethered and non-implanted animals, the habituation time defined in the experimental protocol, environmental factors, genetic drift, and importantly, the state in which the mice are included in the experiments. Indeed, *SAPAP3-KO* mice that already present advanced facial lesions might groom more, as grooming besides being the cause of lesioning is also a behavior executed for wound healing (Spruijt et al., 1992; Young, Schattenkerk, Malt, Koroly, & Li, 1980). To diminish this confounding factor, in our experiment we didn't included *SAPAP3-KO* mice with already advanced body and facial wounds (bleeding wounds, strong skin irritations, and damaged in ears and around eyes). Importantly, we separately analyzed scratching behavior from grooming behavior since these instances may reflect two distinct repetitive behaviors (Berridge & Whishaw, 1992). In the previous mentioned studies with the *SAPAP3-KO* animal model, this distinction is not clearly defined in the methodology and chances are that these RB are both taken together and therefore have an augmented effect in the quantification of total grooming time reported. From our point of view, it is better to analyze these categories separately since scratching in rodents is a rather simple rhythmic movement made by the hind limbs that can be distinguished from the more complicated patterned grooming sequences (Brash et al., 2005). It might be possible that these distinct behaviors may be regulated by circuits arising from different cortical areas, for instance, it has been shown that striatal inputs coming from the anterior cingulate cortex (ACC) are a specific critical circuit element for regulating scratching behavior ((Lu et al., 2018), it would make sense then to categorize it as a different type of RB, one that would fit better into the complex motor tic

category. From our results, both RB are increased in the *SAPAP3-KO* mice compared to wildtype animals and from a translational point of view this is interesting given the frequent comorbidity in patients presenting complex motor tics and compulsive behavior. We observed that optogenetic stimulation in the dorsal medial striatum had a more pronounced effect in alleviating excessive grooming than scratching, perhaps because of the cycling effect that an already irritated skin has on scratching. For instance, S. Chen and colleagues demonstrated in the *Hoxb8* rodent model, a model with a similar phenotype, that skin irritations from compulsive excessive grooming increased scratching behavior worsening body lesions, and that localized lidocaine treatment alleviated scratching caused by a response to chronic itching but did not alter the grooming behavior (S. K. Chen et al., 2010). Apart from our observations in compulsive behavior, the *SAPAP3-KO* model allows the assessment of other dimensions and their relation to compulsivity. In this case, it could be interesting to explore the effect of stimulation in other behavioral measures such as anxiety, since previous studies have reported opposite effects in anxiety alleviation using clinically validated treatments such as fluoxetine (Welch et al., 2007) and DBS (Pinhal et al., 2018) in the *SAPAP3-KO* mutant mice.

2.2. Identification of neurophysiological marker predictive of grooming behaviour

In the context of compulsive behavior, the study of circuits arising from the OFC are of special interest because of the important role in inhibitory control, indeed, when lateral OFC-centromedial striatum circuit is disinhibited, urges of compulsive behaviors are triggered (Jahanshahi et al., 2015). This theory is supported by evidence in OCD patients using functional magnetic resonance imaging (fMRI) and positron-emission tomography (PET) (Menzies et al., 2008). Particularly, imaging studies showed a hyperactivity of the OFC-caudate circuit that is increased by compulsive symptom provocation (McGuire et al., 1994; Milad & Rauch, 2012; S. L. Rauch et al., 1994; Simon et al., 2010). We analyzed functional grooming-related LFP activity by performing *in-vivo* multichannel recording in the IOFC of freely-moving *SAPAP3-KO* mice. A key finding of our study comes from the demonstration of the development of a non-sustained internally generated 1-4 Hz oscillations in the orbitofrontal cortex that temporally predicted grooming initialization. The rise in this oscillations directly correlate to grooming episodes while being more prominent within the one second preceding grooming onset, and were not observed during resting behavior, suggesting that this acute internally generated oscillation could be useful predictor biomarker for self-grooming onset. A previous study have highlighted a difference in the activity of the IOFC previous to aberrant RB onset, it shown that in the *Sapap3* mice there was an elevation in orbitofrontal cortex firing previous to grooming onset (Burguière et al., 2013b). To our knowledge, our data provide the first demonstration of a low-frequency biomarker that is correlated to the prediction of self-grooming behavior. Interestingly, we are not the first ones to have observed low-frequency neural signatures preceding self-initiated movements. Movement-related slow cortical potentials refers to a slow buildup of electrical potential, which reliably precedes

self-initiated movements. It has been proposed as reliable markers and long used as EEG signatures of motor control and are a main feature in Brain-Machine Interfaces but this are mostly measured over the primary motor cortex (Shakeel et al., 2015). Since the low-frequency signature preceded a compulsive behavior, we could ask if this signal could represent an internal state or be translated in an urge that drives the expression of RB, and if so how could it be generated? A recent study presented a very original perspective on that matter, in this study the authors explained how the initiation of an emotional state is related to a somatic change that drives prefrontal cortex (PFC) response to directly participate in sustaining the emotional behavior (Bagur *et al.*, 2018). With this study and a previous one (Karalis et al., 2016), they showed how regular 4Hz breathing in mice feeds back to the brain via the olfactory bulb to train 4Hz oscillations in the PFC and how this predicts freezing behavior. This piece of evidence gives a rationale alternative to explain how low-frequency oscillations that precede behavioral changes related to emotional states origin.

Regarding specific IOFC activity, a recent study provided interesting information regarding IOFC dysfunction in the *SAPAP3-KO* mice. The authors investigated local field potential oscillations in the IOFC of awake mice during rest. They found that compared to wildtype mice, the IOFC of *SAPAP3-KO* mice exhibited network dysfunction, demonstrated by a decreased power of local field potentials that included the delta band (1.5-4 Hz) (Lei et al., 2018). Interestingly, the inverse effect is obtained in the OFC following deep-brain stimulation of the nucleus accumbens, a DBS target for OCD (McCracken & Grace, 2007, 2009). We could imagine that the delta signature that we observed might be related to the recruitment of cortical pyramidal neurons that will, in turn, drive striatal PVi network downstream. Therefore, that power decrease in IOFC could result in less PVi recruited and as a consequence in a hyper activation of MSNs. Indeed, preliminary data from our laboratory showed two interesting points that support this theory. The first point is that in wildtype animals we have seem to find a similar biomarker preceding grooming in the IOFC and the second point is that when compared to *SAPAP3-KO* mice the baseline power of the slow oscillations seems significantly higher than that of the mutant mice. In this sense, there are some interesting question unanswered: 1) what is the causal origin for these functional changes observed in the IOFC and 2) if there is no external signal to trigger the RB how is the precise time of onset determined? Future experiments exploring the synchronization of the delta band with individual neurons may help untangle this story.

2.3. Closed-loop stimulation of striatal interneuron is sufficient to abolish pathological grooming

Although in our study we did not investigate the exact origin of the low-frequency signature we observed in the IOFC, our observations showed that this signature was present across mutant animals, did not seem to be an artefactual event since it was found only in recordings from the IOFC and was recorded from two distinct acquisition setups. Motivated by this finding, we developed a supervised machine learning approach to provide optogenetic stimulation in a context-specific manner. The classification algorithm was designed to consider the different representation of the underlying neural activity of the different electrodes, indeed although multiple electrodes are implanted into the same brain region the size and shape of the sampling field might lightly vary depending on the impedance of the electrode. Using coherent information from multiple recording locations within the OFC allowed us to act upon agreement on the activity of the same region. Due to the fast intervention required to predict a behavior event to come when acquiring neural signals, when choosing an algorithm, we needed an easy to implement for further studies on hardware and that allowed us to obtain results quickly to validate the approach. We believe that cepstral coefficients are an unconventional but efficient alternative to classic feature extraction methods to feed into a number of supervised learning algorithms, and that this approach could be used in other applications than the one presented in this study. Indeed, if the frequency band of interest is known, the frequency scale of triangular filters can be arranged to focus in such frequency band while taking into consideration the contribution of other frequency bands but reducing its influence since those coefficients provide information about the rate of change in the different spectrum bands.

By successfully predicting grooming onset, exploiting the rate change in the 1-4 Hz spectrum band, we were able to investigate the effects of acute optogenetic stimulation in a closed-loop manner. Our results show that closed-loop optogenetic stimulation effectively alleviated compulsive grooming in all *SAPAP3-KO* mice that went through closed-loop experimentation while significantly reducing the stimulation time by 87%. Compared to continuous open-loop stimulation, closed-loop stimulation was more effective in reducing the total time spent in grooming while the reduction in number of events was similar for both approaches. Although having a strong positive efficient effect during closed-loop modulation, it is still not a trivial task to evaluate if closed-loop brain stimulation is a better strategy than open loop. From a translational perspective, we should first investigate the long-term effects of the stimulation and secondly to get a real comparison of power economy, the analysis stage should be implemented in hardware to get a real estimate on the total power consumption.

Here we have provided the first in-vivo closed-loop experiment to alleviate pathological RB in the *SAPAP3-KO* mice. This study gives important evidence of the role of striatal PVI in regulating RB and particularly in their necessity during the temporal window previous to initialization of RB. A crucial point to mention is that the closed-loop approach

presented was a predictive one, since it reacted before RB onset and not to the detection of an on-going RB, therefore the predictive on-demand feedback allowed us to define the temporal specificity characterizing the causal role of PVi in RB. Additionally, the predictive approach implemented may be useful in further experiments as a platform to explore in a closed-loop manner other brain targets for therapeutic purposes. The presented results give a more confident view for future adaptive DBS in patients suffering from RB-related disorders since our online analysis method could be easily implemented in on-board electronics (**Figure 42**). These findings although they raised some intriguing questions, advance our understanding of the neuropathophysiology and circuitry mechanisms that underlie compulsive behaviors, and may help generate and redefine new hypothesis for further investigation.

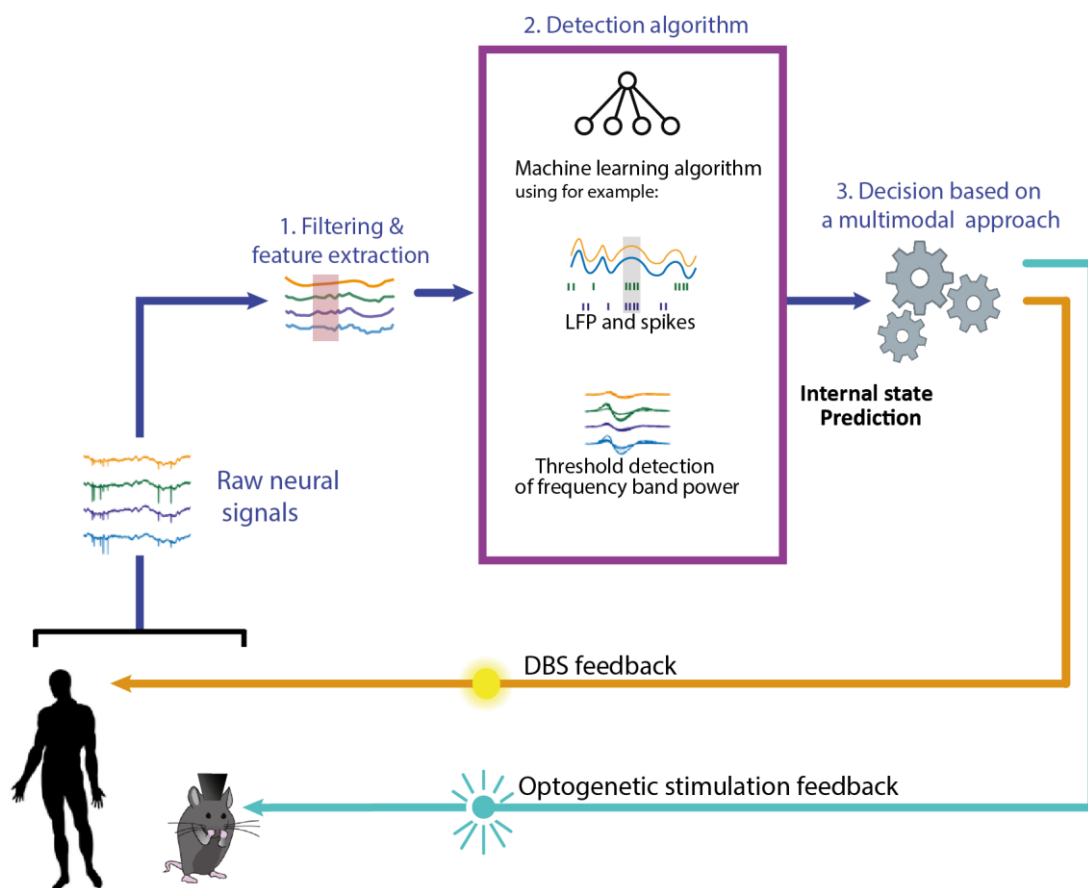


Figure 42. Closed-loop approach in human and mice. Closed-loop focal action of stimulation can yield better responses as it exposes the subject to fewer side effects. As we have shown, in the case of animal experimentation closed-loop optogenetics stimulation can help to test hypothesis on specific neural populations relevant to the regulation of RB. The development of such approach can help encounter technical challenges that can be solved and transfer into the clinic implementation since, globally the same cycle of operations (acquisition of relevant signal features, detection/prediction of the RB to come and feedback) are necessary in animal and human closed-loop applications.

TABLE OF ABBREVIATIONS

Abbreviation	Full name
AAV	Adeno-associated virus
AC	Air conditioning
ACC	Anterior cingulate cortex
AChE	Acetylhydrolase
ADHD	Attention deficit hyperactivity disorder
ASD	Autism spectrum disorder
BDRB	Body-Focused Repetitive Behaviors
BG	Basal ganglia
CB	Compulsive behavior
CBG	Cortico-basal ganglia
CBGTC	Cortico-basal-ganglia-thalamocortical circuit
CBT	Cognitive behavioral therapy
ChAT	Choline acetyltransferase
ChR	Channelrhodopsin
CM-Pf	Centromedian-parafascicular nucleus
CMVT	Chronic motor/vocal tics
CNS	Central nervous system
CPLD	Complex Programmable Logic Device
DA	Dopamine
DBS	Deep brain stimulation
DLPFC	Dorsolateral prefrontal cortex
DLS	Dorso-lateral striatum
DMS	Dorso-medial striatum
DREADD	Designer receptors exclusively activated by designer drugs
DSM-5	Diagnostic and Statistical Manual of Mental Disorders version 5
dVS	Dorsal part of the ventral striatum
EAAC1	Excitatory amino acid carrier 1
ECG	Electrocardiogram
EEG	Electroencephalogram
EMG	Electromyogramme
ET	Essential tremor
FDA	US Food and Drug Administration
fMRI	Functional magnetic resonance imaging
FPGA	Field Programmable Gate Array
FSIs	Fast-spiking interneurons
G	Grooming event
GABA	Gamma-Aminobutyric acid
GP	Globus pallidus
GPe	Globus pallidus (external segment)
GPi	Globus pallidus (internal segment)
GPU	Graphics Processing Unit
HF	High frequency
IC	Internal capsule
LED	Light-Emitting Diode
LFP	Local field potential
IOFC	Lateral OFC
MEA	Microelectrode array
MFCC	Mel-frequency cepstral coefficients
mOFC	Medial OFC
MSN	Medium spiny projection neuron
NAc	Nucleus accumbens
NOS	Nitric oxide synthase
NPY	Neuropeptide Y
OFC	Orbito-frontal cortex

OB	Other behavior event (other than grooming, tic or scratching event).
OC	Obsessive compulsive
OCD	Obsessive compulsive disorder
PD	Parkinson's disease
PET	Positron emission tomography
PFC	Prefrontal cortex
PSD95	Postsynaptic density protein 95
PV	Parvalbumin
PVI	PV+ interneurons
RB	Repetitive behaviors
ROI	Region of interest
RRBs	Restricted and repetitive behaviors
RTOS	Real time operating system
SAPAP3	SAP90/PSD-95-associated protein 3
SN	Substantia nigra
SNc	Substantia nigra (pars compacta)
SNr	Substantia nigra (pars reticulata)
SOM	Somatostatin
SPNs	Spiny projection neurons
SRI	Serotonin reuptake inhibitors
SSRI	Selective serotonin reuptake inhibitor
STN	Subthalamic nucleus
TAN	Tonically active neuron
TRPV1	Transient receptor potential vanilloide 1
TS	Tourette syndrome
TTM	Trichotillomania
VA	Ventralis anterior
Vc	Ventral capsule
VL	Ventralis lateralis
VS	Ventral striatum
VMS	Ventromedial striatum

TABLE OF ILLUSTRATIONS

Figure 1 Habits and goal-directed actions.	10
Figure 2. Compulsive repetitive behavior as a core feature shared between obsessive-compulsive (OC) and autism spectrum disorders.....	16
Figure 3. Goal devaluation procedure to test if OCD patients have a bias toward habits. 17	
Figure 4. Location of basal ganglia nuclei in the human and rat brain.	20
Figure 5. A simplified view of the basal ganglia circuitry showing the direct, indirect and hyperdirect pathways.	21
Figure 6. A simplified representation of a CSTC circuit in a sagittal view of the human brain.....	24
Figure 7. The five circuit model of the BG.	25
Figure 8. Principal functional subdivisions in the cortico-basal ganglia circuits within the human brain.....	26
Figure 9. Striatal functional subdivisions between humans and mice.	27
Figure 10. Schematic representation of the integrative properties of the basal ganglia..	28
Figure 11. Organization of synaptic afferences on a medium spiny neuron.	31
Figure 12. Functional organization of the rodent striatum.	32
Figure 13. Heterogeneity in PVI morphology.	34
Figure 14. Gradient distribution of striatal PVI.	34
Figure 15. Electrophysiological properties of striatal FSIs recorded in vitro.....	35
Figure 16. Synchronous spiking induced by electrotonic coupling of two FSIs.	36
Figure 17. Role of the CSTC circuitry in obsessive–compulsive disorder in humans and compulsive–repetitive behaviors in mice.	46
Figure 18. The SAPAP3-KO mice.....	47
Figure 19. Rodent self-grooming syntactic chain.	51
Figure 20. The condensed history of neuromodulation and how it is closely related to the technological developments of each era.	56
Figure 21. Pictures from the famous experiments in bulls by José Delgado.	60
Figure 22. Possible cell effects of high-frequency DBS.	65

Figure 23. Localization of electrodes for different targets in DBS for OCD.....	67
Figure 24. Effects of electrical vs. optogenetic stimulation of neural tissue.	68
Figure 25. Optogenetic actuator families.....	69
Figure 26. Cre recombinase-based mouse lines in combination with a viral vector.....	70
Figure 27. Different targeting strategies with optogenetic tools in vivo.	71
Figure 28. SAPAP3-KO mutant mice exhibit a deficit in response inhibition.	73
Figure 29. Optogenetic stimulation of IOFC alleviates compulsive grooming.	74
Figure 30. Closed loop control system.....	76
Figure 31. Illustration of an open-loop vs closed-loop DBS paradigm in PD.	77
Figure 32. PubMed citations by year that include the terms “Adaptive brain stimulation.”	79
Figure 33. The cycle of operation in a closed loop approach.....	82
Figure 34. Recording electrodes combined with optical feedback devices for closed-loop neuromodulation.....	83
Figure 35. Home-made drive implant.	120
Figure 36. Custom-made experimental chamber.	121
Figure 37. Real-time closed-loop neuromodulation approach.	123
Figure 38. FPGA based analysis modules.	124
Figure 39 Precision and time response of the FPGA analysis modules.	124
Figure 40. Overview of the neural streamer board.	127
Figure 41. Flow-chart of the “Neural Streamer” software state machine.....	129
Figure 42. Closed-loop approach in human and mice.	169

REFERENCES

- A Vahabzadeh; CJ McDougle. (2014). *Obsessive-Compulsive Disorder. Pathobiology of Human Disease: A Dynamic Encyclopedia of Disease Mechanisms*. Elsevier Inc. <http://doi.org/10.1056/NEJMcp1402176>
- Abelson, J. F., Kwan, K. Y., O’Roak, B. J., Baek, D. Y., Stillman, A. A., Morgan, T. M., ... State, M. W. (2005). Medicine: Sequence variants in SLITRK1 are associated with Tourette’s syndrome. *Science*. <http://doi.org/10.1126/science.1116502>
- Ade, K. K., Wan, Y., Hamann, H. C., O’Hare, J. K., Guo, W., Quian, A., ... Calakos, N. (2016). Increased Metabotropic Glutamate Receptor 5 Signaling Underlies Obsessive-Compulsive Disorder-like Behavioral and Striatal Circuit Abnormalities in Mice. *Biological Psychiatry*, *80*(7), 522–533. <http://doi.org/10.1016/j.biopsych.2016.04.023>
- Adler, C. M., McDonough-Ryan, P., Sax, K. W., Holland, S. K., Arndt, S., & Strakowski, S. M. (2000). fMRI of neuronal activation with symptom provocation in unmedicated patients with obsessive compulsive disorder. *Journal of Psychiatric Research*. [http://doi.org/10.1016/S0022-3956\(00\)00022-4](http://doi.org/10.1016/S0022-3956(00)00022-4)
- Ahmadian, Y., Packer, A. M., Yuste, R., & Paninski, L. (2011). Designing optimal stimuli to control neuronal spike timing. *Journal of Neurophysiology*, *106*(2), 1038–1053. <http://doi.org/10.1152/jn.00427.2010>
- Ahmari, S. E., Spellman, T., Douglass, N. L., Kheirbek, M. A., Simpson, H. B., Deisseroth, K., ... Hen, R. (2013). Repeated cortico-striatal stimulation generates persistent OCD-like behavior. *Science*, *340*(6137), 1234–1239. <http://doi.org/10.1126/science.1234733>
- Al-Galal, S. A. Y., Alshaikhli, I. F. T., & Rahman, A. W. B. A. (2017). Automatic emotion recognition based on EEG and ECG signals while listening to quranic recitation compared with listening to music. In *Proceedings - 6th International Conference on Information and Communication Technology for the Muslim World, ICT4M 2016*. <http://doi.org/10.1109/ICT4M.2016.55>

- Alberti, A. (1886). Contribucion al estudio de las localizaciones cerebrales y a la patogénesis de la epilepsia. *Biedma*.
- Albin, R. L., Young, A. B., & Penney, J. B. (1989). Speculations on the Functional Anatomy of Basal Ganglia Disorders. *Trends in Neurosciences*, 6(1), 73–94. <http://doi.org/10.1146/annurev.ne.06.030183.000445>
- Aldini, G. (1804). Essai théorique et expérimental sur le galvanisme , avec une série d ' expériences faites en présence des commissaires de [...].
- Alkhatib, A. H., Dvorkin-Gheva, A., & Szechtman, H. (2013). Quinpirole and 8-OH-DPAT induce compulsive checking behavior in male rats by acting on different functional parts of an OCD neurocircuit. *Behavioural Pharmacology*. <http://doi.org/10.1097/FBP.0b013e32835d5b7a>
- Alonso, P., López-Solà, C., Real, E., Segalàs, C., & Menchón, J. M. (2015). Animal models of obsessive-compulsive disorder: utility and limitations. *Neuropsychiatric Disease and Treatment*, 11, 1939–55. <http://doi.org/10.2147/NDT.S62785>
- American-Psychiatric-Association. (2013). *Diagnostic and statistical manual of mental disorders* (5th ed.). Washinton, DC.
- Amodio, D. M., & Ratner, K. G. (2011). A memory systems model of implicit social cognition. *Current Directions in Psychological Science*, 20(3), 143–148. <http://doi.org/10.1177/0963721411408562>
- Ansorge, M. S., Zhou, M., Lira, A., Hen, R., & Gingrich, J. A. (2004). Early-life blockade of the 5-HT transporter alters emotional behavior in adult mice. *Science*. <http://doi.org/10.1126/science.1101678>
- Aoyama, K., Sang, W. S., Hamby, A. M., Liu, J., Wai, Y. C., Chen, Y., & Swanson, R. A. (2006). Neuronal glutathione deficiency and age-dependent neurodegeneration in the EAAC1 deficient mouse. *Nature Neuroscience*, 9(1), 119–126. <http://doi.org/10.1038/nn1609>
- Aquilina, O. (2006). A brief history of cardiac pacing. *Images in Paediatric Cardiology*.

[http://doi.org/10.1016/S1443-9506\(02\)90148-4](http://doi.org/10.1016/S1443-9506(02)90148-4)

Armbruster, B. N., Li, X., Pausch, M. H., Herlitze, S., & Roth, B. L. (2007). Evolving the lock to fit the key to create a family of G protein-coupled receptors potently activated by an inert ligand. *Proceedings of the National Academy of Sciences*. <http://doi.org/10.1073/pnas.0700293104>

Ashkan, K., Rogers, P., Bergman, H., & Ughratdar, I. (2017). Insights into the mechanisms of deep brain stimulation. *Nature Reviews Neurology*, 13(9), 548–554. <http://doi.org/10.1038/nrneurol.2017.105>

Atmaca, M., Yildirim, H., Ozdemir, H., Tezcan, E., & Kursad Poyraz, A. (2007). Volumetric MRI study of key brain regions implicated in obsessive-compulsive disorder. *Progress in Neuro-Psychopharmacology and Biological Psychiatry*. <http://doi.org/10.1016/j.pnpbp.2006.06.008>

Bagur1, S., Lefort, J. M., Lacroix, M. M., Lavilléon, G. de, Herry, C., Billand, C., ... Benchenane, K. (2018). Dissociation of fear initiation and maintenance by breathing-driven prefrontal oscillations Authors: *BioRxiv*.

Balleine, B. W., Delgado, M. R., & Hikosaka, O. (2007). The Role of the Dorsal Striatum in Reward and Decision-Making. *Journal of Neuroscience*, 27(31), 8161–8165. <http://doi.org/10.1523/JNEUROSCI.1554-07.2007>

Balleine, B. W., & Dickinson, A. (1998). Goal-directed instrumental action: Contingency and incentive learning and their cortical substrates. *Neuropharmacology*, 37(4–5), 407–419. [http://doi.org/10.1016/S0028-3908\(98\)00033-1](http://doi.org/10.1016/S0028-3908(98)00033-1)

Balleine, B. W., & O'Doherty, J. P. (2010). Human and rodent homologies in action control: Corticostriatal determinants of goal-directed and habitual action. *Neuropsychopharmacology*, 35(1), 48–69. <http://doi.org/10.1038/npp.2009.131>

Bardeen, J., & Brattain, W. H. (1948). The transistor, a semi-conductor triode [14]. *Physical Review*. <http://doi.org/10.1103/PhysRev.74.230>

- Barnes, T. D., Kubota, Y., Hu, D., Jin, D. Z., & Graybiel, A. M. (2005). Activity of striatal neurons reflects dynamic encoding and recoding of procedural memories. *Nature*. <http://doi.org/10.1038/nature04053>
- Bartholow, R. (1874). Experimental investigations into the functions of the human brain. *The American Journal of the Medical Sciences*.
- Bekthereva, N., Grachev, P., Orlova, K. V., & Iatsuk, S. L. (1963). Utilisation of multiple electrodes implanted in the subcortical structure of the human brain for the treatment of hyperkinesia. *Zh. Nevropatol. Psikhiatr. Im. S. S. Korsakova*. <http://doi.org/10.1074/jbc.M115.674101>
- Benabid, A. L., Benazzous, A., & Pollak, P. (2002). Mechanisms of deep brain stimulation. *Movement Disorders*. <http://doi.org/10.1002/mds.10145>
- Benabid, A. L., Pollak, P., Louveau, A., Henry, S., & De Rougemont, J. (1987). Combined (thalamotomy and stimulation) stereotactic surgery of the vim thalamic nucleus for bilateral parkinson disease. *Stereotactic and Functional Neurosurgery*. <http://doi.org/10.1159/000100803>
- Benazzouz, A., Gao, D. M., Ni, Z. G., Piallat, B., Bouali-Benazzouz, R., & Benabid, A. L. (2000). Effect of high-frequency stimulation of the subthalamic nucleus on the neuronal activities of the substantia nigra pars reticulata and ventrolateral nucleus of the thalamus in the rat. *Neuroscience*, *99*(2), 289–295. [http://doi.org/10.1016/S0306-4522\(00\)00199-8](http://doi.org/10.1016/S0306-4522(00)00199-8)
- Bennett, B. D., & Bolam, J. P. (1994). Localisation of parvalbumin-immunoreactive structures in primate caudate-putamen. *Journal of Comparative Neurology*, *347*(3), 340–356. <http://doi.org/10.1002/cne.903470303>
- Benzina, N., Mallet, L., Burguiere, E., N'Diaye, K., & Pelissolo, A. (2000). Cognitive dysfunction in obsessive-compulsive disorder. *Acta Psychiatrica Scandinavica*, *101*(4), 281–285. <http://doi.org/10.1034/j.1600-0447.2000.101004281.x>
- Berke, J. D. (2008). Uncoordinated Firing Rate Changes of Striatal Fast-Spiking Interneurons during Behavioral Task Performance. *Journal of Neuroscience*, *28*(40), 10075–10080.

<http://doi.org/10.1523/JNEUROSCI.2192-08.2008>

Berridge, K. C., Aldridge, J. W., Houchard, K. R., & Zhuang, X. (2005). Sequential super-stereotypy of an instinctive fixed action pattern in hyper-dopaminergic mutant mice: A model of obsessive compulsive disorder and Tourette's. *BMC Biology*, 3, 1–16. <http://doi.org/10.1186/1741-7007-3-4>

Berridge, K. C., & Whishaw, I. Q. (1992). Cortex, striatum and cerebellum: control of serial order in a grooming sequence. *Experimental Brain Research*, 90(2), 275–290. <http://doi.org/10.1007/BF00227239>

Bi, A., Cui, J., Ma, Y. P., Olshevskaya, E., Pu, M., Dizhoor, A. M., & Pan, Z. H. (2006). Ectopic Expression of a Microbial-Type Rhodopsin Restores Visual Responses in Mice with Photoreceptor Degeneration. *Neuron*. <http://doi.org/10.1109/ICCA.2007.4376538>

Bienvenu, O. J., Samuels, J. F., Riddle, M. A., Hoehn-Saric, R., Liang, K. Y., Cullen, B. A. M., ... Nestadt, G. (2000). The relationship of obsessive-compulsive disorder to possible spectrum disorders: Results from a family study. *Biological Psychiatry*, 48(4), 287–293. [http://doi.org/10.1016/S0006-3223\(00\)00831-3](http://doi.org/10.1016/S0006-3223(00)00831-3)

Bienvenu, O. J., Wang, Y., Shugart, Y. Y., Welch, J. M., Grados, M. A., Fyer, A. J., ... Nestadt, G. (2009). Sapap3 and pathological grooming in humans: Results from the OCD collaborative genetics study. *American Journal of Medical Genetics, Part B: Neuropsychiatric Genetics*, 150(5), 710–720. <http://doi.org/10.1002/ajmg.b.30897>

Bindra, D., & Spinner, N. (1958). Response to different degrees of novelty: the incidence of various activities. *Journal of the Experimental Analysis of Behavior*., 341–350. <http://doi.org/10.1901/jeab.1958.1-341>

Bloch, M. H., Landeros-Weisenberger, A., Kelmendi, B., Coric, V., Bracken, M. B., & Leckman, J. F. (2006). A systematic review: Antipsychotic augmentation with treatment refractory obsessive-compulsive disorder. *Molecular Psychiatry*. <http://doi.org/10.1038/sj.mp.4001823>

Blomstedt, P., & Hariz, M. I. (2010). Deep brain stimulation for movement disorders before

- DBS for movement disorders. *Parkinsonism and Related Disorders*, 16(7), 429–433.
<http://doi.org/10.1016/j.parkreldis.2010.04.005>
- Bowery, N. G., & Smart, T. G. (2006). GABA and glycine as neurotransmitters: A brief history. *British Journal of Pharmacology*. <http://doi.org/10.1038/sj.bjp.0706443>
- Boyden, E. S., Zhang, F., Bamberg, E., Nagel, G., & Deisseroth, K. (2005). Millisecond-timescale, genetically targeted optical control of neural activity. *Nature Neuroscience*.
<http://doi.org/10.1038/nn1525>
- Brash, H. M., Mcqueen, D. S., Christie, D., Bell, J. K., Bond, S. M., & Rees, J. L. (2005). A repetitive movement detector used for automatic monitoring and quantification of scratching in mice, 142, 107–114. <http://doi.org/10.1016/j.jneumeth.2004.08.001>
- Breiter, H. C., Rauch, S. L., Kwong, K. K., Baker, J. R., Weisskoff, R. M., Kennedy, D. N., ... Rosen, B. R. (1996). Functional magnetic resonance imaging of symptom provocation in obsessive-compulsive disorder. *Archives of General Psychiatry*.
<http://doi.org/10.1001/archpsyc.1996.01830070041008>
- Burbaud, P., Clair, A. H., Langbour, N., Fernandez-Vidal, S., Goillandeau, M., Michelet, T., ... Mallet, L. (2013). Neuronal activity correlated with checking behaviour in the subthalamic nucleus of patients with obsessive-compulsive disorder. *Brain*, 136(1), 304–317.
<http://doi.org/10.1093/brain/aws306>
- Burgess, A. A., Graybiel, A. M., Burgess, A. A., & Graybiel, A. M. (2018). Inversely Active Striatal Projection Neurons and Interneurons Selectively Delimit Useful Behavioral Article Inversely Active Striatal Projection Neurons and Interneurons Selectively Delimit Useful Behavioral Sequences, 1–14. <http://doi.org/10.1016/j.cub.2018.01.031>
- Burguière, E., Monteiro, P., Feng, G., & Graybiel, A. M. (2013a). Optogenetic Stimulation of Lateral. *Science*, 340(2013), 1243–1246. <http://doi.org/10.1126/science.1232380>
- Burguière, E., Monteiro, P., Feng, G., & Graybiel, A. M. (2013b). Optogenetic stimulation of lateral orbitofronto-striatal pathway suppresses compulsive behaviors. *Science (New York, N.Y.)*, 340(6137), 1243–6. <http://doi.org/10.1126/science.1232380>

- Buzsáki, G., Anastassiou, C. a, & Koch, C. (2012). The origin of extracellular fields and currents-EEG, ECoG, LFP and spikes. *Nature Reviews. Neuroscience*, *13*(6), 407–20. <http://doi.org/10.1038/nrn3241>
- Buzsaki, G., Stark, E., Berenyi, A., Khodagholy, D., Kipke, D. R., Yoon, E., ... Wise, K. D. (2015). Tools for Probing Local Circuits: High-Density Silicon Probes Combined with Optogenetics. *Neuron*, *86*(1), 92–105. <http://doi.org/10.1016/j.neuron.2015.01.028>
- Carden, L., & Wood, W. (2018). Habit formation and change. *Current Opinion in Behavioral Sciences*, *20*, 117–122. <http://doi.org/10.1016/j.cobeha.2017.12.009>
- Chang, J., Wang, Z., Tang, E., Fan, Z., Mccauley, L., Guan, K., ... Wang, C. (2017). Rodent Models of Obsessive Compulsive Disorder: Evaluating Validity to Interpret Emerging Neurobiology. *Neuroscience*. <http://doi.org/10.1038/nm.1954>.Inhibition
- Chen, R., Romero, G., Christiansen, M. G., Mohr, A., & Anikeeva, P. (2015). Wireless Magnetothermal Deep Brain Stimulation. *Science*, *347*(6229), 1477–1480.
- Chen, S. K., Tvrdik, P., Peden, E., Cho, S., Wu, S., Spangrude, G., & Capecchi, M. R. (2010). Hematopoietic origin of pathological grooming in Hoxb8 mutant mice. *Cell*, *141*(5), 775–785. <http://doi.org/10.1016/j.cell.2010.03.055>
- Chuhma, N., Mingote, S., Kalmbach, A., Yetnikoff, L., & Rayport, S. (2017). Heterogeneity in Dopamine Neuron Synaptic Actions Across the Striatum and Its Relevance for Schizophrenia. *Biological Psychiatry*, *81*(1), 43–51. <http://doi.org/10.1016/j.biopsych.2016.07.002>
- Couto, J., Linaro, D., Pulizzi, R., & Giugliano, M. (2016). Closed-Loop Methodologies for Cellular Electrophysiology. *Closed Loop Neuroscience*, 187–199. <http://doi.org/10.1016/B978-0-12-802452-2.00013-5>
- Crawford, S., Channon, S., & Robertson, M. M. (2005). Tourette’s syndrome: performance on tests of behavioural inhibition, working memory and gambling. *Journal of Child Psychology and Psychiatry, and Allied Disciplines*. <http://doi.org/10.1111/j.1469-7610.2005.01419.x>

- Crick, F. (1999). The impact of molecular biology on vaccine development. *Phil. Trans. R. Soc. Lond.*, (354), 2021–2025. <http://doi.org/10.2165/00128413-1997111110-00002>
- Davis, S. B., & Mermelstein, P. (1980). Comparison of Parametric Representations for Monosyllabic Word Recognition in Continuously Spoken Sentences. *IEEE Transactions on Acoustics, Speech, and Signal Processing*. <http://doi.org/10.1109/TASSP.1980.1163420>
- de Koning, P. P., Figeer, M., Endert, E., van den Munckhof, P., Schuurman, P. R., Storosum, J. G., ... Fliers, E. (2016). Rapid effects of deep brain stimulation reactivation on symptoms and neuroendocrine parameters in obsessive-compulsive disorder. *Translational Psychiatry*. <http://doi.org/10.1038/tp.2015.222>
- Debru, A. (2006). The power of torpedo fish as a pathological model to the understanding of nervous transmission in Antiquity. *Comptes Rendus - Biologies*. <http://doi.org/10.1016/j.crv.2006.03.001>
- Dek, E. C. P., van den Hout, M. A., Engelhard, I. M., Giele, C. L., & Cath, D. C. (2015). Perseveration causes automatization of checking behavior in obsessive-compulsive disorder. *Behaviour Research and Therapy*. <http://doi.org/10.1016/j.brat.2015.05.005>
- Delgado, J. M. R., Hamlin, H., & Chapman, W. P. (1952). Technique of Intracranial Electrode Implantation for Recording and Stimulation and its Possible Therapeutic Value in Psychotic Patients. *Stereotactic and Functional Neurosurgery*. <http://doi.org/10.1159/000105792>
- Della Flora, E., Perera, C. L., Cameron, A. L., & Maddern, G. J. (2010). Deep brain stimulation for essential tremor: A systematic review. *Movement Disorders*. <http://doi.org/10.1002/mds.23195>
- Deniau, J. M., Mailly, P., Maurice, N., & Charpier, S. (2007). The pars reticulata of the substantia nigra: a window to basal ganglia output. *Progress in Brain Research*, 160, 151–172. [http://doi.org/10.1016/S0079-6123\(06\)60009-5](http://doi.org/10.1016/S0079-6123(06)60009-5)
- Dickinson, A. (1985). Actions and Habits: The Development of Behavioural Autonomy. *Philosophical Transactions of the Royal Society of London. Series B, Biological Sciences*,

308(1135), 67–78. <http://doi.org/10.1098/rstb.1985.0010>

Diniz, J. B., Rosario-Campos, M. C., Hounie, A. G., Curi, M., Shavitt, R. G., Lopes, A. C., & Miguel, E. C. (2006). Chronic tics and Tourette syndrome in patients with obsessive-compulsive disorder. *Journal of Psychiatric Research*, 40(6), 487–493. <http://doi.org/10.1016/j.jpsychires.2005.09.002>

Dolan, R. J., & Dayan, P. (2013). Goals and habits in the brain. *Neuron*, 80(2), 312–325. <http://doi.org/10.1016/j.neuron.2013.09.007>

Dougherty, D. D. (2018). Deep Brain Stimulation: Clinical Applications. *Psychiatric Clinics of North America*, 41(3), 385–394. <http://doi.org/10.1016/j.psc.2018.04.004>

E. Burguiere, P. Monteiro, L. Mallet, G. Feng, A. G. (2016). Striatal circuits, habits, and implications for obsessive-compulsive disorder. *Curr Opin Neurobiol.*, (0), 59–65. <http://doi.org/10.1016/j.conb.2014.08.008>. Striatal

Edna B. Foa, & Kozak, M. J. (1995). DSM-IV Field Trial: Obsessive-Compulsive Disorder. *American Journal of Psychiatry*, 152, 90–96. <http://doi.org/10.1111/j.1600-0447.1994.tb05788.x>

El Hady, A., Maling, N., & McIntyre, C. (2016). Chapter 5 – Local Field Potential Analysis for Closed-Loop Neuromodulation. In *Closed Loop Neuroscience* (pp. 67–80). <http://doi.org/10.1016/B978-0-12-802452-2.00005-6>

Elble, R. J., & McNamara, J. (2016). Using Portable Transducers to Measure Tremor Severity. *Tremor and Other Hyperkinetic Movements (New York, N.Y.)*. <http://doi.org/10.7916/D8DR2VCC>

Elliott, R., Frith, C. D., & Dolan, R. J. (1997). Differential neural response to positive and negative feedback in planning and guessing tasks. *Neuropsychologia*, 35(10), 1395–1404. [http://doi.org/10.1016/S0028-3932\(97\)00055-9](http://doi.org/10.1016/S0028-3932(97)00055-9)

Fenko, L., Yizhar, O., & Deisseroth, K. (2011). The Development and Application of Optogenetics. *Annual Review of Neuroscience*, 34(1), 389–412. <http://doi.org/10.1146/annurev-neuro-061010-113817>

- Figeo, M., De Koning, P., Klaassen, S., Vulink, N., Mantione, M., Van Den Munckhof, P., ... Denys, D. (2014). Deep brain stimulation induces striatal dopamine release in obsessive-compulsive disorder. *Biological Psychiatry*, 75(8), 647–652. <http://doi.org/10.1016/j.biopsych.2013.06.021>
- Fino, E., Vandecasteele, M., Perez, S., Saudou, F., & Venance, L. (2018). Region-specific and state-dependent action of striatal GABAergic interneurons. *Nature Communications*, 9(1). <http://doi.org/10.1038/s41467-018-05847-5>
- Fino, E., & Venance, L. (2010). Spike-timing dependent plasticity in the striatum. *Frontiers in Synaptic Neuroscience*, 2(JUN), 1–10. <http://doi.org/10.3389/fnsyn.2010.00006>
- Flaherty, A. W., & Graybiel, A. M. (2013). Corticostriatal transformations in the primate somatosensory system . Projections from physiologically mapped body-part representations Corticostriatal Transformations in the Primate Somatosensory System . Projections From Physiologically Mapped Body-Part, 66(4), 1249–1263.
- Fontenelle, L. F., Mendlowicz, M. V., & Versiani, M. (2006). The descriptive epidemiology of obsessive-compulsive disorder. *Progress in Neuro-Psychopharmacology and Biological Psychiatry*, 30(3), 327–337. <http://doi.org/10.1016/j.pnpbp.2005.11.001>
- Franklin, M. E., Abramowitz, J. S., Kozak, M. J., Levitt, J. T., & Foa, E. B. (2000). Effectiveness of exposure and ritual prevention for obsessive-compulsive disorder: Randomized compared with nonrandomized samples. *Journal of Consulting and Clinical Psychology*. <http://doi.org/10.1037/0022-006X.68.4.594>
- Franklin, M. E., Harrison, J. P., & Benavides, K. L. (2012). Obsessive-compulsive and tic-related disorders. *Child and Adolescent Psychiatric Clinics of North America*, 21(3), 555–71. <http://doi.org/10.1016/j.chc.2012.05.008>
- Freund, T. F., & Buzsáki, G. (1998). Interneurons of the hippocampus. *Hippocampus*. [http://doi.org/10.1002/\(SICI\)1098-1063\(1996\)6:4<347::AID-HIPO1>3.0.CO;2-I](http://doi.org/10.1002/(SICI)1098-1063(1996)6:4<347::AID-HIPO1>3.0.CO;2-I)
- Friend, D. M., Kemere, C., & Kravitz, A. V. (2015). Quantifying recording quality in in vivo striatal recordings. *Current Protocols in Neuroscience*, 2015(January), 6.28.1-6.28.9.

<http://doi.org/10.1002/0471142301.ns0628s70>

- G E Alexander, M R DeLong, and P. L. S. (1986). Parallel Organization of Functionally Segregated Circuits Linking Basal Ganglia and Cortex. *Annual Review of Neuroscience*, *9*, 357–381. <http://doi.org/10.1146/annurev.neuro.9.1.357>
- Gage, G. J., Stoetzner, C. R., Wiltschko, A. B., & Berke, J. D. (2010). Selective Activation of Striatal Fast Spiking Interneurons during Choice Execution. *Neuron*, *67*(3), 466–479. <http://doi.org/10.1016/j.neuron.2010.06.034>. Selective
- Galarreta, M., & Hestrin, S. (2002). Electrical and chemical synapses among parvalbumin fast-spiking GABAergic interneurons in adult mouse neocortex. *Proceedings of the National Academy of Sciences*, *99*(19), 12438–12443. <http://doi.org/10.1073/pnas.192159599>
- Gerfen, C. R., & Bolam, J. P. (2010). *The Neuroanatomical Organization of the Basal Ganglia. Handbook of Behavioral Neuroscience* (Vol. 20). Elsevier Inc. <http://doi.org/10.1016/B978-0-12-374767-9.00001-9>
- Gernert, M., Hamann, M., Bennay, M., Lo, W., & Richter, A. (2000). Deficit of Striatal Parvalbumin-Reactive GABAergic Interneurons Idiopathic Paroxysmal Dystonia. *Journal of Neuroscience*, *20*(18), 7052–7058.
- Gildenberg, P. L. (2002). Spiegel and Wycis - The early years. In *Stereotactic and Functional Neurosurgery*. <http://doi.org/10.1159/000064587>
- Gillan, C. M., Morein-Zamir, S., Urcelay, G. P., Sule, A., Voon, V., Apergis-Schoute, A. M., ... Robbins, T. W. (2014). Enhanced avoidance habits in obsessive-compulsive disorder. *Biological Psychiatry*, *75*(8), 631–638. <http://doi.org/10.1016/j.biopsych.2013.02.002>
- Gillan, C. M., Pappmeyer, M., Morein-Zamir, S., Sahakian, B. J., Fineberg, N. A., Robbins, T. W., & De Wit, S. (2011). Disruption in the balance between goal-directed behavior and habit learning in obsessive-compulsive disorder. *American Journal of Psychiatry*. <http://doi.org/10.1176/appi.ajp.2011.10071062>
- Gillan, C. M., Robbins, T. W., Sahakian, B. J., van den Heuvel, O. A., & van Wingen, G. (2016).

The role of habit in compulsivity. *European Neuropsychopharmacology*, 26(5), 828–840.
<http://doi.org/10.1016/j.euroneuro.2015.12.033>

Gittis, A. H., Leventhal, D. K., Fensterheim, B. A., Pettibone, J. R., Berke, J. D., & Kreitzer, A. C. (2011). Selective Inhibition of Striatal Fast-Spiking Interneurons Causes Dyskinesias. *Journal of Neuroscience*, 31(44), 15727–15731.
<http://doi.org/10.1523/JNEUROSCI.3875-11.2011>

Gittis, A. H., Nelson, A. B., Thwin, M. T., Palop, J. J., & Kreitzer, A. C. (2010). Distinct Roles of GABAergic Interneurons in the Regulation of Striatal Output Pathways. *Journal of Neuroscience*. <http://doi.org/10.1523/JNEUROSCI.4870-09.2010>

Glannon, W., & Ineichen, C. (2016). *Philosophical Aspects of Closed-Loop Neuroscience*. *Closed Loop Neuroscience*. Elsevier Inc. <http://doi.org/10.1016/B978-0-12-802452-2.00019-6>

Gorka, S. M., Phan, K. L., & Shankman, S. A. (2015). Convergence of EEG and fMRI measures of reward anticipation. *Biol Psychiatry*, (112), 12–19.
<http://doi.org/10.1177/0333102415576222>

Grados, M. A. (2010). The Genetics of Obsessive-Compulsive Disorder and Tourette Syndrome: An Epidemiological and Pathway-Based Approach for Gene Discovery. *Journal of the American Academy of Child and Adolescent Psychiatry*, 49(8), 810–819e2.
<http://doi.org/10.1016/j.jaac.2010.04.009>

Grados, M. A., Riddle, M. A., Samuels, J. F., Liang, K.-Y., Hoehn-Saric, R., Bienvenu, O. J., ... Nestadt, G. (2001). The Familial Phenotype of Obsessive-Compulsive Disorder in Relation to Tic Disorders: The Hopkins OCD Family Study. *Society of Biological Psychiatry*. [http://doi.org/10.1016/S0006-3223\(01\)01074-5](http://doi.org/10.1016/S0006-3223(01)01074-5)

Graybiel, A. M. (2008). Habits, Rituals, and the Evaluative Brain. <http://doi.org/10.1146/annurev.neuro.29.051605.112851>

Graybiel, A. M., & Ragsdale, C. W. (1978). Histochemically distinct compartments in the striatum of human, monkeys, and cat demonstrated by acetylthiocholinesterase staining. *Proceedings of the National Academy of Sciences*.

<http://doi.org/10.1073/pnas.75.11.5723>

Greene, D. J., Williams, A. C., Koller, J. M., Schlaggar, B. L., & Black, K. J. (2017). Brain structure in pediatric Tourette syndrome. *Molecular Psychiatry*, 22(7), 972–980. <http://doi.org/10.1038/mp.2016.194>

Greer, J. M., & Capecchi, M. R. (2002). Hoxb8 Is Required for Normal Grooming Behavior in Mice. *Neuron*, 33(1), 23–34. [http://doi.org/10.1016/S0896-6273\(01\)00564-5](http://doi.org/10.1016/S0896-6273(01)00564-5)

Grosenick, L., Marshel, J. H., & Deisseroth, K. (2015). Closed-loop and activity-guided optogenetic control. *Neuron*, 86(1), 106–139. <http://doi.org/10.1016/j.neuron.2015.03.034>

Gross, R. E., & Lozano, A. M. (1997). The surgical management of Parkinson's Disease.

Guehl, D., Benazzouz, A., Aouizerate, B., Cuny, E., Rotg??, J. Y., Rougier, A., ... Burbaud, P. (2008). Neuronal Correlates of Obsessions in the Caudate Nucleus. *Biological Psychiatry*, 63(6), 557–562. <http://doi.org/10.1016/j.biopsych.2007.06.023>

Guru, A., Post, R. J., Ho, Y.-Y., & Warden, M. R. (2015). Making sense of optogenetics. *International Journal of Neuropsychopharmacology*, 13, 694–703. <http://doi.org/10.1093/ijnp/pyv079>

Gyertyán, I. (1995). Analysis of the marble burying response: marbles serve to measure digging rather than evoke burying. *Behavioural Pharmacology*. <http://doi.org/10.1016/j.pbiomolbio.2005.05.012>

Haber, S. N. (2016). Corticostriatal circuitry. *Neuroscience in the 21st Century: From Basic to Clinical, Second Edition*, 1721–1741. http://doi.org/10.1007/978-1-4939-3474-4_135

Haber, S. N., Fudge, J. L., & McFarland, N. R. (2000). Striatonigrostriatal Pathways in Primates Form an Ascending Spiral from the Shell to the Dorsolateral Striatum. *The Journal of Neuroscience*, 20(6), 2369–2382. <http://doi.org/10.1523/JNEUROSCI.20-06-02369.2000>

Hamani, C., Saint-Cyr, J. A., Fraser, J., Kaplitt, M., & Lozano, A. M. (2004). The subthalamic

nucleus in the context of movement disorders. *Brain*, 127(1), 4–20.
<http://doi.org/10.1093/brain/awh029>

Hamani, C., & Temel, Y. (2012). Deep brain stimulation for psychiatric disease: Contributions and validity of animal models. *Science Translational Medicine*, 4(142).
<http://doi.org/10.1126/scitranslmed.3003722>

Hashimoto, T., Elder, C. M., Okun, M. S., Patrick, S. K., & Vitek, J. L. (2003). Stimulation of the subthalamic nucleus changes the firing pattern of pallidal neurons. *The Journal of Neuroscience: The Official Journal of the Society for Neuroscience*, 23(5), 1916–23.
<http://doi.org/23/5/1916> [pii]

Hélie, S., Ell, S. W., & Ashby, F. G. (2015). Learning robust cortico-cortical associations with the basal ganglia: An integrative review. *Cortex*, 64, 123–135.
<http://doi.org/10.1016/j.cortex.2014.10.011>

Henze, D. A., Borhegyi, Z., Csicsvari, J., Mamiya, a, Harris, K. D., & Buzsáki, G. (2000). Intracellular features predicted by extracellular recordings in the hippocampus in vivo. *Journal of Neurophysiology*, 84(1), 390–400. <http://doi.org/84:390-400>

Henze, D., Harris, K., Borhegyi, Z., Csicsvari, J., Mamiya, A., Hirase, H., ... Buzsáki, G. (2009). Simultaneous intracellular and extracellular recordings from hippocampus region CA1 of anesthetized rats. *CRCNS;org*. <http://doi.org/http://dx.doi.org/10.6080/K02Z13FP>

Herron, J. A., Thompson, M. C., Brown, T., Chizeck, H. J., Ojemann, J. G., & Ko, A. L. (2017). Chronic electrocorticography for sensing movement intention and closed-loop deep brain stimulation with wearable sensors in an essential tremor patient. *Journal of Neurosurgery*, 127(3), 580–587. <http://doi.org/10.3171/2016.8.JNS16536>

Holzer, J. C., Goodman, W. K., McDougle, C. J., Baer, L., Boyarsky, B. K., Leckman, J. F., & Price, L. H. (1994). Obsessive-compulsive disorder with and without a chronic tic disorder. A comparison of symptoms in 70 patients. *British Journal of Psychiatry*, 164(APR.), 469–473. <http://doi.org/10.1192/bjp.164.4.469>

Ineichen, C., Glannon, W., Temel, Y., Baumann, C. R., & Surucu, O. (2014). A critical reflection

- on the technological development of deep brain stimulation (DBS). *Frontiers in Human Neuroscience*, 8(September), 1–7. <http://doi.org/10.3389/fnhum.2014.00730>
- Iturrate, I., Chavarriaga, R., Montesano, L., Minguetz, J., & Millán, J. D. R. (2015). Teaching brain-machine interfaces as an alternative paradigm to neuroprosthetics control. *Scientific Reports*. <http://doi.org/10.1038/srep13893>
- Jahanshahi, M., Obeso, I., Rothwell, J. C., & Obeso, J. A. (2015). A fronto-striato-subthalamic-pallidal network for goal-directed and habitual inhibition. *Nature Reviews Neuroscience*, 16(12), 719–732. <http://doi.org/10.1038/nrn4038>
- Jech, R., Urgošík, D., Tintěř, J., Nebuželský, A., Krásenský, J., Liščák, R., ... Růžička, E. (2001). Functional magnetic resonance imaging during deep brain stimulation: A pilot study in four patients with parkinson's disease. *Movement Disorders*, 16(6), 1126–1132. <http://doi.org/10.1002/mds.1217>
- Jeffrey L. Cummings. (1993). Frontal-Subcortical Circuits and Human Behavior. *Archives of Neurology*, 50, 873–880.
- Jose A. Obeso, Rodriguez-Oroz, M. C., Benitez-Temino, B., Blesa, F. J., Jorge Guridi, M., Marin, C., & Manuel Rodriguez. (2009). Functional Organization of the Basal Ganglia: Therapeutic Implications for Parkinson's Disease. *Movement Disorders*, 3(76). <http://doi.org/10.1002/mds.22062>
- Kalanithi, P. S. A., Zheng, W., Kataoka, Y., DiFiglia, M., Grantz, H., Saper, C. B., ... Vaccarino, F. M. (2005). Altered parvalbumin-positive neuron distribution in basal ganglia of individuals with Tourette syndrome. *Proceedings of the National Academy of Sciences*, 102(37), 13307–13312. <http://doi.org/10.1073/pnas.0502624102>
- Kalueff, A. V., & Tuohimaa, P. (2005). Mouse grooming microstructure is a reliable anxiety marker bidirectionally sensitive to GABAergic drugs. *European Journal of Pharmacology*, 508(1–3), 147–153. <http://doi.org/10.1016/j.ejphar.2004.11.054>
- Kalueff, A. V., Wayne Aldridge, J., Laporte, J. L., Murphy, D. L., & Tuohimaa, P. (2007). Analyzing grooming microstructure in neurobehavioral experiments. *Nature Protocols*, 2(10),

2538–2544. <http://doi.org/10.1038/nprot.2007.367>

- Kalueff, A. V., Stewart, A. M., Song, C., Berridge, K. C., Graybiel, A. M., & Fentress, J. C. (2016). Neurobiology of rodent self-grooming and its value for translational neuroscience. *Nature Reviews Neuroscience*, *17*(1), 45–59. <http://doi.org/10.1038/nrn.2015.8>
- Karalis, N., Dejean, C., Chaudun, F., Khoder, S., Rozeske, R. R., Wurtz, H., ... Herry, C. (2016). 4-Hz oscillations synchronize prefrontal – amygdala circuits during fear behavior, (October 2015). <http://doi.org/10.1038/nn.4251>
- Kaszás, A., Spitzer, K., Kerekes, B. P., Szalay, G., Rózsa, B., Bagó, A., ... Ulbert, I. (2014). Combined two-photon imaging, electrophysiological, and anatomical investigation of the human neocortex in vitro . *Neurophotonics*, *1*(1), 011013. <http://doi.org/10.1117/1.nph.1.1.011013>
- Kataoka, Y., Kalanithi, P. S. A., Grantz, H., Schwartz, M. L., Saper, C., Leckman, J. F., & Vaccarino, F. M. (2010). Decreased number of parvalbumin and cholinergic interneurons in the striatum of individuals with tourette syndrome. *Journal of Comparative Neurology*, *518*(3), 277–291. <http://doi.org/10.1002/cne.22206>
- Katayama, K., Yamada, K., Ornthanalai, V. G., Inoue, T., Ota, M., Murphy, N. P., & Aruga, J. (2010). Slitrk1-deficient mice display elevated anxiety-like behavior and noradrenergic abnormalities. *Molecular Psychiatry*. <http://doi.org/10.1038/mp.2008.97>
- Kawaguchi, Y. (1993). Physiological, Morphological, and Histochemical Characterization of 3 Classes of Interneurons in Rat Neostriatum. *Journal of Neuroscience*. [http://doi.org/10.1016/S0921-8696\(05\)81133-8](http://doi.org/10.1016/S0921-8696(05)81133-8)
- Kemp, M. ., & Powell, T. P. . (1971). The structure of the caudate nucleus of the cat: light and electron microscopy. *Philosophical Transactions of the Royal Society of London*.
- Kessler, R. C., Berglund, P., Demler, O., Jin, R., Merikangas, K. R., & Walters, E. E. (2005). Lifetime Prevalence and Age-of-Onset Distributions of. *Arch Gen Psychiatry*, *62*(June), 593–602. <http://doi.org/10.1001/archpsyc.62.6.593>

- Kimura, M. (1986). The role of primate putamen neurons in the association of sensory stimuli with movement. *Neuroscience Research*. [http://doi.org/10.1016/0168-0102\(86\)90035-0](http://doi.org/10.1016/0168-0102(86)90035-0)
- Kita, H. (1993). GABAergic circuits of the striatum. *Progress in Brain Research*, 99. [http://doi.org/10.1016/S0079-6123\(08\)61338-2](http://doi.org/10.1016/S0079-6123(08)61338-2)
- Kita, H. (2007). Globus pallidus external segment. *Progress in Brain Research*, 160(06), 111–133. [http://doi.org/10.1016/S0079-6123\(06\)60007-1](http://doi.org/10.1016/S0079-6123(06)60007-1)
- Kita, H., & Jaeger, D. (2017). *Organization of the Globus Pallidus. Handbook of Behavioral Neuroscience* (Vol. 24). Elsevier Inc. <http://doi.org/10.1016/B978-0-12-802206-1.00013-1>
- Kita, H., Kosaka, T., & Heizmann, C. W. (1990). Parvalbumin-immunoreactive neurons in the rat neostriatum: a light and electron microscopic study. *Brain Research*, 536(1–2), 1–15. [http://doi.org/10.1016/0006-8993\(90\)90002-S](http://doi.org/10.1016/0006-8993(90)90002-S)
- Koob, G. F., & Volkow, N. D. (2010). Neurocircuitry of addiction. *Neuropsychopharmacology*, 35(1), 217–238. <http://doi.org/10.1038/npp.2009.110>
- Korff, S., J. Stein, D., & H. Harvey, B. (2008). Stereotypic behaviour in the deer mouse: Pharmacological validation and relevance for obsessive compulsive disorder. *Progress in Neuro-Psychopharmacology and Biological Psychiatry*. <http://doi.org/10.1016/j.pnpbp.2007.08.032>
- Krack, P., Hariz, M. I., Baunez, C., Guridi, J., & Obeso, J. A. (2010). Deep brain stimulation: From neurology to psychiatry? *Trends in Neurosciences*, 33(10), 474–484. <http://doi.org/10.1016/j.tins.2010.07.002>
- Kreitzer, A. C. (2009). Physiology and Pharmacology of Striatal Neurons. *Annual Review of Neuroscience*, 32(1), 127–147. <http://doi.org/10.1146/annurev.neuro.051508.135422>
- Kringelbach, M. L., Jenkinson, N., Owen, S. L. F., & Aziz, T. Z. (2007). Translational principles of deep brain stimulation. *Nature Reviews Neuroscience*, 8(8), 623–635. <http://doi.org/10.1038/nrn2196>

- Krook-Magnuson, E., Armstrong, C., Oijala, M., & Soltesz, I. (2013). On-demand optogenetic control of spontaneous seizures in temporal lobe epilepsy. *Nature Communications*, *4*, 1376. <http://doi.org/10.1038/ncomms2376>
- Krook-Magnuson, E., Szabo, G. G., Armstrong, C., Oijala, M., & Soltesz, I. (2014). Cerebellar Directed Optogenetic Intervention Inhibits Spontaneous Hippocampal Seizures in a Mouse Model of Temporal Lobe Epilepsy. *ENeuro*, *1*(1). <http://doi.org/10.1523/ENEURO.0005-14.2014>
- Kumar, R., Lozano, A. M., Sime, E., & Lang, A. E. (2003). Long-term follow-up of thalamic deep brain stimulation for essential and parkinsonian tremor. *Neurology*. <http://doi.org/10.1212/01.WNL.0000096012.07360.1C>
- Kuo, C.-H., White-Dzuro, G. A., & Ko, A. L. (2018). Approaches to closed-loop deep brain stimulation for movement disorders. *Neurosurgical Focus*, *45*(2), E2. <http://doi.org/10.3171/2018.5.FOCUS18173>
- Kuyck, K. van, Brak, K., Das, J., Rizopoulos, D., & Nuttin, B. (2008). Comparative study of the effects of electrical stimulation in the nucleus accumbens, the mediodorsal thalamic nucleus and the bed nucleus of the stria terminalis in rats with schedule-induced polydipsia. *Brain Research*. <http://doi.org/10.1016/j.brainres.2008.01.043>
- Lai, M.-C., Lombardo, M. V, & Baron-Cohen, S. (2013). Autism. *The Lancet*. http://doi.org/10.1007/978-1-4939-3474-4_91
- Laitinen, L. V., Bergenheim, A. T., & Hariz, M. I. (1992). Leksell's posteroventral pallidotomy in the treatment of Parkinson's disease. *Journal of Neurosurgery*. <http://doi.org/10.3171/jns.1992.76.1.0053>
- Langen, M., Bos, D., Noordermeer, S. D. S., Nederveen, H., Van Engeland, H., & Durston, S. (2014). Changes in the development of striatum are involved in repetitive behavior in autism. *Biological Psychiatry*, *76*(5), 405–411. <http://doi.org/10.1016/j.biopsych.2013.08.013>
- Lapidus, K. A. B., Stern, E. R., Berlin, H. A., & Goodman, W. K. (2014). Neuromodulation for

- Obsessive-Compulsive Disorder. *Neurotherapeutics*, 11(3), 485–495.
<http://doi.org/10.1007/s13311-014-0287-9>
- Lee, K., Holley, S. M., Shobe, J. L., Chong, N. C., Cepeda, C., Levine, M. S., ... Levine, M. S. (2017). Parvalbumin Interneurons Modulate Striatal Output and Enhance Performance during Associative Learning Article Parvalbumin Interneurons Modulate Striatal Output and Enhance Performance during Associative Learning. *Neuron*, 93(6), 1451–1463.e4.
<http://doi.org/10.1016/j.neuron.2017.02.033>
- Leekam, S. R., Prior, M. R., & Uljarevic, M. (2011). Restricted and repetitive behaviors in autism spectrum disorders: A review of research in the last decade. *Psychological Bulletin*, 137(4), 562–593. <http://doi.org/10.1037/a0023341>
- Lei, H., Lai, J., Sun, ; Xiaohong, Xu, Q., & Feng, G. (2018). Lateral orbitofrontal dysfunction in the Sapap3 knockout mouse model of obsessive-compulsive disorder, 1–12.
<http://doi.org/10.1503/jpn180032>
- Lewin, A. B., Chang, S., McCracken, J., McQueen, M., & Piacentini, J. (2010). Comparison of clinical features among youth with tic disorders, obsessive-compulsive disorder (OCD), and both conditions. *Psychiatry Research*.
<http://doi.org/10.1016/j.psychres.2009.11.013>
- Lewis, M., & Kim, S. J. (2009). The pathophysiology of restricted repetitive behavior. *Journal of Neurodevelopmental Disorders*, 1(2), 114–132. <http://doi.org/10.1007/s11689-009-9019-6>
- Leyfer, O. T. O., Folstein, S. E. S., Bacalman, S., Davis, N. O., Dinh, E., Morgan, J., ... Lainhart, J. E. (2006). Comorbid psychiatric disorders in children with autism: Interview development and rates of disorders. *Journal of Autism and Developmental Disorders*.
<http://doi.org/10.1007/s10803-006-0123-0>
- Lim, S. A. O., Kang, U. J., & McGehee, D. S. (2014). Striatal cholinergic interneuron regulation and circuit effects. *Frontiers in Synaptic Neuroscience*, 6(SEP), 1–23.
<http://doi.org/10.3389/fnsyn.2014.00022>

- Little, S., & Brown, P. (2012). What brain signals are suitable for feedback control of deep brain stimulation in Parkinson's disease? *Annals of the New York Academy of Sciences*, 1265(1), 9–24. <http://doi.org/10.1111/j.1749-6632.2012.06650.x>
- Little, S., Pogosyan, A., Neal, S., Zavala, B., Zrinzo, L., Hariz, M., ... Brown, P. (2013). Adaptive deep brain stimulation in advanced Parkinson disease. *American Neurological Association*, 74(3), 447–448. <http://doi.org/10.1002/ana.23966>
- Londei, T., Valentini, A. M. V., & G. Leone, V. (1998). Investigative burying by laboratory mice may involve non-functional, compulsive, behaviour. *Behavioural Brain Research*. [http://doi.org/10.1016/S0166-4328\(97\)00162-9](http://doi.org/10.1016/S0166-4328(97)00162-9)
- Löscher, W., Fisher, J. E., Schmidt, D., Fredow, G., Hönack, D., & Iturrian, W. B. (1989). The sz mutant hamster: A genetic model of epilepsy or of paroxysmal dystonia? *Movement Disorders*, 4(3), 219–232. <http://doi.org/10.1002/mds.870040304>
- Lu, Y., Wang, Y., Lu, B., Chen, M., Zheng, X. P., & Liu, X. J. (2018). ACC to Dorsal Medial Striatum Inputs Modulate Histaminergic Itch Sensation, 38(15), 3823–3839. <http://doi.org/10.1523/JNEUROSCI.3466-17.2018>
- Luk, K. C., & Sadikot, A. F. (2001). GABA promotes survival but not proliferation of parvalbumin-immunoreactive interneurons in rodent neostriatum: An in vivo study with stereology. *Neuroscience*, 104(1), 93–103. [http://doi.org/10.1016/S0306-4522\(01\)00038-0](http://doi.org/10.1016/S0306-4522(01)00038-0)
- Mahlon R. DeLong, M., & Thomas Wichmann, M. (2007). Circuits and Circuit Disorders of the Basal Ganglia. *Arch Neurol*, 72(11), 1232. <http://doi.org/10.1001/jamaneurol.2015.2624>
- Maling, N., Hashemiyoan, R., Foote, K. D., Okun, M. S., & Sanchez, J. C. (2012). Increased Thalamic Gamma Band Activity Correlates with Symptom Relief following Deep Brain Stimulation in Humans with Tourette's Syndrome. *PLoS ONE*. <http://doi.org/10.1371/journal.pone.0044215>
- Mallet, L., Mesnage, V., Houeto, J.-L., Pelissolo, A., Yelnik, J., Behar, C., ... Agid, Y. (2002). Compulsions, Parkinson's disease, and stimulation. *The Lancet*, 360, 1302–1304.

[http://doi.org/10.1016/S0140-6736\(17\)31262-X](http://doi.org/10.1016/S0140-6736(17)31262-X)

Mallet, L., Polosan, M., Jaafari, N., Baup, N., Welter, M.-L., Fontaine, D., ... Pelissolo, A. (2008). Subthalamic Nucleus Stimulation in Severe Obsessive–Compulsive Disorder. *New England Journal of Medicine*, 359(20), 2121–2134. <http://doi.org/10.1056/NEJMoa0708514>

Marsh, R., Alexander, G. M., Packard, M. G., Zhu, H., Wingard, J. C., Quackenbush, G., & Peterson, B. S. (2004). Habit learning in Tourette syndrome: A translational neuroscience approach to a developmental psychopathology. *Archives of General Psychiatry*. <http://doi.org/10.1001/archpsyc.61.12.1259>

Martinez-Ramirez, D., Jimenez-Shahed, J., Leckman, J. F., Porta, M., Servello, D., Meng, F. G., ... Okun, M. S. (2018). Efficacy and safety of deep brain stimulation in tourette syndrome the international tourette syndrome deep brain stimulation public database and registry. *JAMA Neurology*. <http://doi.org/10.1001/jamaneurol.2017.4317>

Marzullo, T. C. (2017). The Missing Manuscript of Dr. Jose Delgado's Radio Controlled Bulls. *Journal of Undergraduate Neuroscience Education : JUNE : A Publication of FUN, Faculty for Undergraduate Neuroscience*, 15(2), R29–R35. Retrieved from <http://www.ncbi.nlm.nih.gov/pubmed/28690447><http://www.pubmedcentral.nih.gov/articlerender.fcgi?artid=PMC5480854>

McCracken, C. B., & Grace, A. A. (2007). High-Frequency Deep Brain Stimulation of the Nucleus Accumbens Region Suppresses Neuronal Activity and Selectively Modulates Afferent Drive in Rat Orbitofrontal Cortex In Vivo. *Journal of Neuroscience*, 27(46), 12601–12610. <http://doi.org/10.1523/JNEUROSCI.3750-07.2007>

McCracken, C. B., & Grace, A. A. (2009). Nucleus Accumbens Deep Brain Stimulation Produces Region-Specific Alterations in Local Field Potential Oscillations and Evoked Responses In Vivo. *Journal of Neuroscience*, 29(16), 5354–5363. <http://doi.org/10.1523/JNEUROSCI.0131-09.2009>

McCulloch, W. S., & Pitts, W. (1943). A logical calculus of the ideas immanent in nervous

- activity. *The Bulletin of Mathematical Biophysics*. <http://doi.org/10.1007/BF02478259>
- McFarland, N. R., & Haber, S. N. (2000). Convergent Inputs from Thalamic Motor Nuclei and Frontal Cortical Areas to the Dorsal Striatum in the Primate. *J. Neurosci.* <http://doi.org/20/10/3798> [pii]
- McGuire, P. K., Bench, C. J., Frith, C. D., Marks, I. M., Frackowiak, R. S. J., & Dolan, R. J. (1994). Functional anatomy of obsessive-compulsive phenomena. *British Journal of Psychiatry*. <http://doi.org/10.1192/bjp.164.4.459>
- Menzies, L., Chamberlain, S. R., Laird, A. R., Thelen, S. M., Sahakian, B. J., & Bullmore, E. T. (2008). Integrating evidence from neuroimaging and neuropsychological studies of obsessive-compulsive disorder: The orbitofronto-striatal model revisited. *Neuroscience and Biobehavioral Reviews*, 32(3), 525–549. <http://doi.org/10.1016/j.neubiorev.2007.09.005>
- Milad, M. R., & Rauch, S. L. (2012). Obsessive-compulsive disorder: Beyond segregated cortico-striatal pathways. *Trends in Cognitive Sciences*, 16(1), 43–51. <http://doi.org/10.1016/j.tics.2011.11.003>
- Miller, J. M., Singer, H. S., Bridges, D. D., & Waranch, H. R. (2006). Behavioral therapy for treatment of stereotypic movements in nonautistic children. *Journal of Child Neurology*. <http://doi.org/10.1177/08830738060210020701>
- Mondragón-González, S. L., & Burguière, E. (2017). Bio-inspired benchmark generator for extracellular multi-unit recordings. *Scientific Reports*, 7(September 2016), 1–13. <http://doi.org/10.1038/srep43253>
- Moody, T. ., Merali, Z., & Crawley, J. N. (1988). The Effects of Anxiolytics and Other Agents on Rat Grooming Behavior. *Annals of the New York Academy of Sciences*, 525(1), 281–290. <http://doi.org/10.1111/j.1749-6632.1988.tb38613.x>
- Müller-Vahl, K. R., Grosskreutz, J., Prell, T., Kaufmann, J., Bodammer, N., & Peschel, T. (2014). Tics are caused by alterations in prefrontal areas, thalamus and putamen, while changes in the cingulate gyrus reflect secondary compensatory mechanisms. *BMC Neuroscience*,

15(Cc). <http://doi.org/10.1186/1471-2202-15-6>

Müller, J., Bakkum, D. J., & Hierlemann, A. (2012). Sub-millisecond closed-loop feedback stimulation between arbitrary sets of individual neurons. *Frontiers in Neural Circuits*, 6(January), 121. <http://doi.org/10.3389/fncir.2012.00121>

Müller, S. V., Johannes, S., Wieringa, B., Weber, A., Müller-Vahl, K., Matzke, M., ... Münte, T. F. (2003). Disturbed monitoring and response inhibition in patients with Gilles de la Tourette syndrome and co-morbid obsessive compulsive disorder. *Behavioural Neurology*. <http://doi.org/10.1155/2003/832906>

Naesstrom, M., Blomstedt, P., Hariz, M., & Bodlund, O. (2017). Deep brain stimulation for obsessive-compulsive disorder: Knowledge and concerns among psychiatrists, psychotherapists and patients. *Surgical Neurology International*. http://doi.org/10.4103/sni.sni_19_17

Nagarajan, N., Jones, B. W., West, P. J., Marc, R. E., & Capecchi, M. R. (2017). Corticostriatal circuit defects in Hoxb8 mutant mice. *Molecular Psychiatry*, 23(9), 1–10. <http://doi.org/10.1038/mp.2017.180>

Nambu, A. (2007). Globus pallidus internal segment. *Progress in Brain Research*, 160(06), 135–150. [http://doi.org/10.1016/S0079-6123\(06\)60008-3](http://doi.org/10.1016/S0079-6123(06)60008-3)

Nambu, A., Tokuno, H., & Takada, M. (2002). Functional significance of the cortico, 43, 1–7. [http://doi.org/10.1016/S0168-0102\(02\)00027-5](http://doi.org/10.1016/S0168-0102(02)00027-5)

Namiki, C., Yamada, M., Yoshida, H., Hanakawa, T., Fukuyama, H., & Murai, T. (2008). Small orbitofrontal traumatic lesions detected by high resolution MRI in a patient with major behavioural changes. *Neurocase*, 14(6), 474–479. <http://doi.org/10.1080/13554790802459494>

Nestadt, G., Addington, A., Samuels, J., Liang, K. Y., Bienvenu, O. J., Riddle, M., ... Cullen, B. (2003). The identification of OCD-related subgroups based on comorbidity. *Biological Psychiatry*, 53(10), 914–920. [http://doi.org/10.1016/S0006-3223\(02\)01677-3](http://doi.org/10.1016/S0006-3223(02)01677-3)

- Nestadt G, J, S., MA, R., KY, L., OJ, B., R, H.-S., ... B., C. (2001). The relationship between obsessive–compulsive disorder and anxiety and affective disorders: results from the Johns Hopkins OCD Family Study. *Psychological Medicine*, 31(03), 481–487. <http://doi.org/10.1017/S0033291701003579>
- Neumann, W. (2019). Toward Electrophysiology-Based Intelligent Adaptive Deep Brain Stimulation for Movement Disorders.
- Neumann, W. J., Horn, A., Ewert, S., Huebl, J., Brücke, C., Slentz, C., ... Kühn, A. A. (2017). A localized pallidal physiomaer in cervical dystonia. *Annals of Neurology*. <http://doi.org/10.1002/ana.25095>
- Novotny, M., Valis, M., & Klimova, B. (2018). Tourette syndrome: A mini-review. *Frontiers in Neurology*, 9(MAR), 1–5. <http://doi.org/10.3389/fneur.2018.00139>
- Nuttin, B., Cosyns, P., Demeulemeester, H., Gybels, J., & Meyerson, B. (1999). Electrical stimulation in anterior limbs of internal capsules in patients with obsessive-compulsive disorder. *Lancet*. [http://doi.org/10.1016/S0140-6736\(99\)02376-4](http://doi.org/10.1016/S0140-6736(99)02376-4)
- Parent, A. (1990). Extrinsic connections of the basal ganglia. *Trends in Neurosciences*, 13(7), 254–258. [http://doi.org/10.1016/0166-2236\(90\)90105-J](http://doi.org/10.1016/0166-2236(90)90105-J)
- Parthasarathy, H. B., & Graybiel, a M. (1997). Cortically driven immediate-early gene expression reflects modular influence of sensorimotor cortex on identified striatal neurons in the squirrel monkey. *The Journal of Neuroscience : The Official Journal of the Society for Neuroscience*, 17(7), 2477–2491. <http://doi.org/10.1523/JNEUROSCI.17-07-02477.1997>
- Paul A. Freiberger, Hemmendinger, D., Pottenger, W. M., & Swaine, M. R. (2018). Computer. In *Eyclopedia britannica*. Encyclopædia Britannica, inc.
- Paz, J. T., Davidson, T. J., Frechette, E. S., Delord, B., Parada, I., Peng, K., ... Huguenard, J. R. (2013). Closed-loop optogenetic control of thalamus as a tool for interrupting seizures after cortical injury. *Nature Neuroscience*, 16(1), 64–70. <http://doi.org/10.1038/nn.3269>

- Penfield, W., and Rasmussen, T. (1950). The Cerebral Cortex of Man: Clinical Study of Localization of Function. *Academic Medicine*. <http://doi.org/10.1097/00001888-195009000-00037>
- Perlmutter, J. S., Mink, J. W., Bastian, A. J., Zackowski, K., Hershey, T., Miyawaki, E., ... Videen, T. O. (2002). Blood flow responses to deep brain stimulation of thalamus. *Neurology*. <http://doi.org/10.1212/WNL.58.9.1388>
- Perreault, M. L., Fan, T., Alijaniam, M., O'Dowd, B. F., & George, S. R. (2012). Dopamine D1-D2 receptor heteromer in dual phenotype GABA/glutamate-coexpressing striatal medium spiny neurons: Regulation of BDNF, GAD67 and VGLUT1/2. *PLoS ONE*, 7(3), 1–10. <http://doi.org/10.1371/journal.pone.0033348>
- Piacentini, J., Woods, D. W., SCAHILL, L., WILHELM, S., Peterson, A. L., Chang, S., ... Walkup, J. T. (2010). Behavior Therapy for Children with Tourette Disorder: A randomized Controlled Trial. *Journal of the American Medical Association*, 303(19), 1929–1937. <http://doi.org/10.1001/jama.2010.607>.Corresponding
- Piallat, B., Polosan, M., Fraix, V., Goetz, L., David, O., Fenoy, A., ... Chabardès, S. (2011). Subthalamic neuronal firing in obsessive-compulsive disorder and Parkinson disease. *Annals of Neurology*, 69(5), 793–802. <http://doi.org/10.1002/ana.22222>
- Piña-Fuentes, D., Beudel, M., Little, S., van Zijl, J., Elting, J. W., Oterdoom, D. L. M., ... Tijssen, M. A. J. (2018). Toward adaptive deep brain stimulation for dystonia. *Neurosurgical Focus*, 45(2), E3. <http://doi.org/10.3171/2018.5.FOCUS18155>
- Pinhal, C. M., van den Boom, B. J. G., Santana-Kragelund, F., Fellingner, L., Bech, P., Hamelink, R., ... Denys, D. (2018). Differential Effects of Deep Brain Stimulation of the Internal Capsule and the Striatum on Excessive Grooming in Sapap3 Mutant Mice. *Biological Psychiatry*, 84(12), 917–925. <http://doi.org/10.1016/j.biopsych.2018.05.011>
- Pisani, A., Bonsi, P., Picconi, B., Tolu, M., Giacomini, P., & Scarnati, E. (2001). Role of tonically-active neurons in the control of striatal function: Cellular mechanisms and behavioral correlates. *Progress in Neuro-Psychopharmacology and Biological Psychiatry*, 25(1), 211–

230. [http://doi.org/10.1016/S0278-5846\(00\)00153-6](http://doi.org/10.1016/S0278-5846(00)00153-6)

Pittenger, C., Krystal, J. H., & Coric, V. (2006). Glutamate-modulating drugs as novel pharmacotherapeutic agents in the treatment of obsessive-compulsive disorder. *NeuroRx*. <http://doi.org/10.1016/j.nurx.2005.12.006>

Planert, H., Szydlowski, S. N., Hjorth, J. J. J., Grillner, S., & Silberberg, G. (2010). Dynamics of Synaptic Transmission between Fast-Spiking Interneurons and Striatal Projection Neurons of the Direct and Indirect Pathways. *Journal of Neuroscience*. <http://doi.org/10.1523/JNEUROSCI.5139-09.2010>

Pollak, P., Benabid, A. L., Gross, C. H., Gao, D. M., Laurent, A., Benazzouz, A., & Perret, J. (1993). Effets de la stimulation du noyau sous-thalamique dans la maladie de Parkinson. *Revue Neurologique*, 149(3), 175–176.

Priori, A., Giannicola, G., Rosa, M., Marceglia, S., Servello, D., Sassi, M., & Porta, M. (2013). Deep brain electrophysiological recordings provide clues to the pathophysiology of Tourette syndrome. *Neuroscience and Biobehavioral Reviews*. <http://doi.org/10.1016/j.neubiorev.2013.01.011>

Pujol, J., Soriano-Mas, C., Alonso, P., Cardoner, N., Menchón, J. M., Deus, J., & Vallejo, J. (2004). Mapping structural brain alterations in obsessive-compulsive disorder. *Archives of General Psychiatry*. <http://doi.org/10.1001/archpsyc.61.7.720>

Purves, D., Augustine, G. J., Fitzpatrick, D., Katz, L. C., LaMantia, A.-S., McNamara, J. O., & Williams, S. M. (2001). *Neuroscience, 2nd Edition*. Sinauer Associates, Inc. <http://doi.org/978-0878937257>

Ramanathan, S., Hanley, J. J., Deniau, J.-M., & Paul, B. J. (2002). Synaptic Convergence of Motor and Somatosensory Cortical Afferents onto GABAergic Interneurons in the Rat Striatum Sankari. *The Journal of Neuroscience*. <http://doi.org/10.1532/HSF98.20051110>

Rapanelli, M., Frick, L. R., & Pittenger, C. (2017). The Role of Interneurons in Autism and Tourette Syndrome. *Trends in Neurosciences*, 40(7), 397–407. <http://doi.org/10.1016/j.tins.2017.05.004>

- Rapanelli, M., Frick, L. R., Xu, M., Groman, S. M., Jindachomthong, K., Tamamaki, N., ... Pittenger, C. (2017). Targeted Interneuron Depletion in the Dorsal Striatum Produces Autism-like Behavioral Abnormalities in Male but Not Female Mice. *Biological Psychiatry*, *82*(3), 194–203. <http://doi.org/10.1016/j.biopsych.2017.01.020>
- Rappel, P., Marmor, O., Bick, A. S., Arkadir, D., Linetsky, E., Castrioto, A., ... Eitan, R. (2018). Subthalamic theta activity: A novel human subcortical biomarker for obsessive compulsive disorder. *Translational Psychiatry*, *8*(1). <http://doi.org/10.1038/s41398-018-0165-z>
- Rauch, S. (2002). Predictors of Fluvoxamine Response in Contamination-related Obsessive Compulsive Disorder A PET Symptom Provocation Study. *Neuropsychopharmacology*, *27*(5), 782–791. [http://doi.org/10.1016/S0893-133X\(02\)00351-2](http://doi.org/10.1016/S0893-133X(02)00351-2)
- Rauch, S. L., Jenike, M. A., Alpert, N. M., Baer, L., Breiter, H. C. R., Savage, C. R., & Fischman, A. J. (1994). Regional Cerebral Blood Flow Measured during Symptom Provocation in Obsessive-Compulsive Disorder using Oxygen 15—Labeled Carbon Dioxide and Positron Emission Tomography. *Archives of General Psychiatry*. <http://doi.org/10.1001/archpsyc.1994.03950010062008>
- Reeves, S. L., Fleming, K. E., Zhang, L., & Scimemi, A. (2016). M-Track: A New Software for Automated Detection of Grooming Trajectories in Mice. *PLoS Computational Biology*, *12*(9), 1–19. <http://doi.org/10.1371/journal.pcbi.1005115>
- Robbins, T. W., & Costa, R. M. (2017). Habits. *Current Biology*, *27*(22), R1200–R1206. <http://doi.org/10.1016/j.cub.2017.09.060>
- Robinson, H. P. C., & Kawai, N. (1993). Injection of digitally synthesized synaptic conductance transients to measure the integrative properties of neurons. *Journal of Neuroscience Methods*. [http://doi.org/10.1016/0165-0270\(93\)90119-C](http://doi.org/10.1016/0165-0270(93)90119-C)
- Rosin, B., Slovik, M., Mitelman, R., Rivlin-Etzion, M., Haber, S. N., Israel, Z., ... Bergman, H. (2011). Closed-loop deep brain stimulation is superior in ameliorating parkinsonism. *Neuron*, *72*(2), 370–384. <http://doi.org/10.1016/j.neuron.2011.08.023>

- Rotge, J. Y., Guehl, D., Dilharreguy, B., Tignol, J., Bioulac, B., Allard, M., ... Aouizerate, B. (2009). Meta-Analysis of Brain Volume Changes in Obsessive-Compulsive Disorder. *Biological Psychiatry*. <http://doi.org/10.1016/j.biopsych.2008.06.019>
- Roth, R. M., Saykin, A. J., Flashman, L. A., Pixley, H. S., West, J. D., & Mamourian, A. C. (2007). Event-Related Functional Magnetic Resonance Imaging of Response Inhibition in Obsessive-Compulsive Disorder. *Biological Psychiatry*, 62(8), 901–909. <http://doi.org/10.1016/j.biopsych.2006.12.007>
- Rubenstein, J., & Rakic, P. (2013). *Neural Circuit Development and Function in the Brain*.
- Rudebeck, P. H., & Murray, E. A. (2009). Amygdala and orbitofrontal cortex lesions differentially influence choices during object reversal learning. *Building*, 28(33), 8338–8343. <http://doi.org/10.1523/JNEUROSCI.2272-08.2008.Amygdala>
- Rymar, V. V., Sasseville, R., Luk, K. C., & Sadikot, A. F. (2004). Neurogenesis and Stereological Morphometry of Calretinin-Immunoreactive GABAergic Interneurons of the Neostriatum. *Journal of Comparative Neurology*, 469(3), 325–339. <http://doi.org/10.1002/cne.11008>
- Santos, F. J., Costa, R. M., & Tecuapetla, F. (2011). Stimulation on demand: Closing the loop on deep brain stimulation. *Neuron*, 72(2), 197–198. <http://doi.org/10.1016/j.neuron.2011.10.004>
- Savica, R., Stead, M., Mack, K. J., Lee, K. H., & Klassen, B. T. (2012). Deep brain stimulation in Tourette syndrome: A description of 3 patients with excellent outcome. *Mayo Clinic Proceedings*. <http://doi.org/10.1016/j.mayocp.2011.08.005>
- Saxena, S., & Rauch, S. L. (2000a). Functional neuroimaging and the neuroanatomy of obsessive-compulsive disorder. *Psychiatric Clinics of North America*. [http://doi.org/10.1016/S0193-953X\(05\)70181-7](http://doi.org/10.1016/S0193-953X(05)70181-7)
- Saxena, S., & Rauch, S. L. (2000b). Functional neuroimaging and the neuroanatomy of obsessive-compulsive disorder. *Psychiatric Clinics of North America*, 23(3), 563–586. [http://doi.org/10.1016/S0193-953X\(05\)70181-7](http://doi.org/10.1016/S0193-953X(05)70181-7)

- Schuetze, M., Park, M. T. M., Cho, I. Y. K., Macmaster, F. P., Chakravarty, M. M., & Bray, S. L. (2016). Morphological alterations in the thalamus, striatum, and pallidum in autism spectrum disorder. *Neuropsychopharmacology*, *41*(11), 2627–2637. <http://doi.org/10.1038/npp.2016.64>
- Schuurman, P. R., Liebrand, L. C., Denys, D., Caan, M. W. A., van Wingen, G. A., van den Munckhof, P., & Figeet, M. (2018). Individual white matter bundle trajectories are associated with deep brain stimulation response in obsessive-compulsive disorder. *Brain Stimulation*, *12*(2), 353–360. <http://doi.org/10.1016/j.brs.2018.11.014>
- Sciamanna, E. (1882). Fenomeni prodotti dall'applicazione della corrente elettrica sulla dura madre et modificazione del polso cerebrale. *Memorie Della Classe Di Scienza Fisiche, Matematiche e Naturali*.
- Scimemi, A., Tian, H., & Diamond, J. S. (2009). Neuronal Transporters Regulate Glutamate Clearance, NMDA Receptor Activation, and Synaptic Plasticity in the Hippocampus. *Journal of Neuroscience*, *29*(46), 14581–14595. <http://doi.org/10.1523/JNEUROSCI.4845-09.2009>
- Sem-Jacobsen, C. W. (1965). DEPTH ELECTROGRAPHIC STIMULATION AND TREATMENT OF PATIENTS WITH PARKINSON'S DISEASE INCLUDING NEUROSURGICAL TECHNIQUE. *Acta Neurologica Scandinavica*. <http://doi.org/10.1111/j.1600-0404.1965.tb01899.x>
- Shakeel, A., Navid, M. S., Anwar, M. N., Mazhar, S., Jochumsen, M., & Niazi, I. K. (2015). A Review of Techniques for Detection of Movement Intention Using Movement-Related Cortical Potentials, 2015.
- Shanahan, N. A., Holick Pierz, K. A., Masten, V. L., Waeber, C., Ansorge, M., Gingrich, J. A., ... Dulawa, S. C. (2009). Chronic Reductions in Serotonin Transporter Function Prevent 5-HT1B-Induced Behavioral Effects in Mice. *Biological Psychiatry*. <http://doi.org/10.1016/j.biopsych.2008.09.026>
- Shmelkov, S. V., Hormigo, A., Jing, D., Proenca, C. C., Bath, K. G., Milde, T., ... Rafii, S. (2010). Slitrk5 deficiency impairs corticostriatal circuitry and leads to obsessive-compulsive-like

- behaviors in mice. *Nature Medicine*, 16(5), 598–602. <http://doi.org/10.1038/nm.2125>
- Shute, J. B., Okun, M. S., Opri, E., Molina, R., Rossi, P. J., Martinez-Ramirez, D., ... Gunduz, A. (2016). Thalamocortical network activity enables chronic tic detection in humans with Tourette syndrome. *NeuroImage: Clinical*, 12, 165–172. <http://doi.org/10.1016/j.nicl.2016.06.015>
- Simon, D., Kaufmann, C., Müsch, K., Kischkel, E., & Kathmann, N. (2010). Fronto-striato-limbic hyperactivation in obsessive-compulsive disorder during individually tailored symptom provocation. *Psychophysiology*. <http://doi.org/10.1111/j.1469-8986.2010.00980.x>
- Sironi, V. A. (2011). Origin and Evolution of Deep Brain Stimulation. *Frontiers in Integrative Neuroscience*, 5(August), 1–5. <http://doi.org/10.3389/fnint.2011.00042>
- Smolinsky, A. N., Bergner, C. L., Laporte, J. L., & Kalueff, A. V. (2011). Mood and Anxiety Related Phenotypes in Mice, 63, 4–7. <http://doi.org/10.1007/978-1-61779-313-4>
- Somogyi, P., Bolam, J. P., & Smith, A. D. (1981). Monosynaptic cortical input and local axon collaterals of identified striatonigral neurons. A light and electron microscopic study using the golgi-peroxidase transport-degeneration procedure. *Journal of Comparative Neurology*, 195(4), 567–584. <http://doi.org/10.1002/cne.901950403>
- Spruijt, B. M., van Hooff, J. A., & Gispen, W. H. (1992). Ethology and neurobiology of grooming behavior. *Physiological Reviews*, 72(3), 825–852. <http://doi.org/10.1152/physrev.1992.72.3.825>
- Squire, Larry; Berg, Darwin; Bloom, Floyd; du Lac, Sascha; Ghosh, Anirvan; Spitzer, N. (2008). *The spinal and Peripheral motor system*. <http://doi.org/10.1016/B978-0-12-385870-2.00032-9>
- Squire, L., Berg, D., Bloom, F., du Lac, S., Ghosh, A., & Spitzer, N. (2008). *Fundamental Neuroscience*. <http://doi.org/10.1016/B978-0-12-385870-2.00032-9>
- Srinivasan, S. S., Maimon, B. E., Diaz, M., Song, H., & Herr, H. M. (2018). Closed-loop functional optogenetic stimulation. *Nature Communications*, 9(1), 5303.

<http://doi.org/10.1038/s41467-018-07721-w>

- Sturm, V., Lenartz, D., Koulousakis, A., Treuer, H., Herholz, K., Klein, J. C., & Klosterkötter, J. (2003). The nucleus accumbens: A target for deep brain stimulation in obsessive-compulsive- and anxiety-disorders. *Journal of Chemical Neuroanatomy*, *26*(4), 293–299. <http://doi.org/10.1016/j.jchemneu.2003.09.003>
- Swain, J. E., Scahill, L., Lombroso, P. J., King, R. A., & Leckman, J. F. (2007). Tourette syndrome and tic disorders: A decade of progress. *Journal of the American Academy of Child and Adolescent Psychiatry*, *46*(8), 947–968. <http://doi.org/10.1097/chi.0b013e318068fbcc>
- Szechtman, H., Ahmari, S. E., Beninger, R. J., Eilam, D., Harvey, B. H., Edemann-Callesen, H., & Winter, C. (2017). Obsessive-compulsive disorder: Insights from animal models. *Neuroscience and Biobehavioral Reviews*, *76*, 254–279. <http://doi.org/10.1016/j.neubiorev.2016.04.019>
- Szechtman, H., Sulis, W., & Eilam, D. (1998). Quinpirole induces compulsive checking behavior in rats: A potential animal model of obsessive-compulsive disorder (OCD). *Behavioral Neuroscience*. <http://doi.org/10.1037/0735-7044.112.6.1475>
- Szydlowski, S. N., Pollak Dorocic, I., Planert, H., Carlen, M., Meletis, K., & Silberberg, G. (2013). Target Selectivity of Feedforward Inhibition by Striatal Fast-Spiking Interneurons. *Journal of Neuroscience*, *33*(4), 1678–1683. <http://doi.org/10.1523/JNEUROSCI.3572-12.2013>
- Tan, T. C., & Black, P. M. L. (2002). Sir Victor Horsley (1857-1916): pioneer of neurological surgery. *Neurosurgery*, *50*(3), 607–611; discussion 611. <http://doi.org/10.1227/00006123-200203000-00032>
- Tecuapetla, F., Jin, X., Lima, S. Q., Costa, R. M., Tecuapetla, F., Jin, X., ... Costa, R. M. (2016). Complementary Contributions of Striatal Projection Pathways to Action Initiation and Execution Article Complementary Contributions of Striatal Projection Pathways to Action Initiation and Execution. *Cell*, *166*(3), 703–715. <http://doi.org/10.1016/j.cell.2016.06.032>
- Tepper, J. M., Abercrombie, E. D., & Bolam, J. P. (2007). Basal ganglia macrocircuits. *Progress in Brain Research*, *160*, 3–7. [http://doi.org/10.1016/S0079-6123\(06\)60001-0](http://doi.org/10.1016/S0079-6123(06)60001-0)

- Tepper, J. M., & Koós, T. (2017). *GABAergic Interneurons of the Striatum. Handbook of Behavioral Neuroscience* (Vol. 24). Elsevier Inc. <http://doi.org/10.1016/B978-0-12-802206-1.00008-8>
- Tepper, J. M., Tecuapetla, F., Koós, T., & Ibáñez-Sandoval, O. (2010). Heterogeneity and Diversity of Striatal GABAergic Interneurons. *Frontiers in Neuroanatomy*, 4(December), 1–18. <http://doi.org/10.3389/fnana.2010.00150>
- Terakita, A. (2005). The opsins. *Genome Biology*, 1–8.
- Thelen, E. (1980). Determinants of amounts of stereotyped behavior in normal human infants. *Ethology and Sociobiology*, 1(2), 141–150. [http://doi.org/10.1016/0162-3095\(80\)90004-7](http://doi.org/10.1016/0162-3095(80)90004-7)
- Ting, J. T., & Feng, G. (2011). Neurobiology of obsessive-compulsive disorder: Insights into neural circuitry dysfunction through mouse genetics. *Current Opinion in Neurobiology*, 21(6), 842–848. <http://doi.org/10.1016/j.conb.2011.04.010>
- Tye, K. M., & Deisseroth, K. (2012). Optogenetic investigation of neural circuits underlying brain disease in animal models. *Nature Neuroscience*, 13(April). <http://doi.org/10.1038/nrn3171>
- Uhlhaas, P. J., & Singer, W. (2006). Neural Synchrony in Brain Disorders: Relevance for Cognitive Dysfunctions and Pathophysiology. *Neuron*, 52(1), 155–168. <http://doi.org/10.1016/j.neuron.2006.09.020>
- van den Boom, B. J. G., Pavlidi, P., Wolf, C. J. H., Mooij, A. H., & Willuhn, I. (2017). Automated classification of self-grooming in mice using open-source software. *Journal of Neuroscience Methods*, 289, 48–56. <http://doi.org/10.1016/j.jneumeth.2017.05.026>
- Viswanathan, A., Jimenez-Shahed, J., Baizabal Carvallo, J. F., & Jankovic, J. (2012). Deep brain stimulation for tourette syndrome: Target selection. *Stereotactic and Functional Neurosurgery*. <http://doi.org/10.1159/000337776>
- Vlasits, A. (2016). He may have invented one of neuroscience's biggest advances. But you've

never heard of him. *STAT*.

- Voigts, J., Siegle, J. H., Pritchett, D. L., & Moore, C. I. (2013). The flexDrive: an ultra-light implant for optical control and highly parallel chronic recording of neuronal ensembles in freely moving mice. *Frontiers in Systems Neuroscience*, 7(May), 1–9. <http://doi.org/10.3389/fnsys.2013.00008>
- Voon, V., Derbyshire, K., Rück, C., Irvine, M. A., Worbe, Y., Enander, J., ... Bullmore, E. T. (2015). Disorders of compulsivity: a common bias towards learning habits. *Molecular Psychiatry*. <http://doi.org/10.1038/mp.2014.44>
- Vu, M.-A. T., Adali, T., Ba, D., Buzsaki, G., Carlson, D., Heller, K., ... Dzirasa, K. (2018). A Shared Vision for Machine Learning in Neuroscience. *The Journal of Neuroscience*, 38(7), 0508-17. <http://doi.org/10.1523/JNEUROSCI.0508-17.2018>
- Warden, M. R., Cardin, J. A., & Deisseroth, K. (2014). Optical Neural Interfaces. *Annual Review of Biomedical Engineering*, 16(1), 103–129. <http://doi.org/10.1146/annurev-bioeng-071813-104733>
- Welch, J. M., Lu, J., Rodriguiz, R. M., Trotta, N. C., Peca, J., Ding, J.-D., ... Feng, G. (2007). Cortico-striatal synaptic defects and OCD-like behaviours in Sapap3-mutant mice. *Nature*, 448(7156), 894–900. <http://doi.org/10.1038/nature06104>
- Welter, M.-L., Burbaud, P., Fernandez-Vidal, S., Bardinet, E., Coste, J., Piallat, B., ... Mallet, L. (2011). Basal ganglia dysfunction in OCD: subthalamic neuronal activity correlates with symptoms severity and predicts high-frequency stimulation efficacy. *Translational Psychiatry*, 1(5), e5. <http://doi.org/10.1038/tp.2011.5>
- Welter, M. L., Houeto, J. L., Bonnet, A. M., Bejjani, P. B., Mesnage, V., Dormont, D., ... Pidoux, B. (2004). Effects of High-Frequency Stimulation on Subthalamic Neuronal Activity in Parkinsonian Patients. *Archives of Neurology*, 61(1), 89–96. <http://doi.org/10.1001/archneur.61.1.89>
- Wilson, C. J. (1980). Fine Structure and Synaptic Connections of the Common Spiny Neuron of the Rat Neostriatum : A Study Employing Intracellular Injection of Horseradish Peroxidase

- Charles J . Wilson and Philip M . Groves Department of Psychology , University of Colorado , Bo. *The Journal of Comparative Neurology*, 194(April 1979), 599–615.
- Wiltschko, A. B., Johnson, M. J., Iurilli, G., Peterson, R. E., Katon, J. M., Pashkovski, S. L., ... Datta, S. R. (2015). Mapping Sub-Second Structure in Mouse Behavior. *Neuron*, 88(6), 1121–1135. <http://doi.org/10.1016/j.neuron.2015.11.031>
- Windels, F., Bruet, N., Poupard, A., Urbain, N., Chouvet, G., Feuerstein, C., & Savasta, M. (2000). Effects of high frequency stimulation of subthalamic nucleus on extracellular glutamate and GABA in substantia nigra and globus pallidus in the normal rat. *European Journal of Neuroscience*. <http://doi.org/10.1046/j.1460-9568.2000.00296.x>
- Wolmarans, D. W., Stein, D. J., & Harvey, B. H. (2017). Social behavior in deer mice as a novel interactive paradigm of relevance for obsessive-compulsive disorder (OCD). *Social Neuroscience*. <http://doi.org/10.1080/17470919.2016.1145594>
- Woods, A., Smith, C., Szewczak, M., Dunn, R. W., Cornfeldt, M., & Corbett, R. (1993). Selective serotonin re-uptake inhibitors decrease schedule-induced polydipsia in rats: a potential model for obsessive compulsive disorder. *Psychopharmacology*. <http://doi.org/10.1007/BF02244910>
- Worbe, Y., Marrakchi-kacem, L., Lecomte, S., Valabregue, R., Poupon, F., Guevara, P., ... Poupon, C. (2015). Altered structural connectivity of cortico-striato-pallido-thalamic networks in Gilles de la Tourette syndrome, (2014), 472–482. <http://doi.org/10.1093/brain/awu311>
- Wu, H., Ghekiere, H., Beeckmans, D., Tambuyzer, T., Van Kuyck, K., Aerts, J. M., & Nuttin, B. (2015). Conceptualization and validation of an open-source closed-loop deep brain stimulation system in rat. *Scientific Reports*, 4(Cl), 1–6. <http://doi.org/10.1038/srep09921>
- Xu, M., Li, L., & Pittenger, C. (2016). Ablation of fast-spiking interneurons in the dorsal striatum, recapitulating abnormalities seen post-mortem in Tourette syndrome, produces anxiety and elevated grooming. *Neuroscience*, 324, 321–329.

<http://doi.org/10.1016/j.neuroscience.2016.02.074>

- Xu, P., Grueter, B. A., Britt, J. K., McDaniel, L., Huntington, P. J., Hodge, R., ... Pieper, A. A. (2013). Double deletion of melanocortin 4 receptors and SAPAP3 corrects compulsive behavior and obesity in mice. *Proceedings of the National Academy of Sciences*, *110*(26), 10759–10764. <http://doi.org/10.1073/pnas.1308195110>
- Xu, Z. C., Wilson, C. J., & Emson, P. C. (1989). Restoration of the corticostriatal projection in rat neostriatal grafts: electron microscopic analysis. *Neuroscience*. [http://doi.org/10.1016/0306-4522\(89\)90129-2](http://doi.org/10.1016/0306-4522(89)90129-2)
- Yarom, Y. (1991). Rhythmogenesis in a hybrid system-interconnecting an olivary neuron to an analog network of coupled oscillators. *Neuroscience*. [http://doi.org/10.1016/0306-4522\(91\)90053-Q](http://doi.org/10.1016/0306-4522(91)90053-Q)
- Yelnik, J. (2008). Modeling the organization of the basal ganglia. *Revue Neurologique*, *164*(12), 969–976. <http://doi.org/10.1016/j.neurol.2008.04.019>
- Yin, H. H., Mulcare, S. P., Hilário, M. R. F., Clouse, E., Holloway, T., Davis, M. I., ... Costa, R. M. (2009). Dynamic reorganization of striatal circuits during the acquisition and consolidation of a skill. *Nature Neuroscience*. <http://doi.org/10.1038/nn.2261>
- Yizhar, O., Fenno, L. E., Davidson, T. J., Mogri, M., & Deisseroth, K. (2011). Optogenetics in Neural Systems. *Neuron*, *71*(1), 9–34. <http://doi.org/10.1016/j.neuron.2011.06.004>
- Young, M., Schattenkerk, M. E., Malt, R. A., Koroly, M. J., & Li, A. K. (1980). Nerve growth factor: acceleration of the rate of wound healing in mice. *Proceedings of the National Academy of Sciences*, *77*(7), 4379–4381. <http://doi.org/10.1073/pnas.77.7.4379>
- Zandt, F., Prior, M., & Kyrios, M. (2007). Repetitive behaviour in children with high functioning autism and obsessive compulsive disorder. *Journal of Autism and Developmental Disorders*. <http://doi.org/10.1007/s10803-006-0158-2>
- Zhang, F., Aravanis, A. M., Adamantidis, A., Lecea, L. De, Deisseroth, K., An, L. de L., & Deisseroth, K. (2007). Circuit-breakers: optical technologies for probing neural signals

and systems. *Nature Reviews Neuroscience*, 581, 8694. <http://doi.org/10.1038/nrn2192>

Zhang, F., Gradinaru, V., Adamantidis, A. R., Durand, R., Airan, R. D., De Lecea, L., & Deisseroth, K. (2010). Optogenetic interrogation of neural circuits: Technology for probing mammalian brain structures. *Nature Protocols*, 5(3), 439–456. <http://doi.org/10.1038/nprot.2009.226>

Zhao, S., Ting, J. T., Atallah, H. E., Qiu, L., Tan, J., Gloss, B., ... Feng, G. (2011). Cell type-specific channelrhodopsin-2 transgenic mice for optogenetic dissection of neural circuitry function. *Nature Methods*. <http://doi.org/10.1038/nmeth.1668>

Zinner, S. H., & Mink, J. W. (2010). Movement Disorders I: Tics and Stereotypies. *Pediatrics in Review*, 31(6), 223–233. <http://doi.org/10.1542/pir.31-6-223>

Zuchner, S., Wendland, J., Ashley-Koch, A., Collins, A., Tran-Viet, K., Quinn, K., ... Murphy, D. (2010). Multiple rare SAPAP3 missense variants in trichotillomania and OCD. *Molecular Psychiatry*, 14(1), 6–9. <http://doi.org/10.1038/mp.2008.83>. Multiple

RESUME EN FRANÇAIS

Dans la vie de tous les jours, pour avoir un comportement efficace, nous nous appuyons sur des habitudes et des routines, c'est-à-dire des facultés que nous avons acquises et automatisées. Lorsque des comportements sont répétés dans un contexte uniforme, le lien associatif entre le contexte et l'action augmente progressivement jusqu'à ce que, par leur répétition régulière, ces comportements deviennent automatiques. Alors que cette faculté d'automatiser plus efficacement peut être bénéfique, la limite de comportements répétitifs sains est ténue. En effet, les circuits cortico-striataux sont affectés par plusieurs pathologies dans lesquelles une dysrégulation de l'expression d'actions automatiques débouche sur des comportements répétitifs pathologiques. On trouve comme troubles neuropsychiatriques caractérisés par des comportements répétitifs pathologiques comme principal symptôme, les troubles obsessionnels compulsifs (TOC) pour lesquels la répétition de routines ou de rituels complexes (compulsions) peut sérieusement affecter la qualité de vie du patient. L'apparition de comportements répétitifs pathologiques peut résulter d'une surexpression de séquences comportementales complexes et habituelles (compulsions) et il a été montré que ces fonctions sont gérées par les circuits cortico-striataux. Pour ce projet de thèse, nous nous concentrons sur un substrat neurophysiologique suspecté de jouer un rôle crucial dans l'apparition et dans la régulation des comportements répétitifs : le réseau d'interneurones du striatum. En effet, les interneurones du striatum exercent un contrôle important sur l'excitabilité du striatum en contrôlant dynamiquement l'entrée et la sortie des neurones épineux moyens. Parmi ceux-ci, le réseau inhibiteur d'interneurones à parvalbumine (PV) forme un large réseau d'inhibition du *feed-forward* dans les neurones épineux moyens et est crucial pour la régulation des fonctions du réseau de sortie du striatum. Un déficit de contrôle inhibiteur par les interneurones à parvalbumine est corrélé à une augmentation des décharges des neurones épineux moyens chez la souris *SAPAP3-KO*, un modèle animal des comportements compulsifs que nous avons utilisés dans notre étude et qui exprime un comportement compulsif d'auto-toilettage. Par une stimulation optogénétique des interneurones à parvalbumine dans la partie dorsale médiale du striatum, nous avons pu empêcher de façon efficace des toilettages compulsifs et on a pu les réduire à des niveaux normaux. De plus, nous avons identifié un biomarqueur électrophysiologique interne non constant dans la bande delta dans le cortex orbitofrontal latéral qui précédait l'apparition des événements d'auto-toilettage. Ce biomarqueur a servi à déclencher la stimulation optogénétique des interneurones PV dans une approche en boucle fermée pour laquelle il s'est avéré être un biomarqueur fiable. La stimulation optogénétique à la demande a effectivement réduit les démarrages d'événements d'auto-toilettage. Conformément à notre intérêt pour les expérimentations en boucle fermée, nous avons contribué à la *toolbox* de neuroscience avec une série de développements techniques qui nous ont aidés à acquérir des données neuronales et qui fournissent un *framework* qui sera utile pour de futures approches en boucle fermée. Nos résultats ont aidé à comprendre les mécanismes biologiques sous-jacents lors de la régulation de comportements répétitifs en suggérant que les interneurones à parvalbumine du striatum sont essentiels à la régulation de l'expression des comportements répétés. Nous avons également fourni un nouveau cadre expérimental pour la prédiction des comportements répétitifs qui pourrait être utilisé pour des tests avec d'autres cibles thérapeutique ou d'autres hypothèses. Ensemble, ces résultats ont non seulement un intérêt pour avancer dans la compréhension en recherche fondamentale des circuits sur lesquels reposent les comportements répétitifs, mais ils présentent également un intérêt clinique immédiat à des fins thérapeutiques pour les troubles de comportements répétitifs.